博士論文

Study on the influence of retro-reflective coatings on the thermal environment of building groups

再帰反射材料が建築物群の温熱環境に及ぼす影響に関する研究

2023 年 6 月

王 京

WANG JING

Study on the influence of retro-reflective coatings on the thermal environment of building groups

ABSTRACT

The urban population growth has led to a denser urban pattern, and high-rise and high-density building groups have become the urban development theme. Many building surfaces made of concrete and asphalt are affected by solar radiation easily, leading to the deterioration of regional thermal environment and the increase of building energy consumption. So far, there have been a lot of green technologies including increasing green plants and water areas, changing building layouts, etc., but these strategies are not well suitable for high-rise high-density buildings.

Owing to the solar radiation is the main cause effecting building thermal environment, the high-reflective coatings (HR-coatings) have attracted much attention due to they can effectively reflect solar radiation in summer. However, the radiant heat from nearby buildings or streets is increased, and can not improve the worsening heat island effect.

Based on this, recently, retro-reflective coatings (RR-coatings) have drawn the attention of many scholars, which can reflect solar radiation back along the incident direction. Theoretically, the temperatures of building surfaces and energy consumption will be reduced when it is applied to the buildings. At present, the application research of this coatings in buildings is a brand-new topic.

In Chapter 1, Background and purpose of the study. The research backgrounds were introduced, which included due to the increase of population and high-rise and high-density buildings caused by urbanization, the thermal environment of regional buildings deteriorated and energy consumption increased. After demonstrating the limitation of other green technologies, based on the fact that solar radiation was the main source of building thermal gain, HR-coatings with a wide range of application and RR-coatings attracted attention in recent years were proposed. And the research status, research purpose and research significance were introduced. Finally, the research structure was explained.

In Chapter 2, Literature review of the application of retro-reflective coatings in buildings. The relevant research of RR-coatings was reviewed, and the focuses were the optical property, which mainly included the fundamental types and property improvement, measurement methods of solar reflectivity and retro-reflectivity, and application efficiency of RR-coatings, which mainly included the effect on urban thermal environment and building energy consumption, among which the impact on the urban thermal environment was elaborated from

the urban albedo, building surface temperature and air temperature. Finally, future directions were proposed on possible studies and applications.

In Chapter 3, Methodology and performance evaluation index. This chapter mainly introduced the basic experimental systems and performance evaluation index of optical performance and thermal performance of RR-coatings, and simulation software and evaluation index applied in the simulation research of the effect on building energy load, which laid the foundation for the related analysis of the following chapters. Firstly, the optical performance experiment was introduced. The solar reflectance and angle distribution of glass bead RR-coatings, prism RR-coatings and HR-coatings were measured using the optical property measuring instruments. Secondly, the thermal performance experiments were introduced, which included the experimental plans, the basic experimental models, and the performance evaluation indexes, which mainly included the regional albedo, wall temperature and air temperature in the enclosed space. Thirdly, based on the software of Energyplus, the impact of RR-coating on the thermal environment of buildings was preliminarily determined, and the effect of building surface retro-reflectivities on energy load of an enclosed educational building in Qingdao was simulated, and the evaluation index included daily, monthly and yearly energy load.

In Chapter 4, Study on spectral properties of retro-reflective coatings. The integrating sphere was used to measure the global reflectivity, and a self-developed instrument was used to measure the angular distribution at different incident angles. The result showed that the global-reflectivity of glass bead RR-coatings and prism RR-coatings were 64.74% and 51.44%, respectively. However, the retro-reflectivity of prism RR-coatings was higher than that of glass bead RR-coatings at the smaller incident angles with the values of 25.22% and 21.67%, respectively (at incidence angles of 10∘ and 30∘). For larger incidence angles including 50∘ and 70∘, two RR-coatings mainly showed specular-reflection property. RR-pattern facades could reduce the wall surface temperature of nearby buildings, compared to general facades.

In Chapter 5, An experimental comparison on regional thermal environment of the high-density enclosed building groups with retro-reflective and high-reflective coatings. This chapter built two small-scaled high-density enclosed building group models and covered by RR-coatings and HR-coatings, respectively. The urban albedo, wall temperature and air temperature were contrastively analyzed. Experimental results showed that compared with HR-coating model, RR-coating model had better cooling potential, and its regional albedo was increased by 5.53%. And air temperature in the enclosed space of RR-coating model was 2.24°C lower than that of HR-coating model, but they were higher than outdoor natural air temperature.

Moreover, compared to HR-coatings, covering RR-coatings could reduce the peak and average wall temperature by 2.47°C~15.25°C & 0.30°C~3.82°C in the daytime and 1.35°C~7.91°C% & 0.25°C~4.38°C in the nighttime, and the application in the roof and east wall had the higher efficiency.

In Chapter 6, Influence of the building enclosed forms on thermal contribution of retro-reflective and high-reflective coatings. In this chapter, three typical forms of high-density buildings, namely the Determinant Form (D-Form), Three-Sided Enclosed Form (TSE-Form) and Four-Sided Enclosed Form (FSE-Form), were proposed, and HR-coatings and RR-coatings were employed. The albedo, wall temperature, and air temperature were monitored. Experimental results showed that the higher the enclosed degree of buildings covered by HR-coatings, the poorer the regional thermal environment and the higher the heat island efficiency. However, the opposite was true for enclosed buildings with RR-coatings. RR-coatings had a better thermal contribution than HR-coatings, and the higher the enclosure degree of buildings, the higher the improvement efficiency of RR-coatings. Compared with HR-coatings, RR-coatings increased the maximum and average regional albedos by 0.67%~3.42% and 1.36%~5.59%, respectively, and lowered the maximum and average temperatures by 0.26°C~7.05°C and 0.02°C~4.83°C for model walls and 0.59°C~4.41°C and 1.80°C~3.06°C for outdoor air, respectively.

In Chapter 7, An experimental evaluation on thermal contribution of retro-reflective and high-reflective coatings in an enclosed building in summer and winter. This chapter evaluated the thermal contribution of RR-coatings and HR-coatings in an enclosed building in both summer and winter. And the regional albedos, wall temperatures, and air temperatures were measured. Experimental results showed that both in summer and winter, compared with HR-coatings, RR-coatings had higher regional albedos, lower wall temperatures and air temperatures, however, the differences were smaller in winter, which would lead to more thermal benefits in summer caused by RR-coatings than thermal penalties in winter. For the regional albedos, the maximum differences in summer and winter were 4.99% and 2.46%, and the values were 2.74°C~11.61°C and 1.39°C~5.61°C for the wall temperatures, 2.10°C and 0.39°C for the air temperatures.

In Chapter 8, The effect of building surface retro-reflectivity on energy load and CO_2 emission of an enclosed building. This chapter analyzed the effect of surface reflectivity on energy load of an educational buildings. The daily, monthly and yearly energy load were simulated based on the Energyplus software, and CO_2 emissions were also calculated. The numerical results showed for daily energy load in four typical seasons, there was a positive

correlation between the daily energy load and building surface reflectivities in January, April and October, and a negative correlation in July. For monthly energy load, the building cooling and heating load were the most in January and August, respectively. For annual energy load, the higher the reflectivity, the lower the cooling load and the higher the heating load. When the building surface reflectivity was 0.7, the annual energy load were the least, with the value of 148.23 $\mathrm{kWh/m^2}$. In addition, the CO_2 emissions was also the lowest, with the value of 24.79 $\mathrm{kg/m^2}$. According to the relation between solar reflectivities and retro-reflectivities of prism RR-coatings mentioned in the published articles, When the building surface retro-reflectivity was 0.47, the total annual energy load and CO_2 emissions were the least.

In Chapter 9, Conclusion and prospect. The main research conclusions of each chapter were summarized, and the contents of the future research were expounded.

STRUCTURE OF THIS PAPER

Study on the influence of retro-reflective coatings on the thermal environment of building groups

Chapter One
Background and Purpose of the Study
1.1 Research source and background
1.2 Research status
1.3 Research purpose and significance
1.4 Research structure

Chapter Two
Literature Review of the application of retro-reflective coatings in buildings
2.1 Introduction
2.2 Review methods and synthesis of evidence
2.3 Retro-reflective coatings and their optical property
2.4 Measurement methods of solar reflectivity and retro-reflectivity
2.5 Application efficiency of retro-reflective coatings
2.6. Conclusion and outlook

Chapter Three
Methodology and performance evaluation index
3.1 Optical performance experiment
3.2 Thermal performance experiment
3.3 Building energy load simulation
3.4 Summary

Chapter Four
Study on spectral properties of retro-reflective coatings
4.1 Introduction
4.2 Optical property of RR-Coatings
4.3 Thermal effect of optical structure
4.4 Conclusion

Core Chapters

Chapter Five
An experimental comparison on regional thermal environment of the high-density enclosed building groups with retro-reflective and high-reflective coatings

5.1 Introduction
5.2 Description of the comparative experiment
5.3 Experiment results and discussion
5.4 Conclusion

Chapter Six
Influence of the building enclosed forms on thermal contribution of retro-reflective and high-reflective coatings
6.1 Introduction
6.2 Description of the comparative experiment
6.3 Experiment results
6.4 Discussion
6.5 Conclusion

Chapter Seven
An experimental evaluation on thermal contribution of retro-reflective and high-reflective coatings in an enclosed building in summer and winter
7.1 Introduction
7.2 Experiment platform and point latout
7.3 Experiment results and discussion
7.4 Conclusion

Chapter Eight
The effect of building surface retro-reflectivity on energy load and CO_2 emission of an enclosed educational building
8.1 Introduction
8.2 Description of the simulation
8.3 Result and discussion
8.4 Conclusion

Chapter Nine
Conclusion and prospect
9.1 Conclusion
9.2 Prospect

TABLE OF CONTENTS

Chapter 7 An experimental evaluation on thermal contribution of retro-reflective and high-reflective coatings in an enclosed building in summer and winter

Chapter 8 The effect of building surface retro-reflectivity on energy load and CO_2 emission of an enclosed building

Background and purpose of this study

Chapter 1 Background and purpose of the study

1.1 Research source and background

1.1.1 Research source

This subject was from the National Natural Science Foundation of China under Grant No. 51908302, and the title was Effect of retro-reflective coatings on the regional thermal environment and energy consumption in the high-rise and high-density building groups. The research period was from 2020.01.01 to 2022.12.31, and the project was finished.

The main research content of this project was to reveal the influence mechanism of retro-reflective coatings (RR-coatings) on regional thermal environment and building energy consumption of high-rise and high-density buildings. In addition, to provide the directions of improving the application performance of RR-coatings, the angular resolution spectrometer system was developed to realize the spectral measurement of RR-coatings at any incidence angles. And to predict the long-term performance of RR-coatings, long-term outdoor exposure experiment and accelerated aging experiment using the aging instrument were carried out.

1.1.2 Research background

The urbanization of the world continued to accelerate, and according to the Population Perspectives study, the world would continue to urbanize over the next 30 years, rising from 56% in 2021 to 68% in 2050. Compared to rural areas, the urban areas would absorb almost all of the future world population growth, as shown in Fig. 1-1. As the carrier of economic development, the cities had the higher population density and more industries. Therefore, there were problems such as traffic congestion, decrease of urban greening rate, etc.
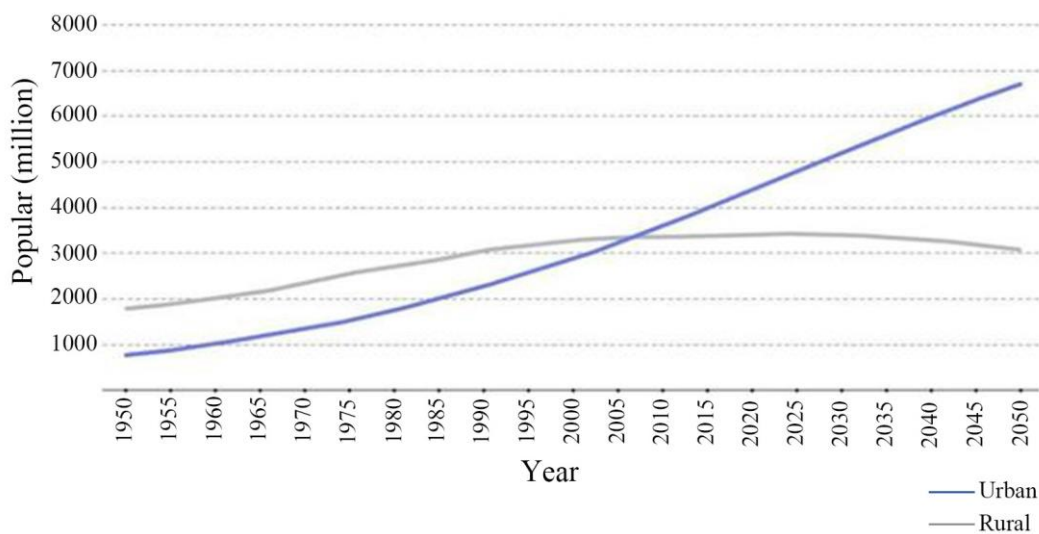
Fig. 1-1. Global Urban and Rural Population Changes and Projections (1950-2050)
Source: State of the World's Cities Report 2022

China, as a country with a population of more than 1.4 billion, ranked among the top in the world. However, the population distribution was uneven geographically, and the total amount of land resources was large and the per capital was small, and the land area available for construction was limited. Coupled with the large-scale rapid urbanization process , high-rise buildings and super high-rise buildings became the effective measures to solve the problem of land resource shortage. In recent years, the vigorous development of science, technology and economic strength has laid a solid foundation for the construction of high-rise buildings and super high-rise buildings, and more and more high-rise buildings and super high-rise buildings appeared in developed areas and emerging cities [1-3]. According to the report released by the World Council on Tall Buildings and Urban Habitat (CTBUH), in 2020, among the 106 super high buildings with a height of more than 200m completed in the world, 56 super tall buildings were located in China, accounting for 53% of the total, as shown in Fig. 1-2. With the shortage of land in urban centers, intensive land use would become a trend and the city would enter the high-rise era. It could make full use of limited space to expand living space. High-rise buildings with large volume entities had an impact on the spatial composition and regional environment [4-6].
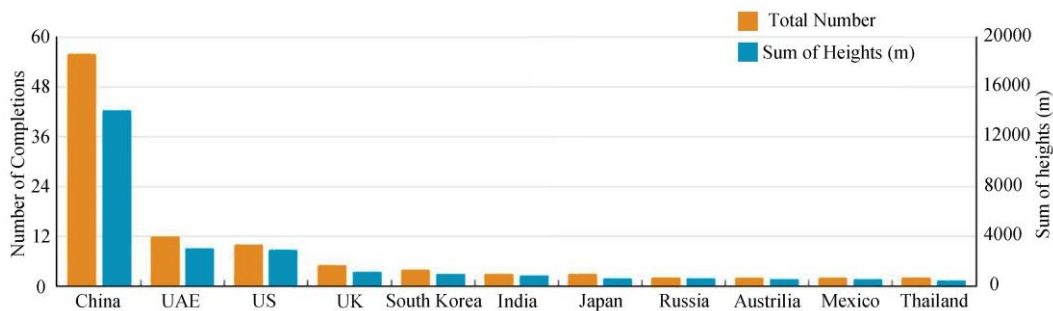
Fig. 1-2. Distribution of countries where high-rise buildings over 200m were completed in 2020

Source: CTBUH Prospective Industry Research Institute

With the increasing number of high-rise buildings, unreasonable planning and layout would also lead to the deterioration of urban environment. The distribution of high-rise buildings affected the urban environment mainly in the following aspects:

(1) The external surface of high-rise buildings and the thermal environment inside the building were susceptible to the sudden change of external climate, forcing people to use artificial air conditioning environment on a large scale, artificial air conditioning emissions a lot of heat to make hot streets more hot, further worsening the urban thermal environment;

(2) Due to the increasingly scarce land resources, the functional zoning of urban planning, the city concentrated the construction of high-rise buildings together, resulting in the excessive

density of high-rise buildings, which further aggravated the urban heat island effect;

(3) The improper location of some high-rise buildings in the city, resulting in poor airflow in a certain area of the city, and the heat island effect was formed.

Urban heat island effect, generally speaking, was the development of urbanization led to great changes in the underlying surface structure of the city, and led to concentrated energy consumption emission in the city, which made the temperature in the city higher than that in the outer suburbs [7]. In the meteorological isotherm map of the near-surface atmosphere, the temperature in the suburbs was low and had little change, while that in the urban area was obvious high. Since this island represented a hot urban area, it was vividly called the urban heat island, as shown in Fig. 1-3. The larger the difference between the city and the surrounding suburbs, the stronger the heat island effect of the city [8]. With the acceleration of urbanization, the volume and function of cities were constantly expanding, and the intensity of urban heat island was also gradually increasing. Which destroyed the sustainable development of environment, resources and population [9, 10], as shown in Fig. 1-4.
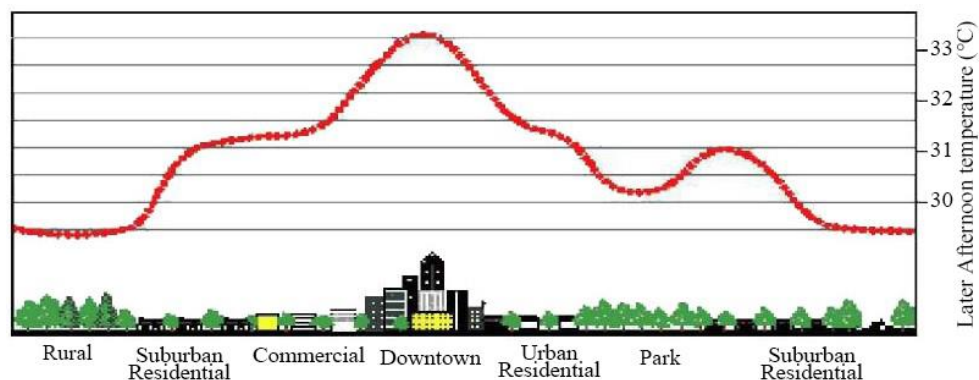
Fig. 1-3. Schematic diagram of urban heat island
Source: https://baike.baidu.com/

Fig. 1-4. Sustainable development of environment, resources and population
Source: https://baike.baidu.com/

Environmental and meteorological scientists developed the concept of urban thermal environment based on the study of urban heat island. Urban thermal environment referred to the physical environment closely related to people's physical health and productivity. The shape of the thermal environment in a city area was the result of the energy distribution and exchange of the environment, and was the comprehensive representation of all kinds of energy flow or exchange paths.

With the rapid development of the city, the scale of the city was getting bigger and bigger, and the city's thermal environment was getting worse [11, 12]. Good regional thermal environment which had appropriate wind speed and fresh air could make people feel comfortable. However, the continuous outward and upward development mode of the city enabled more and more high-rise buildings to be built in the central area of the city, and the population in the residential area became more dense, which created a large amount of living heat and the degradation of the regional thermal environment. When the density and number of high-rise buildings groups was large, the wind speed in this area would be smaller than that in other areas of the city, and there may be a windless area, which would reduce the air ventilation efficiency in this area, which would lead to high air temperature in this area, and further worsen the air pollution. In recent years, the quality of the thermal environment in cities had received a lot of attention. In particular, various countries have set some standards for the evaluation or control of the environment quality.

The thermal environment within the city was influenced by the big air environment within the city. Besides this, there were other factors related to the regional thermal environment. For example, the urban construction surfaces, which included city road, construction layout, materials used in construction and the property of buildings, etc.; The aspects of the environment included solar radiation, urban wind environment and human heat removal, etc.; The physical manifestation related to the urban thermal environment included the solar radiation intensity, air and gas mobility, long wave radiation between the ground and the building surfaces, heat transfer between air and gas, heat conduction, heat storage, etc [13-17], as shown in Fig. 1-5.

With the development of the city, the natural ground soil was replaced by artificial coatings, and the natural ground surfaces were changed into reflective surfaces [18]. Artificial construction coatings used had stronger thermal conductivity than the plant and soil in the suburbs, which could absorb and store more solar radiation [19]. Due to less water evaporation, the air among city was heated. Plants could shade the sun's radiation, clean air and increase air humidity, etc., which could improve the regional thermal environment. The heat generated by

human activity in urban development was huge. And at the same time, a large number of harmful air bodies and solid pollutants were discharged into the air of the city due to human generative activity, which changed the composition of the air among the city, and formed the city's regional air pollution. The high-rise buildings produced a complex influence on wind direction and wind speed [20]. The hard ground with high density buildings was more coarse than the others, thus lowering the wind speed in the city. The "city gorge" formed by the high-rise buildings and streets reduced the wind speed in the area and led to less heat dissipation in the surrounding spaces.
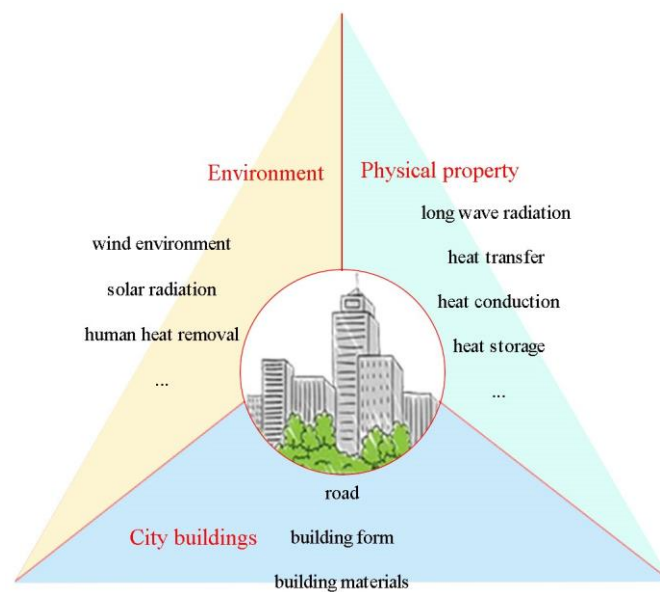
Fig. 1-5. Influencing factors of regional thermal environment
Source: By myself

Energy conservation and emission reduction was necessary to ease the energy crisis. The three main bodies of total social energy consumption were industrial energy consumption, transportation energy consumption and building energy consumption. Its energy consumption was characterized by large total amount and high degree of concentration, which was directly linked to economic production. As an energy consumption directly related to the degree of social urbanization, the proportion of building energy consumption in the total social energy consumption was also increasing.

In 2009, energy consumption in construction reached 717 million tons of standard coal, accounting for 23.39% of the total energy consumption in the whole society. From 2000 to 2009, the average annual growth rate of building energy consumption reached 10%. The United Nations Intergovernmental Panel on Climate Change (IPCC) pointed out in its Fourth Assessment Report (2007) that by 2030, the global construction sector could have an annual

emission reduction potential of 6 billion tons of CO_2-equivalent, the highest among all sectors, as shown in Fig. 1-6. Building energy conservation research is an important way to solve the global energy dilemma and achieve the CO_2 emission reduction target in the future. At present, China was in a critical period of accelerating industrialization, urbanization and new rural construction. In the face of the global impact of climate change, China, as a responsible major country, had been actively taking responsibility for reducing carbon emissions. At the World Climate Conference in Copenhagen in 2009, the Chinese government put forward the goal of "4045" energy conservation and emission reduction, that was, to reduce carbon dioxide emissions per unit of GDP by 40 to 45% from the 2005 by 2020, and formulated relevant domestic statistical, monitoring and assessment methods to implement it.
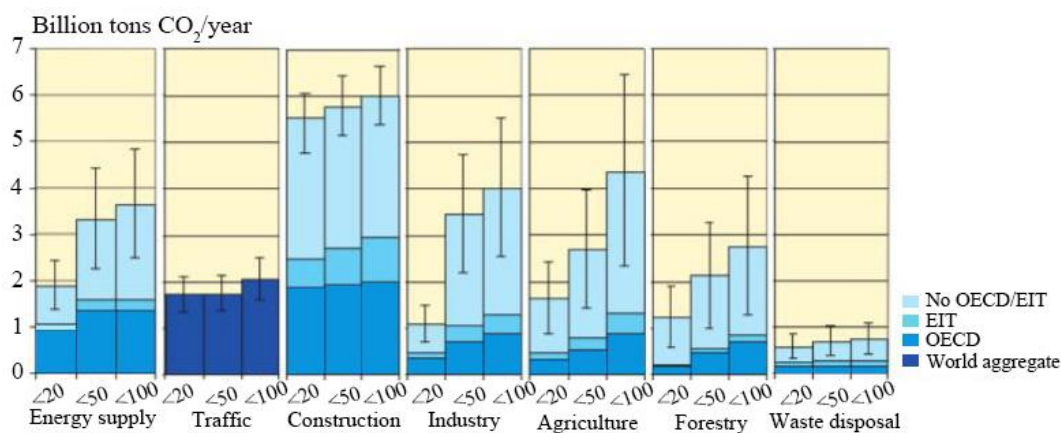
Fig. 1-6. Cost and potential prediction of carbon emission reduction by industry in 2030
Source: Framework Convention on Climate Change from United Nations

About the definition of building energy consumption, there were mainly two ways, one was the building terminal energy consumption, referred to the use of the internal energy consumption, including lighting, elevators, electrical appliances and air conditioning; one was building associated energy consumption, which referred to building materials production energy consumption and construction energy consumption.

Building energy conservation referred to the effective use of energy in the whole process of building use under the condition of ensuring and improving building comfort and quality of life, that was, reducing energy consumption and improving energy efficiency. The building energy mentioned here included the energy consumption of heating, air conditioning, hot water supply, lighting, elevators, cooking, household appliances and so on. Among them, heating, air conditioning and lighting energy consumption accounted for more than 70%. In summer, air conditioning energy consumption in some areas accounted for more than 50% of building energy consumption, as shown in Fig. 1-7.
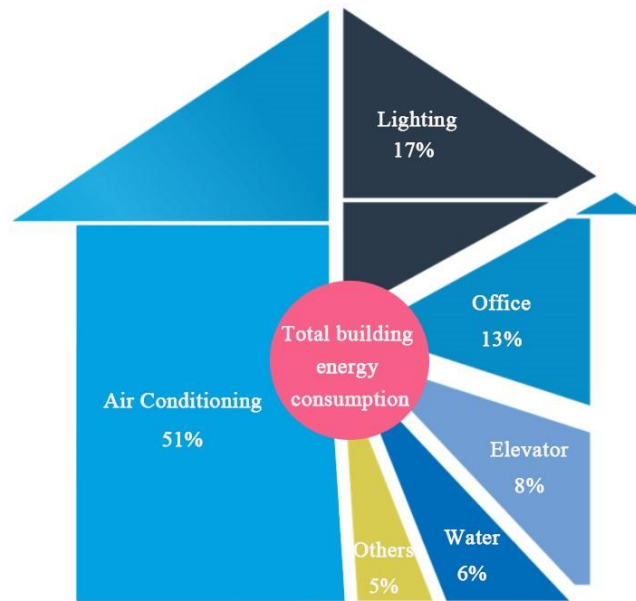
Fig. 1-7. Proportion of air conditioning energy consumption
Source: China HVAC and Refrigeration Association

With the increase of urban heat island intensity, the heating load of urban residential buildings decreased and the cooling load increased, and the decrease of annual average heating load was greater than the increase of annual average cooling load. Urban heat island effect had a very important influence on building energy consumption. Li et al. [21] believed that urban heat island effect could reduce heating energy consumption by 18.7% on average and increased cooling energy consumption by 19.0% on average. Sun et al. [22] pointed out that when heat island effect was ignored, the total amount of building energy used in cold climate zones dominated by heating was significantly overestimated, while the total amount of building energy used in hot climate zones dominated by cooling was underestimated.

At present, the building industry as a whole had the problems of high energy consumption, low efficiency, low thermal insulation performance of the peripheral protection structure, large power consumption of air conditioning in summer, and high energy consumption of heating in winter in the north. In recent years, the global temperature rose as a whole, especially in cities. As the main component of building energy consumption, air conditioning was growing at a rate of more than 10 million units every year, leading to the continuous growth of air conditioning load in summer, and the proportion of air conditioning energy consumption in building energy consumption also rose rapidly. When air conditioning was used intensively in summer, the air conditioning load in Beijing, Shanghai, Guangzhou and other first-tier cities accounted for about 40% of the city's peak load. Some scholars predicted that in China, with the rapid growth of the country's economy and the continuous improvement of people's living standards, the construction industry accounted for 35% of the total electricity consumption [23].

On the one hand, building energy were showing a rigid growth trend. At present, the proportion of building energy consumption in China was less than 30%. According to the experience of developed countries, with the acceleration of urbanization and the continuous improvement of people's living standards, the proportion of building energy consumption would reach 40%. On the other hand, the construction sector would bear an increasing burden of reducing emissions. With the continuous improvement of science technology and the acceleration of industrialization, the technical equipment level, production industrial level and energy utilization efficiency of the industry would be significantly improved. Both the energy consumption per unit output value and the energy consumption per unit product would show a downward trend, and the energy conservation and emission reduction potential of the industrial field would decline. The realization of China's energy conservation and emission reduction targets would inevitably rely more on building energy conservation. In addition, the current stage was a key opportunity to promote building energy conservation, China was carrying out a huge scale of urban and rural construction, the construction area was growing rapidly.

With the continuous acceleration of urbanization, the compact city model has been widely accepted by China's cities, and high-rise and high-density building groups have become the theme of urban development [24, 25]. The urban thermal environment problems represented by heat island effect become more and more obvious [26], and the regional thermal environment problems of high-rise and high-density buildings were particularly prominent, with local overheating, poor ventilation and other serious problems. In the deteriorating regional thermal environment, users' dependence on artificial energy increased, and air-conditioning energy consumption increased significantly in summer [27]. However, high air conditioning energy consumption would increase the heat load of building groups and worsen the regional thermal environment of building groups again [27], thus forming a vicious cycle of "regional thermal environment deterioration - air conditioning energy consumption intensification", as shown in Fig. 1-8.
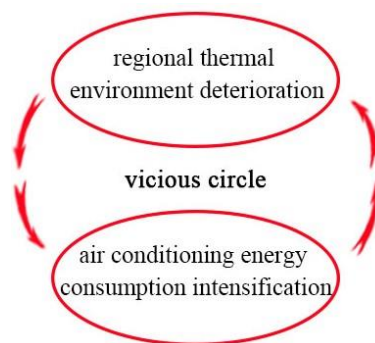
Fig. 1-8. Diagram of the vicious cycle

Therefore, it was very important to study the regional thermal environment and energy consumption of high-rise and high-density buildings. The regional thermal environment of high-rise and high-density buildings was influenced by many factors such as greening area, and water area, spatial combination of buildings.

For the green area, green space not only beautified urban landscape, but also converted solar radiation that would otherwise be converted into soil heat storage into latent heat by shielding solar radiation and transpiration and photosynthesis of leaves and wood bodies, thereby increasing urban air humidity and reducing surface temperature and air temperature above green space, thus alleviating the "heat island" phenomenon [28]. Theoretically, when the coverage rate of green vegetation increased by 10%, the measured maximum temperature was about 2.5% lower than the theoretical value (without considering the effect of greening on heat island effect), and the temperature difference at night was larger than that in the daytime. The coverage rate was inversely proportional to the heat island intensity, with the coverage rate ranging from 30% to 50%, the heat island effect was significantly improved to significantly weakened. When the vegetation coverage exceeded 3 square kilometers and its coverage rate exceeded 60%, the temperature difference between the urban center and the natural vegetation in the suburbs was not much, indicating that green vegetation could effectively improve the heat island effect. The low temperature area formed by the centralized green space vegetation in the city could divide the urban heat island and reduce the influence of the urban heat island [29]. At present, a large proportion of the construction of new high-rise buildings in Chinese cities was in the green belt on the edge of cities. Take Beijing for example, in 1958, the overall urban planning of Beijing determined that the area of its peripheral green belt was 314 square kilometers. With the development of urbanization, by 2000, the reserved suburban green exclusion zone has been reduced from 314 square kilometers to 150 square kilometers, and the decline trend continued. However, in the two periods from 1958 to 1983 and 1993, the city area increased from 600 to 700 square kilometers to 1040 square kilometers, the area of outer green isolation zone in Beijing gradually reduced and disappeared, and the function of improving the urban thermal environment was gradually disappearing.

According to the measured results, planting trees at appropriate locations around buildings could reduce indoor cooling load by 10-40%, indicating that greening had a certain effect on reducing environmental temperature [30]. Through the transpiration, water traveled from the root to the plant leaves, where it turned into water vapor and was released to the atmosphere [31]. Therefore, the green plants could regulate indoor relative humidity and air temperature [32]. Moreover, Mangone et al. [33] found that when plants were placed in the room, participants' thermal comfort increased by an average of approximately 12.0% and the thermal

comfort levels were increased by approximately 1.79 and 1.95 times in both experimental rooms respectively. Rodgers et al. [34] designed the plant wall as an integrated component of a home HVAC system and the overall air temperature would drop. Fernandez Canero et al. [35] built an active plant wall system and confirmed the cooling effect of plant walls, their results showed an average reduction in indoor air temperature could be 4∘C. Moreover, the shorter the distance from the plant wall, the higher the reduced air temperature and the cooling efficacy was better under the warm and dry environment [36]. Abdo et al. [37-39] designed the plant module and experimental set-up, and it was found that an increase in relative humidity was accompanied by a decrease in temperature in the range of 1-3∘C, when the planted substrate was in a saturated moist state, no matter in unplanted and planted the green plant [37, 39]. The green plant types had the certain influence on reducing the air temperature [38]. In a recent study, Meng et al. [40] combined a living wall with air conditioning and showed a significant improvement in thermal comfort in room and its relative humidity was reduced by 2.6%, and the volunteers' average temperature was closer to the neutral skin temperature, compared to the referred room, which indicated the subjective evaluation was improved on indoor thermal environment by the volunteers participating in the experiment. Smith et al. [41] studied the effect of office plants on the indoor environment and found that the relative humidity in the rooms increased after plants were introduced indoors. Lohr et al. [42] did an experiment to explore the effect of indoor plants on particulate matter accumulation, and it was found that the relative humidity was higher in the presence of plants than in their absence. In the study of Rodgers et al. [34], indoor average relative humidity was increased by approximately 7% in the presence of plants and classrooms with the green plants had the greater relative humidity and higher comfort levels, which was important for indoor thermal environment in winter.

Therefore, increasing green area was an effective way to improve urban heat island effect and outdoor thermal environment. At the same time, increasing urban greening could also improve urban landscape. At present, the purpose of greening was to achieve visual landscape effects. In urban construction, the net green area of local plots was more than 15% [43]. However, in order to achieve a certain ecological effect of the vegetation in the development plot, the area needed to reach a certain number, and it also needed a combination of multiple types of plants. Otherwise, the expected effect could not be achieved.

For the water area, water was the basic material conditions for the survival and development of cities. The heat capacity of water body was much higher than that of land, and it had a strong heat storage capacity, so the rise and fall of water body was much more moderate than that of land [44]. There were two kinds of convection heat transfer and latent heat transfer between water and air. The surface layer of water received the long-wave radiation from the sun and the

sky. Owing to the specific heat of water was larger than that of air, water needed to absorb more heat of vaporization in the evaporation process, which could significantly reduce the temperature near the ground [45]. Even if water absorbed a lot of heat from the air, the temperature of the surface layer could still be lower than that of the air, which played a certain role in regulating the local microclimate.

Ranhao et al. studied the relationship between water body and UHI intensity and found UHI efficiency of city was positive with built-up proportion and negative with water body and landscape shape index [46]. Murakawa et al. observed that the air temperature could decrease more than 5°C around a river in warmer season and this effect could also be amplified via wind [47]. In summer, this cooling function improved apparently human thermal comfort feeling in waterfront area. In addition, this effect would be magnified in maximum in areas within 10-20m of rivers [48]. Katayama et al. [49] have documented a 1-3°C difference in air temperature between the river and the city during the warmer season in Japan. Similarly, observations made by Hathway and Sharples [50] have demonstrated the cooling effect of a small river in the Sheffield, United Kingdom, with an average temperature difference of nearly 1°C during hot weather conditions. In Fukuoka, Japan, Ishii et al. [51] found that a large pond had a 3°C cooling effect that extended up to 400 m from the pond. Furthermore, because of limited space in cities, even small bodies of water could have a horizontal cooling effect. Chen et al. [52] have found an average air temperature reduction of 1.3 °C near a small lake in Guangzhou, China. Likewise, in the tropical climate of Singapore, Jusuf et al. [53] have observed that bodies of water with added water walls were able to reduce the air temperature by up to 1.8 °C on a typical hot day. A study by Robitu et al. [54] also shown that a 4 m^2 pond was able to reduce the surrounding air temperature.

Since water bodies could improve the thermal environment, purify and reduce air pollution, it was necessary to actively and reasonably preserve and protect water bodies in the future urban development and construction, and increase efforts to dredging water systems and rivers, cleaning up lakes, etc., so as to ensure the cleanliness and fluidity of water quality in water bodies. In the thermal environment of a city, the reasonable layout and use of water could improve the local micro-environment, so that various types of water in the city, such as lakes, pools, fountains, streams would be able to effectively regulate the city's temperature, and alleviate the heat island effect [55].

For the building forms, there were three types of building forms: single building, building group and cluster building [56]. The architectural complex composed of multiple building monomers was the building group, and the basic unit in the community was the building

monomer. The form, location and direction of monomer buildings and the spatial pattern of building groups determined the thermal environment of the community [57]. There were two types of monomer forms - tower and slab. Compared with slab building, tower building had smaller wind area on four sides and less blocking effect of air flow, which was conducive to the air flow in the community. When the long side of a slab building faced the wind direction, it had a great obstruction effect on the air flow and was easy to form a large "wind shadow area" in the downwind area on its back. Therefore, the negative impact of slab building on the wind environment of the community was relatively large. However, the "wind shadow area" at the downwind of the back of the high-rise building was about 6 times the height of the high-rise building [59]. Therefore, the height of the building and the windward direction of the long side of the building would have a certain impact on the wind and thermal environment of the regional space where the building was located [60].

Among them, the specialized urban design could promote the urban heat island reduction efficiently, but it was too complex to yet a practical approach [61-63]. Increasing the green infrastructure could reduce the amount of infrared radiation and lower the urban surface temperature effectively [64-67], but this technology often needed to provide some land and irrigation water for plants [68]. Moreover, due to the high density of cities, land resources were increasingly scarce, and the available area of green space was limited, and it was difficult to apply in the built urban areas with the higher heat island intensity. In addition, several studies had shown that planted roofs have little effect on outdoor air temperature [69].

However, solar radiation heat was the main energy source of buildings [70]. The energy of sunlight radiated to the surface of the earth about $750w/m^2$ per second. The huge energy provided essential conditions for people's survival and living. While the sunlight brings great energy to people, the strong sunlight that shined on the surface of objects on the earth for a long time would make the surface temperature too high, causing many problems to people's daily life and industrial production [71, 72].

The sun was a natural heat source in the natural environment [73], and the environment's reception of solar radiation determined the thermal characteristics of the environment. Its principle was the heat exchange between the atmosphere and the surface of the earth in the natural environment. Sunlight passed through the atmosphere and was absorbed and reflected by the ground in the form of direct radiation and scattering light. The ground absorbed the short-wave radiation and the temperature rises. The heat energy radiated outward in the form of long wave, which raised the temperature of the atmosphere. As a large part of the long-wave radiation was absorbed by the lower layer of the atmosphere and the surface of the earth, there

was a continuous heat exchange between the atmosphere and the surface in the form of radiation and convection, so that the greenhouse effect was formed. The artificial thermal comfort environment created by human beings was to defend against and adapted to the impact of climate change on human beings [74, 75].

As shown in Fig. 1-9, tall buildings could intercept more solar radiation, and the intercepted solar radiation was reflected and absorbed many times between high-density buildings, so the comprehensive absorption rate of solar radiation was higher. The heat generated by solar radiation caused the building surface temperature to rise, and the heat was transmitted to the room through the envelope, increasing the building cooling load. Therefore, solar radiation was one of the main reasons for building air conditioning energy consumption. It was one of the effective ways to alleviate the harsh thermal environment to solve the high solar radiation heat problem of high-rise and high-density buildings.
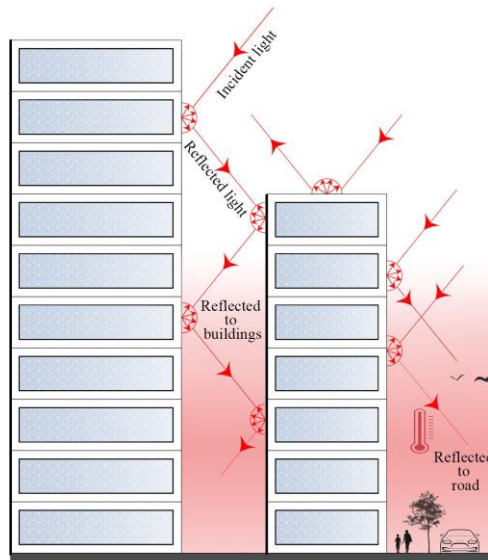
Fig. 1-9. Schematic diagram of ideal solar radiation path for high-rise and high-density buildings

At present, increasing the solar radiation reflectance of building surface was an effective way to reduce the solar radiation heat of building, and high reflective coatings with high solar radiation reflectance were born [76]. Reflective coatings had attracted much attention due to they could effectively reflect solar radiation in summer, and maintain a low building surface temperature, and reduce the heat transfer of building [77-79].

By selecting appropriate resin oxides and production technology, the coating with high reflectivity could be made to reflect sunlight and reduce the surface temperature of objects [80]. At first, this kind of coating was to meet the needs of aerospace and military. Later, because it

could effectively prevent heat conduction to the internal space and improve the thermal and humid environment, it had been applied to the external walls of buildings and other fields. Zingre et al. [81] assessed the effect of cool roof on the thermal behavior of a residential buildings, and found the maximum indoor free-floating temperature reductions were between 2°C~7.5°C. Pereza et al. [82] found that the heat gain of buildings with a high-reflective roof was 9% less than that of the buildings with an ordinary roof. Mohamed et al. [83] found that compared to typical roofs, HR-roofs were capable of reducing cooling loads by about 45%. Baneshi et al. [84] found compared with typical coatings, the building with optimized coatings could reduce the cooling load by 4-31%. Kadri et al. [85] studied the indoor temperature and energy consumption of a double skin roof coupled with thermo-reflective paint and found the indoor operative temperature was reduced by 5°C, and the cooling loads was reduced by 572 kWh. Bansal et al. [86] used two wood enclosures, one painted black and the other painted white to measure the inside air temperature. During hours with maximum solar radiation in New Delhi, India, the black enclosure recorded 7∘C higher air temperature than the white enclosure. In the research carried out by Cheng et al. [87] in the hot humid climate of Hong Kong, the maximum air temperature inside the black test cell was higher by about 6 or 12∘C than the white one depending on the thermal mass. Winandy and Beaumont [88] performed experiments using five outdoor chambers during a three year period in Madison, US. The chamber covered with black shingles was 5∘C–8∘C warmer than the white shingled chamber. Nahar et al. [89] developed a series of experiments, but now they considered passive cooling techniques for concrete roofs. The cell that incorporated pieces of white glazed tiles on the roof reduced the air temperature by 11∘C. The cell painted with white cement on the roof reduced the temperature 5.4∘C. Similarly, Hamdan et al. [90] demonstrated that white glazed tiles were more effective than white cement for cooling the environment inside test cells with concrete roofs in Amman, Jordan. Suman and Verma [91] examined a reflective coating on different types of roofs using experimental rooms in Roorkee, India. In the rooms with asbestos and galvanized roof, the air temperature difference was about 1.5∘C between the room with reflective roof and the reference room. Meanwhile, the reflective coating on a reinforced concrete roof led to a reduction of 2.8∘C indoor air temperature. In another study of test cells, Yu et al. [92] evaluated the influence of different coatings on the walls of two masonry models located at Xi'an Jiaotong University, when the reflectance of the walls increased, the maximum decrease of the indoor air temperature was 4.67∘C with an average diurnal temperature decrease of 3.53∘C.

However, HR-coatings reflected solar radiation by diffuse reflection, and the reflected solar radiation would be received by nearby buildings or streets. It could be seen that HR-coatings

only transfered the heat radiated by the target building to adjacent buildings. Therefore, HR-coatings had a significant energy-saving effect on a single building, while had a low potential for improving the thermal environment of the whole building group. It even further worsened the regional thermal environment [93].

Based on this, this project proposed the RR-coatings, a new coatings with the ability to reflect solar thermal radiation out along the original direction. Fig. 1-10 showed the schematic diagram of the retro-reflection optical properties of the most common RR-coatings. For the glass bead RR-coatings, the incident sunlight was reflected along the incident direction through two refractions on the glass microsphere boundary and one reflection by using the highly-reflective coating. For the prism RR-coatings, the incident sunlight was reflected through two refractions on the prism boundary and multiple reflections on the reflective layer [94].
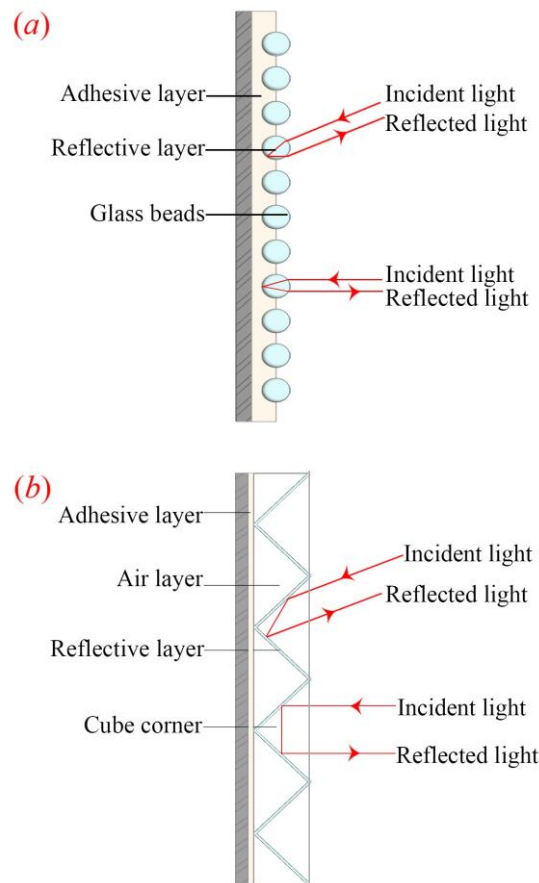
Fig. 1-10. The schematic diagram of the retro-reflection optical properties of the RR-coatings (a) glass bead RR-coatings and (b) prism RR-coatings

Fig. 1-11 showed the effect diagram of the impact of HR-coatings and RR-coatings on the regional thermal environment of the building groups. It could be seen that compared with the HR-coatings, the RR-coatings had better improvement on both the target building and its

surrounding thermal environment.
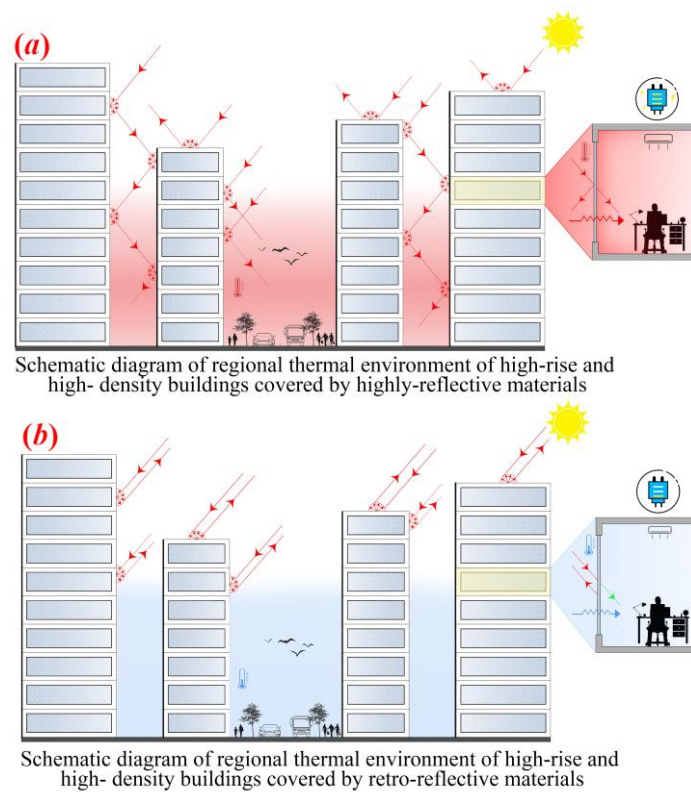
Fig. 1-11. The effect diagram of the impact of RR-coatings and HR-coatings on the regional thermal environment of the building groups

The problems of regional thermal environment in high-rise and high-density building groups had been exposed, and the rapid urbanization development of the country was still raging, some adverse effects like regional thermal environment deterioration and energy consumption increase would be more significant. RR-coatings showed a large potential in reducing the solar radiation, regulating the regional thermal environment and reducing the building energy consumption.

1.2 Research status

For the the research object and its applications in buildings, scholars at home and abroad have made some explorations, but it is still in the preliminary stage. Related research has focused on three aspects.

First, the optical properties of RR-coatings, including global reflectance and retro-reflectance. Yuan J.H. et al. [95] from Osaka City University tested the reflectance of RR-coatings by using the heat balance method. Sakai H. et al. [96] analyzed the influence of different optical structures on the optical properties of RR-coatings, and showed that the prism RR-coatings

have the highest reflectivity. Rossi F. et al. [97] tested the reflection characteristics of five kinds RR-coatings and found that there was an obvious diffusion phenomenon along the retro-reflection path. Morini E. et al. [98] studied the effect of coatings aging on the optical properties of RR-coatings and believed that the reflection characteristics of RR-coatings were less affected by aging. It was not difficult to find from the above research that the reflection characteristics testing technology of RR-coatings was basically mature, but the reflection characteristics optimization of RR-coatings was in the embryonic stage. When the incidence angle of solar radiation was large, the problem of the large attenuation of retro-reflection characteristics of RR-coatings has not been reasonably solved. At noon and afternoon in hot summer, the outdoor thermal environment was the most severe, at this time, the solar radiation incidence angle on the building wall was large, and the retro-reflection characteristics of the RR-coatings were difficult to play. This mismatch seriously restricted the application prospect of the RR-coatings in the construction field.

Secondly, the influence of RR-coatings on the regional thermal environment. Yuan J.H. et al. [99] used a two-dimensional model to analyze the influence of RR-coatings on the thermal environment of blocks, indicating that RR-coatings could increase the urban albedo and reduce the proportion of solar radiation absorbed by the city canyon. Rossi F. et al [100] established a model of urban canyons and found that compared with conventional HR-coatings, RR-coatings had a better effect on mitigating local heat. Morini E. et al. [101] found that the RR-coatings decreased five percent of urban canyons radiate heat. Qin Y.H. et al. [102] established two small-size building models, which were respectively covered by HR-coatings and RR-coatings, the results showed that the temperature around the model with HR-coatings was obviously higher. It could be seen from the above studies that, no matter in breadth or depth, the limitations of the research on the impact of RR-coatings on urban and regional thermal environment were very obvious. The use characteristics of RR-coatings on the exterior surface of buildings and the influence of the spatial form of buildings on the application effect of RR-coatings have not been involved.

Thirdly, the influence of RR-coatings on building energy consumption. Meng X. et al. [103] studied the air conditioning energy consumption was reduced by 20% to 25% under the condition of the maximum solar radiation intensity was $800W/m^2$. Yuan J.H. et al. [104] found that the RR-coatings could reduce the heating load by 15%, but increase cooling load by 5% through simulation with the meteorological conditions in Shanghai. The above literature only took single buildings as the research object, and it only showed the thermal reflection characteristics of RR-coatings, but did not show the retro-reflection characteristics. The actual effect evaluation of RR-coatings was very one-sided.

In conclusion, as a new type of reflection coatings, the optimization of reflection characteristics and the practical application experience in construction engineering were in the initial stage. There was no mature theoretical research and reference method for some problems, such as the optimization of RR-coatings, the influence mechanism of coatings reflection characteristics on building thermal environment and energy consumption.

1.3 Research purpose and significance

1.3.1 Research purpose

Based on a deep understanding of the formation mechanism of the thermal environment of high-rise and high-density buildings, the influence of RR-coatings on the regional thermal environment was proposed to alleviate the problem including deteriorated outdoor thermal environment. On the one hand, the optical properties of RR-coatings were studied, including global reflectance and retro-reflectance. On the other hand, through comparative experiments, the influence of RR-coatings and HR-coatings on the building thermal environment were studied by monitoring the variation of regional albedos, wall temperatures and air temperatures, which were mainly focused on the summer benefit and winter penalty of RR-coatings, and the effect of building forms on the thermal contribution of coatings. Finally, the effect of wall reflectivities on energy load of an enclosed educational building in Qingdao was simulated based on the software of Energyplus, and the optimum retro-reflectivity was converted.

1.3.2 Research significance

The research in the field of building energy conservation has important strategic and practical significance no matter from the macro national level, or from the micro regional level. As one of the three energy consumption industries, the energy consumption and carbon dioxide emission of construction industry have not been given due attention. Especially because of the lack of statistical information about building energy consumption, the whole country was unclear about the situation of energy consumption, to a great extent, hindering the development of building energy-saving work. To realize the low energy consumption, low emission in the whole life cycle of the building, was the internal requirement of achieving the goal of energy saving and emission reduction, and walking the road of modern sustainable development. From the regional level, with the gradual deepening of urbanization construction, the increase of total construction will become an inevitable trend. According to the development experience of developed countries, the increase of urbanization rate would further increase the proportion of building energy consumption in the final energy consumption of the whole society. At the same time, the improvement of living standards also led to the improvement of people's requirements

for the comfort of buildings, which meant that the energy consumption demand and carbon emissions in the construction sector will continue to intensify. Through the analysis of the potential of building energy saving in our country, we could make a scientific planning of each channel and tasks of building energy saving and formulated reasonable policy tools, which would help reduce building energy saving cost, realize energy saving emission reduction effectively.

First of all, based on the actual problems of the deteriorating thermal environment and high building energy consumption of high-rise and high-density buildings in the urbanization development, the thermal environment of buildings would be improved based on people and local conditions, and fundamentally the quality of life of urban residents would be improved. Secondly, the RR-coatings had unique reflection characteristics, which could reduce the building surface temperature and alleviate the urban heat island phenomenon. However, since the research on the RR-coatings as the building exterior surface coatings was a new content after the solar thermal reflection coating, the research started late and received less attention. The research content was refined into the application of the RR-coatings in the field of buildings. Therefore, the application research of RR-coatings had important economic, environmental and social benefits.

1.4 Research structure

1.4.1 Research content

Theoretically, due to its retro-reflection property, the RR-coatings could reduce the total amount of absorbed solar radiation and inhibit the temperature rise, thus weakening the heating ability of the surrounding air and inhibiting the temperature rise of the block, and thus the thermal environment would be improved.

Given that the application potential of RR-coatings in improving thermal environment and urban heat island effect, in this paper, the RR-coatings were applied in the building exterior surface, and studied the application potential through a series of experiment and simulation. The main research contents involved in this topic were as follows:

(1) The solar reflectance of the RR-coatings under the full spectrum and the retro-reflectance under different incidence angles were studied. The latter was of great significance for explaining the influence of the RR-coatings on the thermal environment of buildings.

(2) The influence of RR-coatings on the thermal environment of buildings were studied. Two groups of scaled building complex models covered by HR-coatings and RR-coatings were established, the change of albedos, the wall temperatures and the central air temperatures were

analyzed. And the effect of building forms on the application benefit of RR-coatings were analyzed, three typical forms of high-density buildings were proposed, namely the Determinant Form (D-Form), Three-Sided Enclosed Form (TSE-Form) and Four-Sided Enclosed Form (FSE-form).

(3) To know about the climate adaptability HR-coatings and RR-coatings was important for the building engineering applications. For a more comprehensive assessment of thermal contribution of HR-coatings and RR-coatings, the coatings were applied on two small-scale models of high-density enclosed building groups, and monitored the regional albedos, wall temperatures and air temperatures in both summer and winter.

(4) To research the effect of building surface retro-reflectivities on the energy load of an enclosed educational building, based on the results of a previously published paper on the air temperature difference resulted by covering RR-coatings, the daily, monthly and yearly energy load of an actual three-sided enclosed educational building in Qingdao, China were simulated based on the software of Energyplus, and CO_2 emissions were also calculated.

1.4.2 Research flow

Fig. 1-12. Chapter names and basic structure

Chapter One
Background and Purpose of the Study
1.1 Research source and background
1.2 Research status
1.3 Research purpose and significance
1.4 Research structure

Chapter Two
Literature Review of the application of retro-reflective coatings in buildings
2.1 Introduction
2.2 Review methods and synthesis of evidence
2.3 Retro-reflective coatings and their optical property
2.4 Measurement methods of solar reflectivity and retro-reflectivity
2.5 Application efficiency of retro-reflective coatings
2.6. Conclusion and outlook

Chapter Three
Methodology and performance evaluation index
3.1 Optical performance experiment
3.2 Thermal performance experiment
3.3 Building energy load simulation
3.4 Summary

Chapter Four
Study on spectral properties of retro-reflective coatings
4.1 Introduction
4.2 Optical property of RR-Coatings
4.3 Thermal effect of optical structure
4.4 Conclusion

Core Chapters

Chapter Five
An experimental comparison on regional thermal environment of the high-density enclosed building groups with retro-reflective and high-reflective coatings
5.1 Introduction
5.2 Description of the comparative experiment
5.3 Experiment results and discussion
5.4 Conclusion

Chapter Six
Influence of the building enclosed forms on thermal contribution of retro-reflective and high-reflective coatings
6.1 Introduction
6.2 Description of the comparative experiment
6.3 Experiment results
6.4 Discussion
6.5 Conclusion

Chapter Seven
An experimental evaluation on thermal contribution of retro-reflective and high-reflective coatings in an enclosed building in summer and winter
7.1 Introduction
7.2 Experiment platform and point latout
7.3 Experiment results and discussion
7.4 Conclusion

Chapter Eight
The effect of building surface retro-reflectivity on energy load and CO_2 emission of an enclosed educational building
8.1 Introduction
8.2 Description of the simulation
8.3 Result and discussion
8.4 Conclusion

Chapter Nine
Conclusion and prospect
9.1 Conclusion
9.2 Prospect

Fig. 1-13. Introduction of chapters

The chapter names and basic structure of this paper were shown in Fig. 1-12, and the introduction of chapters was shown in Fig. 1-13. The main contents included the following:

In Chapter 1, Background and Purpose of the Study:

With the acceleration of urbanization, the population gathered from rural areas to cities, and the number of high-rise buildings in cities increased, leading to the deterioration of regional thermal environment and the increase of building energy consumption. There was a vicious cycle between the two, which was not conducive to sustainable development. So far, there have been a lot of green technologies, including increasing green plants, water area, changing building layout, etc., but these strategies were not applied to high-rise and high-density buildings. Considering that solar radiation was the main source of building heat gain, high reflective materials and retro-reflective coatings were proposed. The research status of these materials was introduced in detail. It was pointed out that due to their special optical properties, the application potential of retro-reflective coatings in architecture was great. The purpose and significance of this paper were introduced. Finally, the chapter structure of the article was explained.

In Chapter 2, Literature review of the application of RR-coatings in buildings:

High-rise and high-density buildings were increasing with the rapid urban development, which led to many urban thermal environment problems represented by the urban heat island. The traditional HR-coatings could reduce the solar radiation gain of buildings to alleviate urban heat island by the diffuse reflection, but the reflected solar radiation would be absorbed by the surrounding urban surfaces and thereby, the urban heat gain would not be reduced or even increased due the multiple absorption of thermal radiation in building groups. To overcome the inherent defect of HR-coatings, RR-coatings were proposed to reflect solar radiation along the incident radiation and had gradually attracted much attention due to their unique reflection characteristics. However, the review on RR-coatings had not been published to summarize the development status and potential deficiencies of RR-coatings. This review focused on the development, performance measurement of RR-coatings, while the application efficiency of RR-coatings was described on urban thermal environment and building energy consumption comprehensively. Finally, future directions were proposed on possible studies and applications.

In Chapter 3, Methodology and performance evaluation index:

The main purpose of this chapter was to introduce the basic experimental system, simulation system and evaluation index of the impact of RR-coatings on the thermal environment and energy load of regional buildings, which laid the foundation for the analysis of related research in the following chapters. Firstly, the optical property measuring instruments were developed to measure the solar reflectance and angle distribution of two typical RR-coatings. Secondly, a number of experimental plans were developed, and the basic experimental models were established, and the performance evaluation indicators were determines, which included

regional albedo, wall temperature and air temperature, and based on the experimental data obtained, the thermal performance of RR-coatings was analyzed. Finally, based on the software of Energyplus, the impact of RR-coating on the thermal environment of buildings was preliminarily determined and the effect of wall reflectivities on energy load of an enclosed educational building in Qingdao was simulated, and the evaluation index included daily, monthly and yearly energy load.

In Chapter 4, Experimental study on spectral properties of retro-reflective coatings:

RR-coatings received much attention due to it could reflect the solar radiation along the incident direction, which was different with the traditional HR-coatings with the property of diffuse reflection. For the purpose of optical properties optimization and building application improvement, the spectral characteristics of glass bead RR-coatings and prism RR-coatings were measured. The integrating sphere was used to measure the global reflectivity, and a self-developed instrument was used to measure the angular distribution at different incident angles. The result showed that the global- reflectivity of glass bead RR-coatings and prism RR-coatings were 64.74% and 51.44%, respectively. However, the retro-reflectivity of prism RR-coatings was higher than glass bead RR-coatings at the smaller incident angles with the values of 25.22% and 21.67%, respectively (at 10∘ and 30∘ of incidence). For larger incidence angles including 50∘and 70∘, two RR-coatings mainly showed specular-reflection property.

In Chapter 5, An experimental comparison on regional thermal environment of the high-density enclosed building groups with retro-reflective and high-reflective coatings:

HR-coatings were used to reduce the building heat gain and thereby, alleviate urban heat island, but the solar radiation reflected by HR-coatings would be absorbed by the surrounding urban surfaces and urban thermal gain will not be reduced or even increase. To overcome this inherent optical defect of HR-coatings, RR-coatings were proposed to reflect solar radiation along the incident direction with the potential to improve the urban thermal environment. To compare their improvement efficiency of thermal performance, two small-scale high-density enclosed building group models were built and covered by RR-coatings and HR-coatings, respectively. The urban albedo, wall surface temperature and air temperature were contrastively analyzed in two models. Experimental results showed compared with HR-coating model, RR-coating model had better cooling potential, and its regional albedo was increased by 5.53%. And air temperature in enclosed space of RR-coating model was 2.24℃ lower than that of HR-coating model, but they were higher than outdoor natural air temperature. Moreover, compared to HR-coatings, covering RR-coatings could reduce the peak and average wall temperature by 2.47℃~15.25℃ & 0.30℃~3.82℃ in the daytime and 1.35℃~7.91℃% & 0.25℃~4.38℃ in

the nighttime, and its application in the roof and east wall had the high efficiency.

In Chapter 6, Influence of the building enclosed forms on thermal contribution of retro-reflective and high-reflective coatings:

There were more high-density urban spaces and their forms prominently affected the regional thermal environment, especially for the spatial distribution of solar thermal radiation. Under this condition, the contribution efficiency of reflective coatings should be reevaluated to improve the regional thermal environment. Three typical forms of high-density buildings, namely the Determinant Form (D-Form), Three-Sided Enclosed Form (TSE-Form) and Four-Sided Enclosed Form (FSE-Form), were proposed. HR-coatings and RR-coatings were employed with the different reflective mechanisms, while the albedo, wall temperature, and air temperature were monitored. Experimental results showed that the higher the enclosed degree of buildings covered by HR-coatings, the poorer the regional thermal environment and the higher the heat island efficiency. However, the opposite was true for enclosed buildings with RR-coatings. RR-coatings had a better thermal contribution than HR-coatings, and the higher the enclosure degree of buildings, the higher the improvement efficiency of RR-coatings. Compared with HR-coatings, RR-coatings increased the maximum and average regional albedos by 0.67%~3.42% and 1.36%~5.59%, respectively, and lowered the maximum and average temperatures by 0.26°C~7.05°C and 0.02°C~4.83°C for model walls and 0.59°C~4.41°C and 1.80°C~3.06°C for outdoor air, respectively.

In Chapter 7, An experimental evaluation on thermal contribution of retro-reflective and high-reflective coatings in an enclosed building in summer and winter:

The solar radiation was one of the main factors affecting the thermal environment of regional buildings, and reflective coatings could increase the solar reflectance of the building surface and reduce the solar heat gain. In summer, it could effectively improve the regional thermal environment, but in winter, it might be ineffective, or even counterproductive. This study aimed to experimentally evaluate the thermal contribution of RR-coatings and HR-coatings with the different reflective mechanisms in an enclosed building in both summer and winter. And the regional albedos, wall temperatures, and air temperatures were measured. Experimental results showed that both in summer and winter, compared with HR-coatings, RR-coatings had higher regional albedos, lower wall temperatures and air temperatures, however, the differences were smaller in winter, which would lead to more thermal benefits in summer caused by RR-coatings than thermal penalties in winter. For the regional albedos, the maximum differences in summer and winter were 4.99% and 2.46%, and the values were 2.74°C~11.61°C and 1.39°C~5.61°C for the wall temperatures, 2.10°C and 0.39°C for the air temperatures.

In Chapter 8, The effect of building surface retro-reflectivity on energy load and CO_2 emission of an enclosed building:

The building surface reflectivity determines the amount of reflected solar radiation, which indirectly affects the cooling and heating load of the building. Therefore, building surface retro-reflectivity is important on the energy load and CO_2 emissions of buildings. The effect of surface retro-reflectivity on daily, monthly and yearly energy load were simulated based on the Energyplus software, and CO_2 emissions was also caluculated. The numerical results showed for daily energy load in four typical seasons, there was a positive correlation between the daily energy load and building surface reflectivities in January, April and October, and a negative correlation in July. For monthly energy load, the building cooling and heating load were the most in January and August, respectively. For annual energy load, the higher the reflectivity, the lower the cooling load and the higher the heating load. When the building surface reflectivity was 0.7, the annual energy load were the least, with the value of 148.23 $\mathrm{kWh/m^2}$. In addition, the CO_2 emissions was also the lowest, with the value of 24.79 $\mathrm{kg/m^2}$. According to the relation between solar reflectivities and retro-reflectivities of prism RR-coatings mentioned in the published articles, When the building surface retro-reflectivity was 0.47, the total annual energy load and CO_2 emissions were the least.

In Chapter 9, Conclusion and Prospect:

The main research conclusions were summarized, and the content of the future research was expounded.

References

[1] T. Saroglou, I.A. Meir, T. Theodosiou, B. Givoni. Towards energy efficient skyscrapers. Energy and Buildings 149 (2017) 437-449.

[2] L. Leung, S.D. Ray. New York city energy benchmarking data paper type: low-energy tall buildings? Room for improvement as demonstrated by New York city energy benchmarking data. Int. J. High-Rise Build. 2 (2013) 285-291.

[3] H.M. Sachs. Opportunities for Elevator Energy Efficiency Improvements, American Council for an Energy-Efficient Economy, Washington, 2005, pp. 11.

[4] P. Simmonds. ASHRAE Design Guide for Tall, Supertall, and Megatall Building Systems, American Society of Heating, Refrigerating and Air Conditioning Engineers, Atlanta, GA, 2015.

[5] C.K. Cheung, R.J. Fuller, M.B. Luther. Energy-efficient envelope design for high-rise apartments. Energy Build. 37 (2005) 37-48.

[6] F. Yik. Cooling energy evaluation for high-rise residential buildings in Hong Kong, Energy Build. 37 (2005) 345-351.

[7] W. Zhang, Y.Q. Li, C.G. Zheng, Y.B. Zhu. Surface urban heat island effect and its driving factors for all the cities in China: Based on a new batch processing method. Ecological Indicators 146 (2023) 109818.

[8] F. Pan, J.Z. Pei, G.W. Zhang, Y. Wen, J.P. Zhang, R. Li. Building the cooling roads with high thermal conductivity pavements to relieve urban heat island effect. Construction and Building Materials 346 (2022) 128276.

[9] R.R. Liu, X.B. Dong, X.C. Wang, P. Zhang, M.X. Liu, Y. Zhang. Relationship and driving factors between urbanization and natural ecosystem health in China. Ecological Indicators 147 (2023) 109972.

[10] Y. Xiao, H. Huang, X.M. Qian, L.Y. Zhang, B.W. An. Can new-type urbanization reduce urban building carbon emissions? New evidence from China. Sustainable Cities and Society 90 (2023) 104410.

[11] J.Y. Ren, J. Yang, F. Wu, W. Sun, X.M. Xiao, J.H. Xia. Regional thermal environment changes: Integration of satellite data and land use/land cover. Iscience 26 (2023) 105820.

[12] Z.W. Yu, Y.W. Yao, G.Y. Yang, X.G. Wang, H. Vejre. Strong contribution of rapid urbanization and urban agglomeration development to regional thermal environment dynamics and evolution. Forest Ecology and Management 15 (2019) 214-225.

[13] Z. Jandaghian, H. Akbari. Increasing urban albedo to reduce heat-related mortality in Toronto and Montreal, Canada. Energy Build. 237 (2021) 110697

[14] A.T. Hayes, Z. Jandaghian, M.A. Lacasse, A. Gaur, H. Lu, A. Laouadi, H. Ge, L. Wang. Nature-based solutions (NBSs) to mitigate urban heat island (UHI) effects in Canadian cities. Buildings 12 (7) (2022).

[15] T. Hong, Y. Xu, K. Sun, W. Zhang, X. Luo, B. Hooper. Urban microclimate and its impact on building performance: a case study of San Francisco. Urban Clim. 38 (2021) 100871.

[16] S. Manavvi, E. Rajasekar. Environment, Evaluating outdoor thermal comfort in "Haats"–The open air markets in a humid subtropical region. Build. Environ. 190 (2021) 107527.

[17] B. Liu, Z. Lian, R.D. Brown. Effect of landscape microclimates on thermal comfort and physiological wellbeing. Sustainability 11 (19) (2019) 5387.

[18] H.Q. Xu, T.T. Shi, M.Y. Wang, C.Y. Fang, Z.L. Lin. Predicting effect of forthcoming population growth–induced impervious surface increase on regional thermal environment: Xiong'an New Area, North China. Building and Environment 136 (2018) 98-106.

[19] O. Bucklin, A. Menges, F.L. Amtsberg, H. Drexler, A. Rohr, O.D. Krieg. Mono-material wood wall: Novel building envelope using subtractive manufacturing of timber profiles to improve thermal performance and airtightness of solid wood construction. Energy & Buildings 254 (2022) 111597.

[20] M. Shirzadi, Y. Tominaga. CFD evaluation of mean and turbulent wind characteristics around a high-rise building affected by its surroundings. Building and Environment 225 (2022) 109637.

[21] Li X M, Zhou Y Y, Yu S. Urban heat island impacts on building energy consumption: A review of approaches and findings. Energy 174 (2019) 407-419.

[22] Y Sun, G Augenbroe. Urban heat island effect on energy application studies of office buildings. Energy and Buildings 2014, 77(7): 171-179.

[23] Z. Wu, Q.S. Jia, X. Guan. Optimal control of multiroom HVAC system: An event-based approach. IEEE Transactions on Control Systems Technology 24 (2015) 662-669.

[24] Y. Wang, D. Mauree, Q. Sun, H. Lin, J.L. Scartezzini, R. Wennersten. A review of approaches to low-carbon transition of high-rise residential buildings in China. Renewable and Sustainable Energy Reviews 131 (2020) 109990.

[25] W. Pan, M. Pan. A dialectical system framework of zero carbon emission building policy for high-rise high-density cities: Perspectives from Hong Kong. Journal of Cleaner Production 205 (2018) 1-13.

[26] Y.H. Qin. A review on the development of cool pavements to mitigate urban heat island effect. Renewable and Sustainable Energy Reviews 52 (2015) 445-459.

[27] X. Meng, T. Luo, Z.Y. Wang, W. Zhang, B. Yan, J.L. Ouyang, E.S. Long. Effect of RR-coatings on building indoor temperature conditions and heat flow analysis for walls. Energy and Buildings 127 (2016) 488-498.

[28] D Orazio M., Di Perna C., Di Giuseppe E. Green roof yearly performance: A case study in a highly insulated building under temperate climate. Energy and Buildings 55 (2012) 439-

451.

[29] K. Georgios, J. Darkwa. Support for the integration of green roof constructions within Chinese building energy performance policies. Energy 65 (2014) 71-79.

[30] C.Y. Jim. Air-conditioning energy consumption due to green roofs with different building thermal insulation. Applied Energy 128 (2014) 49-59.

[31] L.J. Deng, Q.H. Deng. The basic roles of indoor plants in human health and comfort, Environ. Sci. Pollut. Control Ser. 25 (2018) 36087-36101.

[32] D.E. Salt, M. Blaylock, N.P. Kumar, V. Dushenkov, B.D. Ensley, I. Chet, I. Raskin, Phytoremediation: a novel strategy for the removal of toxic metals from the environment using plants. Biotechnology (NY) 13 (1995) 468-474.

[33] G. Mangone, S.R. Kurvers, P.G. Luscuere, Constructing thermal comfort: investigating the effect of vegetation on indoor thermal comfort through a four-season thermal comfort quasi-experiment. Build. Environ. 81 (2014) 410-426.

[34] K. Rodgers, R. Handy, W. Hutzel. Indoor air quality (IAQ) improvements using biofiltration in a highly efficient residential home. J. Green Build. 8 (2013) 22-27.

[35] R. Fern´andez-Ca˜nero, L.P. Urrestarazu, A. Franco Salas. Assessment of the cooling potential of an indoor living wall using different substrates in a warm climate, Indoor Built Environ. 21 (2012) 642-650.

[36] L. P´erez-Urrestarazu, R. Fern´andez-Ca˜nero, A. Franco, G. Egea. Influence of an active living wall on indoor temperature and humidity conditions. Ecol. Eng. 90 (2016) 120-124.

[37] P. Abdo, B.P. Huynh. An experimental investigation of green wall bio-filter towards air temperature and humidity variation. J. Build. Eng. 39 (2021) 102244.

[38] P. Abdo, B.P. Huynh. Effect of passive green wall modules on air temperature and humidity, in: Proceedings of the ASME 2018 International Mechanical Engineering Congress and Exposition, vol. 7, 2018, pp. 9-15. Fluids Engineering. Pittsburgh, Pennsylvania, USA.

[39] P. Abdo, B.P. Huynh, V. Avakian. Effect of green wall modules on air temperature and humidity, Development and Applications in Computational Fluid Dynamics; Industrial and Environmental Applications of Fluid Mechanics; Fluid Measurement and Instrumentation; Cavitation and Phase Change, in: Proceedings of the ASME 2018 5th Joint US-European Fluids Engineering Division Summer Meeting, vol. 2, 2018, pp. 15–20. Montreal, Quebec, Canada.

[40] X. Meng, L.Y. Yan, F.D. Liu. A new method to improve indoor environment: combining the living wall with air-conditioning. Build. Environ. 216 (2022) 108981.

[41] A. Smith, M. Pitt. Healthy workplaces: plantscaping for indoor environmental quality. Facilities 29 (2011) 169-187.

[42] V.I. Lohr, C.H. Pearson-mims. Particulate matter accumulation on horizontal surfaces in interiors: influence of foliage plants. Atmos. Environ. 30 (1996) 2565-2568.

[43] O.S. Eddine, B.R.S. David. Experimental and numerical investigation of urban street canyons to evaluate the impact of green roof inside and outside buildings. Applied Energy 114 (2014) 273-282.

[44] N. Nishimura, etc. Novel Water Facilities for Creation of Comfortable Urbran Micrometeorology. Solar Energy 64 (1998) 197-207.

[45] A. Hassaan, A. Mahmoud. Analysis of the microclimatic and human comfort conditions in an urban park in hot and arid regions. Building and Environment 46 (2011) 2641-2656.

[46] R.H. Sun, L.D. Chen. How can urban water bodies be designed for climate adaptation? Landsc Urban Plan 105 (1-2) (2012) 27-33.

[47] S. Murakawa, T. Sekine, K. &Narita. Study of the effects of a river on the thermal environment in an urban area. Energy Build 15 (1990) 993-1001.

[48] J. Xu, Q. Wei, X. Huang, X. Zhu, G. Li. Evaluation of human thermal comfort near urban water body during summer. Build. Environ. 45 (2009) 1072-1080.

[49] T. Katayama, T. Hayashi, Y. Shiotsuki, H. Kitayama, A. Ishii, M. Nishida. Cooling effects of river and sea breeze on thermal environment in a built up area. Energy and Buildings 15-16 (1990-1991) 973-978.

[50] E. A. Hathway, S. Sharples. The interaction of rivers and urban form in mitigating the Urban Heat Island effect: A UK case study. Building and Environment 58 (2012) 14-22.

[51] A. Ishii, S. Iwamoto, T. Katayama, T. Hayashi, Y. Shiotsuki, H. Kitayama. A comparison of field surveys on the thermal environment in urban areas surroundings a large pond: When filled and when drained. Energy and Buildings 16 (1991) 965-971.

[52] X. L. Chen, H.M. Zhao, P.X. Li, Z.Y. Yin. Remote sensing image-based analysis of the relationship between urban heat island and land use/cover changes. Remote Sensing of Environment 104 (2006) 133-146.

[53] S.K. Jusuf, N.H. Wong, N.I. Syafii. Influence of water feature on temperature condition hot humid climate. Presented in iNTA-SEGA 2009 -bridging innovation, technology and tradition.

[54] M. Robitu, C. Isard, D. Groleau, M. Musy. Energy balance study of water ponds and its influence on building energy consumption. Building Services Engineering Research and Technology 25 (2004)171-182.

[55] H. Saaroni, B. Ziv. The impact of a small lake on heat stress in a Mediterranean urban park: The case of TelAviv,Israel. International Journal of Biome teorology 47 (2003) 156-165.

[56] Y. Wang, D. Mauree, Q. Sun, H. Lin, J.L. Scartezzini, R. Wennersten. A review of approaches to low-carbon transition of high-rise residential buildings in China. Renew. Sustain. Energy Rev. 131 (2020) 109990.

[57] W. Pan, M. Pan. A dialectical system framework of zero carbon emission building policy for high-rise high-density cities: Perspectives from Hong Kong, J. Cleaner Prod. 205 (2018) 1-13.

[58] L.S. Bar, M.E. Hoffman, Y. Tzamir. Integrated thermal effects of generic built forms and vegetation on the UCL microclimate. Build. Environ 41 (2006) 343-354.

[59] Y.F. Gao, R.M. Yao, B.Z. Lia, E. Turkbeylerc, Q. Luo, A. Shortd. Field studies on the effect of built forms on urban wind environments. Renewable Energy 46 (2021) 148-154.

[60] J. Zhang, L. Xu, V. Shabunko, S.E.R. Tay, H.X. Sun, S.S.Y. Lau, T. Reindl, Impact of urban block typology on building solar potential and energy use efficiency in tropical high-density city, Appl. Energy 240 (2019) 513-533.

[61] J.J. Sarralde, D.J. Quinn, D. Wiesmann, K. Steemers. Solar energy and urban morphology: Scenarios for increasing the renewable energy potential of neighborhood in London. Renewable Energy 73 (2015) 10-17.

[62] G. Lobaccaro, S. Croce, C. Lindkvist, M.C. Munari Probst, A. Scognamiglio, J. Dahlberg, M. Lundgren, M. Wall. A cross-country perspective on solar energy in urban planning: Lessons learned from international case studies. Renew.Sustain. Energy Rev. 108 (2019) 209-237.

[63] D.E. Bowler, L.B. Ali, T.M. Knight, A.S. Pullin. Urban greening to cool towns and cities: A systematic review of the empirical evidence. Landscape Urban Plann. 97 (2010) 147-155.

[64] A.B. Besir, E. Cuce. Green roofs and facades: A comprehensive review, Renew. Sustain.

Energy Rev. 82 (2018) 915-939.

[65] A. Yoshida, D. Hayashi, Y. Shimazaki, S. Kinoshita. Evaluation of thermal sensation in various outdoor radiation environments. Architectural Science Review 62 (2019) 261-270.

[66] M. Manso, I. Teotonio, C.M. Silva, C.O. Cruz. Green roof and green wall benefits and costs: A review of the quantitative evidence. Renew. Sustain. Energy Rev. 135 (2021) 110111.

[67] M. Martin, N.H. Wong, M. Ichinose. Impact of retro-reflective glass façades on the surface temperature of street pavements in business areas of Singapore and Tokyo. IOP Conference Series: Earth Environ. Sci. 294 (2019) 012020.

[68] E. Ng, L. Chen, Y.N. Wang, C. Yuan. A study on the cooling effects of greening in a high-density city: An experience from Hong Kong. Build. Environ. 47 (2012) 256-271.

[69] H. Chen, R. Ooka, H. Huang, T. Tsuchiya. Study on mitigation measures for outdoor thermal environment on present urban blocks in Tokyo using coupled simulation. Build. Environ. 44 (2009) 2290-2299.

[70] Y.H. Qin, J. Liang, K.G. Tan, F.H. Li. A side-by-side comparison of the cooling effect of building blocks with retro-reflective and diffuse-reflective walls. Sol. Energy 133 (2016) 172-179.

[71] Y.C. Ji, J.S. Song, P.Y. Shen. A review of studies and modelling of solar radiation on human thermal comfort in outdoor environment. Building and Environment 214 (2022) 108891.

[72] J.J. Pan, N.P. Li, W. Zhang, Y.D. He, X.H. Hu. Investigation based on physiological parameters of human thermal sensation and comfort zone on indoor solar radiation conditions in summer. Building and Environment 226 (2022) 109780.

[73] M.T. Manzoor, G. Lenci, M.T. Friend. Convection in volumetrically absorbing solar thermal receivers: A theoretical study. Solar Energy 224 (2021) 1358-1368.

[74] Y. A, N.P. Li, Y.D. He, C.Z. Yuan, L.X. Zhou, J.L. Lu. Occupant-centered evaluation on indoor environments and energy savings of radiant cooling systems with high-intensity solar radiation. Solar Energy 242 (2022) 30-44.

[75] G.D. Liu, Z.X. Wang, C.R. Li, S.T. Hu, X.W. Chen, P. Liang. Heat exchange character and thermal comfort of young people in the building with solar radiation in winter. Building and Environment 179 (2020) 106937.

[76] M. Santamouris. Cooling the cities - a review of reflective and green roof mitigation technologies to fight heat island and improve comfort in urban environments. Solar Energy 103

(2014) 82-703.

[77] H. Akbari, D. Kolokotsa. Three decades of urban heat islands and mitigation technologies research. Energy and Buildings 133 (2016) 834-842.

[78] M. Santamouris, A. Synnefa, D. Kolokotsa, V. Dimitriou, K. Apostolakis. Passive cooling of the built environment—use of innovative reflective materials to fight heat islands and decrease cooling needs. International Journal of Low Carbon Technologies 3/2 (2008) 71-82.

[79] A. Synnefa, M. Santamouris, H. Akbari. Estimating the effect of using cool coatings on energy loads and thermal comfort in residential buildings in various climatic conditions. Energy and Buildings 39 (2007) 1167-1174.

[80] R. Levinson, H. Akbari, C. Joseph. Reilly Cooler tile-roofed buildings with near infrared-reflective non-white coatings. Building and Environment 42 (2007) 2591-2605.

[81] K.T. Zingre, M.P. Wan, S.K. Wong, T.B. Winston, I.Y.Leng. Modelling of cool roof performance for double-skin roofs in tropical climate. Energy 82 (2010) 813-826.

[82] I.H. Pérez, Y.O. Gómezb. Thermal evaluation of building roofs with conventional and reflective coatings. Eco-efficient Materials for Reducing Cooling 9 (2021) 247-273.

[83] H. Mohamed, J.D. Chang, M. Alshayed. Effectiveness of High Reflective Roofs in Minimizing Energy Consumption in Residential Buildings in Iraq. Procedia Engineering 118 (2015) 879-885.

[84] M. Baneshi, S. Maruyama. The impacts of applying typical and aesthetically-thermally optimized TiO_2 pigmented coatings on cooling and heating load demands of a typical residential building in various climates of Iran. Energy and Buildings 113 (2016) 99-111.

[85] M. Kadri, A. Bouchair, A. Laafer. "The contribution of double skin roof coupled with thermo reflective paint to improve thermal and energy performance for the 'Mozabit' houses: Case of Beni Isguen's Ksar in southern Algeria". Energy and Buildings 256 (2022) 111746.

[86] N. Bansal, S. Garg, S. Kothari, Effect of exterior surface colour on the thermal performance of buildings, Building and Environment 22 (1992) 31-37.

[87] V. Cheng, E. Ng, B. Givoni, Effect of envelope colour and thermal mass on indoor temperatures in hot humid climate, Solar Energy 78 (2005) 528-534.

[88] J.E. Winandy, R. Beaumont, Roof Temperatures in Simulated Attics, Forest Products Laboratory, 1995, http://www.fpl.fs.fed.us/documnts/fplrp/fplrp543.pdf.

[89] N.M. Nahar, P. Sharma, M.M. Purohit. Performance of different passive techniques for cooling of buildings in arid regions. Building and Environment 38 (2003) 109-116.

[90] M.A. Hamdan, J. Yamin, E.M. Abdel Hafez. Passive cooling roof design under Jordanian climate. Sustainable Cities and Society 5 (2012) 26-29.

[91] B.M. Summan, V.V. Verma. Measured performance of a reflective thermal coating in experimental rooms. Journal of Scientific & Industrial Research 62 (2003) 1152-1157.

[92] B. Yu, Z. Chen, P. Shang, J. Yang. Study on the influence of albedo on building heat environment in year-round. Energy and Buildings 40 (2008) 945-951.

[93] Yang J.C. Wang Z.H., Kaloush K.E. Environmental impacts of reflective materials: Is high albedo a 'silver bullet' for mitigating urban heat island? Renewable and Sustainable Energy Reviews 47 (2015) 830-843.

[94] J. Wang, S.H. Liu, X. Meng, W.J. Gao, J.H. Yuan. Application of RR-coatings in urban buildings: A comprehensive review. Energy and Buildings 247 (2021) 111137.

[95] J.H. Yuan, C. Farnham, K. Emura. A study on the accuracy of determining the retro-reflectance of retro-reflective material by heat balance. Solar Energy 122 (2015) 419-428.

[96] H. Sakai, K. Emura, N. Igawa, H. Iyota. Reduction of Reflected Heat of the Sun by Retro reflective Materials. Journal of Heat Island Institute International 7 (2012) 218-221.

[97] F. Rossi, A.L. Pisello, A. Nicolini, M. Filipponi, M. Palombo. Analysis of retro-reflective surfaces for urban heat island mitigation: A new analytical model. Applied Energy 114 (2014) 621-631.

[98] E. Morini, B. Castellani, A. Nicolini, F. Rossi, U. Berardi. Effects of aging on RR-coatings for building applications. Energy and Buildings 179 (2018) 121-132.

[99] J. H. Yuan, C. Farnham, K. Emura. Development of a retro-reflective material as building coating and evaluation on albedo of urban canyons and building heat loads. Energy and Building 103 (2015) 107-117.

[100] F. Rossi, B. Castellani, A. Presciutti, E. Morini, E. Anderini, M. Filipponi, A. Nicolini. Experimental evaluation of urban heat island mitigation potential of retro-reflective pavement in urban canyons. Energy and Buildings 179 (2018) 121-132.

[101] E. Morini, B. Castellani, E. Anderini, A. Presciutti, A. Nicolini, F. Rossi. Optimized retro-reflective tiles for exterior building element. Sustainable Cities and Society 37 (2018) 146-153.

[102] Y.H. Qin, J. Liang, K.H. Tan, F.H. Li. A side by side comparison of the cooling effect of building blocks with retro-reflective and diffuse-reflective walls. Solar Energy 133 (2016) 172-179.

[103] X. Meng, C.X. Wang, W.J. Liang, S. Wang, P. Li, E.S. Long. Thermal Performance Improvement of Prefab Houses by Covering RR-coatings. Procedia Engineering 121 (2015) 1001-1007.

[104] J.H. Yuan, K. Emura, C. Farnham, H. Sakai. Application of glass beads as retro-reflective facades for urban heat island mitigation: Experimental investigation and simulation analysis. Building and Environment 105 (2016) 140-152.

Literature review of the application of retro-reflective coatings in buildings

Chapter 2 Literature review of the application of RR-coatings in buildings

2.1 Introduction

The urban population growth has led to a denser urban pattern, and high-rise and high-density building groups have become the urban development theme [1-3]. Many urban surfaces made of concrete and asphalt have absorbed solar energy easily [4-6]. Meanwhile, due to the lack of green, water and land spaces in cities, urban thermal environment has become worsened increasingly and one obvious phenomenon observed is the urban heat island, whose main characteristic is the systematic increment of air temperature in the urban area, compared to the rural one [7-9].

Urban heat island will deteriorate urban thermal conditions [10-12] and under the poor thermal conditions due to high heat island intensity, more energy will be consumed for the living improvement and comfort requirements [13,14], while this energy consumption will further enhance this heat island intensity [15]. Therefore, a vicious circle is being built between the worsening of the urban heat island and the increment of energy consumption, and it is a very urgent task to improve the worsening thermal environment and simultaneously reduce energy consumption in buildings.

To alleviate urban heat island, some proposed technologies included the optimization of urban structures [16-18], the increment of green infrastructures [19, 20], the employment of cooling materials on streets and buildings [21, 22], and so on. Among them, the specialized urban design can promote the urban heat island reduction efficiently, but it is too complex to yet a practical approach [23-25]. Increasing the green infrastructure can reduce the amount of infrared radiation and lower the urban surface temperature effectively [26-29], but this technology often needs to provide some land and irrigation water for plants [30]. In addition, several studies have shown that planted roofs have little effect on outdoor air temperature [31, 32].

Employing HR-coatings on building surfaces, which include cool roofing materials and cool-toned roofing materials [33-36], can reduce the average temperature of indoor air [37, 38], and increase the solar reflectance of outer surfaces, which can reduce the cooling load of residential buildings [39]. However, HR-coatings reflect most of the solar radiation in a diffuse manner, and are only suitable for low-rise buildings or roofs. For high-rise and high-density building groups, HR-coatings will reflect solar radiation repeatedly between buildings and roads, and correspondingly, a large amount of solar radiation will be intercepted by urban surfaces through the multiple absorption [40-43], as shown in Fig. 1(a). Therefore, the service efficiency of the traditional HR-coatings is limited, and even the urban heat island can be aggravated [44, 45].

According to the inherent defect of traditional HR-coatings on the reflection direction of solar radiation, RR-coatings are proposed due to the fact that they can reflect solar radiation back along the incident direction, also in a thin layer. Fig. 2-1 compares the regional thermal environment of high-rise and high-density buildings covered by HR-coatings and RR-coatings. As shown, RR-coatings can reflect solar radiation back along the incident direction, which has the essentially difference with the specular and diffuse reflection of HR-coatings [46, 47]. Therefore, employing RR-coatings can decrease the comprehensive urban heat gain on the mechanism, thereby alleviating the urban heat island and lowering the cooling energy consumption.
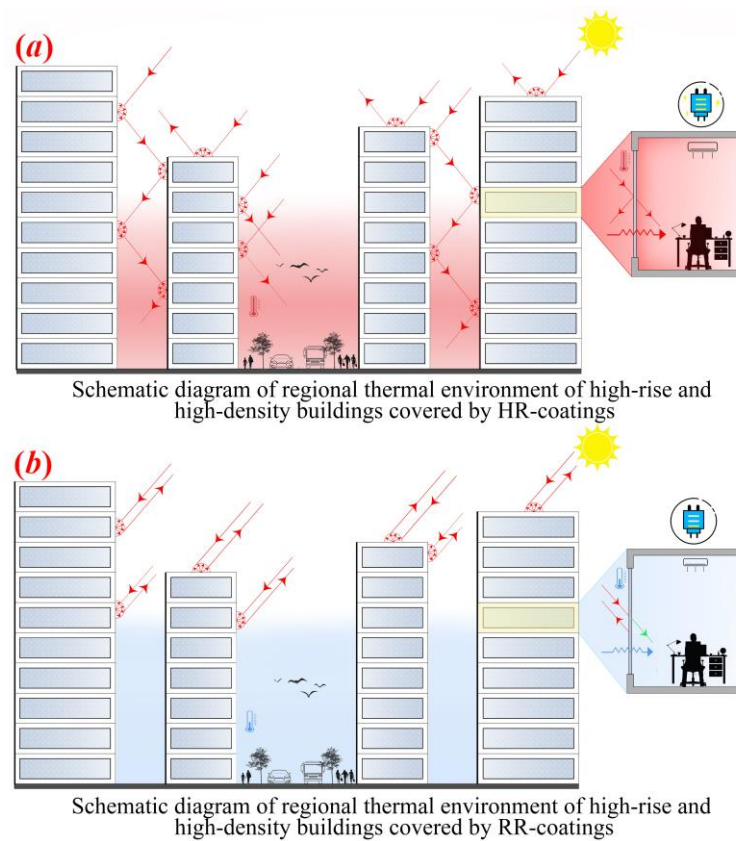
Fig. 2-1. Schematic diagram of regional thermal environment of high-rise and high- density buildings covered by (a) highly-reflective materials and (b) RR-coatings

RR-coatings were developed originally to improve the visibility at night to reflect the illumination source as much as possible [48, 49] and they were widely used in transportation and textile fields [50-54] for various security and decorative purpose [55]. In 2004, Nielsen and Lu [56] described the parameters and related technologies of RR-coatings and proposed the applications of RR-coatings initially in buildings to play their potential in alleviating urban thermal environment and then, more and more scholars have conducted the relative studies in

this area. It has been proved that since RR-coatings can reflect more incident sunlight to the sky, employing it on building facades and roads could be more effective in reducing the total energy consumption, especially in cooling energy consumption [42, 46, 50, 57-64].

Since RR-coatings have shown the large potential on the heat island alleviation and building energy conservation, this review summarizes the recent development of RR-coatings. A detailed illustration was firstly provided on RR-coatings and their properties. Then the measurement methods of reflectivity and retro-reflectivity were analyzed. Next, the review focused on the contribution efficiency of RR-coatings on urban thermal environment and building energy consumption. Finally, future directions were discussed on possible studies and applications.

2.2 Review methods and synthesis of evidence

To review the existing knowledge on RR-coatings applied in buildings systematically, four main databases were consulted (Science Direct, Google Scholar, Web of Science and Summaries of technical papers of AIJ annual meeting). Publications were selected according to the following inclusion criteria:

- Covering the last 20 years (2000-2020) to account for the most recent development, since RR-coatings were proposed by Nielsen and Lu [56] in 2004.

- Focusing on the application on the buildings, including types, measurement methods, application efficiency. When clarifying the initial application in transportation and textile fields, antecedent studies were mentioned, but were not included in the analysis. And the reference about other applicative fields (such as the study of pure optical properties) were excluded to avoid losing the focus on the target.

The 61 published papers were included from 8 countries. Based on authors' affiliations and/or experimental sites, the published studies were predominantly produced in Japan (52.4%), China (11.4%) and Singapore (1.6%) in East Asia, Italy (26.2%), France (1.6%), Switzerland (1.6%) and Spain (1.6%) in Western Europe, and America (3.2%) in North America. Fig. 2-2 presented the number and typology of published papers per year. In 2004, Nielsen and Lu [56] firstly proposed the application of RR-coatings in buildings, and in the following 10 years, most of the papers were published by Sakai's team, and they revealed the optical characteristics of RR-coatings including the retro-reflectivity measurement methods [50, 65, 66] and the directional characteristics [67-69]. From 2014, the published papers concentrated on the durability and the application in buildings of RR-coatings. In addition, it can be clearly seen that the studies on RR-coatings were highly dependent on experiments.
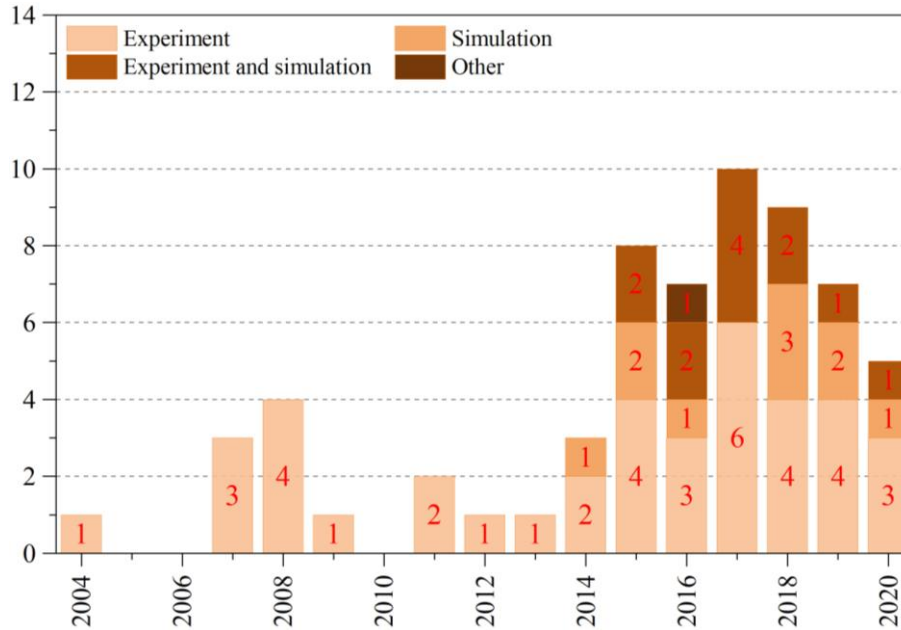
Fig. 2-2. Number and typology of published papers on RR-coatings

2.3 RR-coatings and their optical property

2.3.1 Fundamental types of RR-coatings

Traditional highly-reflective materials reflect the solar radiation in a diffuse manner, while RR-coatings reflect the solar radiation [46] back along the incident direction due to their special optical components with different physical properties [70]. According to the difference of the optical mechanism, RR-coatings could be classified into three categories: glass bead type, capsule type, and prism type. Fig. 2-3 showed the optical mechanism and appearance of three RR-coatings. And based on the prism RR-coatings, the new transparent RR-coatings were proposed and applicated on the windows [71, 72].

(1) Glass bead RR-coatings

The core components are the glass microsphere and the reflective layer. The incident sunlight is reflected along the incident direction through two refractions on the glass microsphere boundary and one reflection by using the highly-reflective coating, as shown in Fig. 2-3 (a). And their solar reflectivity and retro-reflectivity were about 39.1% and 19% [77].

(2) Prism RR-coatings

The core components are the prism cone and the reflective layer. Incident sunlight is reflected through two refractions on the prism boundary and multiple reflections on the reflective layer, as shown in Fig. 2-3(b). Their solar reflectivity and retro-reflectivity were about 83% and 44%

[57, 88].

(3) Capsule RR-coatings

The core components are the glass microsphere, the transparent resin, and the reflective layer. The incident sunlight passes through two refractions on the glass microsphere boundary, two refractions on the interface between glass microsphere and transparent resin, and one reflection on the highly-reflective coating, as shown in Fig. 2-3(c). Their solar reflectivity and retro-reflectivity were about 69% and 18%~20% [57, 88].
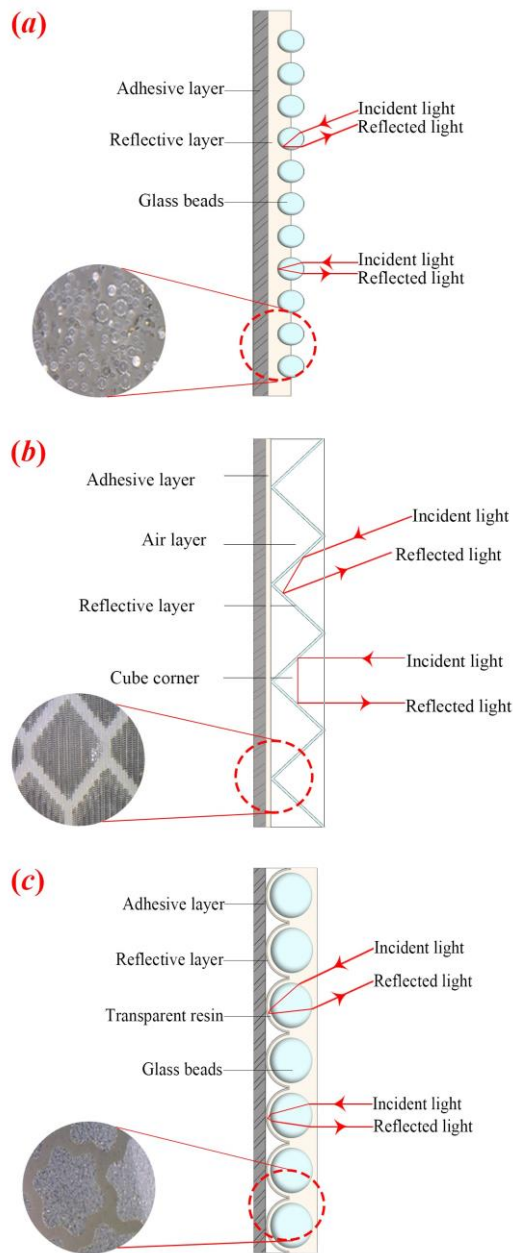
Fig. 2-3. Optical mechanism and appearance of (a) glass-bead RR-coatings, (b) prism RR-coatings and (c) capsule RR-coatings

(4) Transparent RR-coatings

In addition, Han et al. [46] was inspired by Galanthus nivalis petals and built a bio-inspired retro-reflective model based on retro-reflective flower petals of Galanthus nivalis. The cubic-corner retro-reflectors have the acceptance angles between -50° and 50° with the solar reflectance and the retro-reflectance of 71.0%~77.8% and 23.5%~29.5%, respectively. However, it was a pity that this retro-reflective material had not been produced. And Inoue et al. [71] and Ichinose et al. [72] employed the similar mechanism to develop a transparent retro-reflective material, which has the same transparent degree with the normal glass.

2.3.2 Property improvement of RR-coatings

The original purpose of RR-coatings is used for traffic signs and safety clothing to improve the transportation safety, especially in the night [73], so there are some deficiencies for the building application [74, 75]. Therefore, some studies have been done to improve the RR-coatings, especially in the aspects of the reflectivity [76, 77], the durability [55, 57], and the climate adaptability [59, 61], so as to better suit the building application.

（1）For glass bead RR-coatings

For the property improvement of glass bead RR-coatings, more attention was paid on the glass bead from the aspects including the external coating, the size, the refractive index and density of the glass bead.

For the external coatings of glass bead, Castellani et al. [77] covered three type of microspheres on the building tiles. Experimental results showed the reflectivity was increased by clear barium titanate glass microspheres with the total reflectivity and retro-reflectivity of 39.1% and 19%, respectively. However, employing aluminum-coated spheres would halve the total reflectivity, while an additional fluoropolymer coating could also result into the retro-reflectivity increment of 2%~5%. Another study from Castellani et al. [78] also showed there is a strong global reflectance reduction with the aluminum-coated spheres, while the glass microspheres and barium titanate glass microspheres have a reflectance up to 50.6%. And the simple glass microspheres were recommended.

For the glass bead size, Morini et al. [43] built two samples of glass bead RR-coatings with the small glass bead of 0.1mm~0.2mm and 3mm diameters. The experimental result showed RR-coatings with the 0.1mm~0.2mm glass bead had the solar reflectivity of 61%, which was higher than that with the 3mm glass bead of 50%. Meanwhile, they could reflect the solar radiation mainly backward to the incoming direction under the low incidence angle from 10° to 60° and symmetrically with respect to the perpendicular direction under the high incidence

angle more than 60°. In addition, Schwinger et al. [79] built two types of RR-coatings with solid and hollow glass beads and it was found that solid glass bead could obtain the reflectivity of 30%, while the hollow glass bead could only achieve the reflectivity of 5%. This phenomenon is due to the air layer of the hollow glass bead increased the diffuse reflectance of incident light inside the glass bead, resulting in a decrease in the amount of secondary refracted light at the boundary of the microsphere.

For the refractive index of glass bead, Morini et al. [80] compared the performance of two RR-coatings produced by glass bead and clear solid barium titanate bead and their results showed both the glass and the barium tiles had the strong retro-reflectivity of 30% and 32% respectively, but the barium tile has a higher global reflectance, equal to 39%. Yuan et al. [81] measured the reflectivity direction characteristics of glass bead samples with the refractive indexes of 1.9 and 1.5, and found the retro-reflective capacity of glass bead with refractive index of 1.9 was 2-5 times higher than that with refractive index of 1.5, no matter what color reflective layers. And another numerical study of Yuan et al. [76] showed the retro-reflective directional characteristic of glass beads was the most remarkable for the refractive index of 1.93, compared to the refractive index of 1.50 and 2.20. This phenomenon is due to smaller or larger refractive index increased the dispersion of scattered light and reduced the efficiency of retro-reflection.

In addition, Yuan et al. [73] also analyzed the influence of glass bead density by employing two bead densities of $0.15 kg/m^2$ and $0.30 kg/m^2$. Their experimental results found RR-coatings with the high-density glass bead had the larger dependence of incident angles than that with the low-density glass bead, and their retro-reflectance was larger than that with the low-density glass bead at the small incident angles of solar radiation. This phenomenon is due to if the density was smaller, the materials could not form concentrated retro-reflection to the incident light source, and the amount of retro-reflection was less.

（2）**For capsule RR-coatings**

For capsule RR-coatings, only the seasonal applicability improvement had been done. Due to the fact that more reflected solar energy would increase the heating energy consumption in winter, Sakai et al. [69, 82, 83] proposed the concept of selective retro-reflection and developed a new retro-reflective material. Fig. 2-4 showed the optical mechanism of this new retro-reflective material in summer and winter. As shown, taking full use of the solar altitude difference between summer and winter, this new retro-reflective material could reflect the solar radiation in summer and absorb solar radiation in winter by the reasonable location of reflector and absorber coating. However, the structure of these materials was complex and fragile, so

they were adapted for the smaller areas, such as roofs and walls.
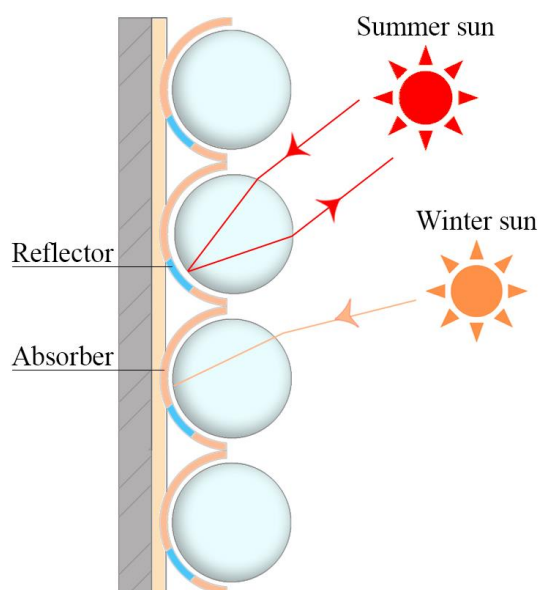
Fig. 2-4. Cross section of the structure of directional-type RR-coatings [69]

（3）**For prism RR-coatings**

For prism RR-coatings, two improvement aspects, including the material durability and the triangular prism shape, had been done. Yuan et al. [84] added a glass covering with high transmission and high strength on prism RR-coatings to improve the durability of prism RR-coatings. And their experimental results showed the reflectivity of these prism RR-coatings kept around 0.81 and was decreased by only 0.02, compared to that without the glass covering, but it could be recovered completely by cleaning after 485 days, which showed the glass covering could maintain the durability and the reflective performance of prism RR-coatings by reducing the impact of external environments including dry-wet cycle of the atmosphere and atmospheric pollutants. And Levinson et al. [62] analyzed the influence of symmetric and asymmetric high-index glass right triangular prisms on the reflection of beam light. It was included that the symmetric high-index glass right triangular prisms had the better performance and that the technologies relying on solar internal reflection may be not suited for walls.

2.3.3 Comprehensive comparison on the different RR-coatings

To encourage the selection and application of RR-coatings to urban surfaces more efficiently, the reflection performance and durability of various RR-coatings will be compared as following.

（1）**Reflection performance**

Reflection performance is the most important evaluation index on reflective materials and included two aspects of the solar reflectivity and retro-reflectivity [77, 78]. Iyota et al. [85]

measured the retro-reflectivity of several commercial RR-coatings, and found that the retro-reflectivity of prism RR-coatings were generally higher than that of glass bead RR-coatings and capsule RR-coatings. This conclusion was supported by the experimental data from Yuan et al. [57], which showed the retro-reflectivity of prism RR-coatings could be as high as 40%, while the retro-reflectivity of two other RR-coatings were about only 20%. However, Iyota et al. [85] pointed out that this situation was only suitable for low incident angles. In the case of the high incident angle, the retro-reflectivity of glass bead RR-coatings was better than that of prism RR-coatings, which were consistent with the conclusion drawn in [68, 73, 81]. This phenomenon is due to the no strict critical angle of the glass bead RR-coatings and capsule RR-coatings, and thereby, they were effective at a wide range of solar positions. However, prism RR-coatings had a critical angle for retroreflection, so its reflection mechanism worked well only within the critical angle. This showed that compared with prism RR-coatings, glass bead RR-coatings were more suitable for external walls and could reduce the impact of noon sunlight on streets and buildings.

（2）Durability

Considering the application of RR-coatings as a building coating, it is also necessary to examine their durability [86]. For glass bead RR-coatings, Morini et al. [87] used the accelerated weathering tester to simulate the natural outdoor exposure conditions for 20 years and found most aging samples had higher global reflectivity but lower the certain retro-reflectivity than new samples and still retain the retro-reflective characteristics. Similarly, Yuan et al. [55] studied the durability of the developed glass bead RR-coatings by exposing the samples to an outdoor environment for 368 days. And it was found that the angular distribution of reflection intensity almost had no significant change, while the solar reflectivity was dropped by 3.3%. In addition, Yuan et al. [57, 88] measured solar reflectivity and retro-reflectivity of the capsule and prism RR-coatings after 25 months of outdoor exposure. Prism RR-coatings showed the better durability after 25 months and their reflectivity and retro-reflectivity could be recovered basically after cleaning. However, the reflectivity and retro-reflectivity for capsule RR-coatings were dropped from 0.69 to 0.51 and from 0.18 to near 0, respectively, and the lower reversion rates were gained after cleaning. This phenomenon is due to the surface degradation of capsule RR-coatings with the obvious cracking. Experimental study of Yuan et al. [84] showed that the durability of RR-coatings could be improved by adding a glass covering. Table 2-1 reviewed the solar reflectivity and retro- reflectivity between before and after aging. It was found that the reflection property of RR-coatings had the certain durability, but it was affected by atmospheric pollutants easily. Meanwhile, it lacks of the long-term exposure experiment of more than 30 years under the real outdoor environment.

Table 2-1. Comparison of solar reflectivity and retro- reflectivity between before and after aging

RR-coatings	Aging time	Solar reflectivity (%)			Retro-reflectivity (%)			Ref.
		Initial	After aging	After cleaning	Initial	After aging	After cleaning	
Capsule	25 mouths	0.69	0.51	0.60	0.18	0.0072	0.087	[57,88]
Prism	25 mouths	0.83	0.81	0.8192	0.44	0.42	0.43	[57,88]
Prism with a glass covering	485 days	0.81	0.79	0.81	-	-	-	[84]
Capsule	485 days	0.80	0.76	0.79	-	-		[84]
Prism	485 days	0.69	0.51	0.62	-	-	-	[84]

2.4 Measurement methods of solar reflectivity and retro-reflectivity

The solar reflectivity and retro-reflectivity are two important evaluation parameters of RR-coatings, and the relative measurement methods and corresponding equipment were developed. The following content reviewed the solar reflectivity, the approximate evaluation and high-precision measurement of retro-reflectivity.

2.4.1 Traditional measurement methods of solar reflectivity

Measurement technologies of solar reflectivity have been basically mature [89-91]. The pyranometer, the spectrophotometer with an integrating sphere, and the spectral solar portable reflector were the traditional measurement methods of solar reflectivity [89-94]. Table 2-2 compared the measurement methods of three traditional measurement methods on solar reflectivity. As shown in Table 2, Pyranometer has many limitations on the measurement sample and the incidence light, compared to spectrophotometer and portable solar reflectometer, and it was employed in the field measurement under the solar radiation. Spectrophotometer with an integrating sphere was usually used in the lab with the small sample, while Portable solar reflectometer has almost no limits.

Table 2-2. Measurement of solar reflectance [89-103]

Measurement methods	Sample characteristics	Sample size	Angle of incidence light	Measurement accuracy	Relevant standard
Pyranometer	Horizontal or low slope	Large surface	less than 45°	Middle	ASTM E1918-06
Spectrophotometer with an integrating sphere	Even	Small surface (approx. 0.1cm^2)	Fixed in the normal range	High	ASTM E903-96
Portable solar reflectometer	Even/uneven	Several square centimeters	--	High	ASTMC1549-2002

Before employing RR-coatings in buildings, it is necessary to analyze the retro-reflective performance of RR-coatings in detail. And in fact, the profile of their reflectance capability does not describe hemispherical shape, as assumed by the Lambert law, which is the basic law of spectrophotometry and describes the relationship among the light absorption intensity, the concentration and the light path length of a certain substance to a certain wavelength [103]. Therefore, the optical properties of RR-coatings in different directions could not be directly tested by the above traditional reflectivity measurement methods.

2.4.2 Approximate evaluation of retro-reflectivity

The retro-reflectivity measurement needs the clear distribution of the reflected light generally, but this measurement has the high demand on the measurement equipment [48, 55]. And thereby, some scholars employed the thermal distribution to estimate the retro-reflectivity of RR-coatings approximately without the clear distribution of the reflected light. Thermal balance theory and equivalent albedo are the main methods.

(1)Thermal balance theory

The thermal balance theory to measure the retro-reflectivity was proposed by Sakai et al. [50, 104]. Fig. 2-5 showed the schematic diagram of thermal balance theory. When the sample was radiated by solar energy, it would absorb the partial energy as displayed by its temperature rise and the rest energy would be reflected by the diffuse reflection, the specular reflection, and the retro-reflection. And the components of the diffuse reflection and the specular reflection were mainly tested by the temperature rise on the opposite surface and the below surface, respectively.

Therefore, the retro-reflectivity could be calculated indirectly from the temperatures of the sample surface, the opposite surface, and the below surface under the condition of the known amount of irradiation. In the laboratory, the various samples were radiated from an oblique downward direction of 45° by an infrared lamp, and the retro-reflectivity was obtained by the thermal measurement.
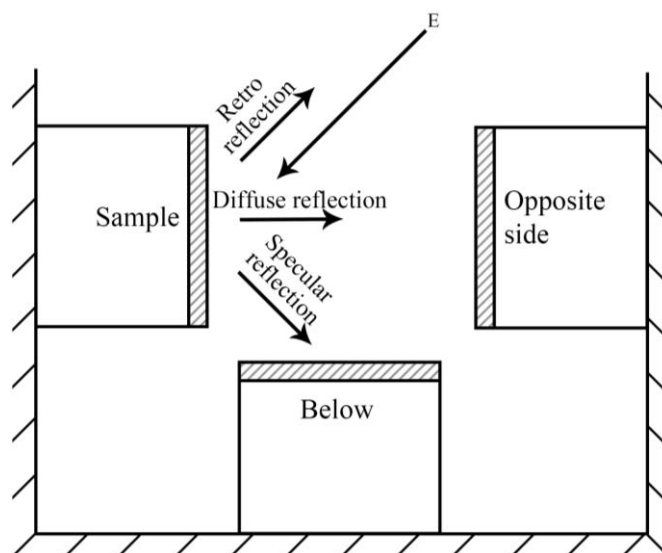
Fig. 2-5. Schematic diagram of thermal balance, proposed in [50, 104]

Sakai et al. [65, 66, 105] and Yuan et al. [57] further improved the thermal balance method, based on Sakai et al. [50, 104] and employed the spectrophotometers to measure the specular reflectance and diffuse reflectance. However, under the outdoor environment, which was different from the ideal environment of laboratories, the errors would be generated easily by sunshine, wind speed and other meteorological conditions, so RR-coatings with known reflectivity were usually used as the reference sample. Further, to minimize the calculation error of solar reflectivity estimated by the thermal balance, Yuan et al. [44] studied the influence of the experimental plate size on the heat loss through experimental calculations and computational fluid dynamics simulations and they proposed a suitable size of the experimental plate.

(2) Equivalent albedo

The equivalent albedo was introduced by Castellani et al. [106] and defined as the ratio between the reflected radiation and the incident radiation over the canyon's ceiling to evaluate the global cooling effect of retro-reflective pavements and facades on a physical model. Morini et al. [107] monitored the trend of the instantaneous albedo, and used the equivalent albedo to demonstrate the effectiveness of RR-coatings, and investigated the effect of different canyon

patterns on the equivalent albedo. Rossi et al. [42] divided the canyon ceiling into an imaginary grid of 90 measurement points and measured the equivalent albedo of every point. And the properties of RR-coatings were compared with those of traditional diffused materials by studying the spatial distribution of albedo at the canyon's ceiling.

(3) Other estimation methods

Inoue et al. [71] defined the effective reflected rate as the proportion of solar radiation reflected upward toward the sky without striking a nearby building to assess the impact on the thermal environment of the surrounding urban area. Levinson et al. [62] estimated the effective solar reflectivity of measurement specimens by comparing their temperatures in the sun to those of reference specimens. Yoshida et al. [108, 109] considered the influence of thermal environment conditions, such as wind speed, temperature, humidity, and radiation by using the fluid mechanics and made a quantitative evaluation of the effect of RR-coatings on the thermal environment of outdoor space in the actual city blocks. Yuan et al. [110] proposed an appropriate analytical model to evaluate the reflective directional characteristics of RR-coatings. Based on Gebhardt theory, which is basically view factors corrected to consider the shortwave inter-reflections between surfaces, Andrea et al. [75] exploited a numerical model based to account for the mutual inter-reflection between surfaces facing in the street canyon.

2.4.3 High-precision measurement methods of retro-reflectivity

The key technology of retro-reflectivity is to gain the clear distribution of the reflected light, especially along the incident direction, and according to this, some measurement systems are proposed and includes the emitting-receiving optical fiber system, the angular distribution measurement method of reflected light and Bi-directional reflectivity measurement method.

(1) The emitting-receiving optical fiber system

One of the challenges in quantifying the retro-reflectivity characteristics of RR-coatings is how to measure the retro-reflected beam in the same direction as the incident beam, which requires the light source and the detector to be at the same angle. Therefore, the fiber system with the light source and the detector was developed in the same probe to measure the retro-reflectivity and according to this method, Sakai et al. [67, 68] firstly designed a test equipment integrated with spectrometers, optical fiber probe and halogen light source to measure the reflection characteristics of RR-coatings. Based on Sakai et al. [67, 68], Yuan et al. [48, 55, 73, 81] developed an emitting-receiving optical fiber system and Fig. 2-6 showed the instrument photo and principal diagram. The fiber probe has seven glass fibers, six of which were used to emit the light and the rest one located at the center was employed to receive the reflected light

from the sample surface. Through the multiple measurement of several types of RR-coatings, the measured values by the emitting-receiving optical fiber system were found to be correlated well with results obtained by an accurate measurement, so the measured value using this system was relative, and not absolute. Yuan et al. [110] took the optical experiment result as the truth value and proposed an appropriate analytical model of evaluating the reflective directional characteristics of RR-coatings. In addition, Ghebrebrhan et al. [54] also design the similar experimental goniometer.
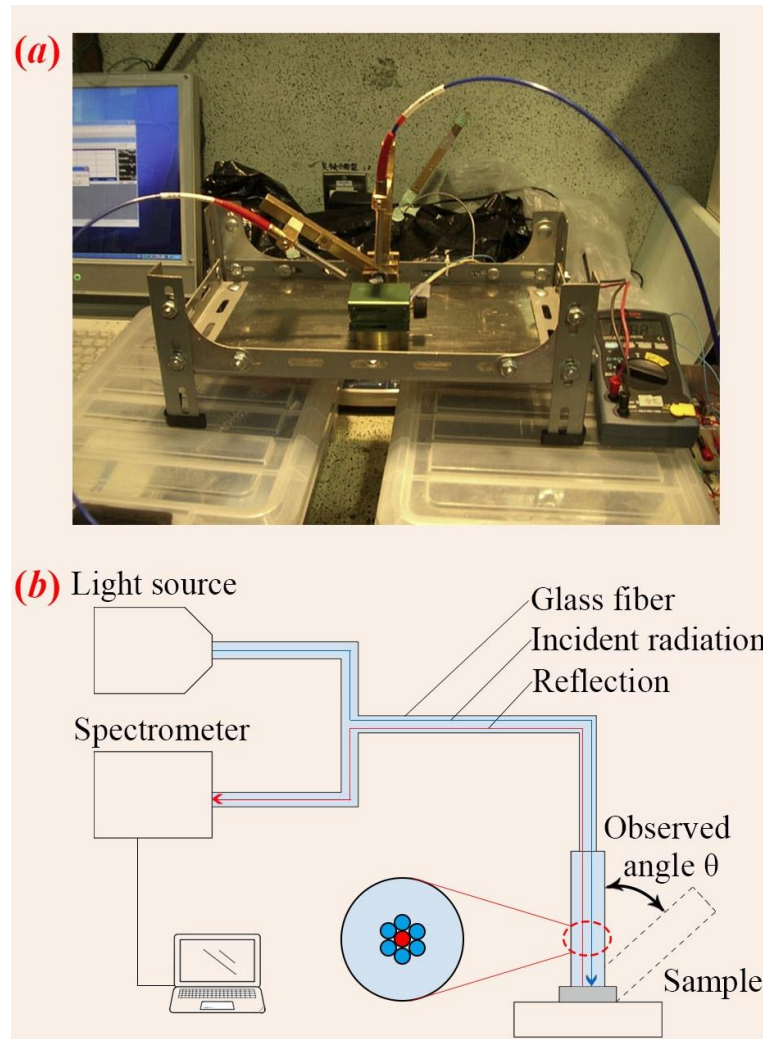
Fig. 2-6. Emitting-Receiving optical fiber system from Yuan et al. [48, 55, 73, 81]: (a) The instrument photo and (b) the system principal diagram

(2) The angular distribution measurement method of reflected light

Rossi et al. [103] designed an ad-hoc experimental facility to measure the angular distribution as shown in Fig. 2-7 and this facility was mainly composed by an artificial solar source and a measurement box, which consisted of a horizontal sample plane made of a highly absorbent

black material, a radiometric probe, and an angular positioner (nine observer angles ranging from -70° to 70°). Because the sample plane could not be tilted, the angular distribution was measured only in one plane. And Rossi et al. [45] improved the above experimental facility. In the improved facility, a semicircular array of 19 fixed photodiodes (observer angles ranging from -90° to 90°) was employed to measure the angular distribution of reflected light, while the sample had different inclinations though rotating its platform.

1. Solar Source   6. Measurement position
2. Box   7. Lens support
3. Lens   8. Shutter
4. Radiometer probe   9. Lamp plan
5. Sample   10. Setup system
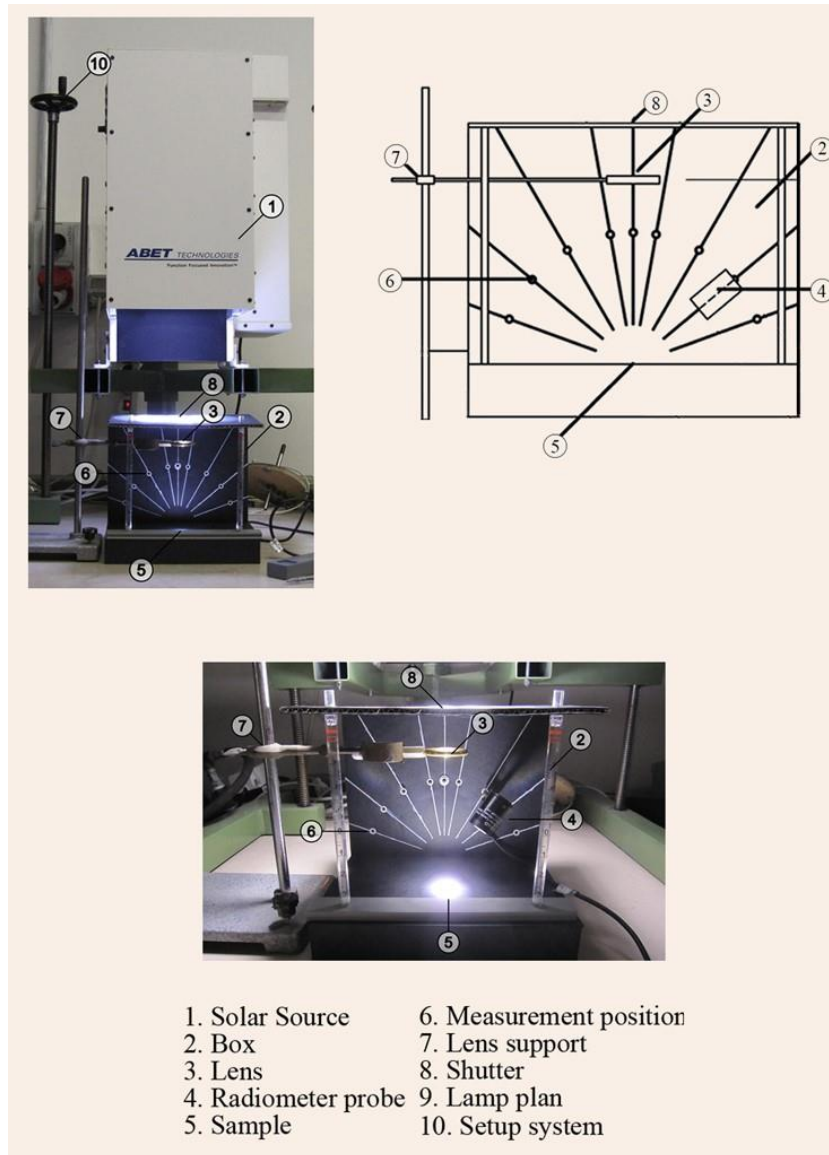
Fig. 2-7. Schematic of measuring the angle distribution of reflected light from Rossi et al. [103]

(3) Bi-directional reflectivity measurement method

Bi-directional reflectivity distribution function can describe the direction distribution of the reflected light and then the radiation flux between any pair of incidence and reflection direction

[111-114]. However, detecting the bi-directional reflectance distribution function of retro-reflective samples by using the goniometer faced a special challenge. If the incidence and reflection direction was close, the light source and the detector would keep out each other. A flat beam splitter was introduced between the light source and the sample. The light from the light source was transmitted to the sample by the beam splitter, while the retro-reflective light was reflected to the detector by the beam splitter.

Belcour et al. [52] presented an improved bi-directional reflectance distribution function goniometer in Fig. 2-8(a). The measurement device included the light source, a beam steerer consisting of two mirrors, a beam splitter, a rotating stage, a rotating arm, and a detector. The main difference compared with a three-dimension isotropic gonio reflectometer was that the detector did not occlude the incoming light source, which was achieved by the beam splitter. It was found that the bi-directional reflectance distribution function value would decrease with the incident angle increment. Ichinose et al. [72] and Harima and Nagahama [115, 116] measured the bi-directional reflectivity of RR-coatings with a two-axis solar gonio-spectrophotometer in Figs. 2-8(b) and 2-8(c), respectively. The device consisted of three different spectral photodetectors, a gonio-spectrophotometer, a half mirror, and a sample table. Grobe [117] developed a novel extension to a goniometer for the measurement of bi-directional reflectivity of retro-reflective coating applied to shutters in Fig. 2-8(d). Light source had a collimator, and the spot size was adjusted to about 10mm in diameter by focusing the beam slightly. And the wavelength dependent transmission and reflection properties were compensated by employing two beam-splitters. The measured data set was compiled into a data-driven reflection model of daylight simulation software.
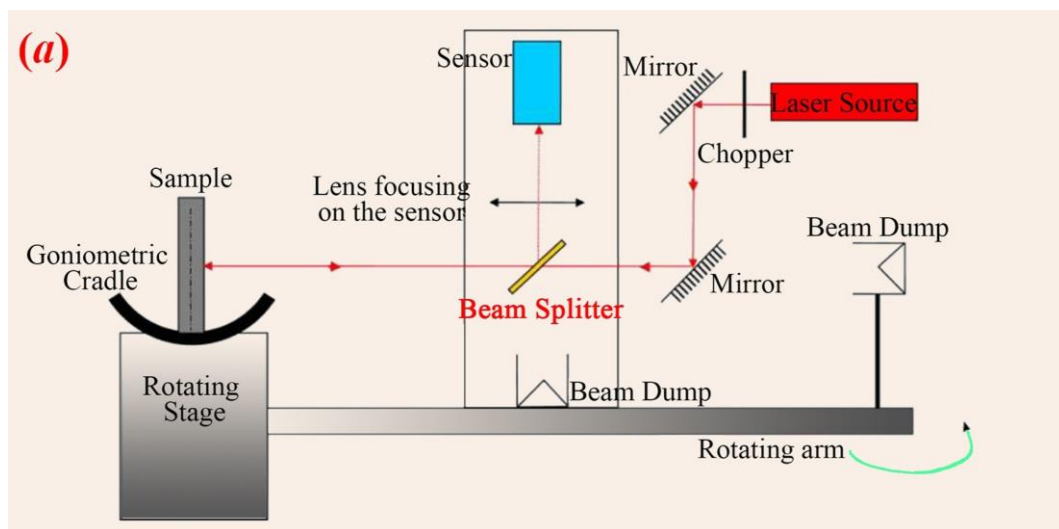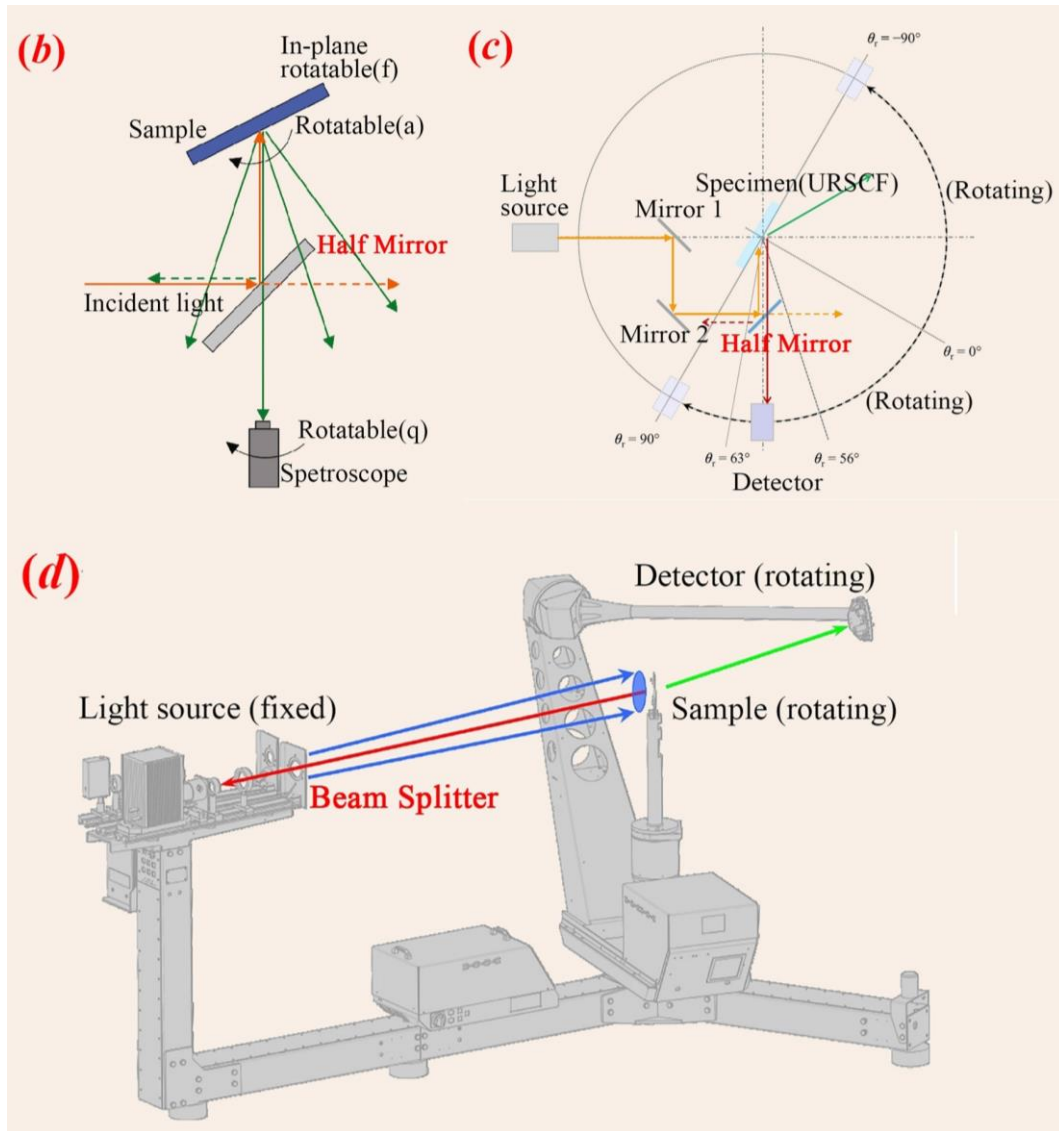
Fig. 2-8. Schematic of measuring bi-directional reflectivity from (a) Belcour et al. [52], (b) Ichinose et al. [57, 72], (c) Harima and Nagahama [115, 116], and (d) Grobe [117]

2.4.4 Comprehensive comparison on the different retro-reflectivity method

RR-coatings reflected the incident radiation along the incoming radiation, so the traditional reflectivity measurement methods were unable to analyze the optical properties of RR-coatings quantitatively in different directions. Their reflectivity should be characterized through specific technologies and procedures, which were able to capture their singular behavior over the hemisphere in different directions [103].

Table 2-3 compared five above measurement methods of retro-reflectivity. As shown in Table 3, the thermal balance method and equivalent albedo method are the evaluation ones with the low measurement accuracy. And the former is easy to cause errors due to the disturbance from

outdoor thermal environment, while the latter produces the large measurement results due to considering the upward diffuse component. And three other methods have the high-precision measurement. Although the emitting-receiving optical fiber method measures the retro-reflectivity, it cannot gain the angle distribution of the reflected light, as the angular distribution method and Bi-directional reflectivity method. In the building application of RR-coatings, the angle distribution of the reflected light is very important to assess the optical properties of RR-coatings comprehensively, so the angular distribution method and Bi-directional reflectivity method are recommended.

Table 2-3 Comparison on the measurement methods of retro-reflectivity

| Method | Measurement accuracy | The reflected light | | Reference |
		Along the incident direction	All direction	
Thermal balance method	Low	No	No	[50, 57, 65, 66, 104, 105]
Equivalent albedo method	Low	No	No	[42, 106, 107]
Emitting-receiving optical fiber method	High	Yes	No	[48, 54, 55, 67, 64, 73, 81]
Angular distribution method	High	Yes	Yes	[45, 103]
Bi-directional reflectivity method	High	Yes	Yes	[52, 72, 115-117]

2.5. Application efficiency of RR-coatings

RR-coatings had the optical property to reflect the incident light back along the incident direction, which leaded to the reduction of the absorbed solar radiation, and thereby the urban thermal environment and energy consumption in buildings must be affected. In the following content, the application efficiency of RR-coatings was reviewed comprehensively on the urban reflectivity, the urban surface temperature, the air temperature, and the energy consumption of buildings.

2.5.1 On the urban reflectivity

RR-coatings can increase the urban reflectivity to reflect more solar radiation, so the urban

radiant heat gain would be reduced correspondingly and thereby, alleviate the urban heat island [118-120]. And urban reflectivity was a comprehensive evaluation index of application efficiency from RR-coatings.

For covering RR-coatings on windows, Yoshida and Mochida [108] covered RR-coatings on windows of an isolated building with window to wall ratio (WWR) of 80% and evaluated the solar radiant environment around an isolated building in summer using Computational Fluid Dynamics (CFD) method coupled with the radiant model. It was estimated that the amount of solar radiation reflected into the sky of the retro-reflective windows increased by 13%, compared to windows with heat-shading films. Another study of Yoshida et al. [109] found that retro-reflective windows reflect 36% more solar radiation into the sky than windows with heat-shading films. Ichinose et al. [72] compared the upward reflected solar irradiance of the low-E glass, the clear float glass, and the clear float glass with retro-reflective film with a reflectance of 60%-70% numerically. Their results showed that the upward reflected solar irradiance was 60%~70% for the retro-reflective film as compared to 45%~55% for the low-E and the clear float glass. And Inoue et al. [121] did the similar study with Ichinose et al. [72] by a comparative experiment and found that the retro-reflective film could reflect about 30% of near-infrared light upwards with the solar incident angle of 60° and that the reflected solar radiation was reduced to approximately 1/3 that of Low-E glass.

For covering RR-coatings on building facades, Inoue et al. [121] simulated the simplified high-rise building model covered by retro-reflective film on all surfaces and found that the retro-reflective film increased the upward reflection ratio of solar radiation by 5% on average. And another study of Inoue et al. [71] showed the annual amount of reflected solar radiation increased by 7%~8%, when all vertical faces of buildings were covered with the saw-tooth type retro-reflective film. Yuan et al. [84] simulated the influence of building surfaces with different reflective characteristics on the albedo of a two-dimensional urban canyons, and found the albedos were increased by up to 10% in summer and 33% in winter due to covering prism retro-reflective coating with a reflectivity of 81% on wall surfaces, compared with diffuse and specular reflection materials. On this basis, Yuan et al. [48] studied the effect of glass beads with refractive indexes of 1.9 and 1.5 on city albedo and their results showed that RR-coatings with a refractive index of 1.9 were more effective in improving urban albedo. In addition, Morini et al. [107] built two building group models (the block pattern and canyon pattern) and found that due to adding RR-coatings, the equivalent albedos were increased by 3% and 7% for the block pattern and the canyon pattern, respectively, compared to conventional construction materials with similar global reflectance.

For covering RR-coatings on the road or pavement in urban canyon, Castellani et al. [106] covered prism RR-coatings with a reflectivity of 62.4% on vertical wall surface and horizontal pavement surface. It was gained that the equivalent albedo on the canyon increased from 89.0% to 94.0% with a consequent reduction of the thermal energy trapped inside the canyon. And in the latter study of Rossi et al. [42], the albedo distribution on the upper horizontal surface of urban canyon was measured by an imaginary grid of 90 measurement points. Their results showed the increased value the maximum albedo could be up to 4.6% for prism RR-coatings with a reflectivity of 62.9%, with respect to the white and beige diffusive materials.

Table 2-4 showed the main outcomes on urban reflectivity by covering RR-coatings on windows, walls, and roads. It can be obviously seen that RR-coatings can increase the urban reflectivity by 3%~36%, which could alleviate the urban thermal island efficiently.

Table 2- 4. Review on the influence of RR-coatings on urban reflectivity

Ref.	Application	Type of RR-coatings (reflectivity)	Method	City	Outcomes on upward reflectivity
Yoshida and Mochida [108]	Windows in a single building (WWR=80%)	Transparent	Sim.	Tokyo, Japan	13%, compared to single glass with heat-shading films
Yoshida et al. [109]	Windows in a street canyon (WWR=80%)	Transparent	Sim.	Tokyo, Japan	Approximately 36%, compared to single glass with heat-shading films
Ichinose et al. [72]	Windows in urban canyon (WWR=60%)	Transparent (60%-70%)	Sim.	Tokyo, Japan	About 15%, compared to the low-E glass and the clear glass
Inoue et al. [121]	A single window	Transparent	Exp.	Tokyo, Japan	33%, compared to the low-E glass
Inoue et	Windows in	Transparent	Sim.	Singapore,	5%, compared to the

al. [121]	high-rise building groups			Bangkok, Tokyo, New York	low-E glass
Inoue et al. [71]	All vertical faces of buildings	--	Sim.	Tokyo, Japan	About 7%~8%, compared to the conventional faces
Yuan et al. [84]	Building walls in urban canyon	Prism (81%)	Sim.	Osaka, Japan	10% in summer and 33% in winter, compared to the north-facing wall with diffuse martials and the south-facing wall with mirror martials
Yuan et al. [48]	Building walls in urban canyon	--	Sim.	Osaka, Japan	More effective (unspecified)
Morini et al. [107]	Building walls in the block pattern	--	Exp.	Terni, Italy	3%, compared to the traditional concrete
Morini et al. [107]	Building walls in the urban canyon pattern	--	Exp.	Terni, Italy	7%, compared to the traditional concrete
Castellani et al. [106]	Pavement and walls in urban canyon	Prism (62.4%)	Exp.	Perugia, Italy	5%, compared to the traditional concrete
Rossi et al. [42]	Roads in urban canyon	Prism (62.9%)	Exp.	Perugia, Italy	4.6%, compared to the white and the beige diffusive materials

2.5.2 On the urban surface temperature

Solar radiation acts directly on urban surfaces and thereby, the urban surface temperature is an important factor on the application efficiency of RR-coatings [122-124]. For covering RR-coatings on the window glass, Martin et al. [30] found compared with the low-E glass, the surface temperature due to using retro-reflective glass with a reflectivity of 42% was reduced by 0.75°C and 7.75°C at least for the pavement surface temperature and glass surface temperature at around 12 pm, respectively. Inoue et al. [121] compared the temperatures of the glass surface and the pavement surface for the single glass, the single glass with retro-reflective film and solar-shading Low-E double glazing, as showed in Fig. 2-9(a) and Fig. 2-9(b) showed the infrared imagery of temperatures in the pavement surface before widows. It was found that the average temperatures in the pavement surface for single-pane glass with RR-coatings were reduced by 1.5°C and 7.9°C compared with the single glass and solar-shading Low-E double glazing, respectively. It showed RR-coatings reflected more solar radiation was reflected upwardly and thereby, urban thermal environment was improved.
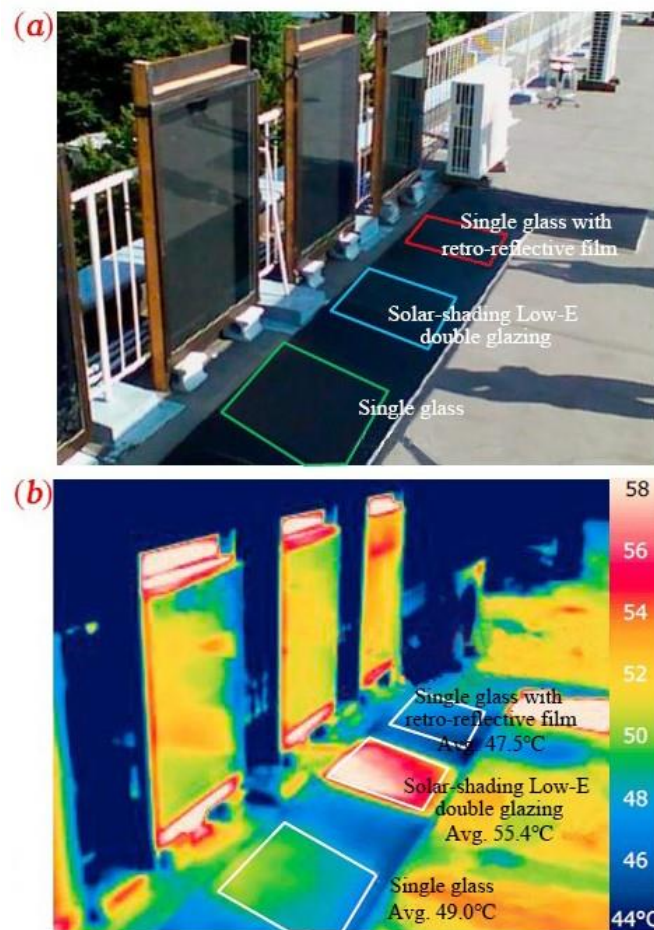
Fig. 2-9. (a) The experimental schematics of three windows and (b) The infrared imagery of temperatures [121]

For covering RR-coatings on buildings, Castellani et al. [78] built two full-scale vertical surfaces covered with glass bead retro-reflective plaster with a reflectivity of 49.2% and diffusive plaster, respectively, as showed in Fig. 2-10(a). And the experimental results showed the globe temperature in the front of the retro-reflective wall does not differ sensibly from values in front of the diffusive wall from the monitoring campaign, but the retro-reflective wall had a lower superficial temperature with respect to the diffusive wall in Fig. 2-10(b).
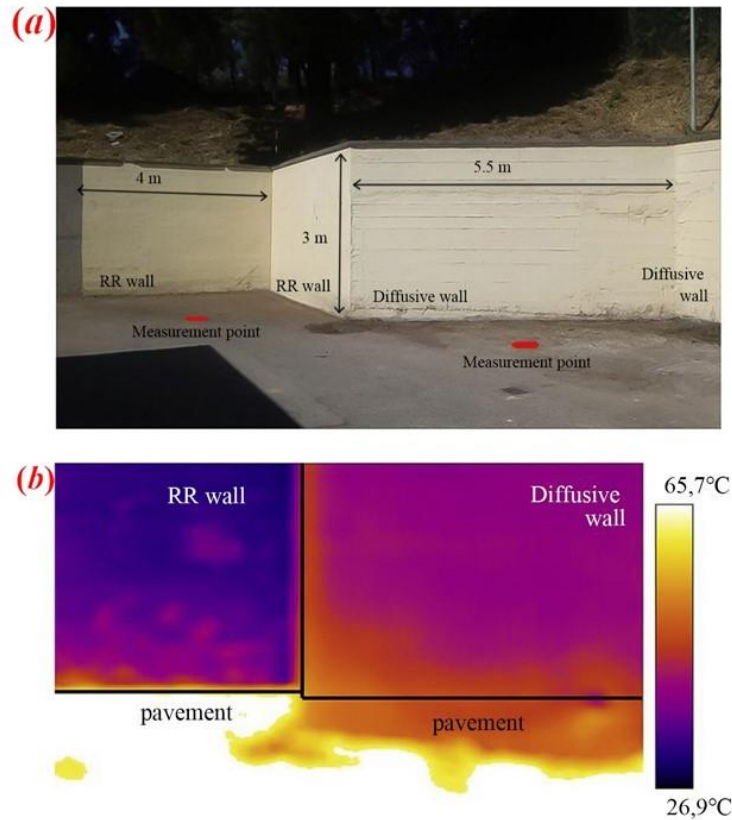
Fig. 2-10. (a) Two full-scale vertical surfaces and (b) the infrared imagery of superficial temperatures of two surface [78]

In addition, Han et al. [46] simulated a system consisting of a stand-alone reference building and a testing surface on the west side to compare the thermal performance of diffusive and transparent retro-reflective surfaces with a reflectivity of 71.0%-77.8%. Their finding showed compared with diffuse surface, the average temperatures were lowered by 0.43°C, 0.85°C, and 0.99°C at 7a.m., 9a.m. and 11a.m, while the maximum temperatures were decreased by 0.66°C, 1.39°C, and 1.64°C at 7a.m., 9a.m. and 11a.m. Meng et al. [15] made a comparative experiment on two building models, one of which was covered by capsule retro-reflective material with a reflectivity of 54.3% and another was taken as a reference. Their experimental results showed adding RR-coatings reduced by 10°C and 25°C for the peak temperatures of inner and outer

surfaces, respectively. Meanwhile, a one-dimensional wall heat transfer model was built for four typical walls and the numerical data indicated that outer surface peak temperatures were lowered by 10°C~20°C, compared with the exterior finishing material due to RR-coatings and that the larger the thermal resistance, the higher the outer surface temperature reduction. Qin et al. [125] built two small-scale building blocks with glass bead RR-coatings with a reflectivity of 54.3% and diffuse-reflective materials as showed in Fig. 2-11(a). Fig. 2-11(b) and 2-11(c) showed outer and inner surface temperatures at the eastern. As shown, outer surface temperatures of retro-reflective surface were 5°C~10°C lower than that of diffuse-reflective surface during early afternoon, while the lowered temperatures were up to about 1.0°C~3.0°C at noontime and about 1°C at night. It showed the retro-reflective wall could keep the building blocks cooler than the diffuse-reflective wall during a sunny climate.
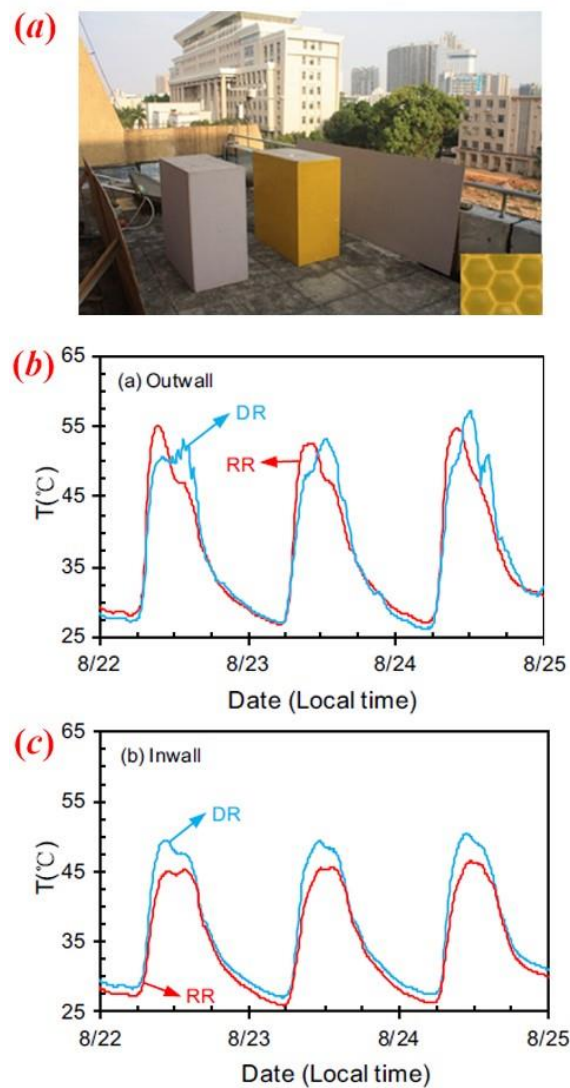
Fig. 2-11. (a) The experiment of two building blocks, (b) outer surface temperature and (c) inner surface temperature [125]

Rossi et al. [63] applied prism RR-coatings with a reflectivity of 62.8% in building envelopes of urban canyons and focused on the temperature trends inside canyons by a summer monitoring campaign. It was found that although RR-coatings had solar reflectance of 62.8%, lower than that of the diffusive sample of 86.5%, the pavement temperatures covered by RR-coatings were always lower than those of diffusive pavements and the maximum difference was 3~7°C during the hottest hours of the day, compared to the white diffuse cooling material. Zhang et al. [126] applied capsule RR-coatings with a reflectivity of 62.3% on tents to improve the poor indoor thermal environment. And adding RR-coatings could reduce outer surface peak temperature by 5.8~15°C and 3.4~5.2°C in the period 10:00~18:00 and 18:00~24:00, while the reduced values in inner surface for peak temperature and average temperature could reach to 9.2°C and 4.9°C, respectively.

Table 2-5 showed the main outcomes on the urban surface temperatures by covering RR-coatings. It was found that covering RR-coatings could reduce urban surface temperature efficiently, which showed the potential benefits of RR-coatings in the urban surface temperature.

Table 2-5. Review on the influence of RR-coatings on urban surface temperatures

Ref.	Application	Type of RR-coatings (reflectivity)	Method	City	Reduced surface temperature
Martin et al. [30]	Highly-glazed facades in urban canyon	Transparent (42%)	Sim.	Tokyo, Japan	0.75°C and 7.75°C for temperatures in the pavement surface and the glass surface, compared to low-E glass
Inoue et al. [121]	Building wall in urban canyon	---	Exp.	Tokyo, Japan	1.5°C and 7.9°C for temperatures in the pavement surface, compared to single-pane glass and solar shading Low-E double glazing

Yoshida et al. [136]	Windows in urban canyon (WWR=80%)	Transparent	Sim.	Tokyo, Japan	4.3°C for the mean radiant temperature, compared to the Low-E double glass
Yoshida and Mochida [108]	Windows in a single building (WWR=80%)	Transparent	Sim.	Tokyo, Japan	6.0°C for the mean radiant temperature, compared to single glass with heat-shading films
Yoshida and Mochida [109]	Windows in a single building (WWR=80%)	Transparent	Sim.	Tokyo, Japan	5°C for the mean radiant temperature, compared to single glass with heat-shading films
Han et al. [46]	Building wall	Transparent (71.0%-77.8%)	Sim.	Minneapolis and Miami, UAS	0.43°C~0.99°C and 0.66°C~1.64°C for the average and peak temperatures in wall surfaces, compared to the diffusive materials
Castellani et al. [78]	full-scale vertical surfaces	Glass bead (49.2%)	Exp.	Perugia, Italy	Keep a lower superficial temperature with respect to the diffusive wall (unspecified)
Meng et al. [15]	Building model	Capsule (54.3%)	Exp. & Sim.	Chengdu, China	5°C~10°C and 4.5°C~25°C for the peak temperatures in inner and outer surface, compared

					with prefab house wall
Qin et al. [125]	Building model	Glass bead (41.8%)	Exp.	Guangxi, China	1.0°C~3.0°C and 5°C~10°C for the peak temperatures in inner and outer surfaces, compared to the diffuse-reflective wall at nighttime
Rossi et al. [63]	Urban canyon model	Prism (62.8%)	Exp.	Perugia, Italy	3°C~7°C for the peak temperature in the pavement, compared to the white diffuse cooling material
Zhang et al. [126]	Tent model	Capsule (62.3%)	Exp.	Chengdu, China	3.4°C~15°C and 4.9°C~9.2°C for the peak temperatures in inner and outer surfaces, compared to tents without RR-coatings

2.5.3 Air temperature

Solar radiation acts directly on urban surfaces, which affects the urban air temperature directly and then indoor air temperature by wall heat transfer concurrently. Therefore, the influence of RR-coatings was reviewed on urban and indoor air temperatures [127-129]. For the urban air temperature, Inoue et al. [71, 121] found the sol-air temperature of transparent single-pane glass with retro-reflective film was nearly 10°C lower than that of Low-E glass. Rossi et al. [63] found that when prism RR-coatings with a reflectivity of 62.8% were applied to the vertical surface of the urban canyon, air temperature decreased by 1% compared with the white diffuse cooling material from the result of a summer monitoring campaign. Yoshida et al. [108, 109] evaluated the thermal comfort for pedestrians in a single building and a two-dimensional square cavity-type street canyon in the summer season. And compared with heat-

shading films, respectively, the new standard effective temperatures windows were lowered by about 1.7°C [108] and 1.2°C [109] for two physical models.

For indoor air temperature, Zhang et al. [130] and Meng et al. [131] covered prism RR-coatings with a reflectivity of 59% and glass bead RR-coatings with a reflectivity of 54.3% on prefab houses, respectively. Their experimental results showed covering RR-coatings on prefab houses could reduce the average and peak temperatures of indoor air by 2.4°C and more than 7°C, compared to the prefab houses without RR-coatings. Zhang et al. [126] covered capsule RR-coatings with a reflectivity of 62.3% on the tent model and found that the peak temperature of indoor air was lowered by 7.0°C, compared to the ordinary tent. The similar research had been conducted by Xu et al. [132] and their experimental data showed the peak and average temperatures of indoor air were reduced by 7.0°C and 3.1°C, respectively, compared with the normal tents.

Table 2-6 showed the main outcomes on air temperatures by covering RR-coatings. As shown, because more solar radiation was reflected by RR-coatings, urban air temperature was reduced efficiently as the evaluation index of the heat island intensity.

Table 2-6. Review on the influence of RR-coatings on air temperature

Ref.	Application	Type of RR-coatings (reflectivity)	Method	City	Reduced air temperatures
Inoue et al. [71, 121]	Window model	---	Exp.	Tokyo, Japan	10°C for urban sol-air temperature, compared to Low-E glass
Rossi et al. [63]	Urban canyon vertical surface	Prism (62.8%)	Exp.	Perugia, Italy	1% for urban air temperature, compared to white diffusive materials
Yoshida and Mochida [108]	Windows in a single building (WWR=80%)	---	Sim.	Tokyo, Japan	1.7°C for the new standard effective temperature, compared to single glass with

					heat-shading films
Yoshida et al. [109]	Windows in a street canyon (WWR=80%)	---	Sim.	Tokyo, Japan	1.2°C for the new standard effective temperature, compared to single glass with heat-shading films
Zhang et al. [130]	Building model	Prism (59%)	Exp.	Chengdu, China	2.4°C for the average air temperature, compared to the prefab house without RR-coatings.
Meng et al. [131]	Building model	Glass bead (54.3%)	Exp.	Chengdu, China	7°C for the peak air temperature, compared to the prefab house without RR-coatings.
Zhang et al. [126]	Tent model	Capsule (62.3%)	Exp.	Chengdu, China	7.7°C for indoor air peak temperature, compared to the ordinary tent
Xu et al. [132]	Tent model	Glass bead (62.3%)	Exp.	Chengdu, China	7.0°C and 3.1°C for the peak and average temperatures of indoor air, compared to the ordinary tent

2.5.4 Building energy consumption

RR-coatings can reflect solar radiation and then improve urban thermal environment. Under this condition, building cooling consumption would be reduced obviously [133-135], but more solar radiation was reflected, which resulted into increasing the heating consumption in winter. The influence of RR-coatings was reviewed on heating and cooling energy consumption as following:

For covering RR-coatings on the window glass, Ichinose et al. [72] investigated the long-term energy conservation of transparent retro-reflective film with a reflectance of 60%- 70% on an office building with a window ratio of 60%, and found that compared with the ordinary transparent glass, the retro-reflective film decreased the total energy consumption by about 20%, but the retro-reflective film had a slight increment due to the thermal insulation effect in winter. Yoshida et al. [136] covered the retro-reflective film with a reflectance of 48.7% on single float glass window on the west side of the building with a window ratio of 80%, and it was found the cooling load was reduced by 489 MJ/h, decreased by 23%, but the heating load was increased by 534 MJ/h, compared to the window with heat shading film and the Low-E double glass.

For covering RR-coatings on building walls, Yuan et al. [84] simulated loads and energy consumption of one floor of a building with air-conditioned area of 605m^2, located in Shanghai, China and it is found that covering RR-coatings with a reflectance of 81% could decrease the cooling loads in summer but increase the heating loads in winter. Compared with no retro-reflective material coating, the cooling and heating loads had the biggest reduction of about 15% and -5% respectively, while the annual cooling and heating loads were decreased by 157 MJ/(m^{2}žyear) and -71 MJ/(m^{2}žyear) respectively. And the equivalent annual carbon dioxide emissions were reduced by about 3.3kg/(m^{2}žyear) due to retro-reflective material coating.

Moreover, Han et al. [46] modeled a bio-inspired retro-reflective envelope applied on a three-floor building with an overall floorage of 900m^2, and found that total energy consumption and cooling energy consumption were reduced by up to 8.2% and 9.8% in different metropolitan areas of the United States. Mauri et al. [74] built a three-floor building with a net floor area of 182m^2 and simulated the cooling and heating energy consumption of this building. Their numerical results showed applying RR-coatings in building facades could decrease the cooling demand from 4.1 kWh/(m^{2}žyear) to 3.5 kWh/(m^{2}žyear) in Milan, from 8.5 kWh/(m^{2}žyear) to 7.8kWh/(m^{2}žyear) in Rome, and from 13.6 kWh/(m^{2}žyear) to 12.6 kWh/(m^{2}žyear) in Palermo, compared to the diffusive material with the same reflectivity. And the corresponding increment in heating energy demands did not affect negatively, since the energy advantages obtained for summer season were higher than the winter energy disadvantage. Zhang et al. [130] took a typical room with a south-facing external wall in an office building of 6900m^2 in Chengdu, China. Their numerical results showed that after applying the prism RR-coatings with a reflectance of 59%, the cooling load could be reduced by about 9.1W/m^2, leading to the 15.2% reduction of electricity consumption in a whole summer, and that the incremental investment for coating could be paid back by 9.1 years in Chengdu. However, energy efficiency would be affected by the weather conditions. The payback periods were 6.8 years and 21 years in

Guangzhou and Harbin, which were affected by the length of the cooling period.

In addition, Xu et al. [132] simulated the energy consumption of tents with 600 mm (Length) × 600 mm (Width) × 600 mm (Height) by building the simulation model, and found after applying the glass bead retro-reflective film with a reflectance of 62.3%, the energy saving rate of the tent was 10.44%. Table 2-7 showed the main outcomes on building energy consumption by covering RR-coatings. As shown, energy conservation efficiency of RR-coatings was quite remarkable, although the heating energy consumption would be increased due to the less solar radiation absorption.

Table 2-7. Review on the influence of RR-coatings on building energy consumption

Ref.	Application	Type of RR-coatings (reflectivity)	Method	City	Reduced energy consumption
Ichinose et al. [72]	Building window	Transparent (60%-70%)	Sim.	Tokyo, Japan	20% for total energy consumption, compared to the normal transparent glass
Yoshida et al. [136]	Building window	---	Sim.	Tokyo, Japan	489 MJ/h (23%) and -534 MJ/h for cooling and heating energy, compared to the Low-E double glass
Yuan et al. [84]	Building walls	Prism (81%)	Sim.	Shanghai, China	19% and -6% for the annual cooling and heating load and 3.3kg/(m^2·year) for the equivalent annual carbon dioxide emissions, compared to no retro-reflective material coating

Han et al. [46]	Urban block vertical surface	Transparent (71.0%-77.8%)	Sim.	Miami and Minneapolis, UAS	8.2% and 9.8% for total energy consumption and cooling energy, compared to the diffusive materials
Mauri et al. [74]	Building walls	---	Sim.	Palermo, Milan, Rome	8.1%~16.1% and -1.1%~-7.6% for cooling and heating energy, compared to the diffusive material with the same reflectivity
Zhang et al. [130]	Building walls	Prism (59%)	Sim.	Chengdu, China	9.1W/m^2 (15.2%) for cooling energy, compared to building without RR-coatings
Xu et al. [132]	Tent model	Glass bead (62.3%)	Sim.	Chengdu, China	10.44% for the total energy, compared to the normal tent

2.6. Conclusion and outlook

RR-coatings are proposed to alleviate the urban thermal island since 2004 and have received much attention, due to the fact that they can reflect solar radiation back along the incident direction. This review mainly summarizes all recent advances on the optical property, measurement methods and application efficiency in buildings covered by RR-coatings. In general, the optical property of RR-coatings was greatly affected by retro-reflective mechanism, the glass refractive index and reflective coating. The measurement methods on the traditional solar reflectivity and retro-reflectivity were discussed in detail. This review focused on a brief summary on the application efficiency about the urban reflectivity, urban surface temperature, urban and indoor air temperature, and building energy consumption. Important conclusions and recommendations are as following:

● Retro-reflectivity is the most important property of RR-coatings. However, there is a great flaw for the present RR-coatings and namely, retro-reflectivity would decay shapely

under the high incidence angle of solar radiation. It is the main optimization direction of RR-coatings.

● Measurement methods of both solar reflectivity and retro-reflectivity have been mature, but applying the reflected radiation along the incident direction strictly to calculate the retro-reflectivity is too harsh to assess the actual contribution of RR-coatings. The effective retro-reflectivity needs to be proposed to evaluate the actual contribution from RR-coatings.

● Due to covering RR-coatings, the sharp improvement of urban reflectivity has been proved, but the more detailed distribution of solar radiation in urban ceilings has not been involved in present published papers. And this detailed distribution was important for building energy consumption and urban thermal environment.

● The influence laws of RR-coatings have been gained on the urban thermal environment and building thermal environment in the model experiment and numerical simulation. It needs long-term monitoring and the following effective assessment on the application efficiency of RR-coatings in the single building or building groups.

● RR-coatings had been certified to reduce the cooling energy consumption at the expense of a certain increment of heating energy consumption and thereby, the energy consumption contribution from RR-coatings has related to local climatic conditions closely and directly. Therefore, the climate applicability of RR-coatings is worthy of discussion.

The challenges and opportunities addressed in this review would provide a direction for future studies on RR-coatings.

References

[1] Y. Wang, D. Mauree, Q. Sun, H. Lin, J.L. Scartezzini, R. Wennersten. A review of approaches to low-carbon transition of high-rise residential buildings in China. Renewable and Sustainable Energy Reviews 131 (2020) 109990.

[2] S.H. Cho, T.K. Lee. A study on building sustainable communities in high-rise and high-density apartments e Focused on living program. Building and Environment 46 (2011) 1428-1435.

[3] W. Pan, M. Pan. A dialectical system framework of zero carbon emission building policy

for high-rise high-density cities: Perspectives from Hong Kong. Journal of Cleaner Production 205 (2018) 1-13.

[4] L. Gustavsson, T. Nguyen, R. Sathre, U.Y.A. Tettey. Climate effects of forestry and substitution of concrete buildings and fossil energy. Renewable and Sustainable Energy Reviews 136 (2021) 110435.

[5] F. Rosso, A.L. Pisello, V.L. Castaldo, C. Fabiani, F. Cotana, M. Ferrero, W. Jin. New cool concrete for building envelopes and urban paving: Optics-energy and thermal assessment in dynamic conditions. Energy and Buildings 151 (2017) 381-392.

[6] T. Kubota, H.S. Lee, A. R. Trihamdani, T.T.T. Phuong, T. Tanaka, K. Matsuo. Impacts of land use changes from the Hanoi Master Plan 2030 on urban heat islands: Part 1. Cooling effects of proposed green strategies. Sustainable Cities and Society 32 (2017) 295-317.

[7] B. Castellani, E. Morini, M. Filipponi, A. Nicolini, M. Palombo, F. Cotana and F. Rossi. Comparative Analysis of Monitoring Devices for Particulate Content in Exhaust Gases. Sustainability 6 (2014), 4287-4307.

[8] A.G. Touchaei, Y. Wang. Characterizing urban heat island in Montreal (Canada)-Effect of urban morphology. Sustainable Cities and Society 19 (2015) 395-402.

[9] M. Karteris, I. Theodoridou, G. Mallinis, E. Tsiros, A. Karteris. Towards a green sustainable strategy for Mediterranean cities: Assessing the benefits of large-scale green roofs implementation in Thessaloniki, Northern Greece, using environmental modelling, GIS and very high spatial resolution remote sensing data. Renewable and Sustainable Energy Reviews 58 (2016) 510-525.

[10] M. Santamouris. Using cool pavements as a mitigation strategy to fight urban heat island—A review of the actual developments. Renewable and Sustainable Energy Reviews 26 (2013) 224-240.

[11] K. Pantavou, G. Theoharatos, A. Mavrakis, M. Santamouris. Evaluating thermal comfort conditions and health responses during an extremely hot summer in Athens. Building and Environment 46 (2011) 339-344.

[12] M. Santamouris, N. Papanikolaou, I. LIVADA, I. Koronakis, C. Georgakis, A. Argiriou, D.N. Assimakopoulos. On the impact of urban climate to the energy consumption of buildings. Solar Energy 70 (2001) 201-216.

[13] S. Hassid, M. Santamouris, N. Papanikolaou, A. Linardi, N. Klitsikas, C. Georgakis,

D.N. Assimakopoulos. The effect of the Athens heat island on air conditioning load. Energy and Buildings 32(2000)131-141.

[14] Y.H. Yau, H.L. Pean. The climate change impact on air conditioner system and reliability in Malaysia - A review. Renewable and Sustainable Energy Reviews 15 (2011) 4939-4949.

[15] X. Meng, T. Luo, Z.Y. Wang, W. Zhang, B. Yan, J.L. Ouyang, E.S. Long. Effect of RR-coatings on building indoor temperature conditions and heat flow analysis for walls. Energy and Buildings 127 (2016) 488-498.

[16] Y. Kikegawa, Y. Genchi, H. Kondo, K. Hanaki. Impacts of city-block-scale countermeasures against urban heat-island phenomena upon a building's energy-consumption for air-conditioning. Applied Energy 83 (2006) 649-668.

[17] E. Jamei, D.R. Ossen, M. Seyedmahmoudian, M. Sandanayake, A. Stojcevski, B. Horan. Urban design parameters for heat mitigation in tropics. Renewable and Sustainable Energy Reviews 134 (2020) 110362.

[18] S. Yin, W. Lang, Y.Q. Xiao. The synergistic effect of street canyons and neighbourhood layout design on pedestrian-level thermal comfort in hot-humid area of China. Sustainable Cities and Society 49 (2019) 101571.

[19] F. Grilo, P. Pinho, C. Aleixo, C. Catita, P. Silva, N. Lopes, C. Freitas, M. Santos-Reis, T. McPhearson, C. Branquinho. Using green to cool the grey: Modelling the cooling effect of green spaces with a high spatial resolution. Science of the Total Environment 724 (2020) 138182.

[20] S. Ziaul, S. Pal. Modeling the effects of green alternative on heat island mitigation of a meso level town, West Bengal, India. Advances in Space Research 65 (2020) 1789-1802.

[21] C. Fabiani, V.L. Castaldo, A.L. Pisello. Thermochromic materials for indoor thermal comfort improvement: Finite difference modeling and validation in a real case-study building. Applied Energy 262 (2020) 114147.

[22] S.W. Lee, C.H. L, E.I.B. S. Reflective thermal insulation systems in building: A review on radiant barrier and reflective insulation. Renewable and Sustainable Energy Reviews 65 (2016) 643-661.

[23] J. Zhang, L. Xu, V. Shabunko, S.E.R. Tay, H.X. Sun, S.S.Y. Lau, T. Reindl. Impact of urban block typology on building solar potential and energy use efficiency in tropical high-

density city. Applied Energy 240 (2019) 513-533.

[24] J.J. Sarralde, D.J. Quinn, D. Wiesmann, K. Steemers. Solar energy and urban morphology: Scenarios for increasing the renewable energy potential of neighborhood in London. Renewable Energy 73 (2015) 10-17.

[25] G. Lobaccaro, S. Croce, C. Lindkvist, M.C. Munari Probst, A. Scognamiglio, J. Dahlberg, M. Lundgren, M. Wall. A cross-country perspective on solar energy in urban planning: Lessons learned from international case studies. Renewable and Sustainable Energy Reviews 108 (2019) 209-237.

[26] D.E. Bowler, L.B. Ali, T.M. Knight, A.S. Pullin. Urban greening to cool towns and cities: A systematic review of the empirical evidence. Landscape and Urban Planning 97 (2010) 147-155.

[27] A.B. Besir, E. Cuce. Green roofs and facades: A comprehensive review. Renewable and Sustainable Energy Reviews 82 (2018), 915-939.

[28] A. Yoshida, D. Hayashi, Y. Shimazaki, S. Kinoshita. Evaluation of thermal sensation in various outdoor radiation environments. Architectural Science Review 62 (2019) 261-270.

[29] M. Manso, I. Teotonio, C.M. Silva, C.O. Cruz. Green roof and green wall benefits and costs: A review of the quantitative evidence. Renewable and Sustainable Energy Reviews 135 (2021) 110111.

[30] M. Martin, N.H. Wong, M. Ichinose. Impact of retro-reflective glass façades on the surface temperature of street pavements in business areas of Singapore and Tokyo. IOP Conference Series: Earth and Environmental Science 294 (2019) 012020.

[31] E. Ng, L. Chen, Y.N. Wang, C. Yuan. A study on the cooling effects of greening in a high-density city: An experience from Hong Kong. Building and Environment 47 (2012) 256-271.

[32] H. Chen, R. Ooka, H. Huang, T. Tsuchiya. Study on mitigation measures for outdoor thermal environment on present urban blocks in Tokyo using coupled simulation. Building and Environment 44 (2009) 2290-2299.

[33] S. Maharjan, K.S. Liao, A.J. Wang, S.A. Curran. Highly effective hydrophobic solar reflective coating for building materials: Increasing total solar reflectance via functionalized anatase immobilization in an organosiloxane matrix. Construction and Building Materials 243 (2020) 118189.

[34] S. Garshasbi, S.J. Huang, J. Valenta, M. Santamouris. On the combination of quantum dots with near-infrared reflective base coats to maximize their urban overheating mitigation potential. Solar Energy 211 (2020) 111-116.

[35] P.K. Thejus, K.V. Krishnapriya, K.G. Nishanth. A cost-effective intense blue colour inorganic pigment for multifunctional cool roof and anticorrosive coatings. Solar Energy Materials and Solar Cells 219 (2021) 110778.

[36] R. Levinson, P. Berdahl, H. Akbari, W. Miller, I. Joedicke, J. Reilly, Y. Suzuki, M. Vondran. Methods of creating solar-reflective nonwhite surfaces and their application to residential roofing materials. Solar Energy Materials and Solar Cells 91 (2007) 304–314.

[37] H. Taha. Meso-urban meteorological and photochemical modeling of heat island mitigation. Atmospheric Environment 42 (2008) 8795-8809.

[38] E. Morini, A. Touchaei, B. Castellani, F. Rossi, F. Cotana. The Impact of Albedo Increase to Mitigate the Urban heat island in Terni (Italy) Using the WRF Model. Sustainability 8 (2016) 999.

[39] A. Synnefa, M. Santamouris, H. Akbari. Estimating the effect of using cool coatings on energy loads and thermal comfort in residential buildings in various climatic conditions. Energy and Buildings 39 (2007) 1167-1174.

[40] Y. Qin. Urban canyon albedo and its implication on the use of reflective cool pavements. Energy and Buildings 96 (2015) 86-94.

[41] Y. Qin, J.E. Hiller. Understanding pavement-surface energy balance and its implications on cool pavement development. Energy and Buildings 85 (2014) 389-399.

[42] F. Rossi, B. Castellani, A. Presciutti, E. Morini, E. Anderini, M. Filipponi, A. Nicolini. Experimental evaluation of urban heat island mitigation potential of retro-reflective pavement in urban canyons. Energy and Buildings 126 (2016) 340-352.

[43] E. Morini, B. Castellani, A. Presciutti, M. Filipponi, A. Nicolini, F. Rossi. Optic-energy performance improvement of exterior paints for buildings. Energy and Buildings 139 (2017) 690-701.

[44] J.H. Yuan, C. Farnham, K. Emura. A study on the accuracy of determining the retro-reflectance of retro-reflective material by heat balance. Solar Energy 122 (2015) 419-428.

[45] F. Rossi, B. Castellani, A. Presciutti, E. Morini, M. Filipponi, A. Nicolini, M. Santamouris. Retroreflective façades for urban heat island mitigation: Experimental

investigation and energy evaluations. Applied Energy 145 (2015) 8-20.

[46] Y.L. Han, J.E. Taylor, A.L. Pisello. Toward mitigating urban heat island effects: Investigating the thermal-energy impact of bio-inspired retro-reflective building envelopes in dense urban settings. Energy and Buildings 102 (2015) 380–389.

[47] J.H. Yuan, K. Emura, H. Sakai. Evaluation of the solar reflectance of highly reflective roofing sheets installed on building roofs. Journal of Building Physics 37 (2012) 170-184.

[48] J.H. Yuan, K. Emura, C. Farnham, H. Sakai. Application of glass beads as retro-reflective facades for urban heat island mitigation: Experimental investigation and simulation analysis. Building and Environment 105 (2016) 140-152.

[49] T. Grosges. Retro-reflection of glass beads for traffic road stripe paints. Optical Materials 30 (2008) 1549-155.

[50] S. Hideki, N. Kazuo, I. Norio. Solar reflection characteristics of RR-coatings: (Part 1) Demonstration experiment of reflection reduction efficiency. Summaries of technical papers of AIJ annual meeting 41056 (2007) 111-112.

[51] É.J. Santos, A.B. Herrmann, S.K. Prado, E.B. Fantin, V.W. Santos, A.V.M. Oliveira, A.J. Curtius. Determination of toxic elements in glass beads used for pavement marking by ICP OES. Microchemical Journal 108 (2013) 233-238.

[52] L. Belcour, R. Pacanowski, M. Delahaie, A. L. Geay, L. Eupherte. Bidirectional reflectance distribution function measurements and analysis of retroreflective materials. Journal of the Optical Society of America A 31 (2014) 2561-2572.

[53] J.E. Hummer, W. Rasdorf, G. Zhang. Linear Mixed-Effects Models for Paint Pavement-Marking Retro reflectivity Data. Journal of Transportation Engineering 137 (2011) 705-716.

[54] M. Ghebrebrhan, L.C. Hoke, F.J. Aranda, M.L. Hoey, D.M. Archambault, J. Perry, L. Belton, D. Ziegler, J.B. Carlson, B.R. Kimball. Design and fabrication of extruded retroreflective polymer fibers. Optical Materials Express 4 (2014) 002656.

[55] J.H. Yuan, K. Emura, C. Farnham. A study on the durability of a glass bead retro-reflective material applied to building facades. Progress in Organic Coatings 120 (2018) 36-48.

[56] R.B. Nilsen, X.J. Lu. Retro reflection Technology. European Symposium on Optics and Photonics for Defence and Security. International Society for Optics and Photonics (2004) 47-60.

[57] J.H. Yuan, K. Emura, C. Farnham. A method to measure retro-reflectance and durability of RR-coatings for building outer walls. Journal of Building Physics 38 (2015) 500-516.

[58] M. Santamouris, G.Y. Yun. Recent development and research priorities on cool and super cool materials to mitigate urban heat island. Renewable Energy 161 (2020) 792-807.

[59] M. Manni, G. Lobaccaro, F. Goia, A. Nicolini. An inverse approach to identify selective angular properties of RR-coatings for urban heat island mitigation. Solar Energy 176 (2018) 662-673.

[60] M. Manni, M. Cardinali, G. Lobaccaro, F. Goia, A. Nicolini, F. Rossia. Effects of retro-reflective and angular-selective RR-coatings on solar energy in urban canyons. Solar Energy 209 (2020) 662-673.

[61] M. Manni, G. Lobaccaro, F. Goia, A. Nicolini, F. Rossi. Exploiting selective angular properties of retro-reflective coatings to mitigate solar irradiation within the urban canyon. Solar Energy 189 (2019) 74-85.

[62] R. Levinson, S. Chen, J. Slack, H. Goudey, T. Harima, P. Berdahl. Design, characterization, and fabrication of solar-retroreflective cool-wall materials. Solar Energy Materials and Solar Cells 206 (2020) 110117.

[63] F. Rossi, E. Morini, B. Castellani, A. Nicolini, E. Bonamente, E. Anderini, F. Cotana. Beneficial effects of retroreflective materials in urban canyons: results from seasonal monitoring campaign. Journal of Physics: Conference Series 655 (2015) 012012.

[64] J.H. Yuan, K. Emura, C. Farnham. Potential for Application of Retroreflective Materials instead of Highly Reflective Materials for Urban Heat Island Mitigation. Urban Studies Research 2016 (2016) 1-10.

[65] K. Haruna, S. Hideki, N. Kazuo, I. Norio. Solar reflection characteristics of RR-coatings: (Part 2) Retroreflectance estimation through outdoor measurement. Summaries of technical papers of AIJ annual meeting 41057 (2007) 113-114.

[66] K. Haruna, S. Hideki, N. Kazuo, I. Norio. Estimating the solar reflectance of RR-coatings by thermal measurement (environment). AIJ Kinki Chapter research meeting 4052 (2007) 205-209.

[67] N. Kazuo, K. Haruna, S. Hideki, I. Norio. Retro-reflectance estimation and the attempt to measure the directional characteristics on RR-coatings. AIJ Kinki Chapter research meeting

4053 (2008) 209-212.

[68] S. Hideki, I. Hiroshi, Nagamura Kazuo, Igawa Norio. Solar reflection characteristics of RR-coatings: (Part 3) Measurement of spectral characteristics and incident angle dependence of retro-reflective components. Summaries of technical papers of AIJ annual meeting 1219 (2008) 437-438.

[69] S. Hideki, I. Hiroshi, N. Kazuo, I. Norio. Evaluation of the incident angle dependence of the solar reflectance of a retroreflective materials. Summaries of technical papers of AIJ annual meeting 41217 (2011) 411-442.

[70] T. Grosges. Retro-reflection of glass beads for traffic road stripe paints. Optical Materials 30 (2008) 1549-1554.

[71] T. Inoue, K. Takase, Y. Saito. Effects of modified near-infrared retro-reflective film on urban thermal environment. Journal of Physics: Conference Series. 1343 (2019) 012191.

[72] M. Ichinosea, T. Inoue, T. Nagahama. Effect of retro-reflecting transparent window on anthropogenic urban heat balance. Energy and Buildings 157 (2017) 157-165.

[73] J.H. Yuan, K. Emura, H. Sakai, C. Farnham, S.Q. Lu. Optical analysis of glass bead RR-coatings for urban heat island mitigation. Solar Energy 132 (2016) 203-213.

[74] L. Mauri, G. Battista, E.L. Vollaro, R.L. Vollaro. Retroreflective materials for building's façades: Experimental characterization and numerical simulations. Solar Energy 171 (2018) 150-156.

[75] V. Andrea, M. Luca, C. Chiara, D.L.V. Roberto. Numerical Model for the Characterization of RR-coatings Behavior in an Urban Street Canyon. Journal of Thermal Science 27 (2018) 456-462.

[76] J.H. Yuan, K. Emura, C. Farnham. Geometrical-optics analysis of reflective glass beads applied to building coatings. Solar Energy 122 (2015) 997-1010.

[77] B. Castellani, E. Morini, E. Anderin M. Filipponi, F. Rossi. Development and characterization of retro-reflective colored tiles for advanced building skins. Energy and Buildings 154 (2017) 513-522.

[78] B. Castellani, A.M. Gambelli, A. Nicolini, F. Rossi. Optic-energy and visual comfort analysis of retro-reflective building plasters. Building and Environment 174 (2020) 106781.

[79] L. Schwinger, S. Lehmann, L. Zielbauer, B. Scharfe, T. Gerdes. Aluminum Coated Micro Glass Spheres to Increase the Infrared Reflectance. Coatings 9 (2019) 9030187.

[80] E. Morini, B. Castellani, E. Anderini, A. Presciutti, A. Nicolini, F. Rossi. Optimized retro-reflective tiles for exterior building element. Sustainable Cities and Society 37 (2018) 146-153.

[81] J.H. Yuan, C. Farnham, K. Emura. Performance of Retro-Reflective Building Envelope Materials with Fixed Glass Beads. Applied Sciences 9 (2019) 1714.

[82] S. Hideki, I. Hiroshi, N. Kazuo, I. Norio. Prototype of RR-coatings and measurement of solar reflection characteristics. AIJ Kinki Chapter research meeting 76 (2011) 1229-1234.

[83] H. Sakai, H. Iyota. Development of Two New Types of Retroreflective Materials as Countermeasures to Urban Heat Islands. International Journal of Thermophysics 38 (2017) 31.

[84] J. Yuan, C. Farnham, K. Emura. Development of a retro-reflective material as building coating and evaluation on albedo of urban canyons and building heat loads. Energy and Buildings 103 (2015) 107-117.

[85] H. Iyota, H. Sakai, K. Emura, N. Igawa, H. Shimada, N. Nishimura. Method for Measuring Solar Reflectance of Retroreflective Materials Using Emitting-Receiving Optical Fiber. Journal of Heat Island Institute International 7 (2012) 2

[86] N. Xie, H. Li, W.Z. Zhao, C. Zhang, B. Yang, H.J. Zhang, Y. Zhang. Optical and durability performance of near-infrared reflective coatings for cool pavement: Laboratorial investigation. Building and Environment 163 (2019) 106334.

[87] E. Morini, B. Castellani, A. Nicolini, F. Rossi, U. Berardi. Effects of aging on RR-coatings for building applications. Energy and Buildings 179 (2018) 121-132.

[88] J.H. Yuan, K. Emura. Changes in Solar Reflectance of Retro-reflective Sheets used on the Outer Wall of Building over Long-term Exposure. Air-conditioning and Sanitary Engineers of Japan Conference in Nagano. 10 (2013) 245-248.

[89] R. Levinson, H. Akbari, P. Berdahl. Measuring solar reflectance—Part II: Review of practical methods. Solar Energy 84 (2010) 1745-1759.

[90] R. Levinson, M. Egolf, S. Chen, P. Berdahl. Experimental comparison of pyranometer, reflectometer, and spectrophotometer methods for the measurement of roofing product albedo. Solar Energy 206 (2020) 826-847.

[91] M. Santamouris, A. Synnefa, T. Karlessi. Using advanced cool materials in the urban built environment to mitigate heat islands and improve thermal comfort conditions. Solar Energy 85 (2011) 3085-3102.

[92] S.S. Soulayman, N. Daude. A correction method for solar radiation measurements made using non-calibrated Eppley-type and Robitzsch-type pyranometers. Applied Energy 52 (195) 125-132.

[93] W. Schmidt. A novel single beam optical spectrophotometer for fast luminescence, absorption, and reflection measurements of turbid materials. Trends in analytical chemistry 12 (1993) 74-82.

[94] A.F. García, F. Sutter, L.M. Arcos, C. Sansom, F. Wolfertstetter, C. Delord. Equipment and methods for measuring reflectance of concentrating solar reflector materials. Solar Energy Materials and Solar Cells 167 (2017) 28-52.

[95] M. Iqbal. Chapter 12- Solar radiation measuring instruments. An Instruction to Solar Radiation. (1983) 335-373.

[96] K.L. Coulson. Chapter 2- Radiation Sensor and Source. Solar and Terrestrial Radiation: Methods and Measurements. (1975) 84-141.

[97] ASTM, 2006. ASTM E1918-06: Standard Test Method for Measuring Solar Reflectance of Horizontal and Low-Sloped Surfaces in the Field.

[98] G.X. Mei, B. Wu, S.K. Ma, Y.H. Qin. A simplified method for the solar reflectance of a finite surface in field. Measurement 110 (2017) 211-216

[99] Y.H. Qin, H.S. He. A new simplified method for measuring the albedo of limited extent targets. Solar Energy 157 (2017) 1047–1055.

[100] ASTM, 1996. ASTM E903-96: Standard Test Method for Solar Absorptance, Reflectance, and Transmittance of Materials Using Integrating Spheres. American Society for Testing and Materials, West Conshohocken, PA.

[101] R. Levinson, M. Egolf, S. Chen, P. Berdahl. Experimental comparison of pyranometer, reflectometer, and spectrophotometer methods for the measurement of roofing product albedo. Solar Energy 206 (2020) 826-847.

[102] ASTM C1549, 2002. Standard Test Method for Determination of Solar Reflectance near Ambient Temperature Using a Portable Solar Reflectometer, ASTM.

[103] F. Rossi, A. L. Pisello, A. Nicolini, M. Filipponi, M. Palombo. Analysis of retro-reflective surfaces for urban heat island mitigation: A new analytical model. Applied Energy 114 (2014) 621-631.

[104] H. Sakai, K. Emura, N. Igawa. Reduction of reflected heat by retroreflective materials.

Journal of Structural and Construction Engineering (Transactions of AIJ) 73 (2008) 1239-1244.

[105] H. Sakai, H. Kobayashi, K. Emura, N. Igawa. Outdoor measurement of solar reflective performance of retroreflective materials. Journal of Structural and Construction Engineering (Transactions of AIJ) 73 (2008) 1713-1718.

[106] B. Castellani, A. Nicolini, A.M. Gambelli, M. Filipponi, E. Morini, F. Rossi. Experimental assessment of the combined effect of retroreflective façades and pavement in urban canyons. IOP Conference Series: Materials Science and Engineering 609 (2019) 072004.

[107] E. Morini, B. Castellani, A. Presciutti, E. Anderini, M. Filipponi, A. Nicolini, F. Rossi. Experimental Analysis of the Effect of Geometry and Facade Materials on Urban District's Equivalent Albedo. Sustainability 9 (2017) 1245.

[108] S. Yoshida, A. Mochida. Evaluation of effects of windows installed with near-infrared rays retro-reflective film on thermal environment in outdoor spaces using CFD analysis coupled with radiant computation. Building Simulation 11 (2018) 1053-1066.

[109] S. Yoshida, S. Yumino, T. Uchida, A. Mochida. Numerical Analysis of the Effects of Windows with Heat Ray Retro-reflective Film on the Outdoor Thermal Environment within a Two-dimensional Square Cavity-type Street Canyon. Procedia Engineering 169 (2016) 384-391.

[110] J.H. Yuan, K. Emura, C. Farnham. Analytical model to evaluate the reflective directional characteristics of RR-coatings. Energy and Buildings 223 (2020) 110169.

[111] P.A. Bennewitz. New scanning gonio-photometer for extended BRTF measurements. Reflection, Scattering, and Diffraction from Surfaces II 7792 (2010).

[112] B. Karamata, M. Andersen. Origin and nature of measurement bias in catadioptric parallel goniophotometers. Optical Society of America 31 (2014) 1040-1048.

[113] L.D. Girolamo. Generalizing the definition of the bi-directional reflectance distribution function. Remote Sensing of Environment 88 (2003) 479-482.

[114] J.R. Zaworski, J.R. Welty, M.K. Drost. Measurement and use of bi-directional reflectance. Heat Mass Transfer 39 (1996) 1149-1156.

[115] T. Harima, T. Nagahama. Evaluation methods for retroreflectors and quantitative analysis of near-infrared upward reflective solar control window film- Part I: Theory and evaluation methods. Solar Energy 148 (2017)177-192.

[116] T. Harima, T. Nagahama. Evaluation methods for retroreflectors and quantitative

analysis of near-infrared upward reflective solar control window film—Part II: Optical properties evaluation and verification results. Solar Energy 148 (2017) 164-176.

[117] L.O. Grobe. Characterization and data-driven modeling of a retro-reflective coating in Radiance. Energy and Buildings 162 (2018) 121-133.

[118] L. Xu, J.Y. Wang, F.P. Xiao, S.E. Badawy, A. A. Potential strategies to mitigate the heat island impacts of highway pavement on megacities with considerations of energy uses. Applied Energy 281 (2021) 116077.

[119] C.Y. Jim. Solar–terrestrial radiant-energy regimes and temperature anomalies of natural and artificial turfs. Applied Energy 173 (2016) 520–534.

[120] J.C. Fernandez, F. Cappelletti, A. Gasparella. Including the effect of solar radiation in dynamic indoor thermal comfort indices. Renewable Energy 165 (2021) 151-161.

[121] T. Inoue, T. Shimo, M. Ichinose, K. Takase, T. Nagahama. Improvement of urban thermal environment by wavelength-selective retro-reflective film. Energy Procedia 122 (2017) 967-972.

[122] H. Shen, H.W. Tan, A. Tzempelikos. The effect of reflective coatings on building surface temperatures, indoor environment and energy consumption—An experimental study. Energy and Buildings 43 (2011) 573–580.

[123] T. Rahman, K. Nagano, J. Togawa. Study on building surface and indoor temperature reducing effect of the natural meso-porous material to moderate the indoor thermal environment. Energy and Buildings 191 (2019) 59-71.

[124] G. Vox, A. Maneta, E. Schettini. Evaluation of the radiometric properties of roofing materials for livestock buildings and their effect on the surface temperature. Biosystems engineering 144 (2016) 26-37.

[125] Y.H. Qin. J. Liang, K.G. Tan, F.H. Li. A side by side comparison of the cooling effect of building blocks with retro-reflective and diffuse-reflective walls. Solar Energy 133 (2016) 172-179.

[126] L.L. Zhang, X. Meng, F. Liu, L. Xu, E.S. Long. Effect of RR-coatings on temperature environment in tents. Case Studies in Thermal Engineering 9 (2017) 122-127.

[127] D. Kumar, M. Alam, P.X.W. Zou, J.G. Sanjayan, R.A. Memon. Comparative analysis of building insulation material properties and performance. Renewable and Sustainable Energy Reviews 131 (2020) 110038.

[128] A. Joudi, H. Svedung, C. Bales, M. Ronnelid. Highly reflective coatings for interior and exterior steel cladding and the energy efficiency of buildings. Applied Energy 88 (2011) 4655-4666.

[129] C.Fabiani, A.L. Pisello, E.B. Zeid, J. Yang, F. Cotana. Adaptive measures for mitigating urban heat islands: The potential of thermochromic materials to control roofing energy balance. Applied Energy 247 (2019) 155-170.

[130] Y. Zhang, E.S. Long, Y.R. Li, P. Li. Solar radiation reflective coating material on building envelopes: Heat transfer analysis and cooling energy saving. Energy Exploration and Exploitation 35 (2017) 748-766.

[131] X. Meng, C.X. Wang, W.J. Liang, S. Wang, P. Li, E.S. Long. Thermal Performance Improvement of Prefab Houses by Covering RR-coatings. Procedia Engineering 121 (2015) 1001-1007.

[132] L. Xu, W. Zhang, W. Wang, B. Gao, M. Chen. Impact of different improvement measures on the thermal performance of ultra-thin envelopes. Energy 203 (2020) 117802.

[133] X.H. Zhou, J. Carmeliet, M. Sulzer, D. Derome. Energy-efficient mitigation measures for improving indoor thermal comfort during heat waves. Applied Energy 278 (2020) 115620.

[134] C. Wang, Y. Zhu, X.F. Gou. Thermally responsive coating on building heating and cooling energy efficiency and indoor comfort improvement. Applied Energy 253 (2019) 113506.

[135] M. Zinzi, E. Carnielo, B. Mattoni. On the relation between urban climate and energy performance of buildings. A three-years experience in Rome, Italy. Applied Energy 221 (2018) 148–160.

[136] S. Yoshida, S. Yumino, T. Uchida, A. Mochida. Effects of windows with heat ray retro-reflective film on outdoor thermal environment and building cooling load. Journal of Heat Island Institute International 2 (2014) 67-72.

Methodology and performance evaluation index

Chapter 3 Methodology and performance evaluation index

The main purpose of this chapter was to establish the basic experiment and simulation system and performance evaluation index of the impact of RR-coatings on the thermal environment of the building area, which laid the foundation for the analysis of related researches in the following chapters. Firstly, the optical property measuring instruments were developed to measure the solar reflectance and angle distribution of two typical RR-coatings. Secondly, a number of experimental plans were developed, and the basic experimental models were established, and the performance evaluation indicators were determines, which included regional albedo, wall temperature and air temperature, and based on the experimental data obtained, the thermal performance of the RR-coatings was analyzed. Finally, based on the software of Energyplus, the impact of RR-coating on the thermal environment of buildings was preliminarily determined and the effect of wall reflectivities on energy load of an enclosed educational building in Qingdao was simulated.

3.1 Optical performance experiment

3.1.1 Evaluation index

(1) Solar reflectance

Objects under sunlight constantly absorbed solar heat, causing the surface temperature to rise. The parameter representing surface heat absorption ability was solar reflectance [1-3]. The higher the solar reflectance, the less solar heat it absorbed.

Conventional solar thermal reflection coatings had both high infrared emissivity and solar reflectance [4, 5]. Therefore, when the surface covered with cooling coating faced the sky under the sun, the high solar reflectance greatly reduced the absorption of solar heat, and the high infrared emissivity made the part of the absorbed heat dissipate from the surface in the form of thermal radiation, so it had a good cooling effect. High solar reflectance and high infrared emissivity were indispensable. For example, silver metal had the highest solar reflectance of 0.97 in nature, and aluminum metal also had a high solar reflectance of 0.82, but the infrared emissivity of metal was usually 0.1. Therefore, when silver and aluminum metal were placed under the sun, although the absorbd solar heat was little, but because of bad heat transfer, the heat built up and eventually it got hot.

Fig. 3-1 showed the energy distribution of solar radiation [6]. It could be seen that about 95% of the energy was concentrated in the range of 400~3000nm. According to the wavelength, the solar radiation could be divided into three stages, among which, the highest energy part was near infrared light, the wavelength between 780~2500nm, its energy accounted for up to 52%, followed by visible light, and the wavelength ranged from 400nm to 780nm, accounting for

43%, and the rest was ultraviolet light with a wavelength of 295~400nm and only 5% of the energy.

According to the analysis of the distribution of solar radiation energy, no matter what kind of object, it would release its own heat by means of radiation, which was called thermal radiation [7]. In nature, as long as its temperature was above absolute zero, thermal radiation would be generated. The energy radiated by an object was mainly affected by its own temperature. If the object itself had a higher temperature, the energy generated in the process of thermal radiation was also relatively higher.
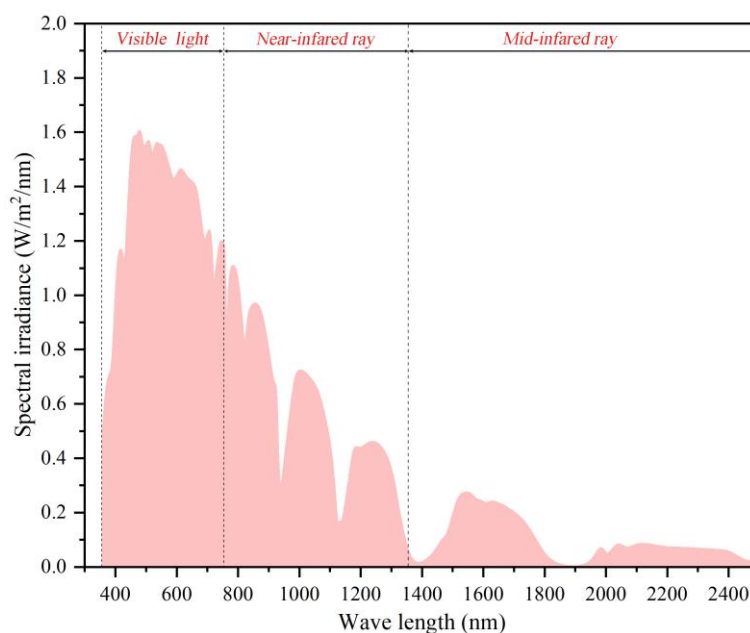
Fig. 3-1. Solar radiation energy distribution

In fact, any object could not only generate thermal radiation itself, but also had a certain influence on it by external thermal radiation. The influence process was usually analyzed by means of transmittance, absorptivity and reflectivity. There was a certain correlation among the three parameters, that was, the sum of the three parameters was 1 [8]. It turned out that there were very few objects that could absorb 1. These objects were called black bodies, and they emitted electromagnetic waves covering all wavelengths.

Near infrared light, visible light two bands carried the highest energy, in order to achieve the ideal heat insulation effect in hot weather, the reflectivity of the coating on the two bands should be increased as high as possible. For radiation-type reflective heat insulation coatings, the principle of heat insulation was to strengthen the reflection ratio of the material in the near infrared light, visible light, when the building was exposed to sunlight, most of the solar radiation could be reflected out, and the absorbed energy was reduced, so that the building

surface temperature under the sunlight was not too high, which reduced the heat transfer, so as to achieve the purpose of heat insulation.

The outer envelope was very critical to the building, which required not only high safety, but also good insulation, especially in hot summer and cold winter areas. The material used in the structure directly determined the indoor temperature, and its surface thermal effect mainly depended on the solar radiation absorption coefficient. For summer, the sun irradiated the structure surface for a long time in the daytime, with the increase of irradiation time, the absorbed heat was increased, and these heat could be transmitted to the room through the structural materials. In order to improve the comfort of the environment, people needed to use a lot of refrigeration equipment. In winter, the difference between indoor and outdoor temperature was higher, and heat was transferred from indoor to outdoor, and the indoor temperature decreased [9-11].

(2) Retro-reflection

The study on the reflection characteristics of RR-coatings should not only consider the solar reflectance, but also the reflection direction characteristics of the coatings, which was particularly important for the comprehensive heat generated by solar radiation in cities [12]. Retro-reflection property referred to the ability of coatings to reflect solar radiation back in the direction of incidence. Retro-reflectance measurement usually required a clear distribution of reflected light, but such measurement had high requirements for measuring equipment [13, 14]. Therefore, the key technique of retro-reflection by some scholars was to obtain a clear distribution of reflected light, especially along the direction of incidence. Based on this, some measurement systems were proposed, including the transmitter-receive fiber system, the angular distribution measurement method of reflected light and the bidirectional reflection measurement method.

Yuan J.H. et al. [15] from Osaka City University proposed to use a spectrophotometer to track the reflected near infrared rays from multiple angles to test the reflection characteristics of regression reflection materials. In addition, they also considered to test the reflectance of the RR-coatings using the thermal balance method [16]. Rossi et al. [17] measured the angular distribution of reflected light by using a semicircular array of 19 fixed photodiodes, while the samples had different slants by rotating their platforms.

In order to evaluate the angular distribution of RR-coatings, a new test equipment was developed, which included macroscopic angular resolution spectral system, halogen light source and spectrometer.

3.1.2 Experiment devices

Solar reflectance and retro-reflectance were two important evaluation parameters of RR-coatings. The corresponding measurement methods and equipment were developed in cooperation with Shanghai Chenchang Instrument Company. Shanghai Chenchang Instrument Co., Ltd. was a scientific and technological instrument equipment company. Its main products included spectrometers and accessories for spectral detection, laboratory microscopy systems and angular resolution systems. It was committed to provide a full range of spectral detection solutions for scientific research and industrial users related to spectral detection.

For the solar reflectance of coatings, a mature integrating sphere device (model: IS50-R5) was adopted, as shown in Fig. 3-2. The measured wavelength covered UV-Vision-near-infrared, ranging from 250-2500 nm, and the color temperature of the light source was 2915 K.

However, for the measurement of retro-reflectance, no mature method was available. The integrating sphere could not be directly used to measure the retro-reflection intensity of the sample, so it was difficult to evaluate the angular distribution and the retro-reflection spectrum of the sample. Therefore, the author developed a visible-near-infrared spectrometer system, as shown in Fig. 3-3. The macroscopic angular resolution spectral system of the system could make the incident light focused on the sample surface well, and the sampling manipulator adopted a precise sliding table, which could rotate 0°~ 360° to realize the retro-reflectance spectral measurement of coatings at any incidence angles.

Fig. 3-2. Integrating sphere equipment
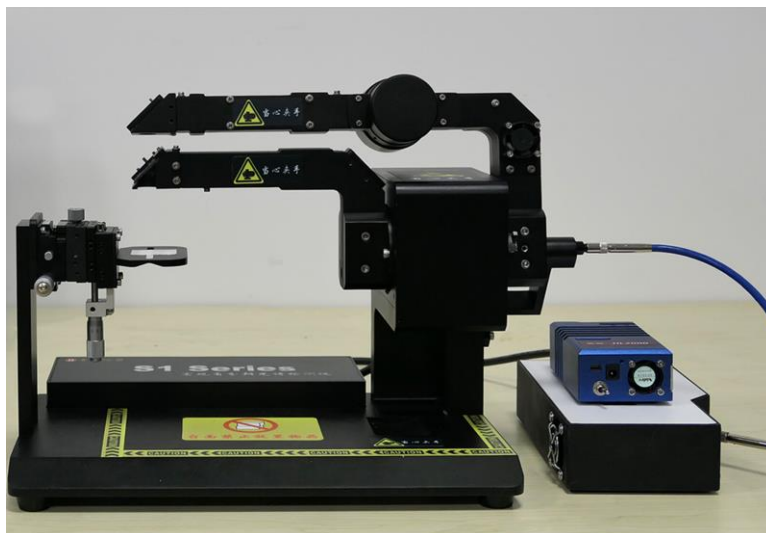
Fig. 3-3. Angular resolution system

3.1.3 Experiment platforms

The experimental site was the Academic Innovation Center of Coastal Human Settlement Environment of Qingdao University of Technology, which had traditional superior discipline resources such as architecture, civil engineering, environment and information. Through the establishment of interdisciplinary teams and the construction of high-level scientific research platform, the effective utilization of marine resources, the protection of marine ecological environment and the construction of green smart city were committed, so as to create a technological innovation brand of Shandong coastal human settlement environment.

Fig. 3-4 showed the test samples and electron microscope magnification of this experiment, which were prism RR-coatings, glass bead RR-coatings and common HR-coatings, respectively. Among them, two kinds of RR-coatings were produced by 3M Company in the United States, and the HR-coatings was domestic.

The solar reflectance of the coating was measured by an integral spectrophotometer with a wavelength range of 250~2500nm. Before the experiment, the instrument setting value, calibration and zeroing of the purple spectrophotometer instrument were carried out. According to the standard solar incident spectrum, it was found that the wavelength of 250~2500nm covered most of the solar energy. According to the instrument conditions, the test wavelength interval was set to 25nm. The the instrument system was set up, and put the three coatings into the spectrophotometer, then the detection was conduct. During the detection process, the data was record at an interval of 25nm. Fig. 3-5 (a) showed the picture taken when detecting the solar reflectance of the RR-coatings. The overall reflectance of the coatings must take into account the energy distribution of ground-based solar radiation. According to ASTME424-71-

2007, the global reflectance (R) could be expressed as

$$r = \frac{\int S_\lambda r(\lambda) d\lambda}{\int S_\lambda d\lambda} \times 100\% \approx \frac{\int_{780}^{2526} S_\lambda r(\lambda) d\lambda}{\int_{780}^{2526} S_\lambda d\lambda} \times 100\% \tag{1}$$

Where r(λ) represented the reflectance based on wavelength, and Sλ represented the solar energy ratio of different wavelengths, whose value could be referred to MIL DTL 64159(MR)-2007.
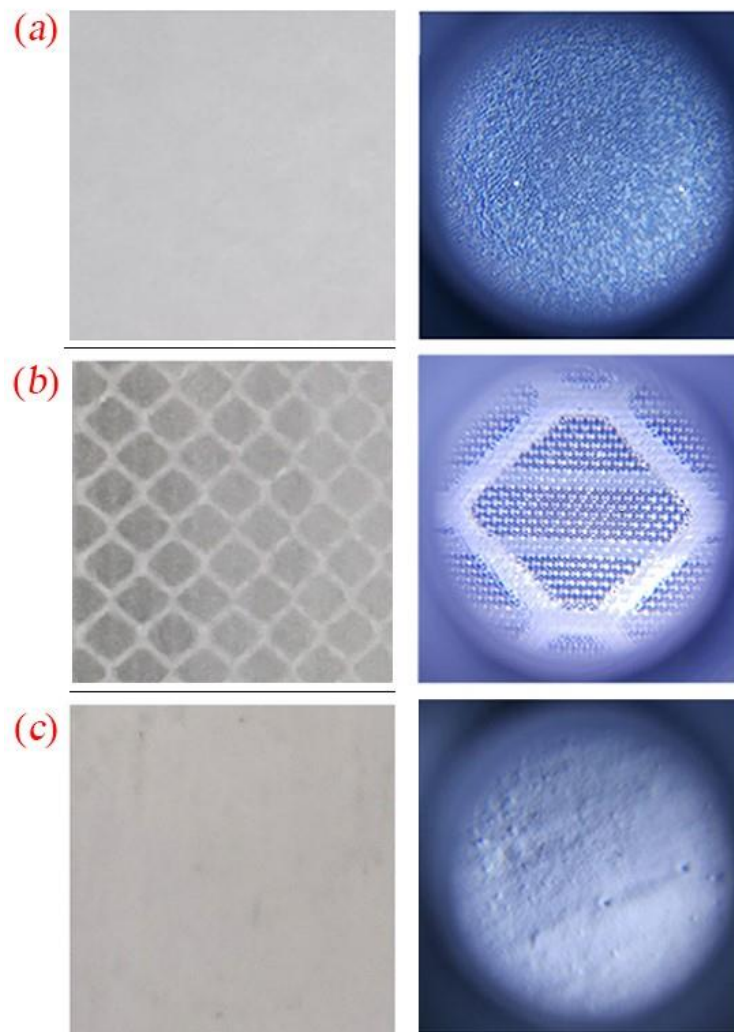
Fig. 3-4. Test sample photographs and electron microscope magnification of the test samples

In order to determine the retro-reflection properties of the two RR-coatings, the angular distribution of the reflected energy of the coatings was measured (from -90° to 90°) by using a specially developed angular resolution test system. Fig. 3-5 (b) was the picture taken when detecting the angle distribution of the RR-coatings. The polar plot showed the amount of the

total reflection value of the sample at each unit angle, spaced at 10° intervals and ranging from -90° to 90°, while the red arrow (the value pointing to the incident Angle η) indicated the beam direction of 10°, 30°, 50°, or 70°. Compared with traditional coatings, both of these RR-coatings exhibited remarkable angular reflection characteristics.
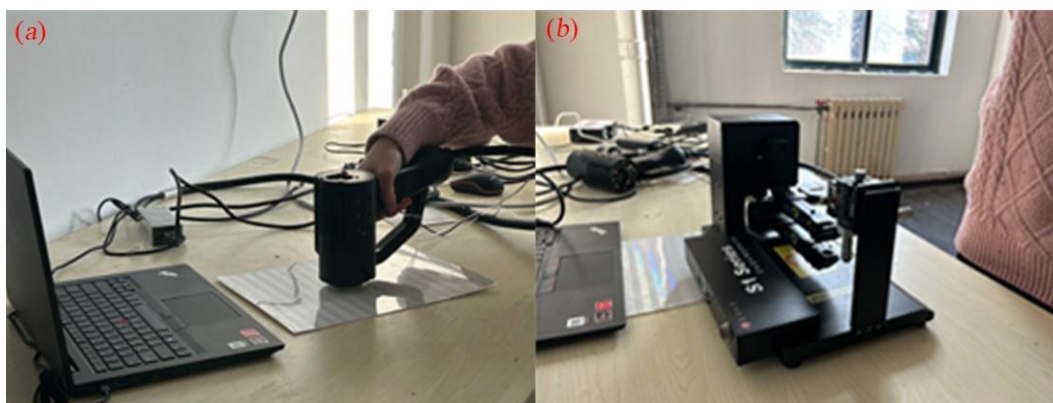
Fig. 3-5. Field photo of (a) solar reflectance measurement and (b) retro-reflectance measurement

3.2 Thermal performance experiment

3.2.1 Evaluation index

(1) Regional albedo

Albedo was a key factor controlling the radiation budget and energy balance of urban ecosystem [18]. Generally, the low albedo of cities leaded to the increase of solar shortwave radiation absorbed by the surface, which promoted the rise of urban temperature and the the worsening of urban heat island [19-21]. Santamouris et al. [22] analyzed albedo and heat-related death cases in 13 regions around the world, it was found that for every 0.1 increase in albedo, the number of deaths due to heat wave decreased by 1.8%. Akbari et al. [23] studied the long-term climate effect of global urban albedo through a model and found that every 0.01 increase in urban albedo had a cooling effect of 10-15K/m² on global temperature, which was equivalent to reducing about 7kg of carbon dioxide emissions. Jandaghian et al. [24] found through simulation that increasing surface albedo such as roof, wall and ground could reduce cooling energy demand by 10% in downtown of Toronto. The micrometeorological environment of urban blocks would have a direct impact on residents' health and quality of life [25, 26]. It could be seen that accurate assessment of urban albedo was very important for relieving urban heat stress and formulating urban energy supply strategy.

Previous studies paid more attention to the overall albedo of the city, ignored the spatial difference of the albedo of inner city blocks [27]. Compared with the natural ecosystem, the

factors affecting the albedo of urban blocks were more complex. The albedo of the natural ecosystem was mainly affected by the solar altitude angle and presented the typical diurnal and seasonal variations [28]. In addition, clouds in the sky affected the surface albedo by blocking and scattering solar radiation. In addition to the above two factors, the albedo of urban blocks was also affected by its own morphological structure (street aspect ratio, sky visibility, landscape elements (vegetation, buildings, etc.) [29-31], affected by the above factors, the albedo inside the city was complex and diverse.

Sugawara et al. [32] found that the albedo in the Tokyo metropolitan area was lower in the area with more buildings and decreased with the increase of the street aspect ratio through the observation method of paired radiometers carried by helicopters. In addition, urban underlying surfaces were often composed of a variety of materials, among which albedo features were highly heterogeneous due to color, texture and radiation properties [33]. Li et al. [34] measured the albedo of different pavement materials on site and conducted long-term monitoring of the albedo, establishing an empirical relationship between the cooling effect of increasing albedo on high temperature pavement and solar radiation. By means of networking, albedo observation was conducted on wood strips, bricks, glass, cement, asphalt and other materials in urban landscape elements, and it was found that the texture, color and surface humidity of urban materials would affect the albedo [35]. Vegetation such as grassland and forest inside the city would also change the urban albedo [36].

The research methods of urban albedo could be divided into field fixed point observation and remote sensing inversion, which had differences in spatio-temporal resolution, cost and other aspects.

Fixed-point observation of external field usually referred to the direct observation of upward and downward short-wave radiation by setting up a radiometer, and calculating the ratio of the two to get the surface albedo. The principle of the field fixed point observation method was simple, and the albedo calculated by this method had high accuracy and high time resolution [37]. In the urban interior with high heterogeneity, the location selection of fixed point observation was very important. Due to high human and material costs, it was often impossible to carry out high-density and large-scale distribution observation in cities, which was suitable for spatial scales below the block scale, especially the reflectance study of single surface coatings and the experimental study of scale models.

Remote sensing inversion referred to the acquisition of ground reflection information by sensors mounted on flight platforms such as aircraft and satellites, and the estimation of surface albedo combined with albedo inversion algorithm [38]. Surface reflectance was obtained after

radiation calibration of sensor data, and albedo conversion was generally completed in two ways: bidirectional reflection distribution function (BRDF model) [39] and empirical linear equation. BRDF model inversion method had high accuracy, but it required a lot of prior knowledge about underlying surface characteristics and careful experimental design [40, 41]. For highly heterogeneous urban areas, it was difficult to obtain BRDF reflection characteristics of complex underlying surfaces, so this method was difficult to be applied in urban research [42, 43]. The premise of empirical linear equation method was that the surface is considered to be Lambertian body, that was, the surface radiation characteristics were isotropic, and the albedo inversion method was formed through the fitting of a large number of remote sensing data [44, 45]. The shortcomings of remote sensing inversion methods based on space shuttle and satellite were mainly high cost and low spatial resolution, which were especially unfavorable to the study of urban interior albedo.

The special form of radiation energy exchange in urban composite built environment was an important factor for the formation of heat island. In urban built environment, due to the multiple reflection of radiation by urban form, special solar energy capture effect was generated, thus generating more energy absorption. It could be seen that the change of local radiation balance caused by solar energy capture effect promoted the formation of urban heat island to a large extent [46]. Albedo was an important indicator to determine the ability of absorbing solar radiation. The composite built environment absorbed more solar radiation and reflected less. This difference was due to the increase of solar radiation absorption due to the multiple reflection of radiation in the urban composite built environment, that was, the special solar energy captured effect in the urban composite built environment.

In this paper, regional albedo was selected as the evaluation index of the impact of HR-coatings and RR-coatings on regional thermal environment. It was not only an important factor determining the amount of solar radiation absorbed by a city, but also represented the ratio of radiation leaving the city surface to radiation reaching the city surface, which was considered as the risk index of urban heat island. At the same time, it was closely related to a variety of urban form elements and influenced by urban form, reflection characteristics of coatings and spatial layout, etc., so it had the potential to be incorporated into the planning to improve the thermal environment. It could be seen that the reflectivity reflected the dual information of urban form and thermal environment at the same time, which could be said to be an important medium for the interaction between urban form and thermal environment in terms of radiation heat transfer. The influence of urban form on thermal environment could be studied from the perspective of reflectivity.

(2) Wall temperature and air temperature

The thermal physical factors related to reflectance were studied in this paper, including wall temperature and air temperature. After the surface received solar radiation, the radiation energy first heated the wall, making the wall temperature rose, which further heated the air temperature. The influence of air temperature on human body was great, affecting people's activities and clothes, which had a certain degree of influence on people's comfort. The influence of wall temperature on human comfort level was roughly the same as that of air temperature, and it had certain influence on indoor air temperature, which indirectly affected human comfort level.

The observation experiment of building wall temperature and its influence on outdoor thermal environment had always been one of the research hotspots at home and abroad. The research content was also continuously refined and in-depth. From simple observation and data analysis at the very beginning to purposefully compare the difference of the environmental impact of various architectural factors, etc. So far, research in this area had become increasingly systematic.

In 1995, S.E.G. Jayamaha et al. [47] also made a comparative analysis of wind speed, air temperature through experiments. It was pointed out that for large area wall, the influence of ambient wind direction on heat flow exchange was not obvious. In 2004, Francisco Sanchez de la Flor et al. [48] went further and analyzed these factors more systematically by building test rooms and specimens and observing them continuously, they obtained correlations between various factors and changes in the thermal properties of the walls. K.nachoi.Livacla et al. [49] also conducted a similar experiment that they selected a street valley in Athens, Greece, and monitored it continuously for 5 days and 5 nights, and recorded the data of wind speed and surface temperature of the underlying surface of the street valley and two building walls. The experimental results showed that there was no obvious relationship between the air temperature distribution in the street valley and the height variation, but in the early morning, a strong temperature inversion was observed, reaching 7.21°C/100m. Through the comparative analysis of the temperature of street canyons facing SSW and NNE, it was concluded that the air temperature distribution of street canyons was a function of street geometry and direction, but at the same time, it was also affected by building materials, optical and thermal properties of street materials and surrounding air temperature.

In this paper, wall temperature and air temperature were selected as evaluation indexes of the impact of HR-coatings and RR-coatings on regional thermal environment. At the same time, it was closely related to a variety of urban form elements and influenced by urban form, reflection characteristics of materials and spatial layout, etc., so it has the potential to be incorporated into

the evaluation of the improvement of the thermal environment.

3.2.2 Experiment devices

The measurement instruments used in this paper were solar radiometer for measuring albedo, multi-channel for measuring wall temperature and air temperature, and climatic parameters. All instruments were purchased from Beijing Shijiantong Technology Co., LTD.

Beijing Shijiantong Technology Co., LTD. was a high-tech enterprise dedicated to the manufacture of intelligent instruments and sensing terminals. The measurement range involved temperature, humidity, heat flow, heat radiation, sunshine radiation, wind speed, air flow, noise, illumination, air quality, meteorology, etc. Products were widely used in building environment, HVAC, industrial environment, ecological meteorology, indoor and outdoor air quality, occupational health, public health, new energy utilization and other fields. Over the years, Jiantong had always brought cutting-edge, professional, easy testing technology and timely service to users. Jiantong Technology had obtained more than 60 software Copyrights and patents (including the number of software Copyrights and patents of wholly-owned subsidiaries).

For the measurement of albedo, the solar radiometer JTR05 was used and the spectral range was 300~300nm, as shown in Fig. 3-6. It could also be used to measure the solar radiation incident on the inclined plane. In accordance with the WMO World Meteorological Organization (CIMO Guide), and suitable for all kinds of harsh environment, and had many other advantages including high sensitivity, accurate measurement, easy to use, maintenance free. Measurement range were 0~2000W/m^2, resolution were 0.1W/m^2, accuracy were ±2%, stability were ±2%, cosine response were ≤± 5% (solar altitude Angle 10°), power supply were 5VDC, standard output were 0-2.5VDC, working environment temperature were -50℃~85℃, humidity were ≤ 100%RH, product weight were 820g.

Fig. 3-6. The solar radiometer JTR05

For temperature measurement, multi-channel touch data recorder TP1000 was adopted, as shown in Fig. 3-7. It supported temperature, humidity, current, voltage, pressure, liquid level, flow, displacement and other tests at the same time, simple appearance design, light and easy to use, wireless remote transmission to the computer IE& mobile phone wechat monitoring.

Connecting the multi-channel multi-channel touch data recorder was a T-type thermocouple probe temperature sensor, as shown in Fig. 3-8. As shown, the heat transfer medium was glass fiber, which had the advantages of fast heat transfer, high precision, good linearity, high stability, good uniformity and high sensitivity. Test range was -200°C~400°C, measuring accuracy was ±0.5°C, resolution was 0.01°C. Thermocouples were all made of welding by ourselves. Therefore, in order to ensure the accuracy of the temperature tested, the thermocouple was fixed on a polystyrene foam board in a relatively closed room to record the indoor air temperature. After continuous observation for several days, the data was analyzed, then eliminated the thermocouples whose change trend of test results was inconsistent with most of the thermocouples until the selected thermocouple met the requirements.

Fig. 3-7. Multi-channel touch data recorder TP1000
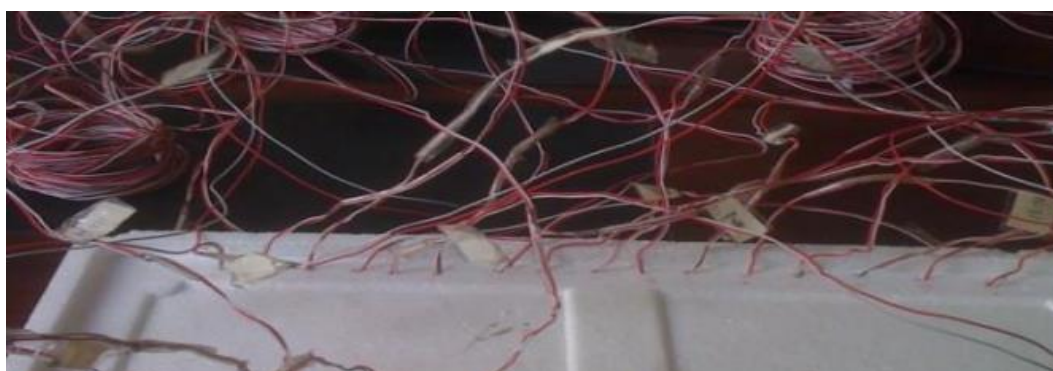
Fig. 3-8. T-type thermocouple probe temperature sensor

For the measurement of outdoor climate parameters, multi-parameter outdoor weather station JTR13 was adopted, as shown in Fig. 3-9. It was an automatic weather station with meteorological data acquisition, storage, processing and transmission functions. The system had stable performance, high detection accuracy, and could operate normally in unattended harsh natural environments. Its perfect software data processing function could meet the requirements of university buildings outdoor climate research and small weather stations. The temperature, relative humidity, wind speed, wind direction, air pressure, rainfall, total radiation, ultraviolet radiation and other parameters could be tested, among which, the test range of wind speed measurement was 360 in 16 directions, measurement accuracy was ±0.1m/s, resolution was 0.1m/s.

Fig. 3-9. Multi-parameter outdoor weather station JTR13

3.2.3 Experiment platforms

All the experiments in this paper were conducted in Qingdao, a coastal city, and the location of Qingdao was shown in Fig. 3-10. This city was characterized by significant seasonal variation, and had both cooling period and heating period. Fig. 3-11 showed the equipotential diagram of outdoor air and solar radiation all the year in Qingdao city of China. The highest temperature was 37.80°C in summer, the lowest air temperatures were -9.61°C in winter. And the highest solar radiation intensity in summer reached 1050kW/m^2, and the solar radiation intensity in winter was much lower than that in summer. And from Fig. 3-11, the winter period included November, December, January, February and March with the average air temperatures

of about -4.01°C, while the summer period included June, July, August, and September with the average air temperatures of about 27.02°C.
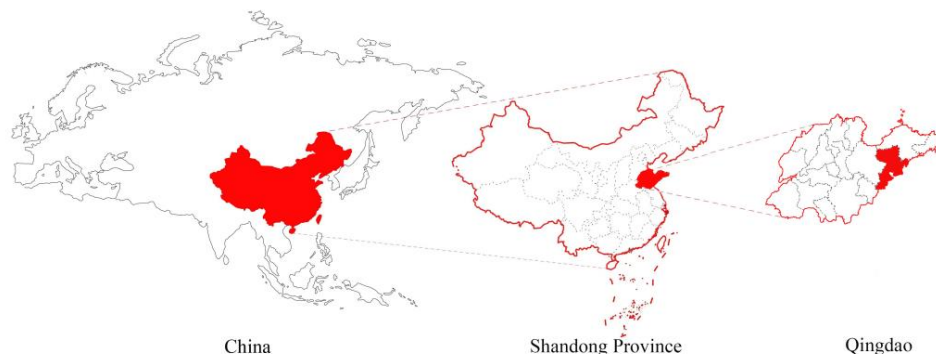
Fig. 3-10. Location of Qingdao in China
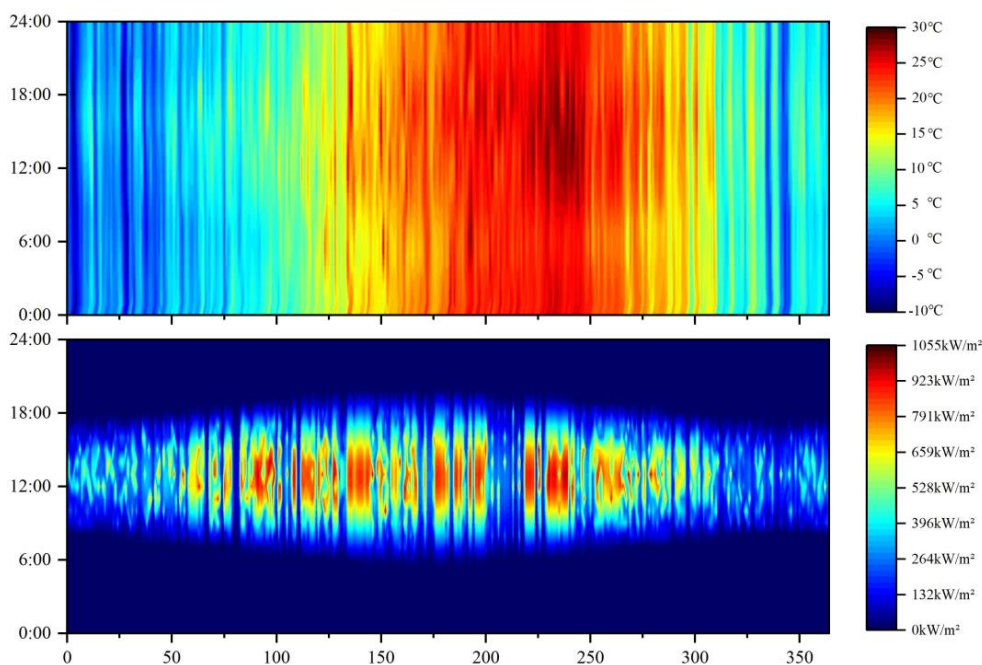
Fig. 3-11. Equipotential diagram of air temperature and solar radiation intensity all the year in Qingdao, China

The experiment was located in the Academic Innovation Center of Coastal Human Settlement Environment of Qingdao University of Technology, which had traditional advantages in disciplines such as architecture, civil engineering, environment and information. By establishing interdisciplinary teams and building high-level scientific research platforms, it was committed to the effective utilization of marine resources, marine ecological environment protection and green smart city construction to build Shandong coastal human settlement environment technology innovation brand.

At present, there were two main ways to conduct experiments. One was to choose 2 rooms,

the size, the air conditioning system settings, thermal performance, energy habits and so on had no difference, then brushed different paint in the rooms, respectively, and then the internal and external surface temperature and humidity in the rooms were monitored to compare the cooling effect of paint. Second was to build a proportional model for the experiment according to the corresponding standards, and determine the thermal properties had no difference, and then the internal and external surface temperature were monitored to compare the cooling effect of the paint. In the experiments of this paper, the second method was used to test the cooling effect of HR-coatings and RR-coatings.

Yuan et al. [15] conducted durability tests on prism RR-coatings after long-term outdoor exposure and concluded that prism RR-coatings had good durability and most suitable as architectural coatings. Therefore, in the three experiments on the influence of HR-coatings and RR-coatings on the thermal environment of building groups, prism RR-coatings and HR-coatings were used, and their samples and light paths were shown in Fig. 3-12.
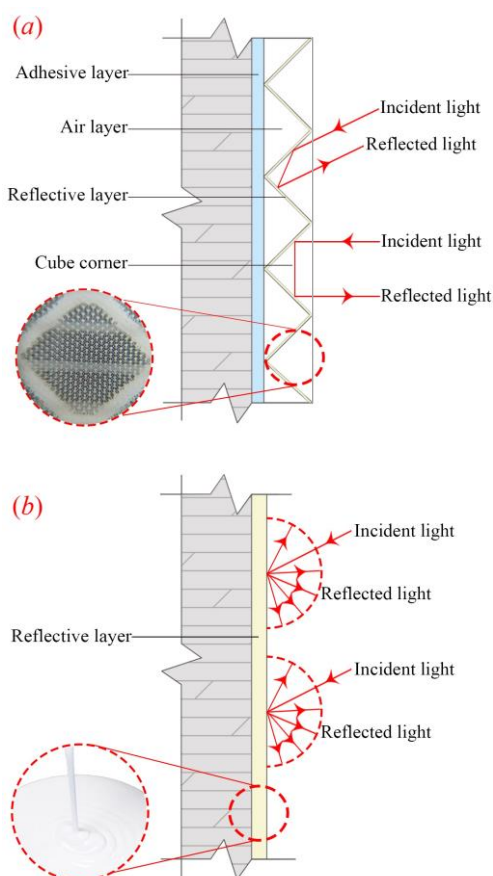
Fig. 3-12. The samples and light paths of (*a*) prism RR-coatings and (*b*) HR-coatings

The first experiment lasted for 96 hours from June 18 to 21, 2021. The experiment focused on the comparative study of the influence of the two coatings on the regional thermal

environment. The experiment platform was shown in the Fig. 3-13. The second experiment lasted for 96 hours from September 12 to 15, 2021. The experiment focused on the comparative study of the influence of different building formed on the thermal contribution of the two coatings. The experiment platform was as shown in the Fig. 3-14.

Fig. 3-13. The first experiment platform
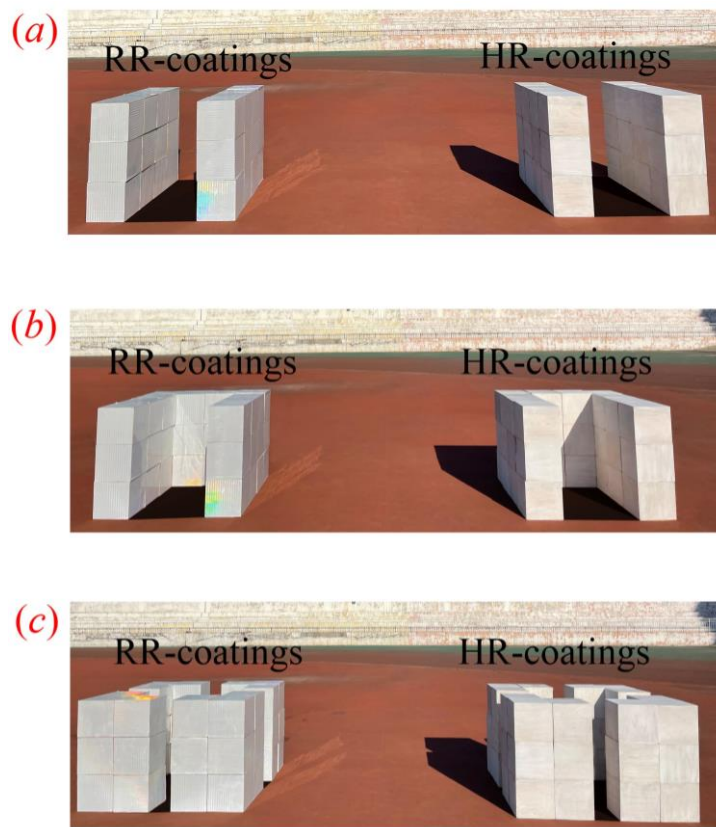
Fig. 3-14. The second experiment platform

The third experiment lasted 96 hours from December 7 to 10, 2022. The experiment focused on the comparative study of the influence of different seasons on the thermal contribution of the two coatings. The experiment platform was as shown in the Fig. 3-13.

3.3 Building energy load simulation

3.3.1 Evaluation index

(1) Building surface temperature

The building surface temperature is related to people's production and labor, and has an important impact on people's daily life, work, transportation and other activities. Climate change is also closely related to the healthy and sustainable development of society. Therefore, temperature change and climate conditions have attracted more and more attention from countries around the world. The global climate has significantly changed in recent years, and its average temperature has shown a rising trend. The environmental problem of climate warming threatens the development of economic life and other aspects of human society, so a series of problems caused by temperature rise should be paid great attention to. In order to deal with the problem of climate change, it is necessary to measure and monitor the temperature change and analyze its temperature change law.

(2) Building energy load

With the improvement of people's requirements for the comfort of living environment, the global building energy consumption was increasing year by year. As an important index affecting the energy consumption of air conditioning system, air conditioning load was obviously affected by outdoor climate conditions of buildings. Researchers at home and abroad have conducted a lot of studies on the relationship between the load of air conditioning system in buildings and outdoor meteorological conditions of buildings.

Akbari et al. [50-52] in the United States conducted a study on the relationship between outdoor ambient temperature and building air conditioning load in Los Angeles. When outdoor temperature increases by 10℃, air conditioning load increased by about 12W/m^2, and annual building energy consumption increased by about 300MW. Stantamouris et al. [53] used TRNSYS to simulate and analyze the deterioration of urban environment in Athens and its impact on the load of building air conditioning system. The results showed that when the heat island intensity in this area exceeded 10℃, the cooling load of building air conditioning system increased by two times and the power consumption increased by three times. COP of air conditioning refrigeration system decreased by 25%. Shimoda et al. [54] analyzed the meteorological observation data of Osaka in the past ten years and found that the urban environment in this area deteriorated in recent years. In the past ten years, the urban environmental temperature increased by about 2℃, resulting in an increase of about 25% in the load of building air conditioning system.

3.3.2 Simulation software introduction

Energy Plus was developed in 1976 by Lawrence Berkeley Laboratory, the United States Army Building Engineering Laboratory, the University of Illinois, Oklahoma State University and others. Building on BLAST and DOE-2, the Energy Plus added a number of new features and features, such as the ability to calculate time steps that could be reduced to 1 min. It was released in 2001 and was still being updated. Energy Plus calculated building heating and cooling loads and dynamic energy consumption throughout the year, and generated detailed reports. It used heat balance method to calculate load and room temperature, and used CTF (Conduction Function) to calculate heat Transfer. CTF was a more accurate reaction coefficient method and was based on wall surface temperature rather than indoor air temperature and therefore had better accuracy, while CTF non-convergence could usually be solved by shortening the time step. Energy Plus used heat and mass transfer to calculate heat and moisture transfer of walls, and used three-dimensional finite difference to calculate soil heat transfer. Kiva Foundation, added in version 8.7.0, was more accurate in calculating heat transfer between indoor ground layer and soil. In addition, Energy Plus provided a detailed description of the performance of the building and could describe the detailed shape information of the building.

3.3.3 Simulation setting

In this paper, we use the software of Energyplus to conduct two simulations. The first was to preliminarily determine the impact of RR-coating on the thermal environment of buildings. Based on the characteristic of RR-coating to reflect solar radiation back along the incident direction was due to its special optical elements with different physical properties. The prism RR-pattern facade was presented in Energyplus software, as shown in Fig. 3-15, and with the general facade as the contrast. The simulation case was shown in Fig. 3-16. A 7-day period was simulated for the investigation of the temperature variations, from 15th July to 21st July. And the weather data from Nanjing, China was input. The temperature difference at the center of the building at 10a.m., 1p.m. and 5 p.m. were researched, when the intensities of solar radiation were quite different.
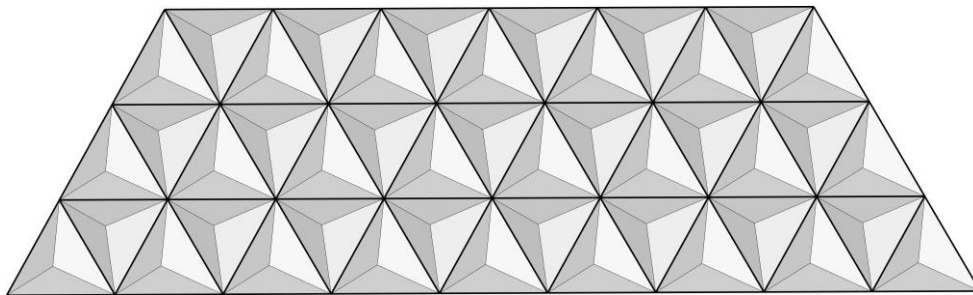
Fig. 3-15. Schematic diagram of prism RR-pattern facade
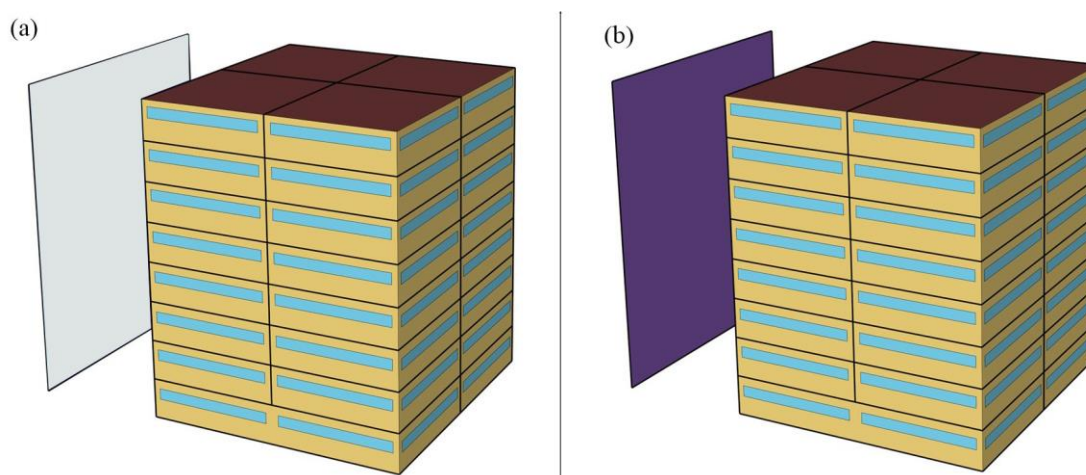
Fig. 3-16. Simulation case of the single building and neighboring testing surface (a) RR-pattern facades, (b) general facades

The second simulation selected the an actual three-sided enclosed educational building, the building model and plan function layout were as shown in Fig. 3-17. Then according to the previous experimental data, that was, compared with the HR-coatings, the RR-coatings of the solar reflectance of about 50% could reduce the space temperature by about 2°C, the reflectance of the building surface was set to 0~1, the step size was 0.1, and the corresponding cooling temperature varied linearly between 0°C and 4°C. However, because there was no coating with complete reflection or absorption in reality, therefore, the reflectance of 0 and 1 were removed. The specific setting of the temperature reduction for different reflectance was shown in Fig. 3-18. Based on these values, changes were made to the weather file, and then entered into EnergyPlus to simulate the daily, monthly and yearly energy load of an actual three-sided enclosed educational building in Qingdao, China, and CO_2 emissions were also calculated.
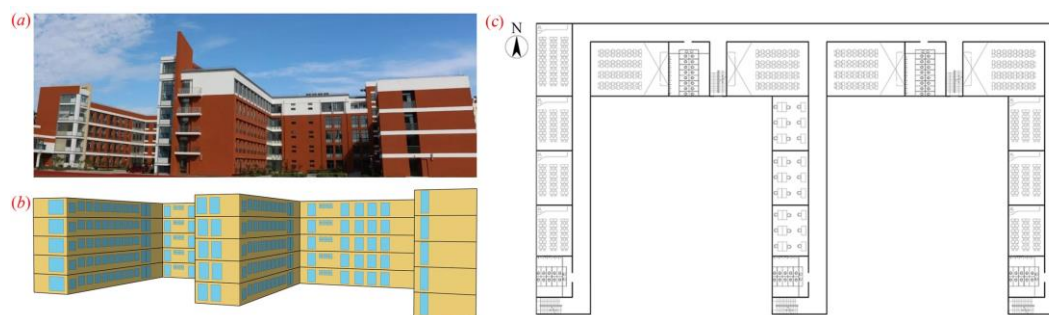
Fig. 3-17. (*a*) Building photo diagram, (*b*) model diagram and (*c*) plan function layout diagram
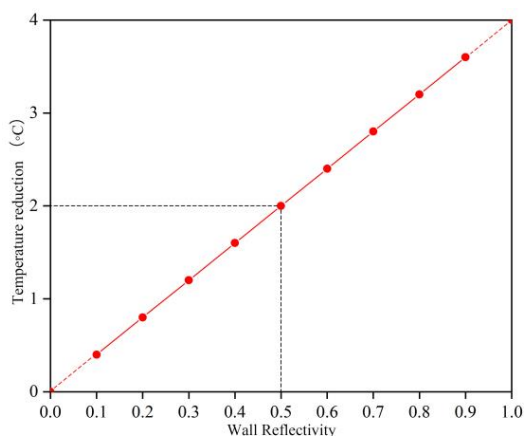
Fig. 3-18. Temperature reduction for different reflectance

3.4 Summary

This chapter briefly introduced the optical performance experiment of RR-coatings and HR-coatings involved in this paper, and the thermal performance experiment of two coatings on the thermal environment of regional buildings, and the building surface temperature and energy load simulation. In addition, the related evaluation indexes were also introduced, including the solar reflectance and retro-reflectance of coatings, the albedo, the wall temperature and air temperature of buildings, and daily, monthly and yearly energy load. And the instruments and measuring methods used in the experiment were also introduced.

References

[1] S.R.A. Dantas, F. Vittorino, K. Loh. Comparison of reflectance to solar radiation between mortars treated with TiO2 and painted mortars after three years of exposure. Journal of Building Engineering 46 (2022) 103829.

[2] M. Governatori, C. Ferrari, T. Manfredini, C. Siligardi. Preparation and characterization of glass ceramic frits with high solar reflectance. Open Ceramics 6 (2021) 100091.

[3] H.K. Zhang, Y.L. Yang, J. Huang, D.S. Fan. Radiative cooling gray paint with high solar reflectance for thermal management of electronic equipment. Solar Energy 241 (2022) 460–466.

[4] Y.P. Chen, J. Zou. Cr and Mg co-doped YAlO3 red cool pigments with high NIR reflectance and infrared emissivity for sustainable energy-saving applications. Ceramics International

[5] K.X. Lin, Y.W. Du, S.R. Chen, L.K. Chao, H.H. Lee, T.C. Ho, Y.H. Zhu, Y.J. Zeng, A.Q.

Pan, C.Y. Tso. Nanoparticle-polymer hybrid dual-layer coating with broadband solar reflection for high-performance daytime passive radiative cooling. Energy & Buildings 276 (2022) 112507

[6] A.N.M.T. Elahi, D. Jensen, M. Ghashami, K. Park, Comprehensive energy balance analysis of photon-enhanced thermionic power generation considering concentrated solar absorption distribution, Sol. Energy Mater. Sol. Cells 226 (2021) 111067.

[7] T.L. Zhang, C. Spece, F. Qi, W. Ying, T.T. Song. Influence of tree location on thermal radiation disturbance of the west wall of summer buildings. Energy & Buildings 273 (2022) 112359.

[8] A. Joudi, H. Svedung, M. Cehlin, M. Ronnelid. Reflective coatings for interior and exterior of buildings and improving thermal performance. Applied Energy 103 (2013) 562–570.

[9] X.W. Su, Z.J. Wang, C. Liu, F.Z. Zhou. Comfort limit for asymmetric thermal radiation from a cold wall in neutral to cool environments.   Building and Environment 218 (2022) 109112.

[10] K.J. Kontoleon, S. Saboor, D. Mazzeo, J. Ahmad, E. Cuce. Thermal sensitivity and potential cooling-related energy saving of masonry walls through the lens of solar heat-rejecting paints at varying orientations. Applied Energy 329 (2023) 120264.

[11] Z.A.A. Absi, M.I.M. Hafizal, M. Ismail. Experimental study on the thermal performance of PCM-based panels developed for exterior finishes of building walls. Journal of Building Engineering 52 (2022) 104379.

[12] J. Wang, S. Liu, X.i. Meng, W. Gao, J. Yuan. Application of RR-coatings in urban buildings: A comprehensive review. Energy Build. 247 (2021) 111137.

[13] J.H. Yuan, K. Emura, C. Farnham, H. Sakai. Application of glass beads as retro-reflective facades for urban heat island mitigation: Experimental investigation and simulation analysis. Build. Environ. 105 (2016) 140-152.

[14]J.H. Yuan, K. Emura, C. Farnham. A study on the durability of a glass bead retro-reflective material applied to building facades. Prog. Org. Coat. 120 (2018) 36-48.

[15] J.H. Yuan, K. Emura, C. Farnham. A method to measure retro reflectance and durability of RR-coatings for building outer walls. Journal of Building Physical 38 (2014) 500-516.

[16] J.H. Yuan, C. Farnham, K. Emura. A study on the accuracy of determining the retro-reflectance of retro-reflective material by heat balance. Solar Energy 122 (2015) 419-428.

[17] F. Rossi, B. Castellani, A. Presciutti, E. Morini, M. Filipponi, A. Nicolini, M. Santamouris. Retroreflective facades for urban heat island mitigation: Experimental investigation and energy evaluations. Appl. Energy 145 (2015) 8-20.

[18] G.S. Campbell. An Introduction to Environmental Biopsics [M]. Heidelberg Science Librar3. Springer New York, 1977, p175-176.

[19] T.R. Oke. The energetic basis of the urban heat Island. Quarterly Journal of the Royal Meteorological Society108 (1982) 1-24.

[20] G.A. Meehl, C. Tebaldi. More Intense, More Frequent, and Longer Lasting Heat Waves in the 21st Century. Science 305(2004) 994-997.

[21] Y. Wang, Z. Guo, J. Han. The relationship between urban heat island and air pollutants and them with influencing factors in the Yangtze River Delta, China. Ecological Indicators 129 (2021) 107976.

[22] M. Santamouris, F. Fiorito. On the impact of modified urban albedo on ambient temperature and heat related Mortality. Solar Energy 216 (2021) 493-507.

[23] H. Akbari, M.H. Damon, D. Seto. The Long-term effect of increasing the albedo of urban Areas. Environmental Research Letters 7 (2012) 024004.

[24] Z. Jandaghian, U. Berardi. Analysis of the cooling effects of higher albedo surfaces during heat waves coupling the Weather Research and Forecasting model with building energy Models. Energy and Buildings 207 (2020) 109627.

[25] T.R. Oke, G. Mills, A. Christen. Urban Climates. Cambridge University Press, 2017, p128-129.

[26] M. Taleghani, D. Sailor, G.A.Ban-Weiss. Micrometeorological simulations to predict the impacts of heat mitigation strategies on pedestrian thermal comfort in a Los Angeles Neighborhood. Environmental Research Letters 11 (2016) 024003.

[27] B.E. Psiloglou, H.D. Kambezidis. Estimation of the ground albedo for the Athens area, Greece. Journal of Atmospheric and Solar-Terrestrial Physics 71 (2009) 943-954.

[28] H. Liu, B. Wang, C. Fu. Relationships between surface albedo, soil thermal parameters and soilmoisture in the semi-arid area of Tongyu, northeastern China. Advances in Atmospheric Sciences 25 (2008) 757-764.

[29] H. Sugawara, T. Takamura. Surface Albedo in Cities: Case Study in Sapporo and Tokyo，Japan. Boundary-Layer Meteorology 153 (2014) 539-553.

[30] M. Aida. Urban albedo as a function of the urban structure?A model Experiment. Boundary-Layer Meteorology 23 (1982) 405-413.

[31] K. Fortuniak. Numerical estimation of the effective albedo of an urban Canyon. Theoretical andApplied Climatology 91 (2007) 245-258.

[32] H. Sugawara, T. Takamura. Surface Albedo in Cities: Case Study in Sapporo and Tokyo, Japan. Boundary-Layer Meteorology 153 (2014) 539-553.

[33] S.R. Gaffin, M. Imhoff, C. Rosenzweig. Bright is the new black—multi-year performance of high-albedo roofs in an urban Climate. Environmental Research Letters 7 (2012) 014029.

[34] H. Li, J. Harvey, A. Kendall. Field measurement of albedo for different land cover materials and effects on thermal Performance. Building and Environment 59 (2013) 536-546.

[35] J. Loveday, G.K. Loveday, J.J. Byrne. Modified i Buttons: A Low-Cost Instrument to Measure the Albedo of Landscape Elements. Sustainability 11 (2019) 6896.

[36] L. Meng, J. Mao, Y. Zhou. Urban warming advances spring phenology but reduces the response of phenology to temperature in the conterminous United States. Proceedings of the National Academy of Sciences 117 (2020) 4228-4233.

[37] F. Rossi, B. Castellani, A. Presciutti, E. Morini, E. Anderini, M. Filipponi, A.Nicolini. Experimental evaluation of urban heat island mitigation potential of retro-reflective pavement in urban canyons. Energy Build. 126 (2016) 340-352.

[38] C.B Schaaf, F. Gao, A.H. Strahler. First operational BRDF, albedo nadir reflectance products from MODIS. Remote Sensing of Environment 83 (2002) 135-148.

[39] W. Lucht, C.B. Schaaf, A.H. Strahler. An algorithm for the retrieval of albedo from space using semiempirical BRDF Models. IEEE Transactions on Geoscience and Remote Sensing 38 (2002) 977-998.

[40] T. Hakala, J. Suomalainen, J.I. Peltoniemi. Acquisition of Bidirectional Reflectance Factor Dataset Using a Micro Unmanned Aerial Vehicle and a Consumer Camera. Remote Sensing 2 (2010) 819-832.

[41] E. Honkavaara, E. Khoramshahi. Radiometric Correction of Close-Range Spectral Image Blocks Captured Using an Unmanned Aerial Vehicle with a Radiometric Block Adjustment. Remote Sensing 10 (2018) 256.

[42] J.F. Burkhart, A. Kylling, C.B. Schaaf. Unmanned aerial system nadir reflectance and

MODIS nadir BRDF-adjusted surface reflectances intercompared over Greenland. The Cryosphere 11 (2017) 1575-1589.

[43] S. Bonafoni, A. Sekertekin. Albedo Retrieval From Sentinel-2 by New Narrow-to-Broadband Conversion Coefficients. IEEE Geoscience and Remote Sensing Letters 17 (2020) 1618-1622.

[44] S. Liang. Narrowband to broadband conversions of land surface albedo I. Remote Sensing of Environment 76 (2001) 213-238.

[45] Y. Qu, S. Liang, Q. Liu. Mapping Surface Broadband Albedo from Satellite Observations: A Review of Literatures on Algorithms and Products. Remote Sensing 7 (2015) 990-1020.

[46] A. Bernabe, M. Musy, H. Andrieu, I. Calmet. Radiative properties of the urban fabric derived from surface form analysis: A simplified solar balance model. Solar Energy 122 (2015) 156-168.

[47] S.E.G. Jayamaha, N.E. Wijeysundera, S.K.Chou. Measurement of the heat transfer coefficient for walls. Building and Environment 32 (1996) 399-407.

[48] F.S. Flor, S.A. Dom′nguez. Modelling microclimate in urban enviroments and assessing its in uence on the performance of surrounding building. Energy and Buildings 36 (2004) 403-413.

[49] K.Niachou, I.Livacla, M.Santamouris. Experimental study of temperature and airflow distribution inside an urban street canyon during hot summer weather conditions—Part I: Air and surface temperatures. Building and Environment 43 (2008) 1383-1392.

[50] H. Akbari, S. Konopacki. Energy effects of heat — island reduction strategies in Toronto, Canadaf. Energy 29 (2004) 191-210.

[51] H. Akbari, M. Pomerantz, H. Taha. Cool Surfaces and Shade Trees to Reduce Energy Use and Improve Air Quality in Urban Area. Solar Energy 70 (2001) 295-310.

[52] R. Levinson, H. Akbari. Effects of composition and exposure on the solar reflectance of portalnd cement concrete. Solar Energy 92 (2012) 1679-1698.

[53] M. Santamouris, N. Papanikolaou, I. Livada. On the impact of urban climate on the energy consumption of buildings. Solar Energy 70(2001) 201-216.

[54] Y. Shimoda, T. Fujii, T. Morikawa. Residential end use energy simulation at city scale. Building and Environment 39 (2004) 959-967.

Study on spectral property of retro-reflective coatings

Chapter 4 Study on spectral properties of retro-reflective coatings

4.1 Introduction

In recent years, high-rise and high-density buildings increased and gradually formed a compact urban development mode [1, 2], which exacerbated the urban heat island effect, and leaded to the deterioration of outdoor thermal environment and the increasement of building energy consumption [3, 4]. Therefore, the application of cooling coatings with high solar reflectivity and thermal emissivity on the buildings was considered as an effective solution [5, 6]. However, the solar radiaiton reflected by the highly-reflective coatings (HR-coatings) would be absorbed by the adjacent buildings and streets, as shown in Fig. 4-1(a), therefore, the highly-reflective coatings had a very limited positive impact on the urban heat island effect among the high-rise buildings [7]. Since 2014, more scholars had paid attention to the retro-reflective coatings (RR-coatings), which could reflect solar radiation along the incident direction, and the optical reflection principle was shown in Fig. 4-1(b). RR-coatings could reduce the solar radiation reached on the adjacent buildings and roads, and improve the surrounding thermal environment and lower the urban heat island [8].

Rossi et al. [9] found that when RR-coatings were applied to the vertical surface of the urban canyon, air temperature decreased by 1% compared with the white diffuse coatings from the result of a summer monitoring campaign. Zhang et al. [10] covered RR-coatings on the tent model and found that the peak temperature of indoor air was lowered by 7.0°C, compared to the ordinary tent. Qin et al. [11] built two small-scale building blocks with both glass bead RR-coatings and HR-coatings, and it was found that the outer surface temperatures of the RR-coatings were 5–10 ∘C lower than that of the HR-coatings during the early afternoon, while the lowered temperatures were up to around 1.0–3 ∘C at noontime and about 1 ∘C at night. Rossi et al. [12] monitored the application of the prism RR-coatings with a reflectivity of 62.8% on the vertical surface of the urban canyons in the summer, and the results showed that the temperature dropped by 1% when compared with the white diffused cooling materials. Yoshida et al. [13] covered the RR-coatings on single float glass and it was found the cooling load was reduced by 489 MJ/h, but the heating load was increased by 534 MJ/h, compared to the window with heat shading film and the Low-E double glass. Yuan et al. [14] simulated the energy consumption of building located in Shanghai, China and it was found that compared with no RR-coatings, the annual cooling and heating loads were decreased by 157 MJ/m2 and -71 MJ/m2, respectively.

In addition, many scholars have studied the optical properties of RR-coatings. Sakai et al. [15] first proposed the thermal balance method, roughly measured and calculated the retro-reflectance of glass beads and capsule RR-coatings. Sakai et al. [16] and Yuan et al. [17] further improved the thermal equilibrium method by using a spectrophotometer to measure the specular

and diffuse reflectance to calculate the retro-reflectance. The method was used to measure the retro-reflectance of prism and capsule RR-coatings at some wavelengths. Yuan et al. [18-20] developed the Emitting-Receiving optical fiber system with a fiber optic probe having seven glass fibers, six of which were used to emit light and the other at the center to receive reflected light, and measured the the angular distribution at some incident angles of glass bead RR-coatings and prism RR-coatings. Rossi et al. [21] designed a special experimental apparatus to measure the angular distribution, which consisted mainly of an artificial solar energy source and a measurement box, and the angular distribution of radiation reflected by five RR-coatings was evaluated at several solar radiation incidence angles. However, owing to the sample plane could not be tilted, the measurement was limited by the angular distribution on one plane. The experimental setup was further improved by Rossi et al. [22]. A semicircular array of 19 fixed photodiodes was used to measure the angular distribution of the reflected light, while the samples could have different inclinations by rotating the platform.

From the above review, it could be seen that the main works about the RR-coatings were focused on the the application effects and measurement of spectral property [23]. And the research of spectral property could be more helpful for the research of related application efficiency. Based on this, this study employed two typical RR-coatings, and measured the global-reflectance and retro-reflectance by IS50-R3 integrating sphere equipment and a special angular resolution test system, which was self-developed. And prism RR-pattern facades were proposed, and take general facades as comparison, conducted surface temperatures simulation of nearby buildings in order to examine their impact on thermal environment preliminarily.
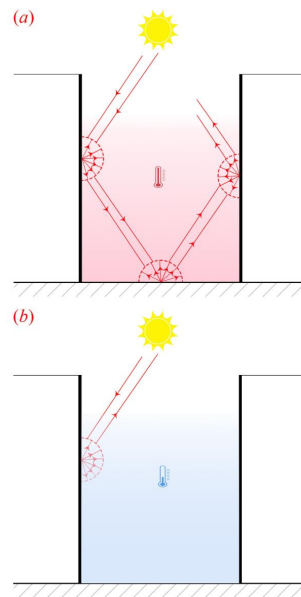
Fig. 4-1. Optical paths of (a) diffuse reflection and (b) retro-reflection

4.2 Optical property of RR-Coatings

4.2.1 Description of RR-coatings

RR-coatings mainly included three categories: glass-beads, prism and capsule. Glass-bead RR-coatings could be manufactured easily and were more effective in reducing the temperature [16, 23]. Prism RR-coatings had better durability and were more suitable for buildings [8]. However, capsule RR-coatings were more fragile and not be widely used [22].

The glass-beads RR-coatings and prism RR-coatings were selected in this study. Fig. 4-2. showed the physical appearance and optical mechanism. For the glass-beads RR-coatings, the incident sunlight was reflected along the incident direction through two refractions on the glass microsphere boundary and one reflection by using the highly-reflective coating. And for the prism RR-coatings, the incident sunlight was reflected through two refractions on the prism boundary and multiple reflections on the reflective layer [22].
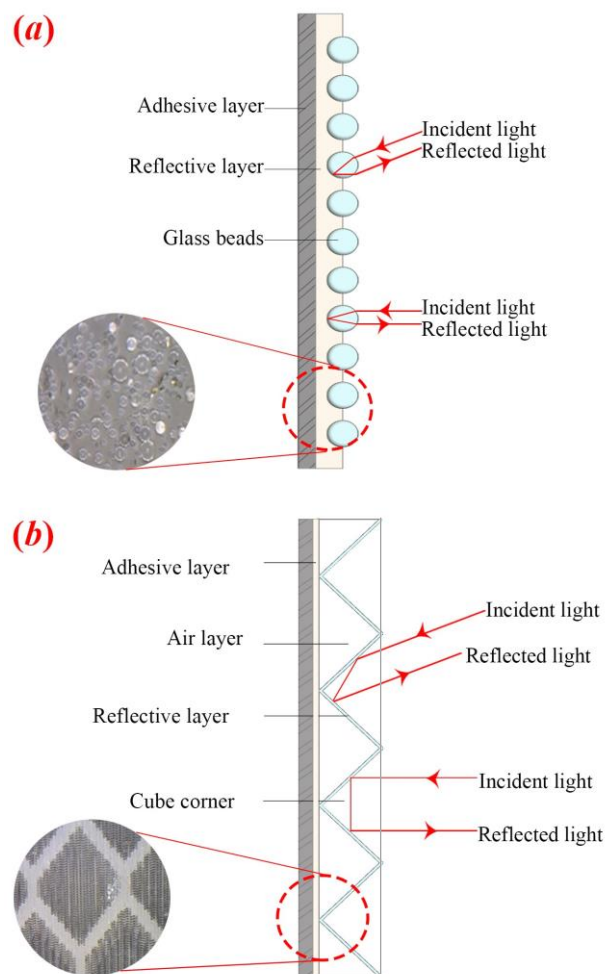
Fig. 4-2. Physical appearance and optical mechanism of (a) glass-beads and (b) prism RR-coatings

4.2.2 Description of measurement equipment

For the global reflectivity, the integrating sphere was employed by use of mature equipment (Model: IS50-R5) with an adaptive wavelength of 250–2500 nm. For the retro-reflectivity, owing to the integrating spheres could not be used directly to measure the retro-reflection of the samples, new testing equipment was self-developed. The measurement system graph and optical principle were shown in Fig. 4-3. It mainly included a macro-angular resolution spectroscopic system, a halogen light source (spectral range 360–2500 nm), a spectrometer (wavelength range 360–2500 nm), many near-infrared quartz glass fibers, and some mechanical components. The light emitted by the halogen lamp entered the incident arm, and the incident arm shined the light source on the sample surface of the sample table at a set incident angle. The receiving arm received the reflected light from the sample at a specific angle and transmitted it through optical fiber to the spectrometer. And the final angular distribution of RR-coating reflectance could be obtained by referring to the angular distribution of the reflectance of the standard aluminum mirror. Table 4-1 showed the specifications for the instruments used in the measurements. The macroscopic angular resolution spectrum system could enable the incident light to be accurately focused onto the sample surface and the sampling manipulator adopts the precise sliding platform, which could achieve the full rotation of 0–360∘ to obtain the spectral measurements at any incident angle.
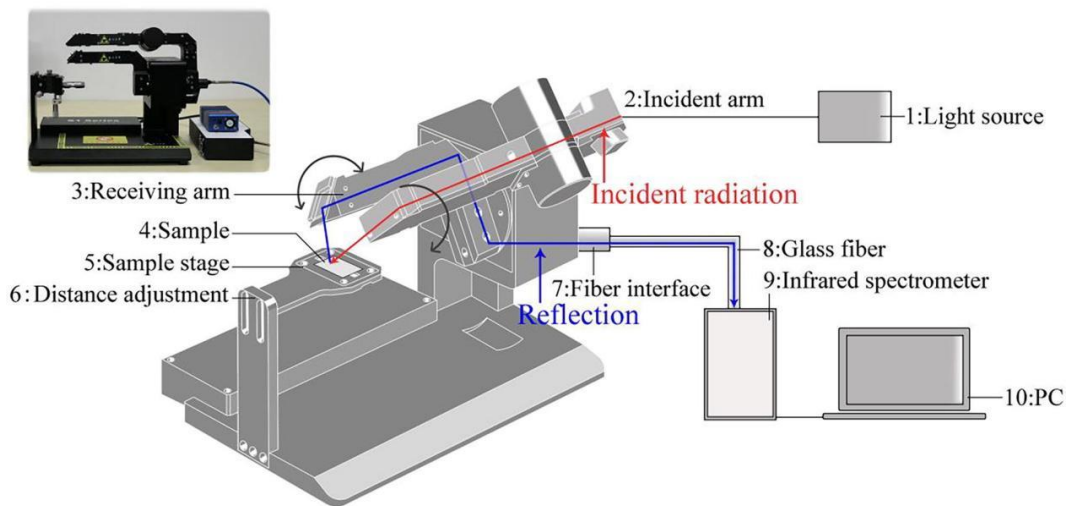
Fig. 4-3. Measurement system graph and optical principle

Table 4-1. Specifications of the instruments used in the measurements

Instrument	Model	Supplier	Resolution	Accuracy	Range	of
					operation	
Spectrometer	EN2500	Shanghai	8 nm	± 0.2 nm	200 nm~	2500

		Chenchang Instrument Equipment Co., ltd			nm
Integrating sphere	IS50-R5	Shanghai Chenchang Instrument Equipment Co., ltd	0°	± 0.2 nm	200 nm~ 2500 nm
Angular resolution test system	S1	Shanghai Chenchang Instrument Equipment Co., ltd	0.1°	± 1 %	0 ~ 360°

4.2.3 Measurement results

(1) Global reflectivity

Fig. 4-4. showed the global reflectance of the glass beads RR-coatings, prisms RR-coatings and a high-reflective coatings (HR-coatings) measured by the IS50-R5 integrating sphere device. As shown, the global reflectivity of the two RR-coatings were changed as the similar rule of the variation of wavelength. However, the glass beads RR-coatings had a higher reflectivity than prism RR-coatings, and they were both lower than that of the HR-coatings. Under the wavelength of 780-2526 nm, where more than 95% of the infrared ray was covered [24], for the reflectivity of glass beads RR-coatings, the lowest value was 53.11% at 823.7 nm and the highest value was 78.35% at 1014.0 nm, while for the prisms RR-coatings, the lowest value was 26.83% at 1682.5 nm and the highest value was 56.65% at 1089.7 nm.

By the weighted-average computation of the ground solar radiation energy distribution, the reflectance of glass-beads RR-coatings, prism RR-coatings and HR-coatings were 64.74%, 51.44% and 73.2%, respectively. Compared to the HR-coatings, these two RR-coatings had the lower globe reflectivity.
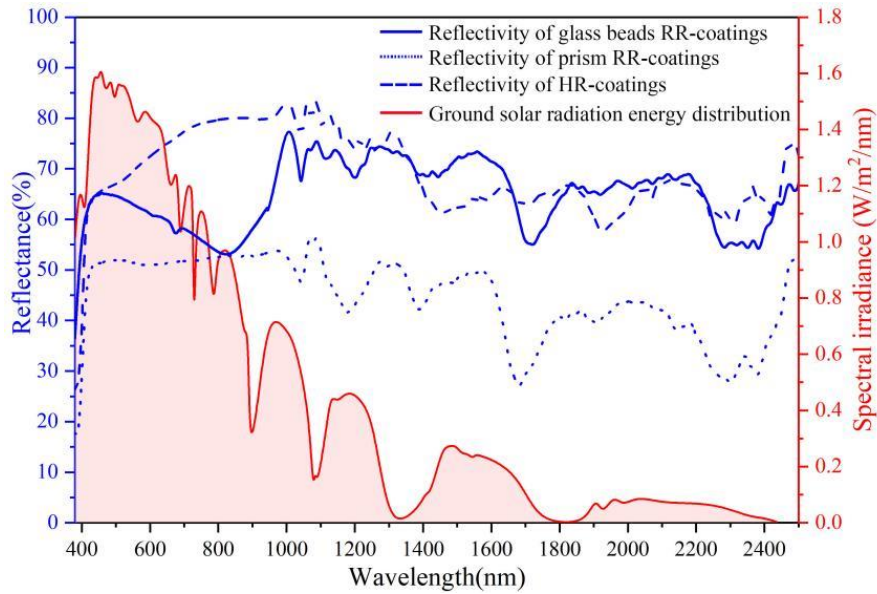
Fig. 4-4. Reflectance spectrum of the glass-beads, prism RR-coatings and the HR-coatings.

(2) Retro-reflectivity

To study the retro-reflectivity of the glass-beads, prism RR-coatings and the HR-coatings, the angular distribution (from -80° to 80°) of reflected radiation for the incident angle of 10°, 30°, 50° and 70° was measured by employment of the self-developed special angular resolution test system, which was shown in Fig. 4-5. The incident solar radiation striked the samples with positive angles of incidence. It could be seen that compared with HR-coatings which had diffuse-reflection property and no retro-reflection property, two kinds of RR-coatings showed the significant retro-reflection property for small incidence angles including 10° and 30°. At 50°, although retro-reflection property was maintained, specular-reflected radiation percentage was obviously higher than the retro-reflected one. At 70°, retro-reflection was completely lost and there was only specular-reflection. It showed the dependency of retro-reflection property of RR-coatings on the lower incident angles.

Table 4-2 showed the angular distribution percentage of the reflected radiation for several angles of the incident radiation. It could be seen that for two RR-coatings, the reflected solar radiation towards the incoming direction, that was retro-reflectivity, decreased with the increasement of the incident angle. For the glass bead RR-coatings, the retro-reflectivity was 21.73% and 19.21%, respectively (at 10° and 30° of incidence), and RR behavior was stronger for prism RR-coatings with the value of 25.22% and 21.67%, respectively. However, for larger incidence angles including 50°and 70°, two RR-coatings mainly showed specular-reflection property. The specular reflectance of glass bead RR-coatings were 18.61% and 28.01%, respectively, and specular-reflection property were also stronger for prism RR-coatings with

the value of 19.60% and 29.97%, respectively. And with the incident angle increased from 0∘and 70∘, the retro-reflectivity of the glass-beads RR-coatings and prism RR-coatings were decreased by 67.69% and 91.67%, respectively.
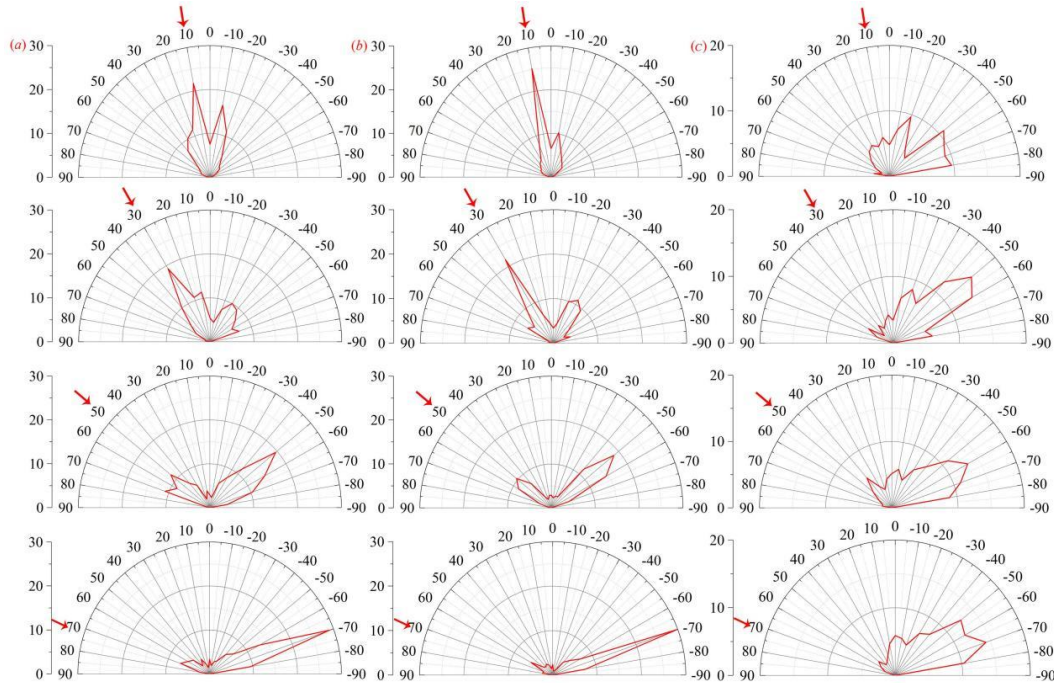
Fig. 4-5. Angular distribution of reflected solar radiation for 10∘, 30∘, 50∘ and 70∘ of (a) the glass-beads, (b) prism RR-coatings and (c) the HR-coating

Table 4-2. Angular distribution percentage of the reflected radiation (from 80∘ to -80∘) for several angles of the incident radiation (10∘, 30∘, 50∘ and 70∘)

Direction of reflected light	Glass-beads RR-coatings				Prism RR-coatings				HR-coatings			
	10	30	50	70	10	30	50	70	10	30	50	70
-80	0.00	0.00	4.00	8.43	0.00	0.00	0.00	10.42	9.64	5.98	8.82	10.32
-70	0.71	5.02	5.32	28.01	0.65	1.03	4.32	29.97	9.04	5.13	11.03	14.29
-60	1.67	3.68	7.41	10.15	1.31	2.69	14.40	10.13	9.64	13.67	13.23	11.90
-50	2.86	3.47	18.61	7.07	3.27	4.48	19.60	7.07	10.84	15.38	11.03	12.70
-40	3.33	5.38	8.53	5.77	3.92	7.41	11.52	4.77	3.61	11.96	8.09	7.94
-30	5.47	10.05	6.88	3.41	4.90	11.08	2.88	2.41	4.82	6.84	6.62	7.14
-20	10.95	5.82	5.88	2.94	6.53	9.84	2.88	0.94	9.64	8.55	4.41	4.76
-10	8.66	4.47	2.31	1.94	10.34	4.48	2.30	1.94	7.23	6.84	5.88	5.56
0	7.52	5.35	2.88	3.36	8.53	3.36	2.88	2.36	4.82	3.42	5.15	5.87
10	21.73	7.47	1.88	1.41	25.22	4.48	2.88	4.41	6.02	4.27	4.41	4.76

20	11.52	8.70	2.02	2.36	13.80	6.72	2.02	4.36	4.82	3.42	2.94	3.17
30	10.14	19.21	5.88	3.83	7.53	21.67	2.88	5.83	5.42	2.56	3.68	2.38
40	7.76	10.94	7.20	2.36	5.90	8.96	9.20	5.36	4.82	3.42	5.88	2.06
50	3.33	4.59	11.60	4.83	2.92	5.60	10.38	2.83	3.61	1.71	3.68	3.17
60	2.38	3.70	5.64	5.66	2.61	6.72	8.64	3.65	2.41	4.27	2.21	2.38
70	2.14	1.12	3.88	7.02	1.96	1.12	2.88	2.10	1.20	2.56	1.47	1.59
80	0.71	1.12	0.58	2.36	0.65	1.12	0.58	2.36	2.41	0.00	1.47	0.00

4.3 Thermal effect of optical structure

It was worth mentioning that in order to determine the influence of RR-coatings on building thermal environment preliminarily, based on the RR-coatings reflected the solar radiation back along the incident direction due to their special optical components with different physical properties, the prism RR-pattern facades were proposed and represented by shadow elements in the software of Energyplus, similar with the surface design in Han et al. [25]. Meanwhile, general facades were as the comparison, and conducted surface temperatures simulation of nearby buildings in order to examine their impact on thermal environment.

4.3.1 Description of RR-facade model

The first step in the simulation was to design a surface model enables similar RR-property investigation in the energy simulation environment. A macro-scale RR-facades design with an array retro-reflector pattern which was a cubic-corner retro-reflector consisting of three mutually perpendicular plane surfaces was proposed, as shown in the Fig. 4-6. The Ideal Loads Air System was adopted for the purpose of studying the HVAC energy consumption of reference buildings.
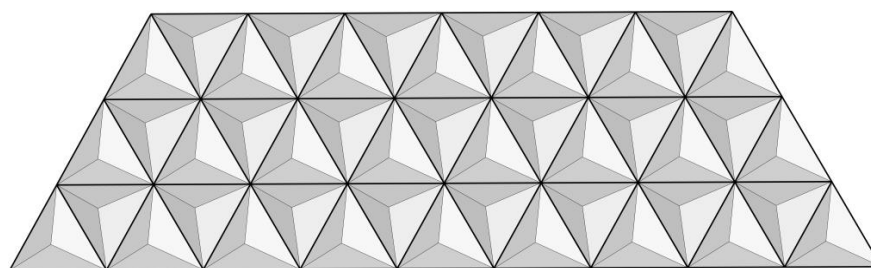
Fig. 4-6. Macro-scale cubic-corner retroreflector array

4.3.2 Description of the simulation case

The simulation case consisted of a single residential building and a neighboring testing surface on the west side, and a general facade was introduced as the comparison. The simulation models were illustrated in Fig. 4-7. The simulation city was Nanjing, and the weather data were from the Energyplus climate file database. The single building had eight floors, with the length,

width and height of 20m* 20m* 24m. The plans of ground-floor and the upper-seven-floors were described in Fig. 4-8, and the first floor was the hall, and other floors were for residence. The information about construction materials were set as shown in the Table 4-3. The diffuse solar reflectance of the exterior vertical facades was set to 40%. The east facade of the building was opposite to the testing surface, and the distance between them was 10m. The testing surface was designed through the shadow elements in the Energyplus. And the conditions of the building load calculation were referred to [26]. Since surface temperatures were influenced by the amount of received solar radiation, this comparative analysis could be conducted correspondingly by studying the temperature variations of the control surface.

A 7-day period was simulated for the investigation of the temperature variations, from 15_{th} July to 21_{st} July. And the weather data from Nanjing, China was input. The temperature difference at the center of the building at 10a.m., 1p.m. and 5 p.m. were researched, when the intensities of solar radiation were quite different.
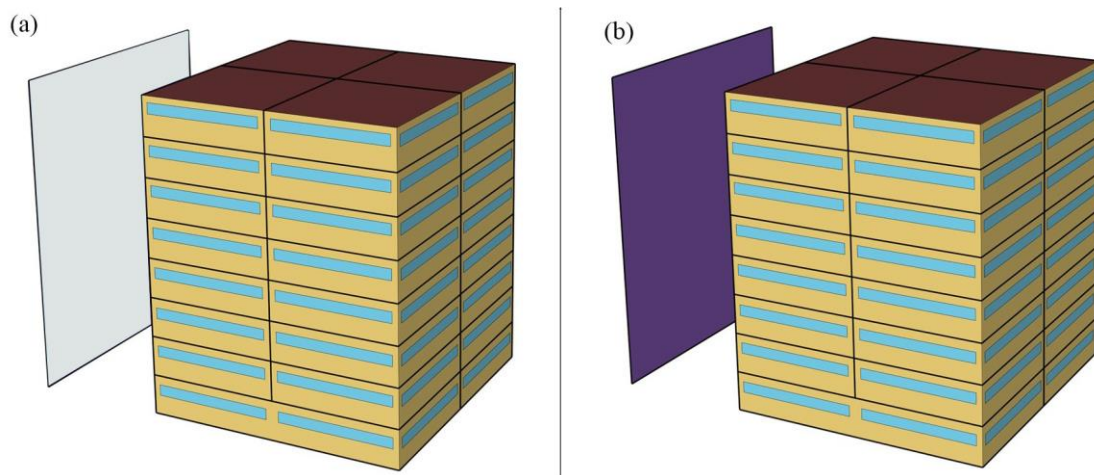
Fig. 4-7. Simulation case of the single building and neighboring testing surface (a) RR-pattern facades, (b) general facades
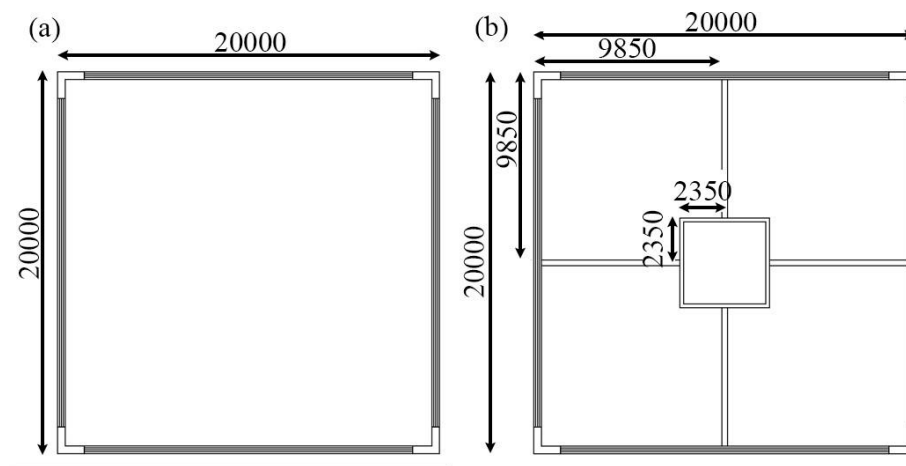
Fig. 4-8. The plans of (a) ground-floor and (b) upper-seven-floors

Table 4-3. Architectural elements description

Architectural elements	Layers materials description and thickness (from outer side, measures in meters)	Thermal properties
External walls	External brickwork: 0.10	K=0.314 W/m²K, Reflectivity=40%
	XPS extruded polystirene: 0.08	
	Concrete block (lightweight): 0.1	
	Gypsum plastering : 0.013	
Internal walls	Gypsum plasterboard: 0.020	K=1.754 W/m²K, Reflectivity=40%
	Air gap and aluminum frame: 0.10	
	Gypsum plasterboard: 0.020	
Ground	External rendering: 0.025	K=0.246 W/m²K, Reflectivity=29%
	Floor structure: 0.20	
	Mineral wool (stone): 0.15	
	Wooden flooring: 0.02	
Roof	Asphalt: 0.010	K=0.250 W/m²K, Reflectivity=40%
	Mineral wool (glass): 0.15	
	Air gap and roof structure: 0.20	
	Plasterboard: 0.015	
Internal floor	Wooden flooring: 0.02	K=1.122 W/m²K, Reflectivity=29%
	Elastomeric foam: 0.005	
	Cast concrete (lightweight): 0.10	
	Gypsum plastering: 0.015	
Window	Clear: 0.003 Air Clear: 0.003	K=2.4 W/m²K, Reflectivity=7%

4.3.3 Results and Discussion

Building surface temperature was an important parameter affecting outdoor thermal environment, which would affect outdoor comfort level directly and the building energy consumption indirectly [27], so the temperatures in exterior walls were studied in this study.

Fig. 4-9 showed the variation of the surface temperatures resulted by two different testing surfaces during the experimental period at 10a.m., 1p.m. and 5p.m., respectively. It could be seen that the temperatures of RR-pattern facades were always lower than those of general facades. For the 10a.m. in the Fig. 4-9(a), the maximum temperature difference was 0.66°C, and the average temperature difference were 0.43°C. For the 1p.m. in the Fig. 4-9(b), the

maximum temperature difference was 1.75℃, and the average temperature difference was 1.57℃. For the 5p.m. in the Fig. 4-9(*c*), the maximum temperature difference was 1.13℃, and the average temperature difference was 1.02℃.

From Fig. 4-9, it showed there were the different temperature reduction in different times and there were the higher temperature reduction efficiencies at 1p.m. This phenomenon was because there were more solar radiation gain in 1 p.m., due to the optical advantages of RR-pattern facade, it could reflect the more solar radiation along the incident direction.
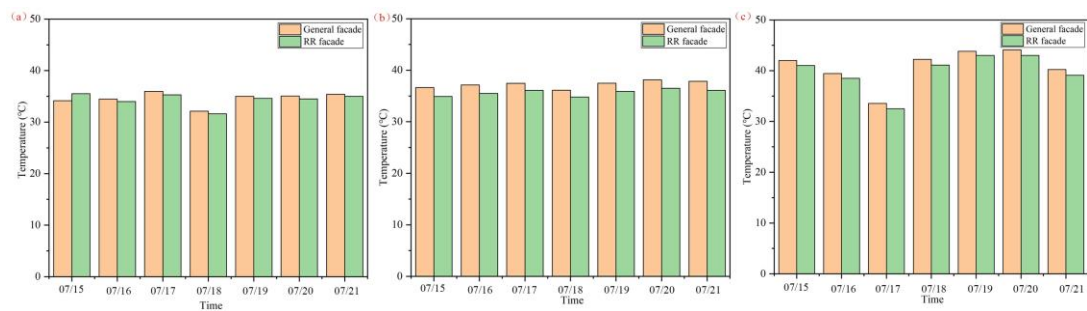
Fig. 4-9. The temperature variations of RR-facades and general facades at (a) 10:00 a.m. (b) 1:00 p.m. (c) 5:00 p.m.

4.4 Conclusion

In this study, two typical RR-coatings (the glass beads and prism RR-coatings) were selected as the basis for detailed spectral measurements and analysis, with conventional HR-coatings as a comparison. The global reflectance spectral of the coatings were measured using an integrating sphere, while a dedicated angular resolution system was developed to measure the retro-reflectance of the two typical RR-coatings, at four representative incidence angles. And prism RR-pattern facades were proposed, and take general facades as comparison, conducted surface temperatures simulation of nearby buildings in order to examine their impact on thermal environment preliminarily. The main conclusions are as follows:

(1) The global reflectivity of glass-beads RR-coatings, prism RR-coatings and HR-coatings were 64.74%, 51.44% and 73.2%, respectively. Compared to the HR-coatings, these two RR-coatings had the lower global reflectivity.

(2) The HR-coatings had only diffuse-reflection property and no retro-reflection property. Two RR-coatings showed the significant retro-reflection property, and at the smaller incidence angles, compared with glass bead RR-coatings, the prism RR-coatings showed the stronger retro-reflection property with the values of 25.22% and 21.67%, respectively (at 10◦ and 30◦ of incidence).

(3) For larger incidence angles including 50◦and 70◦, two RR-coatings mainly showed specular-reflection property. And compared with the glass beads RR-coatings, the prism RR-coatings had the stronger specular-reflection property.

(4) The prism RR-coatings showed the larger dependency of retro-reflection property on the lower incident angles.

(5) RR-pattern facades could reduce the wall surface temperature, compared to general facades. And at the time of 1p.m. when the solar radiation was the highest, there showed the best cooling effect with the peak and average temperatures difference of 1.75°C and 1.57°C.

References

[1] J. Wang, S.H. Liu, Z.F. Liu, X. Meng, C.B. Xu, W.J. Gao, An experimental comparison on regional thermal environment of the high-density enclosed building groups with retro-reflective and high-reflective coatings, Energy Build. 259 (2022), 111864.

[2] W. Pan, M. Pan, A dialectical system framework of zero carbon emission building policy for high-rise high-density cities: perspectives from Hong Kong, J. Clean. Prod. 205 (2018) 1–13.

[3] E.L. Kruger, F.O. Minella, F. Rasia, Impact of urban geometry on outdoor thermal comfort and air quality from field measurements in curitiba, Brazil, Build. Environ. 46 (3) (2011) 621–634.

[4] S. LoweA, An energy and mortality impact assessment of the urban heat island in the us, Environ. Impact Assess. Rev. 56 (JAN. 2016) 139–144.

[5] A. Synnefa, M. Santamouris, H. Akbari, Estimating the effect of using cool coatings on energy loads and thermal comfort in residential buildings in various climatic conditions, Energy Build. 39 (2007) 1167–1174.

[6] M. Santamouris, Cooling the cities - a review of reflective and green roof mitigation technologies to fight heat island and improve comfort in urban environments, Sol. Energy 103 (2014) 682–703.

[7] Y.H. Qing, Urban canyon albedo and its implication on the use of reflective cool pavements, Energy Build. 96 (2015) 86–94.

[8] J.H. Yuan, K. Emura, C. Farnham, A method to measure retro-reflectance and durability of RR-coatings for building outer walls, J. Build. Phys. 38 (6) (2015) 500–516.

[9] F. Rossi, E. Morini, B. Castellani, A. Nicolini, E. Bonamente, E. Anderini, F. Cotana. Beneficial effects of RR-coatings in urban canyons: results from seasonal monitoring campaign. Journal of Physics: Conference Series 655 (2015) 012012.

[10] L.L. Zhang, X. Meng, F. Liu, L. Xu, E.S. Long. Effect of RR-coatings on temperature environment in tents. Case Studies in Thermal Engineering 9 (2017) 122-127.

[11] Y.H. Qin, J. Liang, K.G. Tan, F.H. Li, A side by side comparison of the cooling effect of building blocks with retro-reflective and diffuse-reflective walls, Sol. Energy 133 (2016) 172–179.

[12] F. Rossi, E. Morini, B. Castellani, A. Nicolini, F. Cotana, Beneficial Effects of Retroreflective Materials in Urban Canyons: Results from Seasonal Monitoring Campaign, 33rd UIT Heat Transfer Conference, 2015. June 22-24.

[13] S. Yoshida, S. Yumino, T. Uchida, A. Mochida. Effects of windows with heat ray retro-reflective film on outdoor thermal environment and building cooling load. Journal of Heat Island Institute International 2 (2014) 67-72.

[14] J. Yuan, C. Farnham, K. Emura. Development of a retro-reflective material as building coating and evaluation on albedo of urban canyons and building heat loads. Energy and Buildings 103 (2015) 107-117.

[15] H. Sakai, H.K. Emura, N. Igawa, Reduction of reflected heat by retroreflective materials, J. Struct. Construct. Eng. 73 (2008) 1239–1244.

[16] H. Sakai, H. Kobayashi, K. Emura, N. Igawa, Outdoor measurement of solar reflective performance of retroreflective materials, J. Struct. Construct. Eng. 73 (2008) 1713–1718.

[17] J.H. Yuan, K. Emura, C. Farnham, H. Sakai, Application of glass beads as retro-reflective facades for urban heat island mitigation: experimental investigation and simulation analysis, Build. Environ. 105 (2016) 140–152.

[18] J.H. Yuan, K. Emura, H. Sakai, C. Farnham, S.Q. Lu, Optical analysis of glass bead RR-coatings for urban heat island mitigation, Sol. Energy 132 (2016) 203–213.

[19] J.H. Yuan, C. Farnham, K. Emura, Performance of retro-reflective building envelope materials with fixed glass beads, Appl. Sci. 9 (2019) 1714.

[20] F. Rossi, A.L. Pisello, A. Nicolini, M. Filipponi, M. Palombo, Analysis of retro-reflective surfaces for urban heat island mitigation: a new analytical model, Appl. Energy 114 (2014) 621–631.

[21] F. Rossi, B. Castellani, A. Presciutti, E. Morini, M. Filipponi, A. Nicolini, M. Santamouris, Retroreflective façades for urban heat island mitigation: experimental investigation and energy evaluations, Appl. Energy 145 (2015) 8–20.

[22] J. Wang, S.H. Liu, X. Meng, W.J. Gao, J.H. Yuan, Application of RR-coatings in urban buildings: a comprehensive review, Energy Build. 247 (2021) 111–137.

[23] B. Castellani, E. Morini, E. Anderini, M. Filipponi, F. Rossi, Development and characterization of retro-reflective colored tiles for advanced building skins, Energy Build. 154 (2017) 513–522.

[24] A.N.M.T. Elahi, D. Jensen, M. Ghashami, K. Park. Comprehensive energy balance analysis of photon-enhanced thermionic power generation considering concentrated solar absorption distribution. Solar Energy Materials and Solar Cells, 226 (2021) 111067.

[25] Y.L. Hana, J. E. Taylorb, A.L. Pisello. Toward mitigating urban heat island effects: Investigating the thermal-energy impact of bio-inspired retro-reflective building envelopes in dense urban settings. Energy and Buildings 102 (2015) 380–389.

[26] C.C. Xu, S.H. Li, X.S. Zhang. Energy flexibility for heating and cooling in traditional Chinese dwellings based on adaptive thermal comfort: A case study in Nanjing. Building and Environment 179 (2020) 106952.

[27] I. Hernández-Pérez, J. Xaman, E.V. Macias-Melo, K.M. Aguilar-Castro, I. Zavala-Guillen, I. Hernandez-Lopez, E. Sima. Experimental thermal evaluation of building roofs with conventional and reflective coatings. Energy and Buildings 158 (2018) 569-579.

An experimental comparison on regional thermal environment of the high-density enclosed building groups with retro-reflective and high-reflective coatings

Chapter 5 An experimental comparison on regional thermal environment of the high-density enclosed building groups with retro-reflective and high-reflective coatings

5.1 Introduction

China's urbanization rate will reach 80% in 2050 [1] and the rapid growth of urban population leads to urban congestion. High-density buildings have become the theme of urban development [2, 3]. The urban surface composed of reinforced concrete and asphalt will absorb a large amount of solar radiation, making the urban thermal environment tend to deteriorate [4, 5]. At present, improving the solar reflectivity of building surfaces was an effective way to reduce the heat gain from solar radiation. Highly-reflective coatings (HR-coatings) could increase the solar reflectivity of the external surface of buildings, and reduce the indoor average air temperature by 1°C~3°C [6, 7], and the cooling load by 18%-93% [8]. However, HR-coatings reflect solar radiation in a diffuse way, and the reflected solar radiation will be intercepted by nearby buildings and roads through the multiple absorption. And thereby for high-density building groups, HR-coatings have the low potential of thermal environment improvement [9].

According to the inherent defect of traditional HR-coatings on the reflection direction of solar radiation, more scholars have paid attention to retro-reflective coatings (RR-coatings), which can reflect the solar radiation back along the incident direction since 2004 [10, 11] and proved that the urban albedo could be effectively reduced [12-14]. Yoshida et al. [12] covered exterior windows of buildings with RR-coatings and used CFD software to evaluate the solar radiation environment around individual buildings. It was concluded that RR windows increased the amount of solar radiation reflected to the sky by 13% compared with windows with thermal insulation film. Castellani et al. [13] covered the vertical wall and horizontal road of the canyon model with RR-coatings, and the results showed that the equivalent albedo increased from 89.0% to 94.0%. Rossi et al. [14] set 90 measurement points at the upper level of the canyon model to measure the albedo, and concluded that compared with white and beige diffused materials, the albedo increment of RR-coatings may be as high as 4.6%, which showed RR-coatings could improve the regional thermal environment. Han et al. [15] established a system consisting of an independent reference building and a testing surface on the west side and found that the RR-coatings were effective in reducing the building temperature by up to 1.39°C compared with HR-coatings. Meng et al. [16] covered prefabricated houses with RR-coatings and found that the average and peak temperatures of indoor air decreased by more than 1.5°C and 7°C, respectively, compared with houses without RR-coatings. In addition, RR-coatings can effectively reduce the energy consumption of buildings. Ichinose et al. [17] studied the long-term energy conservation of an office building and found that the RR film decreased the total energy consumption by about 20%. Mauri et al. [18] covered the facade of a three-story building with RR-coatings and simulated the energy consumption of this building. The

numerical results showed that the cooling energy consumption of RR-coatings could be reduced by 16.1% compared to HR-coatings with the same reflectivity.

Additionally, there was some field research conducted through a certain proportion of building models. Morini et al. [19] established building models of block layout and canyon layout, and compared the effectiveness of RR-coatings and traditional building coatings. It was found that the equivalent albedo increased by 3% for block layout and 7% for canyon layout. Qin et al. [20] measured the internal and external wall temperatures of block models with RR-coatings and HR-coatings, and found that the external wall temperature of the model with RR-coatings was 5°C~10°C lower than that of the model with HR-coatings. The above studies mostly focused on the cooling effect of RR-coatings in the oversimplified building models. However, there were great differences between the oversimplified and real building models in the characteristics of thermal environment, and the accuracy of the obtained experimental data remained to be discussed. And there has been a lack of experimental studies on the effects of RR-coatings on the thermal environment of building models based on real buildings.

Nowadays, more buildings have applied the enclosed building form [21] to the land use rate and provide residents with a variety of outdoor resting places and rich combinations of landscapes [22]. However, the enclosed building group easily formed the basin effect, which was averse to natural ventilation and easy to absorb the solar radiation [23]. Therefore, the regional thermal environment was relatively poor in the enclosed building group. Based on this, RR-coatings were applied to the enclosed building group to refine its regional thermal environment with a reference of HR-coatings.

According to the chapter 4, the retro-reflectance property of prism RR-coatings was better than other kinds of RR-caotings, therefore, the prism RR-coatings were applied in this study. Two enclosed building group models were built and covered by prism RR-coatings and HR-coatings respectively, while their thermal environment was contrastively analyzed by employing the urban albedo, wall surface temperature and air temperature to characterize whether the building group model covered by prism RR-coatings could stay cooler than that covered by HR-coatings.

5.2 Description of the comparative experiment

5.2.1 Description of Building Group Models

Enclosed building layout is widely applied in modern urban buildings because of its higher land use efficiency and better outdoor environment, as shown in Fig. 5-1(a). In order to reveal the influence of RR-coatings and HR-coatings on the thermal environment of the public space

of enclosed building groups, a simplified representation of this layout was carried out. The size of the simplified model was shown in Fig. 5-1(b). On the roof of a 7-story building in Qingdao University of Technology, two models with RR-coatings and HR-coatings respectively were made for comparison experiment. In order to be closer to the real urban thermal environment, the black film was laid on the bottom to represent the ground asphalt. The experiment site was shown in Fig. 5-1(c). In spite of much smaller than the real building groups, this model could imitate the real architectural complex to a large extent, because they had the same multiple reflections of sunlight and the solar radiation is the main driving force of building temperature change [20].
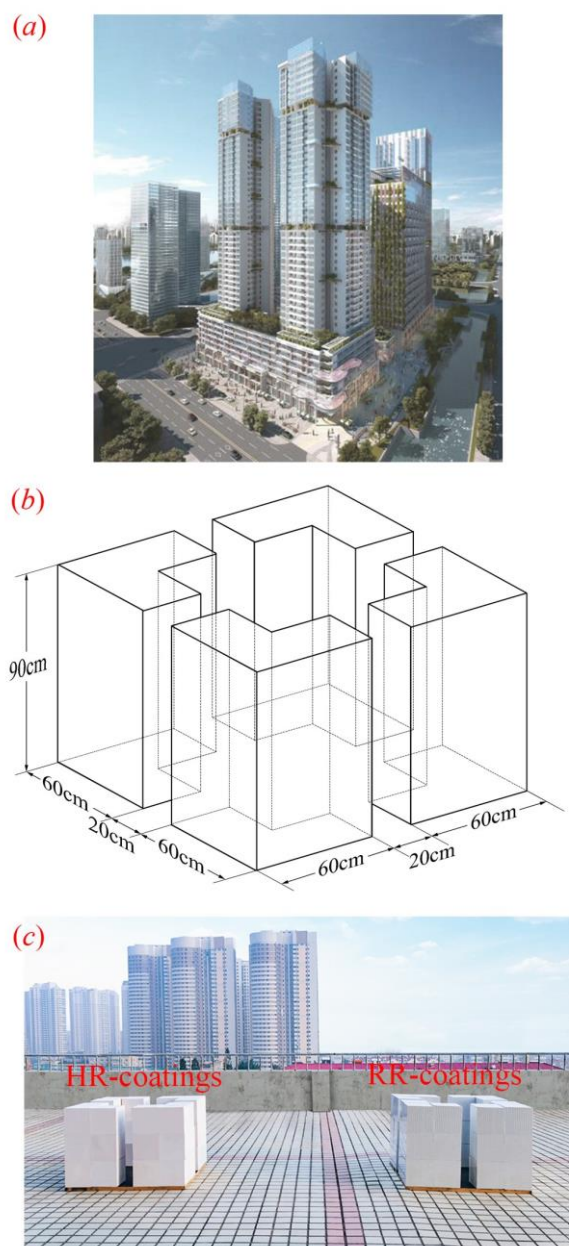
Fig. 5-1. (a) Actual buildings, (b) simplify model dimensions and (c) experimental platform

5.2.2 Layout of measurement point

Fig. 5-2 showed the positions of thermocouples and the solar radiometers. To measure the temperatures at different locations of enclosed building group models, a total of 16 calibrated T-type thermocouples were distributed on the walls and enclosed space. Among them, 1 T-type thermocouple was distributed at the roof, and 3 T-type thermocouples were distributed at the vertical center-line of the east, south, west and north walls respectively to measure the temperature profiles. Each three thermocouples were distributed at 15cm, 45cm, 75cm away from the ground at each height respectively. To measure the solar radiation intensity, in accordance with the procedure published in other works [26], two back-to-back solar radiometers were placed about 0.3m above the center of each model to obtain reflected solar radiation and incident solar radiation, which could be used to calculate the albedos of the whole model [13]. Table 5-1 gave the specification of instruments applied in the experiment. The errors of T-type thermocouples and solar radiometers selected in the experiment were lower than 0.5°C and 2% respectively, and all collected data were automatically recorded in a PC through a data logger at 1-minute intervals for the further data processing.
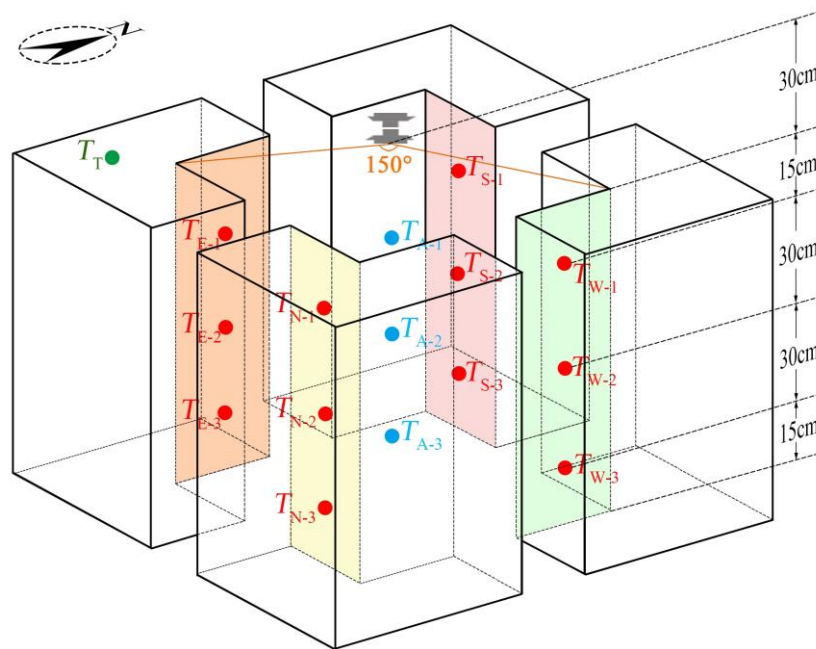
Fig. 5-2. Schematic diagram of the point layout

Table 5-1. Specification of instruments applied in the experiment

Instrument	Resolution	Accuracy	Range of operation
T-type thermocouples	0.01°C	±0.5°C	-200°C ~ +400°C
Solar radiometers	0.01 W/m^2	±2%	0 ~ 2000W/m^2

5.3 Experiment results and discussion

The experiment was undertaken in Qingdao University of Technology from 18th to 21th of June 2021. Fig. 5-3 showed the variation of the outdoor air temperature and the horizontal total radiation with time during the experimental period in Qingdao city. To clarify the influence of solar radiation on the thermal environment of the building group models clearly, the experiment was mainly carried out on sunny days to reduce the cloud disturbance. As shown in Fig. 5, the highest, lowest and average outdoor air temperatures were 37.8°C, 20.4°C and 27.6°C, respectively. The daily temperature difference was more than 10°C, and the highest solar radiation reached 1238W/m².
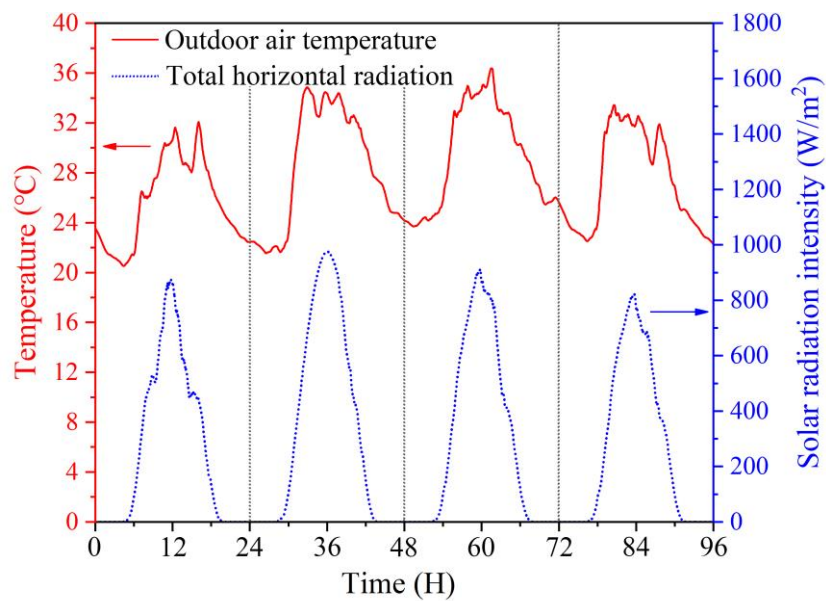
Fig. 5-3. Outdoor thermal environment during the experimental period (air temperature and solar radiation)

5.3.1 Comparison of the regional albedo

Heat gain from solar radiation is an important factor of the formation of regional thermal environment. To evaluate the influence of reflective coatings on the regional thermal environment, the horizontal albedo of regional space was introduced [27], which was defined as the ratio of reflected solar radiation to received solar radiation in the regional space, and could be simplified by the ratio of upward and downward radiation intensity [14].

Fig. 5-4 showed the variation of reflected solar radiation intensity and horizontal albedos with time in two building group models with RR-coatings and HR-coatings. It could be seen that the reflected solar radiation intensity had the same variation law as outdoor solar radiation, but the reflected solar radiation intensity in the RR-coating model was significantly higher than

that in the HR-coating model. The peak difference was 116w/m^2 and its appearance was at 13:00 noon. Compared with HR-coatings, RR-coatings could reduce the solar radiation absorption by about 1407.27kJ/m^2, and the associated reduction rate was about 24.1%. Moreover, from the albedo comparison in Fig. 5-4(b), the regional albedos of the RR-coating model were significantly higher than those of the HR-coating model especially at 6:00-18:00, and the increased percentages were 5.53% and 10.90% for average and peak albedos, respectively. It showed RR-coatings could reduce the regional solar radiation gain, compared with HR-coatings. According to the comparison of albedos, it was easily found that although the solar reflectivity of HR-coatings was 29% higher than that of RR-coatings, RR-coatings could gain the higher albedo improvement than HR-coatings. The core reason was due to that fact that HR-coatings relied more on diffuse reflection, while RR-coatings could reflect the more solar radiation out of the building group along the incident direction.
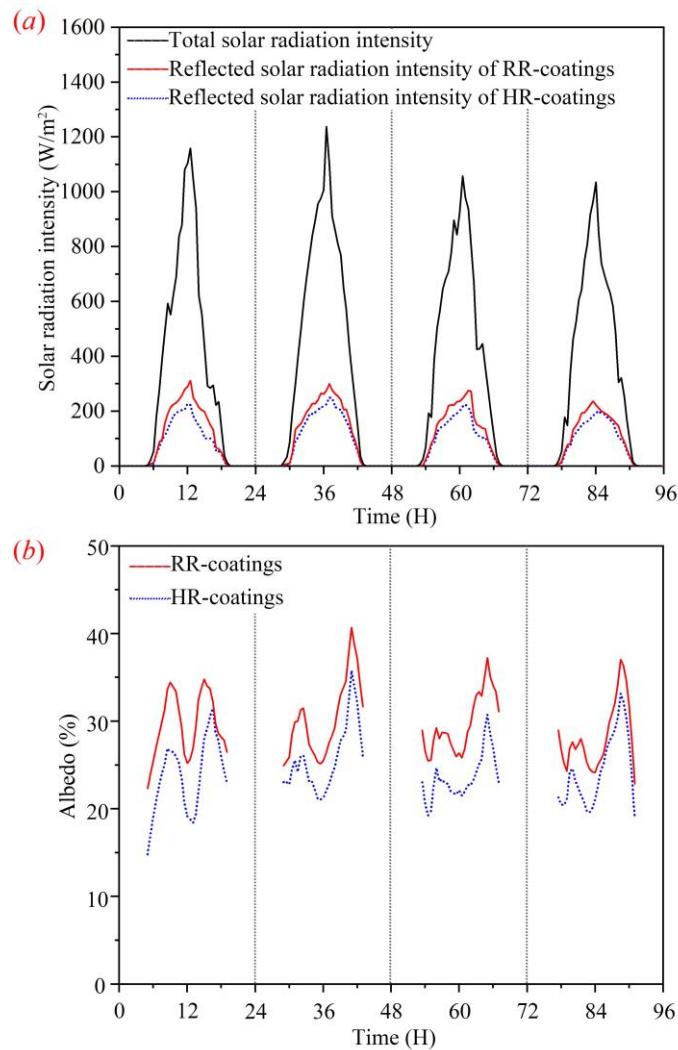
Fig. 5-4. Variation of (a) reflected solar radiation and (b) albedos for RR-coating and HR-coating models

5.3.2 Comparison of wall temperature

Building surface temperature is an important parameter affecting outdoor thermal environment, which will affect outdoor comfort level directly and the building energy consumption indirectly [28], so the temperatures in exterior walls were studied in this study.

Fig. 5-5 showed the variation of the roof temperatures of two building group models with time during the experimental period. It could be seen that the roof temperatures of the RR-coating model were always lower than those of the HR-coating model. In the daytime, the average and maximum reduced temperatures were 3.82°C and 7.71°C respectively, and the maximum temperature reduction appeared at 12:05 due to the high solar radiation intensity. Moreover, the average and maximum reduced temperatures were 3.57°C and 4.44°C in the nighttime, respectively. This phenomenon was mainly due to two following reasons. On the one hand, HR-coating model had the higher thermal storage in the daytime, which could keep the higher wall temperature in the nighttime [20]. On the other hand, RR-coatings had the higher infrared emissivity than HR-coatings, which gained the cold radiation from the sky [29].
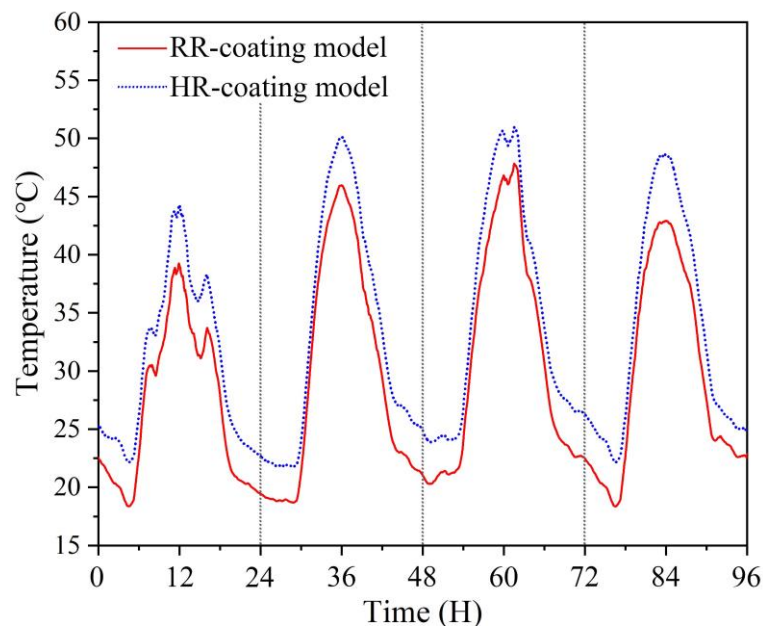
Fig. 5-5. Variation of the roof temperature of RR-coating and HR-coating models with time

Fig. 5-6 showed the temperature variation with time of four walls during the experimental period. As shown, the RR-coating model had always the lower temperatures than the HR-coating model in the east wall in Fig. 5-6(a). In the daytime, the maximum temperature difference appeared at 8:34, when there was the highest solar radiation intensity in the east wall. The maximum temperature differences were 12.8°C, 11.61°C and 15.25°C for T_{E-1}, T_{E-2} and T_{E-}

$_3$, while the average temperature differences were 3.44℃, 1.69℃ and 2.35℃ for T_{E-1}, T_{E-2} and T_{E-3} in the daytime. Meanwhile the maximum temperature differences were 3.73℃, 2.63℃ and 4.74℃ for T_{E-1}, T_{E-2} and T_{E-3}, while the average temperature differences were 3.09℃,0.83℃ and 3.68℃ for T_{E-1}, T_{E-2} and T_{E-3} in the nighttime.

For the south wall in Fig. 5-6(b), the RR-coating model had always the lower temperatures than the HR-coating model. In the daytime, the maximum temperature difference occurred at 12:29, when there was the highest solar radiation intensity in the south wall. The maximum temperature differences were 6.81℃, 7.25℃ and 7.64℃ for T_{S-1}, T_{S-2} and T_{S-3}, while the average temperature differences were 3.28℃, 2.92℃ and 3.18℃ for T_{S-1}, T_{S-2} and T_{S-3} in the daytime. Meanwhile the maximum temperature differences were 7.91℃, 3.65℃ and 3.68℃ for T_{S-1}, T_{S-2} and T_{S-3}, while the average temperature differences were 4.38℃, 3.06℃ and 3.13℃ in the nighttime.

For the west wall in Fig. 5-6(c), the RR-coating model had always the lower temperatures than the HR-coating model, but compared with the east wall and the south wall, the temperature differences of the west wall were not obvious. In the daytime, the maximum temperature difference appeared after 15:00, when there was the highest solar radiation intensity in the western wall. The maximum temperature differences were 4.97℃, 4.6℃ and 5℃ for T_{W-1}, T_{W-2} and T_{W-3}, while the average temperature differences were 1.21℃, 1.08℃ and 1.15℃ for T_{W-1}, T_{W-2} and T_{W-3} in the daytime. Meanwhile the maximum temperature differences were 1.58℃, 1.81℃ and 3.72℃ for T_{W-1}, T_{W-2} and T_{W-3}, while the average temperature differences were 1.08℃, 1.29℃ and 2.09℃ for T_{W-1}, T_{W-2} and T_{W-3} in the nighttime.

For the north wall in Fig. 5-6(d), the RR-coating model always had the lower temperatures than the HR-coating model. However, compared with the east wall, south wall and west wall, the temperature difference on the north wall was the smallest, mainly due to the north wall was always in the shade, and received the least solar radiation. The maximum temperature differences were 2.47℃, 2.7℃ and 2.78℃ for T_{N-1}, T_{N-2} and T_{N-3}, while the average temperature differences were 0.3℃, 0.67℃ and 1.12℃ for T_{N-1}, T_{N-2} and T_{N-3} in the daytime. Meanwhile the maximum temperature differences were 1.35℃, 1.96℃ and 1.47℃ for T_{N-1}, T_{N-2} and T_{N-3}, while the average temperature differences were 0.25℃, 1.03℃ and 1.01℃ for T_{N-1}, T_{N-2} and T_{N-3} in the nighttime.

From Fig. 5-6(d), it showed there was the different temperature reduction in different heights and that there were the higher temperature reduction efficiencies for the upper and lower points, especially in the east and south walls. This phenomenon was because the upper part of the model had the highest sky visibility, leading to the more solar radiation gain in the daytime and

more long-wave radiation in the night, while the lower part of the model received more reflected solar radiation by HR-coatings, compared to RR-coatings. Due to the optical advantages of RR-coatings, it absorbed the lower solar radiation and did not deteriorate the surrounding thermal environment. Meanwhile, there were the different efficiencies of RR-coating applied in the walls with different orientations, compared to HR-coating. East and south walls have the larger temperature reduction than the west and north walls, which was due to the higher solar radiation in east and south walls.
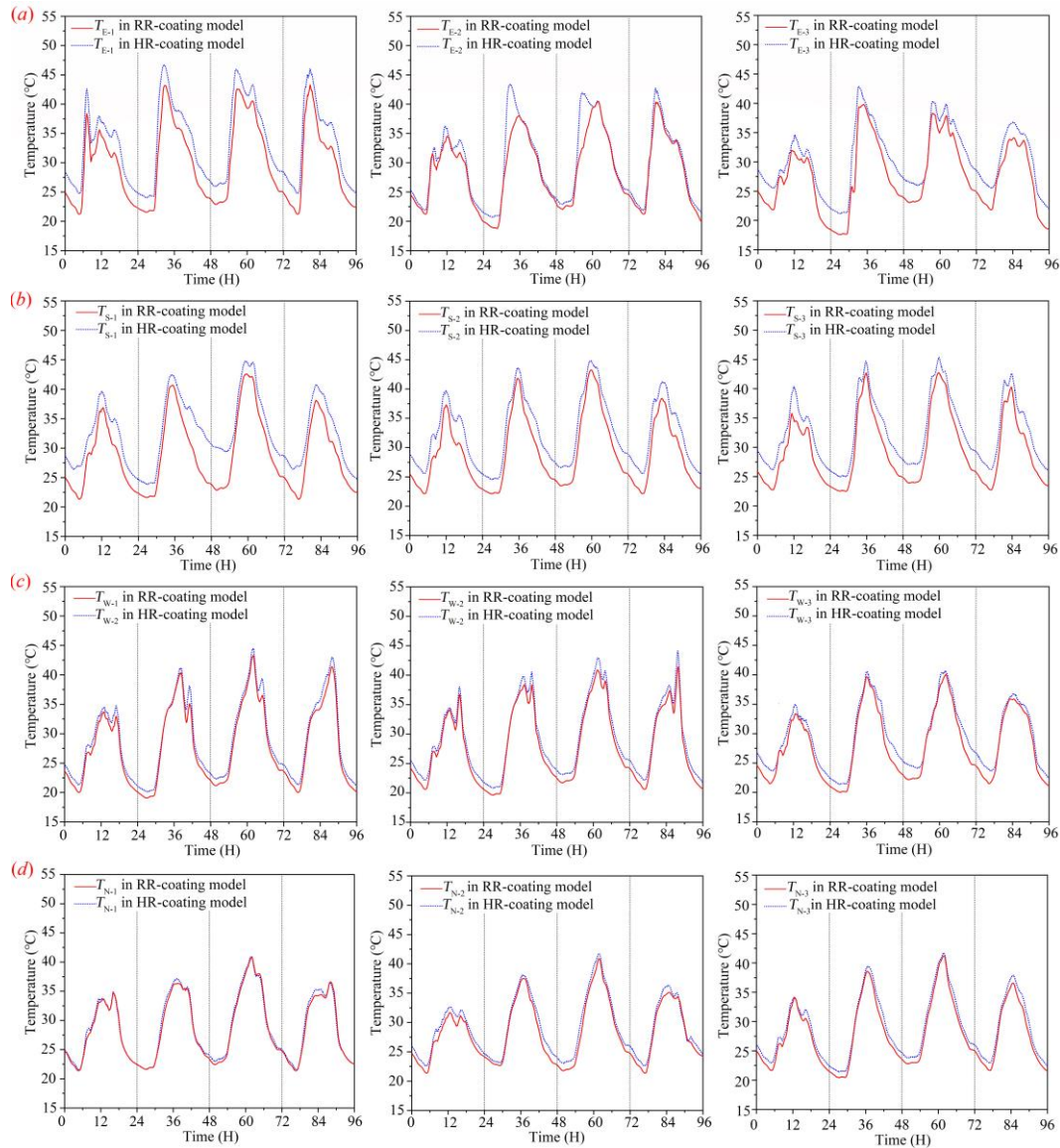
Fig. 5-6. Variation of the wall temperatures in RR-coating and HR-coating models for (a) the east wall, (b) the south wall (c) the west wall and (d) the north wall

Table 5-2 gave the maximum and average temperature difference of wall surfaces between RR-coating and HR-coating models. It could be seen that wall orientation had the certain influence on the reduction efficiency of RR-coatings. The walls with the best cooling efficiency

were the east one in the daytime and the south one & roof in the nighttime. By comparing five wall orientations comprehensively, the east wall had the best cooling effect, followed by the roof and south walls, while the north wall had the poorest cooling effect.

Table 5-2. The maximum and average temperature difference of wall surface between RR-coating and HR-coating models

Wall orientation	Measured points	In the daytime		In the nighttime	
		Peak value	Average value	Peak value	Average value
Roof	T_T	7.71	3.82	4.44	3.57
East wall	T_{E-1}	12.80	3.44	3.73	3.09
	T_{E-2}	11.61	1.69	2.63	0.83
	T_{E-3}	15.25	2.35	4.74	3.68
South wall	T_{S-1}	6.81	3.28	7.91	4.38
	T_{S-2}	7.25	2.92	3.65	3.06
	T_{S-3}	7.64	3.18	3.68	3.13
West wall	T_{W-1}	4.97	1.21	1.58	1.08
	T_{W-2}	4.60	1.08	1.81	1.29
	T_{W-3}	5.00	1.15	3.72	2.09
North wall	T_{N-1}	2.47	0.30	1.35	0.25
	T_{N-2}	2.70	0.67	1.96	1.03
	T_{N-3}	2.78	1.12	1.47	1.01

5.3.3 Comparison of air temperature

Outdoor air temperature is another important index affecting outdoor thermal environment and energy consumption of surrounding buildings [30]. Fig. 5-7 showed the air temperature variation in the enclosed space with time (T_{A-1}, T_{A-2} and T_{A-3}) during the experimental period. As shown in Fig. 5-7, air temperatures in the enclosed space fluctuated almost synchronously with the outdoor natural air temperature, but they were higher than outdoor natural air temperature. It was mainly because the wall temperatures increased after absorbing solar radiation and then the part heat would be transmitted to the air in the enclosed space by natural convection. And due to the retro-reflection effect, the RR-coating model had the lower air temperature in the enclosed space than the HR-coating model.

Table 5-3 showed air temperature of different positions (T_{A-1}, T_{A-2} and T_{A-3}). As shown in Table 5-3, compared to outdoor natural air temperature, the peak and average air temperatures in the enclosed space were increased by 6.74°C~8.09°C and 4.17°C~4.25°C for the HR-coating model, while they were increased by 5.27°C~5.85°C and 1.76°C~2.59°C for the RR-coating model. It showed a large amount of solar radiation was absorbed by buildings, which deteriorated the urban thermal environment. Additionally, compared with the HR-coating model, the peak and average air temperatures were reduced by 1.47°C~2.24°C and 1.62°C~2.49°C respectively by covering RR-coatings, which showed RR-coatings have a significant improvement effect on the outdoor thermal environment due to their retro-reflecive performance.

(a)
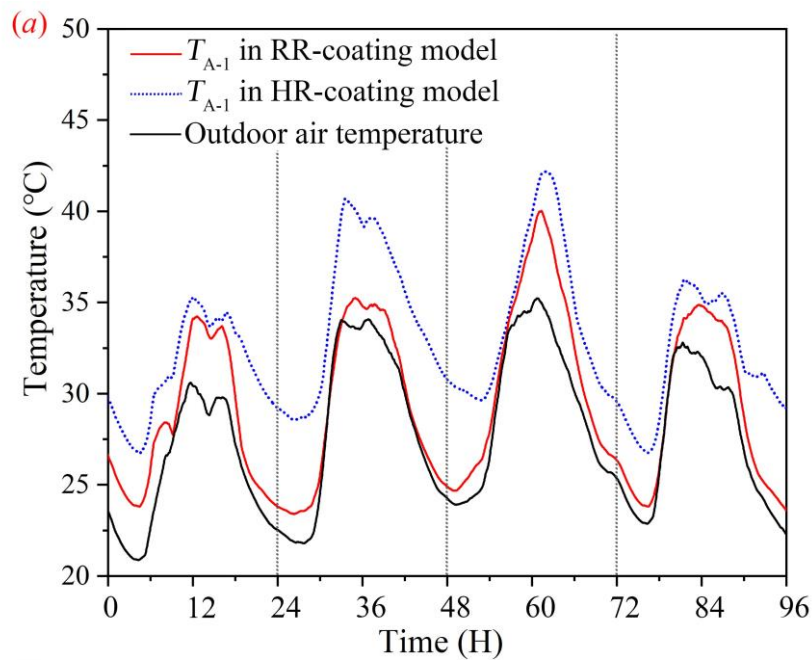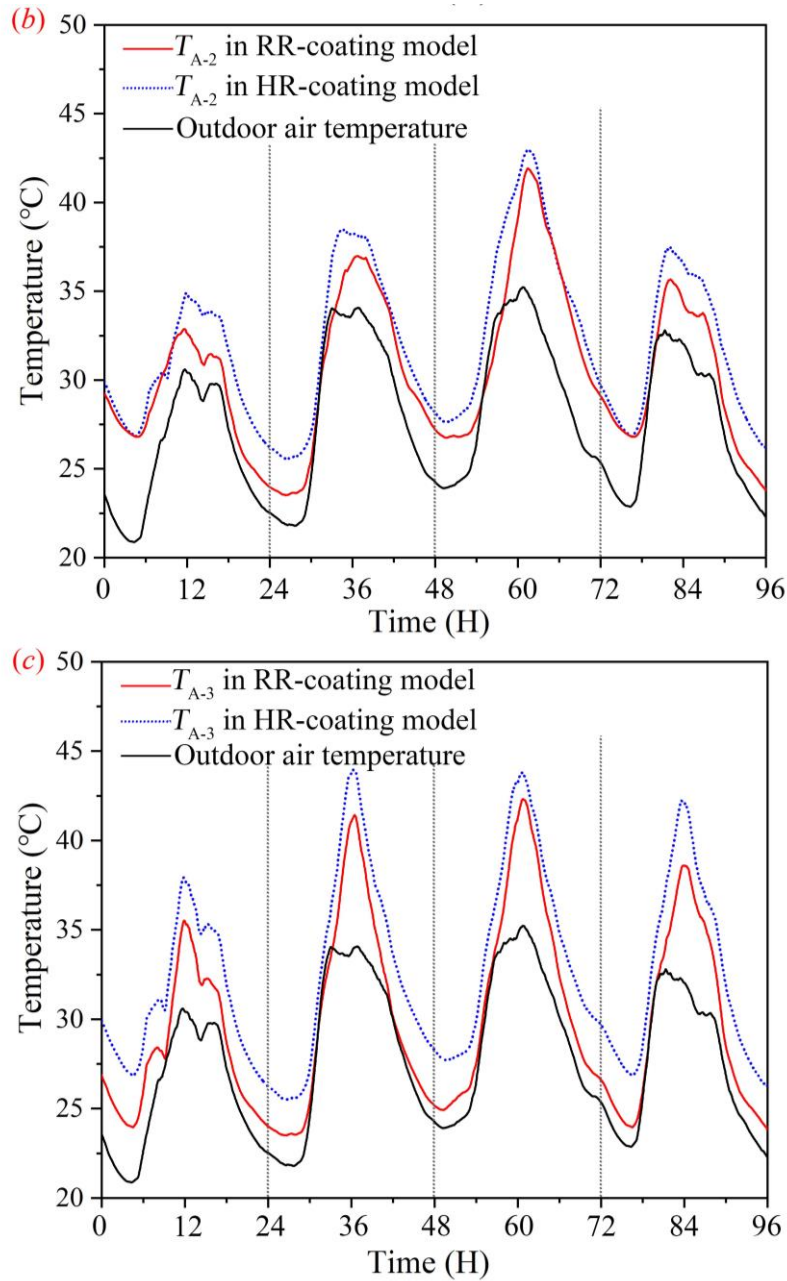
Fig. 5-7. Variation of air temperatures in RR-coating model and HR-coating model with time

Table 5-3. Comparison of air temperature of different positions (T_{A-1}, T_{A-2} and T_{A-3})

Measured points	Natural		HR-coating model		RR-coating model	
	Peak value	Average value	Peak value	Average value	Peak value	Average value
T_{A-1}	37.80	27.64	44.54	31.89	43.07	29.40
T_{A-2}	38.75	27.83	46.51	32.04	44.37	30.42
T_{A-3}	39.80	28.46	47.89	32.63	45.65	30.95

5.4 Conclusion

In this study, RR-coatings and HR-coatings were covered in the high-density enclosed building groups to compare their influence on the regional thermal environment in the enclosed space. And the regional albedo, wall surface temperature and air temperature were employed to evaluate the regional thermal environment improvement. And the following conclusions were drawn:

(1) Compared to the HR-coating model, the RR-coating model could improve the regional albedo and its increased percentages were 5.53% and 10.90% for average and peak regional albedos, due to that fact that HR-coatings relied more on diffuse reflection, while RR-coatings could reflect the more solar radiation out of the building group along the incident direction.

(2) RR-coatings could reduce the wall surface temperature, compared to HR-coatings. The east wall showed the best cooling effect with the peak and average temperatures reduced by 11.61℃~15.25℃ and 1.69℃~2.35℃ in the daytime, while the south wall showed the cooling effect with the peak and average temperatures reduced by 3.65℃~7.91℃ and 3.06℃~4.38℃ in the nighttime.

(3) The wall orientation had the large influence on its cooling efficiency. And by comparing five wall orientations, the east wall had the best cooling effect, followed by the roof and south walls, while the north wall had the poorest cooling effect.

(4) Compared with the HR-coating model, the peak and average air temperatures were reduced by 1.47℃~2.24℃ and 1.62℃~2.49℃ respectively by covering RR-coatings, which showed RR-coatings have a significant improvement effect on the outdoor thermal environment.

References

[1] National Bureau of Statistics (NBS), 2019. Statistical communiqué of the People's Republic of China on the 2018 national economic and social development, http://www.stats.gov.cn/tjsj/zxfb/201902/t20190228_1651265.html. Access date: 25 July 2019.

[2] Y. Wang, D. Mauree, Q. Sun, H. Lin, J.L. Scartezzini, R. Wennersten. A review of approaches to low-carbon transition of high-rise residential buildings in China. Renewable and Sustainable Energy Reviews 131 (2020) 109990.

[3] W. Pan, M. Pan. A dialectical system framework of zero carbon emission building policy for high-rise high-density cities: Perspectives from Hong Kong. Journal of Cleaner Production

205 (2018) 1-13.

[4] L. Gustavsson, T. Nguyen, R. Sathre, U.Y.A. Tettey. Climate effects of forestry and substitution of concrete buildings and fossil energy. Renewable and Sustainable Energy Reviews 136 (2021) 110435.

[5] F. Rosso, A.L. Pisello, V.L. Castaldo, C. Fabiani, F. Cotana, M. Ferrero, W. Jin. New cool concrete for building envelopes and urban paving: Optics-energy and thermal assessment in dynamic conditions. Energy and Buildings 151 (2017) 381-392.

[6] H. Taha. Meso-urban meteorological and photochemical modeling of heat island mitigation. Atmospheric Environment 42 (2008) 8795-8809.

[7] E. Morini, A. Touchaei, B. Castellani, F. Rossi, F. Cotana. The Impact of Albedo Increase to Mitigate the Urban heat island in Terni (Italy) Using the WRF Model. Sustainability 8 (2016) 999.

[8] A. Synnefa, M. Santamouris, H. Akbari. Estimating the effect of using cool coatings on energy loads and thermal comfort in residential buildings in various climatic conditions. Energy and Buildings 39 (2007) 1167-1174.

[9] J.C. Yang Z.H. Wang, K.E. Kaloush. Environmental impacts of reflective materials: Is high albedo a 'silver bullet' for mitigating urban heat island? [J]. Renewable and Sustainable Energy Reviews, 2015(47), 830-843.

[10] R.B. Nilsen, X.J. Lu. Retro reflection Technology. European Symposium on Optics and Photonics for Defence and Security. International Society for Optics and Photonics (2004) 47-60.

[11] J. Wang, S.H. Liu, X. Meng, W.J. Wei, J.H. Yuan. Application of RR-coatings in urban buildings: A comprehensive review. Energy and Buildings 247 (2021) 111137.

[12] S. Yoshida, A. Mochida. Evaluation of effects of windows installed with near-infrared rays retro-reflective film on thermal environment in outdoor spaces using CFD analysis coupled with radiant computation. Building Simulation 11 (2018) 1053-1066.

[13] B. Castellani, A. Nicolini, A.M. Gambelli, M. Filipponi, E. Morini, F. Rossi. Experimental assessment of the combined effect of retroreflective façades and pavement in urban canyons. IOP Conference Series: Materials Science and Engineering 609 (2019) 072004.

[14] F. Rossi, B. Castellani, A. Presciutti, E. Morini, E. Anderini, M. Filipponi, A. Nicolini. Experimental evaluation of urban heat island mitigation potential of retro-reflective pavement

in urban canyons. Energy and Buildings 126 (2016) 340-352.

[15] Y.L. Han, J.E. Taylor, A.L. Pisello. Toward mitigating urban heat island effects: Investigating the thermal-energy impact of bio-inspired retro-reflective building envelopes in dense urban settings. Energy and Buildings 102 (2015) 380–389.

[16] X. Meng, T. Luo, Z.Y. Wang, W. Zhang, B. Yan, J.L. Ouyang, E.S. Long. Effect of RR-coatings on building indoor temperature conditions and heat flow analysis for walls. Energy and Buildings 127 (2016) 488-498.

[17] M. Ichinosea, T. Inoue, T. Nagahama. Effect of retro-reflecting transparent window on anthropogenic urban heat balance. Energy and Buildings 157 (2017) 157-165.

[18] L. Mauri, G. Battista, E.L. Vollaro, R.L. Vollaro. Retroreflective materials for building's façades: Experimental characterization and numerical simulations. Solar Energy 171 (2018) 150-156.

[19] E. Morini, B. Castellani, A. Presciutti, E. Anderini, M. Filipponi, A. Nicolini, F. Rossi. Experimental Analysis of the Effect of Geometry and Facade Materials on Urban District's Equivalent Albedo. Sustainability 9 (2017) 1245.

[20] Y.H. Qin. J. Liang, K.G. Tan, F.H. Li. A side by side comparison of the cooling effect of building blocks with retro-reflective and diffuse-reflective walls. Solar Energy 133 (2016) 172-179.

[21] E. Mertens. Bioclimate and city planning- open space planning. Atmospheric Environment 33 (1999) 4115-4123.

[22] D. Lai, Z.W. Lian, W.W. Liu, C.R. Guo, W. Liu, K.X. Liu, Q.Y. Chen. A comprehensive review of thermal comfort studies in urban open spaces. Science of the Total Environment 742 (2020), 140092.

[23] M. Xu., B. Hong, J.Y. Mi, S.S. Yan. Outdoor thermal comfort in an urban park during winter in cold regions of China. Sustainable Cities and Society 43 (2018) 208–220.

[24] J.H. Yuan, K. Emura, C. Farnham. A method to measure retro-reflectance and durability of RR-coatings for building outer walls. Journal of Building Physics 38 (2015) 500-516.

[25] American Society for Testing and Materials (ASTM). ASTM E903–12: Standard Test Method for Solar Absorptance, Reflectance, and Transmittance of Materials Using Integrating Spheres; ASTM International: West Conshohocken, PA, USA, 2012.

[26] M. Aida. Urban Albedo as a Function of the Urban Structure-A Model Experiment.

Bound Layer Meteorol. 1982, 23, 405–413.

[27] I.A. Meir, D. Pearlmutter, Y. Etzion. On the microclimatic behavior of two semi-enclosed attached courtyards in a hot dry region. Building and Environment 30 (1995) 563-572.

[28] I. Hernández-Pérez, J. Xaman, E.V. Macias-Melo, K.M. Aguilar-Castro, I. Zavala-Guillen, I. Hernandez-Lopez, E. Sima. Experimental thermal evaluation of building roofs with conventional and reflective coatings. Energy and Buildings 158 (2018) 569-579.

[29] J. Hollick. Nocturnal radiation cooling tests. Energy Procedia 30 (2012) 930 – 936.

[30] A. Aboelata. Reducing outdoor air temperature, improving thermal comfort, and saving buildings' cooling energy demand in arid cities – Cool paving utilization. Sustainable Cities and Society 68 (2021) 102762.

Influence of the building enclosed forms on thermal contribution of retro-reflective and high-reflective coatings

Chapter 6 Influence of the building enclosed forms on thermal contribution of retro-reflective and high-reflective coatings

6.1 Introduction

With the continuous increase in the urban population, urban forms have become more compact [1], and there are more high-density buildings [2, 3]. Many enclosed building groups have been formed. In these enclosed building groups, the typical forms are the canyon one, semienclosed one, and courtyard one [4, 5]. Urban building forms significantly affect the urban climate. Compared with the relatively open spaces of non-enclosed building forms, solar radiation will be reflected more times in enclosed spaces [6]. This will lead to more absorbed solar radiation by the surrounding urban surfaces, and the regional thermal environment will thus be affected [7]. Therefore, the great pressure is posed from perspectives of the global economy and energy [8, 9] and human comfort and health [10, 11]. Corresponding mitigation technologies have been proposed to counteract the negative effects [12-14], and technologies using cool materials on streets and buildings have been widely applied and are effective [15, 16].

High-reflective coatings (HR-coatings) have a high solar reflectivity of approximately 40%-98%, and a high infrared emissivity of approximately 90% [17, 18]. This could reduce the building cooling load by approximately 18-93% [19]. However, for high-density urban areas, the solar radiation reflected will be intercepted by nearby buildings and roads [20-22], as shown in Fig. 6-1(a). Therefore, the application of HR-coatings cannot solve the problems related to the thermal environment of high-density urban spaces [23]. In contrast to HR-coatings, retro-reflective coatings (RR-coatings) can reflect solar radiation in the incidence direction and reduce the solar radiation reaching adjacent buildings and roads, as shown in Fig. 6-1(b). Due to the advantage of the optical characteristics and better thermal contribution of RR-coatings, more scholars are already working on it [24, 25].

Sakai et al. [26] and Yuan et al. [27] measured the retro-reflectance of RR-coating samples by heat balance theory, and found that the retro-reflectance of prism RR-coating samples could reach 40%, while the retro-reflectance of glass bead and capsule samples were only approximately 20%. Yuan et al. [28] studied the changes of solar-reflectance and retro-reflectance of RR-coatings after they were exposed outdoors for approximately 25 months, and found that prism RR-coatings had better durability. Rossi et al. [29] evaluated the angular reflectance of RR-coatings under several solar radiation angles, and found that when the incident angle exceeded a certain value, RR-coatings lost their retro-reflective performance.
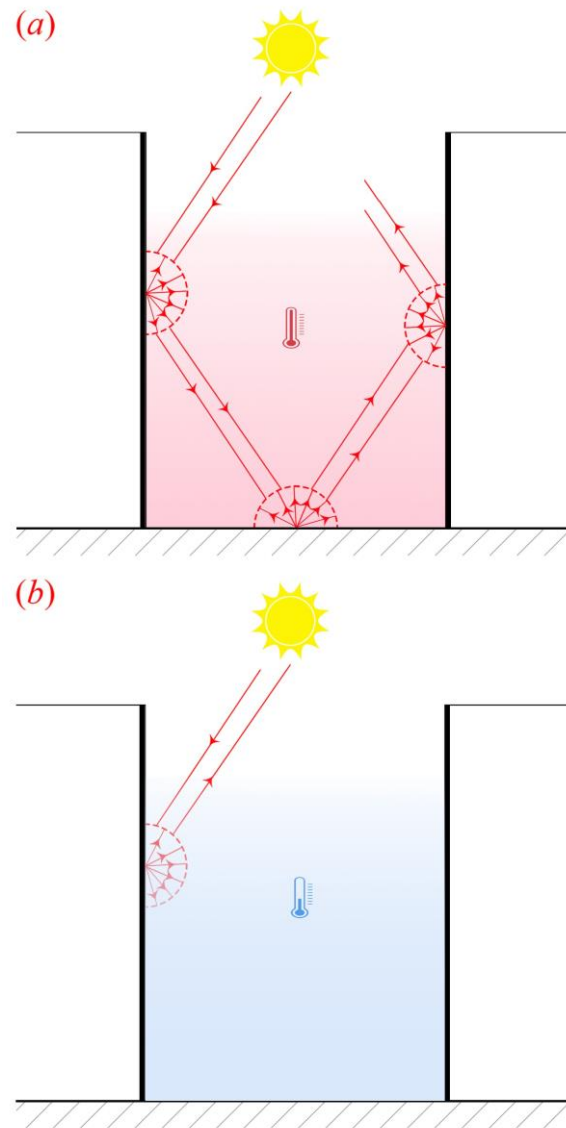
Fig. 6-1. Schematic diagram of the regional thermal environment of high-density buildings covered by (a) HR-coatings and (b) RR-coatings

RR-coatings have also been demonstrated to be effective in improving the regional thermal environment. For example, Inoue et al. [30] simulated a building block and found that the upward reflected solar radiation increased by 5% after the RR-coatings were applied to the glass windows. Inoue et al. [31] simulated urban blocks in Tokyo and calculated that when the buildings were covered with RR-coatings, the amount of reflected solar radiation increased from 7% to 8%. Castellani et al. [32] found that compared with HR-coatings, the equivalent albedo of canyons covered by RR-coatings increased by 5% through field measurement. Morini et al. [33] compared the effect of RR-coatings and conventional construction materials on two building group models (the block pattern and canyon pattern) and found that the albedos were increased by 3% and 7%, respectively. It could be seen that RR-coatings could increase the

albedos of buildings, both for block pattern and canyon pattern, which were two widely studied building forms. However, there was little difference in the albedos between them. Yoshida et al. [34, 35] studied the thermal comfort of pedestrians in street canyons in summer, and found that the mean radiation temperature and standard effective temperature around a glass window with RR-coatings were approximately 6.0°C and 1.7°C lower than those around the window with shading film, respectively.

It could be seen that most of these studies were based on the urban scenario of single street canyons or blocks. The influence of urban geometric forms on the thermal contribution of RR-coatings and HR-coatings was ignored, especially from the enclosed forms of building groups. Based on this, this study mainly focused on exploring the potential contribution to improve the regional thermal environment by employing prism RR-coatings and HR-coatings on the different urban geometric forms. After simplifying the actual high-density buildings, three typical forms of high-density buildings were proposed, namely the Determinant Form (D-Form), Three-Sided Enclosed Form (TSE-Form) and Four-Sided Enclosed Form (FSE-form). The prism RR-coatings and HR-coatings were employed on the three building forms. The regional albedo, wall temperature and air temperature were monitored to compare the thermal contribution of coatings on the high-density buildings with three enclosed forms.

6.2 Description of the comparative experiment

6.2.1 Experimental building models

With the urban construction accelerating, the number of high-density buildings is increasing [40]. High-density building forms mainly include the canyon form, semienclosed form, and courtyard form [4, 5]. To facilitate the further analysis, these three building forms were simplified as D-Form, TSE-Form and FSE-Form. Meanwhile, to analyze the influence of building forms deeply, the difference of building facades was ignored and all building facades were covered by RR-coating or HR-coatings. Fig. 6-2 shows the typical enclosed forms of high-density buildings and their simplified models in the experiment. To analyze the contribution efficiency of different reflective coatings, HR-coatings and RR-coatings were applied to the experimental model surfaces. Meanwhile, there was a black film on the bottom to simulate the ground asphalt in the actual environment. Since the solar radiation was the main cause of building temperature changes [41], and the multiple reflections of sunlight among building models had the same mechanism as the real one, the three groups of building models could imitate the real buildings.
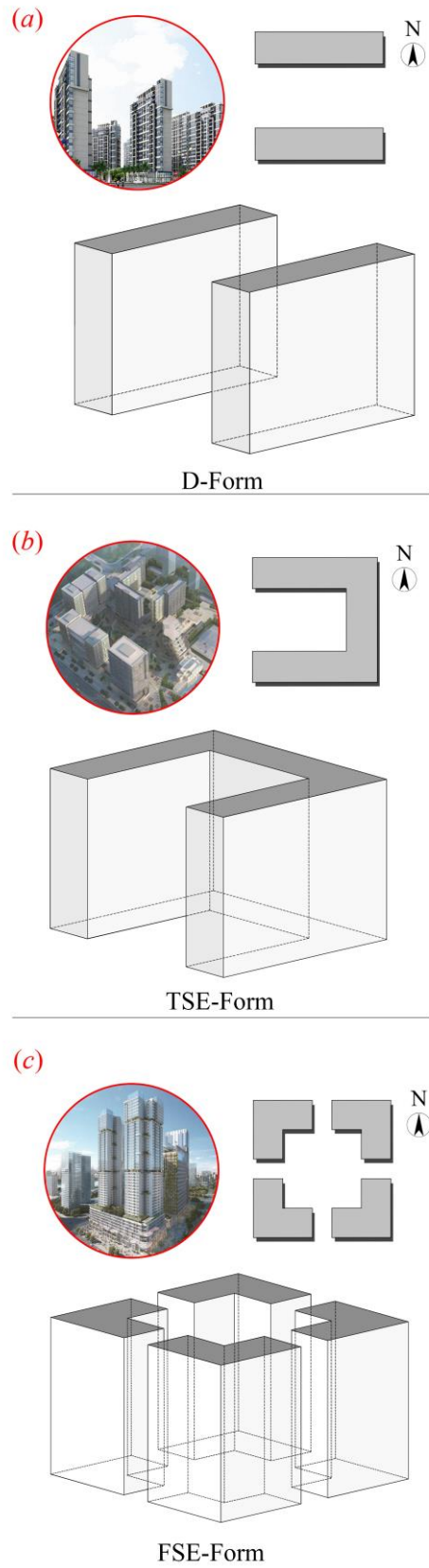
Fig. 6-2. Enclosed forms of high-density buildings: (a) D-Form building s, (b) TSE-Form buildings and (c) FSE-Form buildings

6.2.2 Measurement points

To efficiently evaluate the thermal contribution of coatings, three indicators were measured, including the regional albedo, wall temperature and air temperature. Fig. 6-3 shows the positions of the solar radiometers and T-type thermocouples in each group. To obtain the regional albedo, two opposite solar radiometers were set to obtain reflected solar radiation and incident solar radiation. They were at approximately 0.3m above the enclosed space of each model. T-type thermocouples were distributed on all model walls to test the model wall temperatures. And one T-type thermocouple was in the center of the enclosed space to test air temperatures.

Table 6-1 shows the specifications of the used instruments. As shown, the accuracies of the T-type thermocouples and solar radiometers were 0.5°C and 2% respectively. The temperature data and solar radiation data collected were recorded through the data recorder at 10-minute intervals. The accuracies of spectrometer and angular resolution test system were 0.2nm and 1% respectively. They were used to measure the global reflectance and retro-reflectance of two coatings respectively. All instruments were calibrated.

Table 6-1. Specifications of instruments used in the experiment

Instrument	Model	Supplier	Resolution	Accuracy	Range of operation
T-type thermocouples	TP1000	Beijing Century Jiantong Technology Co., LTD	0.01°C	± 0.5°C	-200°C ~ +400°C
Solar radiometers	JTR05	Shenzhen Topurui Electronics Co., LTD	0.1W/m²	± 2%	0~2000W/m²
Spectrometer	EN2500	Shanghai Chenchang Instrument Equipment Co., LTD	8nm	± 0.2nm	200nm ~ 2500nm
Angular resolution test	S1	Shanghai Chenchang	0.1°	± 1%	0~360°

system	Instrument
	Equipment
	Co., LTD
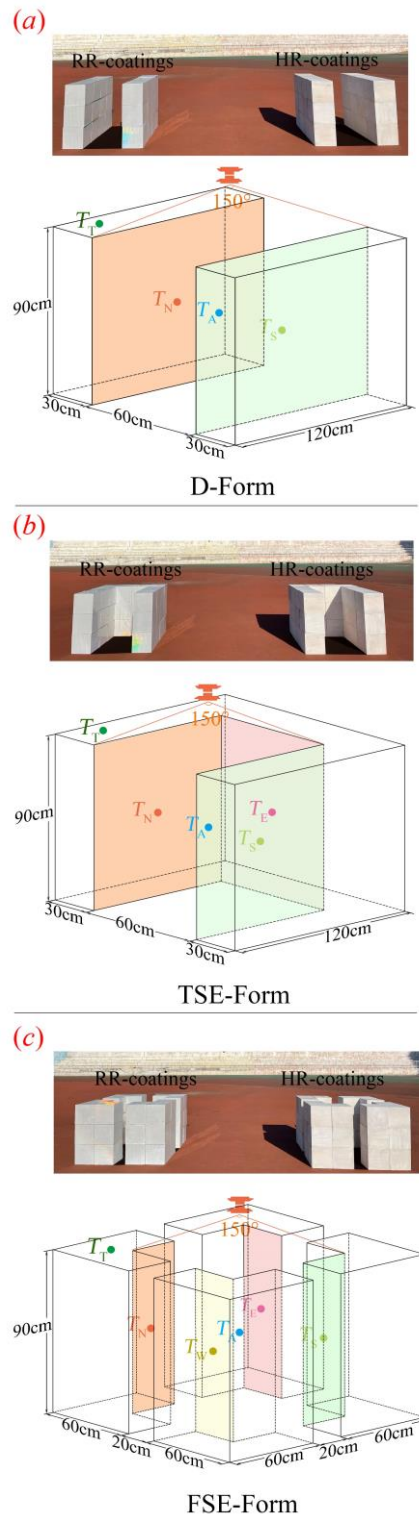
Fig. 6-3. Experimental platform and schematic diagram of the point layout (a) D-Form buildings, (b) TSE-Form buildings and (c) FSE-Form buildings

6.3 Experimental results

The experiment was undertaken in Qingdao city from the 12th to 15th of September 2021. Fig. 6-4 shows the outdoor air temperature and the solar radiation during the experimental period. To clarify the thermal contribution of two coatings more clearly and reduce the disturbance of cloud, the experiment was mainly carried out on sunny days with high solar radiation. As shown in Fig. 6-4, the minimum, maximum and average values of outdoor air temperatures were 15.90°C, 32.71°C, and 22.67°C, respectively, and the highest solar radiation was up to 881.00 W/m². Therefore, all differences in the regional thermal environment could be attributed to the differences in building forms and coatings, the effectiveness of the comparative experiment could be guaranteed.
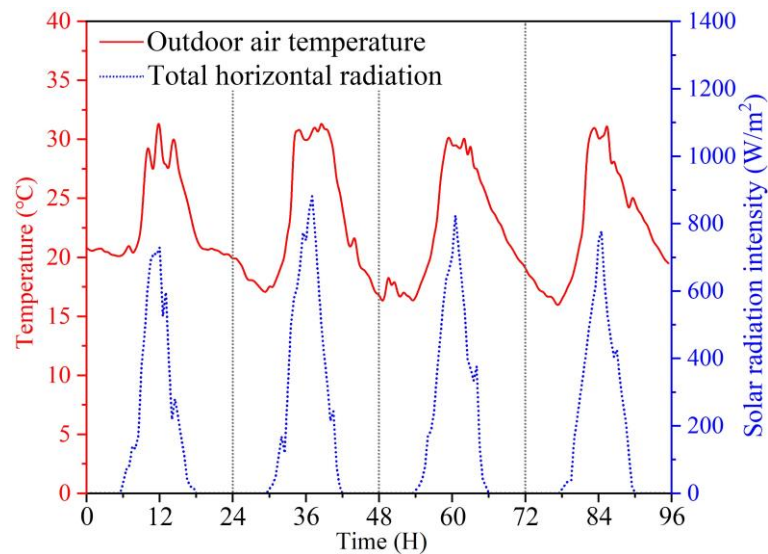
Fig. 6-4. Variation in outdoor air temperature and solar radiation during the experimental period

6.3.1 Comparison of the regional albedo

One of the main factors affecting the regional thermal environment is the capacity of urban buildings to absorb solar energy. It tends to raise the outside air temperature, further augmenting the need for summer cooling energy and decreasing the need for winter heating energy [42]. To quantitatively evaluate this impact, the regional albedo was introduced and calculated as the ratio of reflected and incident solar radiation by the regional space [21]. Fig. 6-5 shows the horizontal albedos for three building forms with RR-coatings and HR-coatings, respectively. It could be clearly seen that compared with HR-coating models, RR-coating models had the higher regional albedos, although RR-coatings had the lower solar reflectance. From D-Form to FSE-Form, it was easily found that the albedo improvement due to covering RR-coatings was increasing, compared to those of HR-coatings. It indicated that the higher the enclosed

degree of buildings, the higher the contribution efficiency of RR-coatings on improving the regional albedo.

Table 6-2 shows the maximum and average albedos of the three building models with RR-coatings and HR-coatings. From the D-Form to the FSE-Form, the maximum and average albedos were increased by 1.39% and 3.23% for the RR-coating model, respectively. However, they were reduced by 1.36% and 1.00% for the HR-coating model, respectively. Moreover, RR-coatings could gain a higher regional albedo than HR-coatings, and the higher the enclosure degree of building groups, the higher the regional albedo. The maximum and average albedos of the building models with RR-coatings were 0.67%~3.42% and 1.36%~5.59% higher than those with HR-coatings. It showed RR-coatings could increase the regional albedos to a greater extent than HR-coatings, especially for the higher enclosure buildings. In addition, for the three building forms, the maximum albedo differences occurred almost at the noon when the solar altitude angles were higher. This finding were consistent with some published studies [43]. However, from the angular distribution, it could be found that RR-coatings have only specular-reflection at high incident angles and no retro-reflection. It would result in a decrease in albedo. The reason for the maximum differences appeared at noon could be attributed to the experimental location, Qingdao. The latitude of Qingdao is approximately 37°09′, and the maximum height angle of the sun at noon during experimental period is approximately 57°. And within the range, RR-coatings still have retro-reflection property which can reflect more solar radiation out of the models.
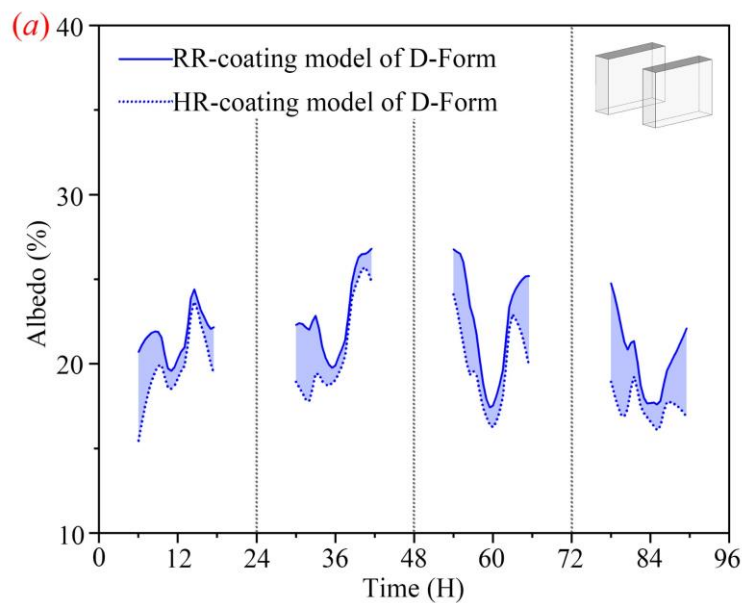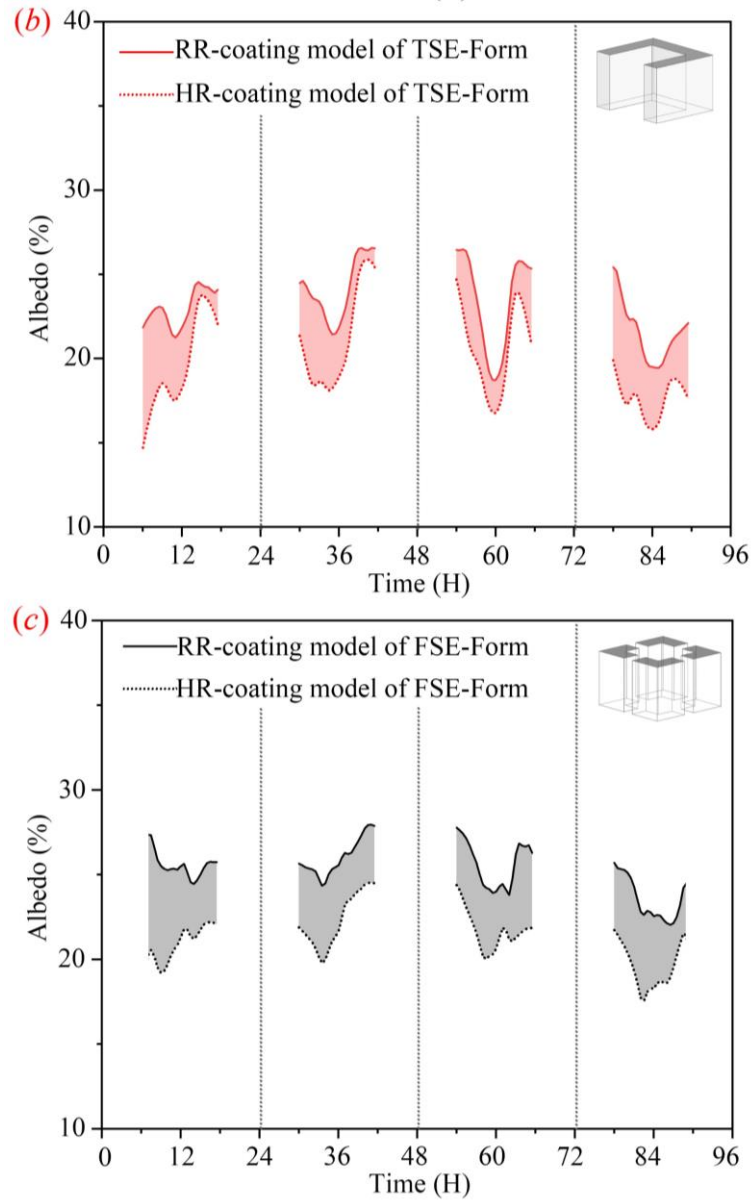
Fig. 6-5. Variation in regional albedos for (a) D-Form buildings, (b) TSE-Form buildings and (c) FSE-Form buildings

Table 6-2. Comparison of maximum and average albedos of three building models

Building forms	Maximum value (%)			Average value (%)		
	RR-coatings	HR-coatings	Difference Value	RR-coatings	HR-coatings	Difference Value
D-Form	26.54	25.87	0.67	21.85	20.49	1.36

TSE-Form	26.81	25.71	1.10	23.01	19.72	3.29
FSE-Form	27.93	24.51	3.42	25.08	19.49	5.59

6.3.2 Comparison of wall temperatures

Wall temperature is one of parameters affecting the regional thermal environment. It affects human thermal comfort and the building energy consumption [44]. Therefore, the wall temperatures were studied in this study.

Figs. 6-6-Figs. 6-8 show the wall temperatures in the interior enclosing spaces for D-Form, TSE-Form and FSE-Form during the experimental period, respectively. It can be seen clearly that the wall temperatures of the RR-coating models were lower than those of the HR-coating models, although the RR-coatings had a lower solar reflectivity. However, there are the obvious difference in three models of high-density buildings.

From D-Form buildings to FSE-Form buildings, the temperature differences in walls and roofs gradually increased between RR-coatings and HR-coatings. It indicated that the higher the enclosed degree of buildings, the higher the contribution efficiency of RR-coatings on reducing surface temperatures, compared to HR-coatings. This phenomenon was mainly resulted from that solar radiation could be reflected more times in the building groups of the higher enclosed spaces. Therefore, the solar radiation had the higher impact on the regional thermal environment. Under this condition, the defect of HR-coatings was magnified on the diffuse reflection, as shown in Fig. 6-1(a). And RR-coatings had the higher contribution efficiency owing to the advantages of optical properties, as shown in Fig. 6-1(b). Moreover, the natural ventilation would be weakened in the building groups with the higher enclosure degree. The thermal effect of solar radiation on building surfaces were intensified.

In addition, compared to HR-coating, the thermal contribution of RR-coating was different for the walls in different orientations, especially for TSE-Form and FSE-Form. Compared with the west and north walls, the roof, east and south walls had a better thermal contribution. This phenomenon was due to the higher solar radiation in the east and south walls. It showed the roof and the east and south walls were the better choices to cover the RR-coatings.
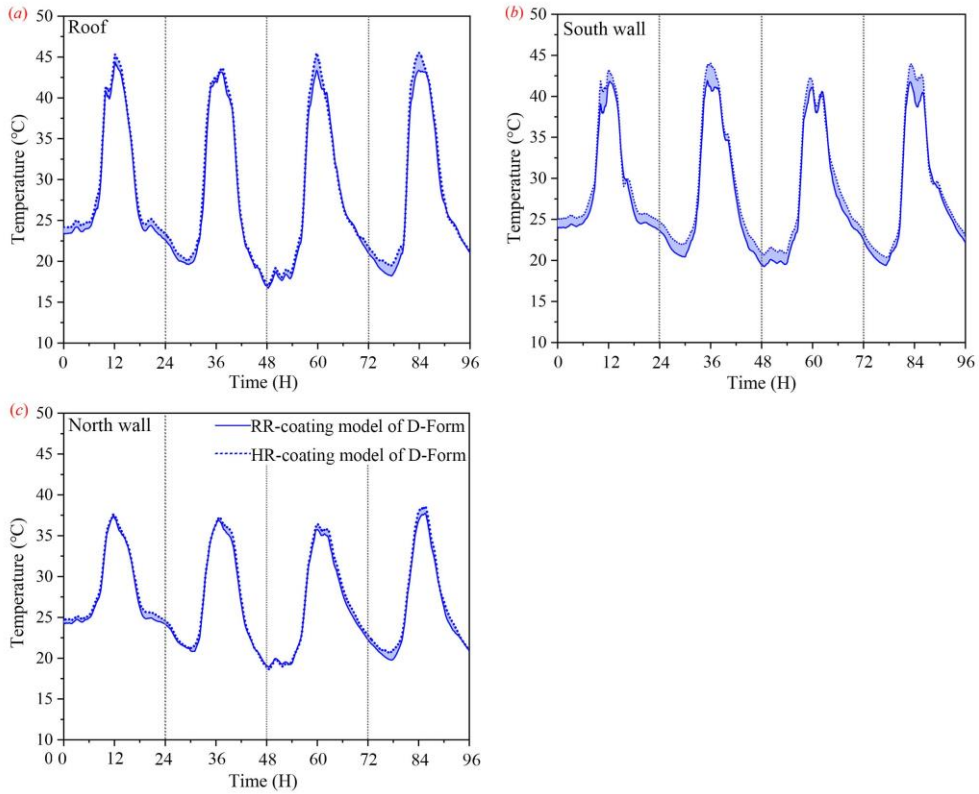
Fig. 6-6. Variation in the wall temperatures for D-Form buildings
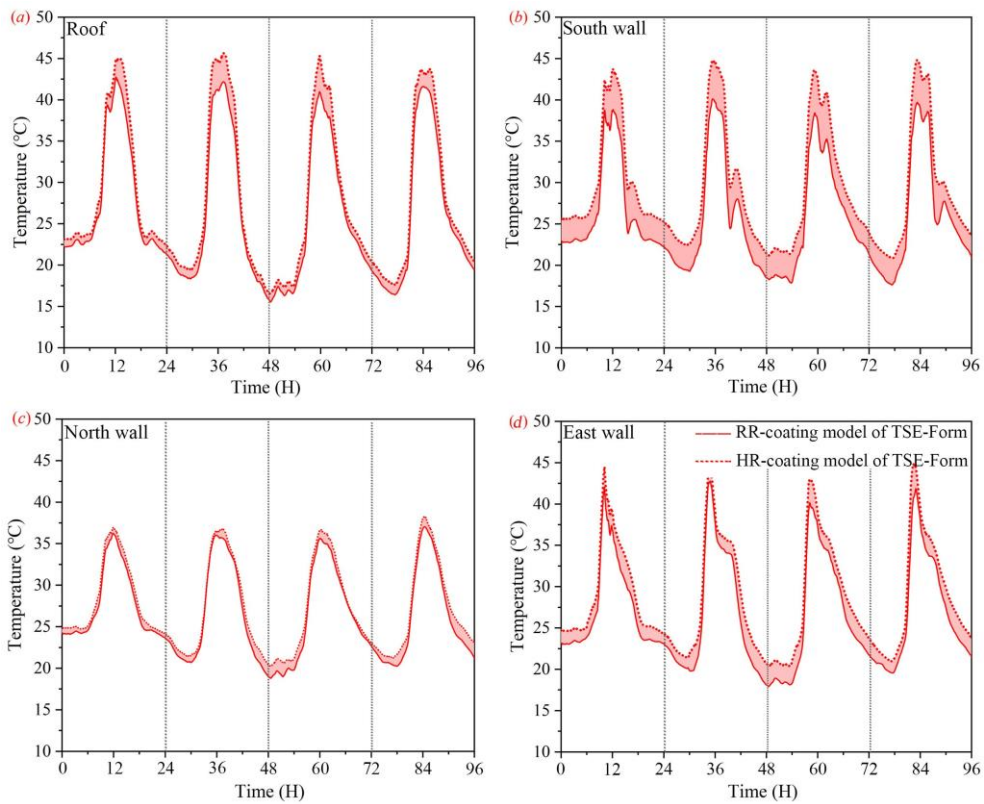
Fig. 6-7. Variation in the wall temperatures for TSE-Form buildings
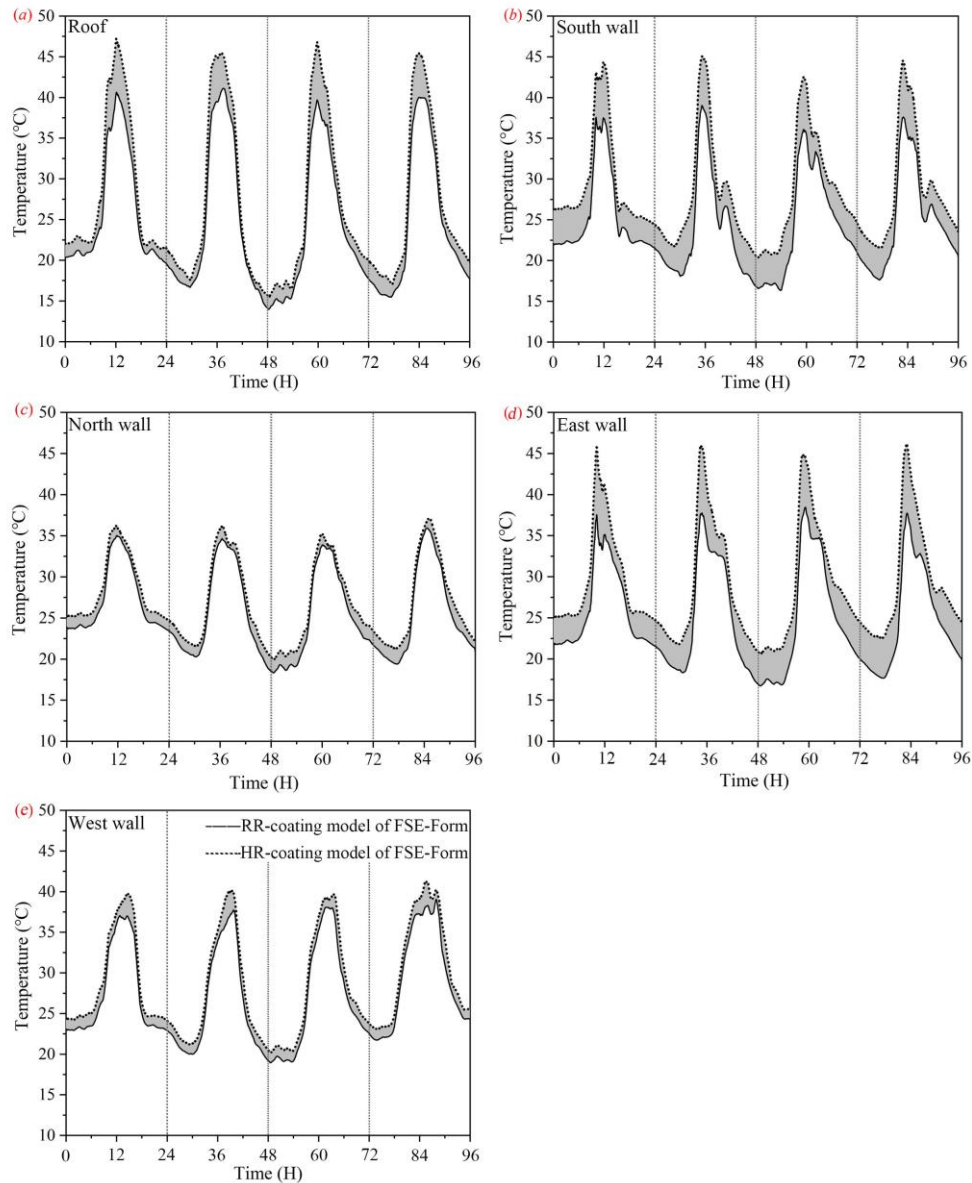
Fig. 6-8. Variation in the wall temperatures for FSE-Form buildings

Table. 6-3 shows the maximum and average wall temperatures of the three building forms with RR-coatings and HR-coatings. As shown in Table 6-3, the enclosure forms of buildings had the higher impacts on the contribution efficiency of RR-coatings and HR-coatings. From D-Form to FSE-Form, the peak and average wall temperatures of the RR-coating models decreased by 1.41°C~3.13°C and 0.89°C~3.23°C, respectively. However, it was on the contrary for HR-coating models, where the peak and average wall temperatures increased by 1.00°C~1.23°C and 0.29°C~0.66°C, respectively. In addition, compared to the HR-coating models, the RR-coating model had a lower wall temperature. The values were also affected by the enclosure degree and wall direction. On the one hand, from D-Form to FSE-Form, the wall temperature differences increased by 2.64°C~4.13°C and 1.18°C~3.97°C for the peak and

average values, respectively. On the other hand, the east wall had the higher temperature differences with peak and average values of 7.05°C and 4.21°C for FSE-Form. The above data showed that RR-coatings could obtain lower wall temperatures on wall surfaces more effectively than HR-coatings, especially for the higher enclosure buildings and walls that received the higher solar radiation. Similar to the variation of albedos, for the three building forms, the maximum wall temperature differences occurred almost at the noon with higher solar altitude angles. Those findings were consistent with some published studies [43, 44]. The reasons for this phenomenon were as follows. Firstly, the incidence solar radiation angles were under 60°, RR-coatings still have retro-reflection property. Secondly, in the morning, the absolute retro-reflection advantage of RR-coatings made the temperatures of the building walls were always lower.

Table 6-3. Comparison of maximum and average wall temperatures of three building forms

Wall orientation	Building forms	Maximum value			Average value		
		RR-coatings	HR-coatings	Difference Value	RR-coatings	HR-coatings	Difference Value
Roof	D-Form	45.63	47.31	1.68	27.79	27.81	0.02
	TSE-Form	43.71	47.63	3.92	26.21	27.84	1.63
	FSE-Form	42.50	48.31	5.81	24.56	28.41	3.85
South wall	D-Form	45.53	46.61	1.08	27.81	28.67	0.86
	TSE-Form	43.21	47.10	3.89	25.78	28.91	3.13
	FSE-Form	43.10	47.80	4.70	24.50	29.33	4.83
North wall	D-Form	38.31	38.57	0.26	26.67	27.12	0.45
	TSE-Form	37.90	39.30	1.40	26.51	27.15	0.64
	FSE-	36.90	39.80	2.90	25.78	27.41	1.63

	Form						
	TSE-Form	45.11	47.30	2.19	26.66	28.73	2.07
East wall	FSE-Form	42.15	49.20	7.05	24.96	29.17	4.21
West wall	FSE-Form	41.04	43.82	2.78	26.32	28.94	2.62

6.3.3 Comparison of air temperatures

Outdoor air temperature is an of the important index to evaluate the regional thermal environment [45]. Fig. 6-11 shows the variation in air temperature in the enclosed space of the three building forms during the experimental period. Air temperatures in the enclosed space were always higher than natural air temperatures. This phenomenon was due to the fact that the absorbed heat by building surfaces was released into air temperature by natural convection. And due to the retro-reflection effect, compared to HR-coating models, there were lower air temperatures in the RR-coating models. From the D-Form buildings to the FSE-form buildings, the air temperature differences between the enclosed spaces in the models with two coatings gradually increased. It indicated that the higher the enclosed degree of buildings, the larger the air temperature reduced by RR-coatings. This phenomenon was mainly due to the higher surface temperature in building groups with the higher enclosure degree, as shown in Figs. 6-6-Figs. 6-8. Also due to the higher enclosure degree, the natural ventilation was weakened, and thereby, the hot air did not dissipate quickly by the airflow.

Table 6-4 compares the maximum and average air temperatures of the three building forms. As shown in Table 6-4, compared with the HR-coating model, the air temperatures in the enclosed space of the RR-coating model were lower. And the higher the enclosure degree of the building groups, the higher the temperature differences. From D-Form to FSE-Form, the peak and average air temperatures of the RR-coating models decreased by 2.30°C and 1.12°C, respectively. However, the opposite was true for the HR-coating models, where the peak and average air temperatures increased by 1.52°C and 0.14°C, respectively. The above analysis showed that RR-coatings could reduce air temperatures in the enclosure spaces more than HR-coatings, especially for the higher enclosure buildings. Similarly, for the three building forms, the maximum air temperature differences occurred almost at the noon. The finding was consistent with some published studies [33, 43]. The phenomenon could be attributed to the effective angles of retro-reflection property of RR-coatings.
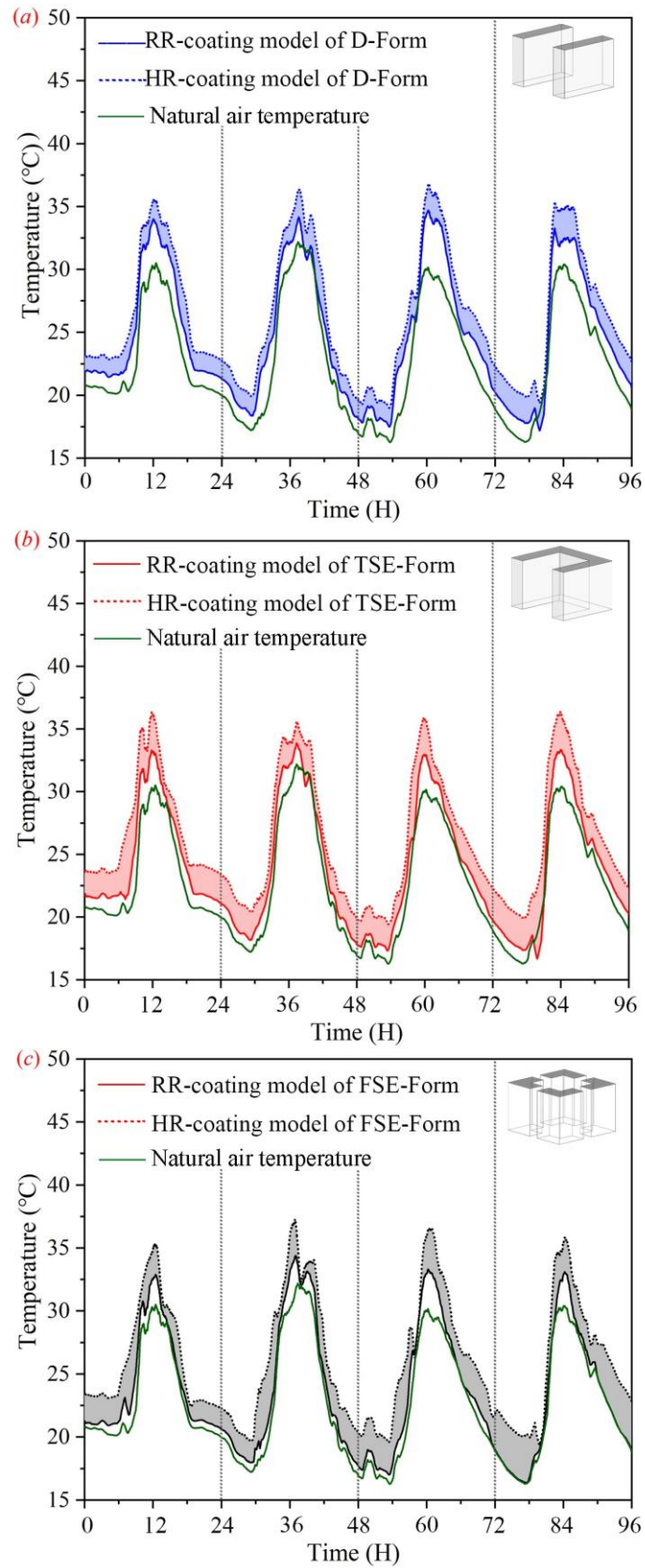
Fig. 6-9. Variation of air temperatures for (a) D-Form buildings, (b) TSE-Form buildings, and (c) FSE-Form buildings

Table 6- 4. Comparison of maximum and average air temperatures of three building forms

Building forms	Peak value			Average value		
	RR-coatings	HR-coatings	Difference Value	RR-coatings	HR-coatings	Difference Value
D-Form	37.80	38.39	0.59	24.60	26.40	1.80
TSE-Form	36.30	38.91	2.61	23.80	26.43	2.53
FSE-Form	35.50	39.91	4.41	23.48	26.54	3.06

6.4 Discussion

This study indicated that RR-coatings had a higher improvement in the regional thermal environment than HR-coatings, including the increase in albedo, and the reduction in wall and air temperature, although RR-coatings had a lower solar reflectance.

For the albedo, it was found that compared with HR-coatings, RR-coatings could increase the maximum and average regional albedo by 0.67%~3.42% and 1.36%~5.59%, respectively. It indicated that RR-coatings could reflect back more solar radiation to the sky and decrease multiple reflections among the buildings due to the retro-reflectivity. This finding was similar to the mounting evidence on the albedo. For example, Castellani et al. [32] found that compared with HR-coatings, the equivalent albedo of urban canyons covered by RR-coatings increased by 5%. And Rossi et al. [21] found that the maximum albedo of urban canyons increased by 4.6% for RR-coatings, with respect to the white and beige diffusive materials. In this study, it was found that compared with HR-coatings, the average albedo of D-Form buildings covered by RR-coatings could increase by 1.36%. The reason why the finding was lower than existing results may lie in different experimental locations. In one of our previously published studies [43], it was found that compared with HR-coating, the regional albedo of FSE-Form buildings covered by RR-coatings could increase by 5.53%. It was consistent with the finding of this study. However, Qin et al. [37] found the building with HR-coatings would stay cooler than that with RR-coatings when the solar radiation was of high value (the hours around noon). That was different with the finding in this study. The main reason for the difference was the height angle of the sun varied from regions.

For the wall temperature, it was found that RR-coatings could lower the maximum and

average temperatures by 0.26°C~7.05°C and 0.02°C~4.83°C, respectively. Similarly, Rossi et al. [21] applied RR-coatings in building envelopes of urban canyons, and found that the south-oriented facade temperatures could be reduced by 7.68°C. In this study, similar to urban canyons, it was found that the wall temperature of the D-Form covered by RR-coatings could be reduced by 1.08°C. The differences between the results were mainly due to the different experimental locations. Of course, there have also been many studies on the thermal contribution of RR-coatings in other buildings with different forms. For example, Meng et al. [47] found that compared with the building model without RR-coatings, the model covered by RR-coatings could reduce the maximum temperatures of inner and outer surfaces by 10°C and 25°C. It was also found that the top, south and east walls were the better choices for covering with RR-coatings, which was the same as the conclusion drawn in this paper. This phenomenon was due to the walls could receive more solar radiation. Qin et al. [37] found that outer surface temperatures of the small-scale building blocks with RR-coatings were 5°C~10°C lower than those with diffuse-reflective surfaces. Zhang et al. [48] found that after applying RR-coatings on tents, the peak outer wall temperature could be reduced by 5.8~15°C and 3.4~5.2°C in the periods 10:00~18:00 and 18:00~24:00, respectively. It could be seen that no matter what kinds of application, RR-coatings could decrease the wall temperature in different degrees.

For the air temperature, previous studies have focused more on indoor air temperatures. For example, Meng et al. [25] found that compared to prefabricated houses without RR-coatings, covering RR-coatings could reduce the average and peak indoor air temperatures by 1.5°C and 7°C, respectively. Zhang et al. [48] found that compared to the ordinary tent, the peak indoor air temperature of the tent model was lowered by 7.0°C. Only a study has focused on the outdoor air temperature. For example, Rossi et al. [33] found that compared with the white diffuse cooling material, the air temperature of the urban canyon decreased by 1% after covering RR-coatings on the vertical surface. In this study, it was found that due to the retro-reflection effect, compared to HR-coating models, there were lower air temperatures in the RR-coating models. And the RR-coatings could lower the maximum and average air temperatures by 1.80°C~3.06°C.

In addition, unlike the previous studies those focused on single building form, this study evaluated the thermal contribution of RR-coatings and HR-coatings on three building forms. It was found that the higher the enclosure degree of buildings covered by RR-coatings, the better the thermal environment, including the albedo, wall temperature, and air temperature. This was in contrast to existing research [49, 50] which demonstrated that the higher the enclosure degree of buildings, the worse the thermal environment. This phenomenon occurred was owing to the building groups of the higher enclosure degree would weaken the natural ventilation, and the

solar radiation had a higher impact on the regional thermal environment. The optical characteristic of RR-coatings resulted in less absorbed solar radiation.

This study analyzed the influence of the building enclosed forms on thermal contribution of RR-coating and HR-coating based on three groups of scaled building models. The provided evaluations had the certain theoretical significance for the coating application on high-rise buildings and compared with HR-coatings, RR-coatings were more suitable for buildings with a higher enclosure degree. The employed experimental models were somewhat different from the real high-rise buildings. Further studies were expected to make a dimensional analysis of data to translate the behavior of the small-scale building into that of a real building. However, there were the same qualitative regularities. It was believed that any differences would not greatly change or reverse the conclusion obtained [41].

6.5 Conclusions

In this study, the influence of enclosed building forms on the thermal contribution of reflective coatings was evaluated. It was found RR-coatings had a higher improvement in the regional thermal environment than HR-coatings, although RR-coatings had a lower solar reflectance. The higher the enclosure degree of buildings, the higher the improvement efficiency of RR-coatings. The reason for those was due to the optical property of RR-coatings. However, from the angular distribution of reflected radiation, it could be found that the existing RR-coatings might lose retro-reflectivity when the solar radiation was high. To make RR-coatings have better improvement of thermal environment, the new RR-coatings with retro-reflectivity in a bigger angle range need to be designed. In addition, the experimental conditions were somewhat different from real conditions in urban areas. Therefore, the following research will also be focused on the numerical simulation and the field measurement to explore the effect of RR-coatings and HR-coating on thermal environment and human thermal comfort based on real buildings.

References

[1] J. Fahed, E. Kinab, S. Ginestet, L. Adolphe. Impact of urban heat island mitigation measures on microclimate and pedestrian comfort in a dense urban district of Lebanon. Sustainable Cities and Society 61 (2020) 102375.

[2] Y. Wang, D. Mauree, Q. Sun, H. Lin, J.L. Scartezzini, R. Wennersten. A review of approaches to low-carbon transition of high-rise residential buildings in China. Renewable and Sustainable Energy Reviews 131 (2020) 109990.

[3] W. Pan, M. Pan. A dialectical system framework of zero carbon emission building policy for high-rise high-density cities: Perspectives from Hong Kong. Journal of Cleaner Production 205 (2018) 1-13.

[4] L.S. Bar, M. E. Hoffman, Y. Tzamir. Integrated thermal effects of generic built forms and vegetation on the UCL microclimate. Building and Environment 41 (2006) 343-354.

[5] Y.F. Gao, R.M Yao, B.Z. Lia, E. Turkbeylerc, Q. Luo, A. Shortd. Field studies on the effect of built forms on urban wind environments. Renewable Energy 46 (2021) 148-154.

[6] D.L. Liu, H.H. Zhao, J.P. Liu. Rule of long-wave radiation in enclosed building space. Energy and Buildings 182 (2019) 311-321.

[7] E. Jamei, P. Rajagopalan, M. Seyedmahmoudian, Y. Jamei. Review on the impact of urban geometry and pedestrian level greening on outdoor thermal comfort. Renewable and Sustainable Energy Reviews 54 (2016) 1002-1017.

[8] F. Rossi, E. Bonamente, A. Nicolini, E. Anderini, F. Cotana. A carbon footprint and energy consumption assessment methodology for UHI -affected lighting systems in built areas. Energy and Buildings 114 (2016) 96-103.

[9] M. Santamouris. On the energy impact of urban heat island and global warming on buildings. Energy and Buildings 82 (2014) 100-113.

[10] X. Meng, L. Meng, Y. Gao, H.R. Li. A comprehensive review on the spray cooling system employed to improve the summer thermal environment: application efficiency, impact factors, and performance improvement. Building and Environment 217 (2022) 109065

[11] F. Rossi, E. Anderini, B. Castellani, A. Nicolini, E. Morini. Integrated improvement of occupants' comfort in urban areas during outdoor events. Building and Environment 93 (2015) 285-292.

[12] X. Meng, L.Y. Yan, F.D. Liu. A new method to improve indoor environment: Combining the living wall with air-conditioning. Building and Environment 216 (2022) 108981

[13] F.D. Liu, L.Y. Yan, X. Meng. A review on indoor green plants employed to improve indoor environment. Journal of Building Engieering 53 (2022) 104542

[14] M. Zhang, C.B. Xu, L. Meng, X. Meng. Outdoor comfort level improvement in the traffic waiting areas by using a mist spray system: An experiment and questionnaire study. Sustainable Cities and Society 71 (2021) 102973

[15] C. Fabiani, V.L. Castaldo, A.L. Pisello. Thermochromic materials for indoor thermal

comfort improvement: Finite difference modeling and validation in a real case-study building. Applied Energy 262 (2020) 114147.

[16] S.W. Lee, C.H. Lim, E.I.B. Salleh. Reflective thermal insulation systems in building: A review on radiant barrier and reflective insulation. Renewable and Sustainable Energy Reviews 65 (2016) 643-661.

[17] H. Akbari, D. Kolokotsa. Three decades of urban heat islands and mitigation technologies research. Energy and Buildings 133 (2016) 834-842.

[18] M. Santamouris, A. Synnefa, D. Kolokotsa, V. Dimitriou, K. Apostolakis, Passive cooling of the built environment-use of innovative reflective materials to fight heat islands and decrease cooling needs. International Journal of Low Carbon Technologies 3/2 (2008) 71-82.

[19] A. Synnefa, M. Santamouris, H. Akbari. Estimating the effect of using cool coatings on energy loads and thermal comfort in residential buildings in various climatic conditions. Energy and Buildings 39 (2007) 1167-1174.

[20] Y. Qin. Urban canyon albedo and its implication on the use of reflective cool pavements. Energy and Buildings 96 (2015) 86-94.

[21] F. Rossi, B. Castellani, A. Presciutti, E. Morini, E. Anderini, M. Filipponi, A. Nicolini. Energy and Buildings 126 (2016) 340-352.

[22] E. Morini, B. Castellani, A. Presciutti, M. Filipponi, A. Nicolini, F. Rossi. Optic-energy performance improvement of exterior paints for buildings. Energy and Buildings 139 (2017) 690-701.

[23] F. Rossi, B. Castellani, A. Presciutti, E. Morini, M. Filipponi, A. Nicolini, M. Santamouris. Retroreflective façades for urban heat island mitigation: Experimental investigation and energy evaluations. Applied Energy 145 (2015) 8-20.

[24] J. Wang, S.H. Liu, X. Meng, W.J. Wei, J.H. Yuan. Application of RR-coatings in urban buildings: A comprehensive review. Energy and Buildings 247 (2021) 111137.

[25] X. Meng, C.X. Wang, W.J. Liang, S. Wang, P. Li, E.S. Long. Thermal Performance Improvement of Prefab Houses by Covering RR-coatings. Procedia Engineering 121 (2015) 1001-1007.

[26] H. Sakai, H. Kobayashi, K. Emura, N. Igawa. Outdoor measurement of solar reflective performance of retroreflective materials. Journal of Structural and Construction Engineering (Transactions of AIJ) 73 (2008) 1713-1718.

[27] J.H. Yuan, K. Emura, C. Farnham. A method to measure retro-reflectance and durability of RR-coatings for building outer walls. Journal of Building Physics 38 (2015) 500-516.

[28] J.H. Yuan, K. Emura. Changes in Solar Reflectance of Retro-reflective Sheets used on the Outer Wall of Building over Long-term Exposure. Air-conditioning and Sanitary Engineers of Japan Conference in Nagano. 10 (2013) 245-248.

[29] F. Rossi, A.L. Pisello, A. Nicolini, M. Filipponi, M. Palombo. Analysis of retro-reflective surfaces for urban heat island mitigation: a new analytical model. Appl. Energy 114 (2014) 621-631.

[30] T. Inoue, T. Shimo, M. Ichinose, K. Takase, T. Nagahama. Improvement of urban thermal environment by wavelength-selective retro-reflective film. Energy Procedia 122 (2017) 967-972.

[31] T. Inoue, K. Takase, Y. Saito. Effects of modified near-infrared retro-reflective film on urban thermal environment. Journal of Physics: Conference Series 1343 (2019) 012191.

[32] B. Castellani, A. Nicolini, A.M. Gambelli, M. Filipponi, E. Morini, F. Rossi. Experimental assessment of the combined effect of retroreflective façades and pavement in urban canyons. IOP Conference Series: Materials Science and Engineering 609 (2019) 072004.

[33] E. Morini, B. Castellani, A. Presciutti, E. Anderini, M. Filipponi, A. Nicolini, F. Rossi. Experimental Analysis of the Effect of Geometry and Facade Materials on Urban District's Equivalent Albedo. Sustainability 9 (2017) 1245.

[34] S. Yoshida, A. Mochida. Evaluation of effects of windows installed with near-infrared rays retro-reflective film on thermal environment in outdoor spaces using CFD analysis coupled with radiant computation. Building Simulation 11 (2018) 1053-1066.

[35] S. Yoshida, S. Yumino, T. Uchida, A. Mochida. Numerical Analysis of the Effects of Windows with Heat Ray Retro-reflective Film on the Outdoor Thermal Environment within a Two-dimensional Square Cavity-type Street Canyon. Procedia Engineering 169 (2016) 384-391.

[36] J.H. Yuan, K. Emura, H. Sakai, C. Farnham, S.Q. Lu. Optical analysis of glass bead RR-coatings for urban heat island mitigation. Solar Energy 132 (2016) 203-213.

[37] P.K. Thejus, K.V. Krishnapriya, K.G. Nishanth. A cost-effective intense blue colour inorganic pigment for multifunctional cool roof and anticorrosive coatings. Solar Energy Materials and Solar Cells 219 (2021) 110778.

[38] S. Garshasbi, S.J. Huang, J. Valenta, M. Santamouris. On the combination of quantum dots with near-infrared reflective base coats to maximize their urban overheating mitigation potential. Solar Energy 211 (2020) 111-116.

[39] A.N.M.T. Elahi, D. Jensen, M. Ghashami, K. Park. Comprehensive energy balance analysis of photon-enhanced thermionic power generation considering concentrated solar absorption distribution. Solar Energy Materials and Solar Cells, 226 (2021) 111067.

[40] X. Yang, Y. Li. The impact of building density and building height heterogeneity on average urban albedo and street surface temperature. Building and Environment 90 (2015) 146-156.

[41] Y.H. Qin. J. Liang, K.G. Tan, F.H. Li. A side-by-side comparison of the cooling effect of building blocks with retro-reflective and diffuse-reflective walls. Solar Energy 133 (2016) 172-179.

[42] R. Levinson, H. Akbari1, P. Berdahl. Measuring solar reflectance—Part I: Defining a metric that accurately predicts solar heat gain. Solar Energy 84 (2010) 1717–1744.

[43] J. Wang, S.H. Liu, Z.F. Liu, M. Xi, C.B. Xu, W.J. Gao. An experimental comparison on regional thermal environment of the high-density enclosed building groups with retro-reflective and high reflective coatings. Energy and Buildings 259 (2022) 111864.

[44] Y.L. Han, J.E. Taylor, A.L. Pisello. Toward mitigating urban heat island effects: Investigating the thermal-energy impact of bio-inspired retro-reflective building envelopes in dense urban settings. Energy and Buildings 102 (2015) 380–389.

[45] I. Hernández-Pérez, J. Xaman, E.V. Macias-Melo, K.M. Aguilar-Castro, I. Zavala-Guillen, I. Hernandez-Lopez, E. Sima. Experimental thermal evaluation of building roofs with conventional and reflective coatings. Energy and Buildings 158 (2018) 569-579.

[46] A. Aboelata. Reducing outdoor air temperature, improving thermal comfort, and saving buildings' cooling energy demand in arid cities – Cool paving utilization. Sustainable Cities and Society 68 (2021) 102762.

[47] X. Meng, T. Luo, Z.Y. Wang, W. Zhang, B. Yan, J.L. Ouyang, E.S. Long. Effect of RR-coatings on building indoor temperature conditions and heat flow analysis for walls. Energy and Buildings 127 (2016) 488-498.

[48] L.L. Zhang, X. Meng, F. Liu, L. Xu, E.S. Long. Effect of RR-coatings on temperature environment in tents. Case Studies in Thermal Engineering 9 (2017) 122-127.

[49] E. Ahmadian, B. Sodagar, C. Bingham, A. Elnokaly, G. Mills. Effect of urban built form and density on building energy performance in temperate climates. Energy and buildings 236 (2021) 110762.

[50] Q.T. Deng, G.B. Wang, Y.T. Wang, H. Zhou, L. Ma. A quantitative analysis of the impact of residential cluster layout on building heating energy consumption in cold IIB regions of China. Energy and Buildings 253 (2021) 111515.

An experimental evaluation on thermal contribution of retro-reflective and high-reflective coatings in an enclosed building in summer and winter

Chapter 7 An experimental evaluation on thermal contribution of retro-reflective and high-reflective coatings in an enclosed building in summer and winter

7.1 Introduction

Rapid urbanization leads to the intensification of urban heat island phenomenon, which mainly manifests as the air temperatures in cities were much higher than that in the surrounding countryside [1]. It is unfavorable to the sustainable development of environment, resources and population [2]. The demand for improving urban thermal environment and reducing energy use is increasing [3]. Some green technologies have been proposed, included the increment of green infrastructures [4], the employment of specialized urban design [5] and so on. However, solar radiation has a great influence on the buildings heat gain, therefore reflective coatings have attracted more attention due to they could effectively reflect solar radiation, and maintain a lower building surface temperature, and reduce the heat transfer [6-10]. Currently, reflective coatings mainly include high-reflective coatings (HR-coatings) with a wide range of application [11-13] and retro-reflective coatings (RR-coatings), which have attracted attention in recent years [14, 15].

For the HR-coatings, Yang et al. [16] provided a synthetic overview of potential environmental impacts of reflective coatings at a variety of scales, ranging from energy load on a single building to regional hydroclimate, and found that most of the existing experimental and modeling studies about HR-coatings showed certain thermal benefits, including temperature reduction and energy savings. Pereza et al. [17] found that the heat gain of buildings with a high-reflective roof was 9% less than that of the buildings with an ordinary roof. Mohamed et al. [18] found that high-reflective roof were capable of reducing cooling loads by about 45%. Baneshi et al. [19] found compared to the residential building with typical coatings, the building with optimized coatings which with higher reflectivity could reduced the annual cooling load by 4-31%, while increased the annual heating load demand by 1.7-10%. However, HR-coatings could only reflect solar radiation back to the sky if there were no high-rise buildings around, otherwise, a part of the reflected sunlight would be absorbed by surrounding buildings [20]. Salvati et al. [21] found that an increase in surface reflectance in urban canyons had an adverse effect on outdoor thermal comfort because increased surface reflection led to an increase of mean radiant temperature. Therefore, HR-coatings have limited effect on thermal environment improvement of enclosed buildings [15].

Different from the HR-coatings, RR-coatings could reflect the solar radiation back along the incident direction [22], and the absorbed solar radiation by surrounding buildings would be reduced, which would have a certain improvement on the thermal environment and energy consumption. This coatings were originally used in transportation and textile fields for various security and decorative purpose [23]. In 2004, Nielsen and Lu [24] proposed the applications of RR-coatings in buildings to alleviate urban heat island phenomenon. And from then on, more

and more scholars have paid attention to relative research. Some studies focused on the optical property improvement of RR-coatings. Sakai et al. [25] developed a new RR-coatings, which could reflect the solar radiation in summer and absorb solar radiation in winter by the reasonable location of reflector and absorber coating. Yuan et al. [26] added a glass covering with high transmission and high strength on prism RR-coatings to improve the durability. And some studies focused on the influence of RR-coatings on the thermal environment of buildings. Yoshida et al. [27] covered the RR-coatings on exterior windows of buildings and it was found the reflected solar radiation was increased by 13%. Inoue et al. [28] simulated a high-rise building model, and covered all surfaces with RR-coatings and found that the upward reflected solar radiation was increased by 5% on average. Zhang et al. [29] applied RR-coatings on tents, and found the outer surface peak temperature was reduced by 5.8°C~15°C in the period of 10:00~18:00, while the inner surface peak temperature was reduced by 9.2°C~4.9°C. Rossi et al. [30] found that the air temperature could decrease by 1% when RR-coatings were covered on the urban canyon surface. In one of our previous studies [31], it was also found that when covering with RR-coatings, the regional albedos could be increased by 3.42%, and the wall temperatures and outdoor air could drop by 7.05°C and 3.06°C, respectively. Yuan et al. [26] discovered that when covering RR-coatings, the annual cooling loads of a building in Shanghai could be reduced by 157 MJ/m². Yoshida et al. [32] covered the RR-coatings on a single float glass window on the west of the building, and it was found the cooling load was decreased by 23%.

From the above review, it could be seen that most of the studies focused on the effect of reflective coatings in summer, while there was few on that in winter, especially for the RR-coatings. Therefore, different from previous studies, this study mainly focused on the seasonal evaluation of RR-coatings on thermal performance of buildings, which is important in in the areas of hot summers and cold winters with great demands for both cooling load and heat load. Based on this, two coatings were separately covered on the scaled building models, and the regional albedos, wall temperatures and air temperatures in two seasons were monitored.

7.2 Experiment platform and point layout

In the comparative experiment, courtyard-type high-density buildings were selected as the research subject owing to the higher land use efficiency and better outdoor environment [33], and for the further analysis, the building form was simplified as shown in Fig. 7-1(a), and the building facades were covered by prism RR-coatings and HR-coatings, respectively. To be closer to the real urban thermal environment, the black film was laid on the bottom to represent the ground asphalt. Owing to the comparative experiment were conducted at the same time in

summer and winter, respectively, the differences in experimental results could be attributed to the covered coatings, which could ensure the validity of the experiment.

To comprehensively study the thermal contribution of coatings, three indicators were applied, including the regional albedo, wall temperature and air temperature. Fig. 7-1(b) showed the positions of measurement instruments. For the regional albedo, two back-to-back solar radiometers were set to obtain reflected solar radiation and incident solar radiation. For the wall temperature and air temperature, 1 T-type thermocouple were placed on the center of walls in all directions and the enclosed space, respectively.

Table 7-1 shows the specifications of the used instruments. As shown, the accuracies of the solar radiometers, T-type thermocouples and anemograph were 2%, 0.5∘C and 0.1m/s, respectively. And before the experiment, all instruments were calibrated to ensure their test accuracy.
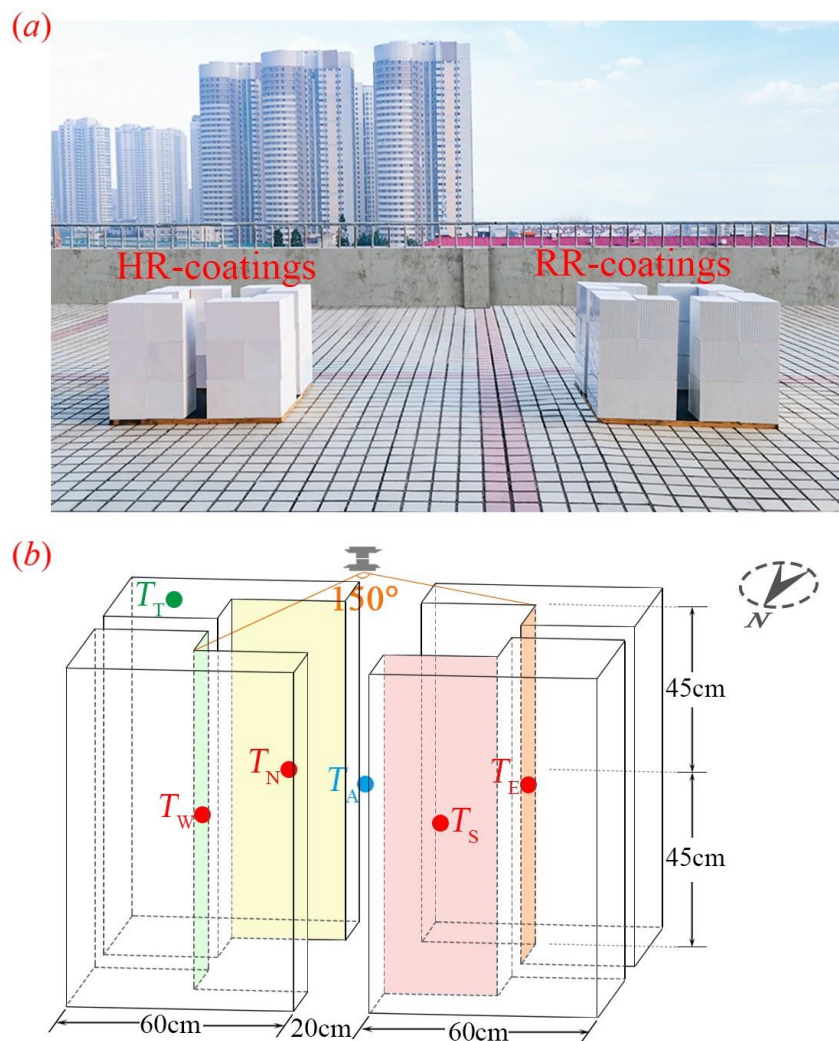
Fig. 7-1. Experimental platform and point layout

Table 7-1 Specification of instruments applied in the experiment

Instrument	Resolution	Accuracy	Range of operation
Solar radiometers	$0.1 W/m^2$	$\pm 2\%$	$0 \sim 2000 W/m^2$
T-type thermocouples	$0.01°C$	$\pm 0.5°C$	$-200°C \sim +400°C$
Anemograph	$0.1 m/s$	$\pm 0.1 m/s$	$0.4 \sim 60 m/s$

7.3 Experiment results and discussion

The comparative experiment was conducted from 18th to 21st of June 2021, and from 7th to 10th of December 2022 in Qingdao city, China, respectively. Owing to the solar radiation was the main cause effecting building thermal environment [34], the experiment was carried out on sunny days with less cloud disturbance. Fig. 7-2 showed the variation of horizontal radiation, outdoor air temperature and wind speed with time during the experimental periods. It could be seen that the horizontal radiation and outdoor air temperature in summer were much higher than those in winter, while the wind speed was opposite. For the horizontal radiation, in summer, the highest solar radiation reached 1238.0 W/m^2, while the value was 572.2 W/m^2 in winter. For the outdoor air temperatures, the highest, the lowest and the average values in summer were 37.8°C, 20.4°C and 27.6°C, respectively, while those values in winter were 15.3°C, 1.1°C and 7.5°C, respectively. And for the outdoor wind speed, the highest wind speed in summer and winter were 4.0 m/s and 5.4m/s, respectively.
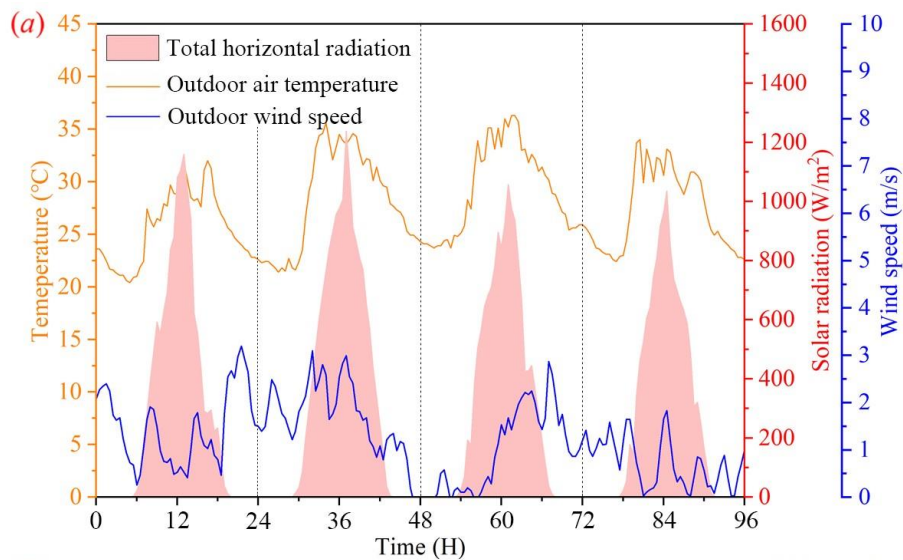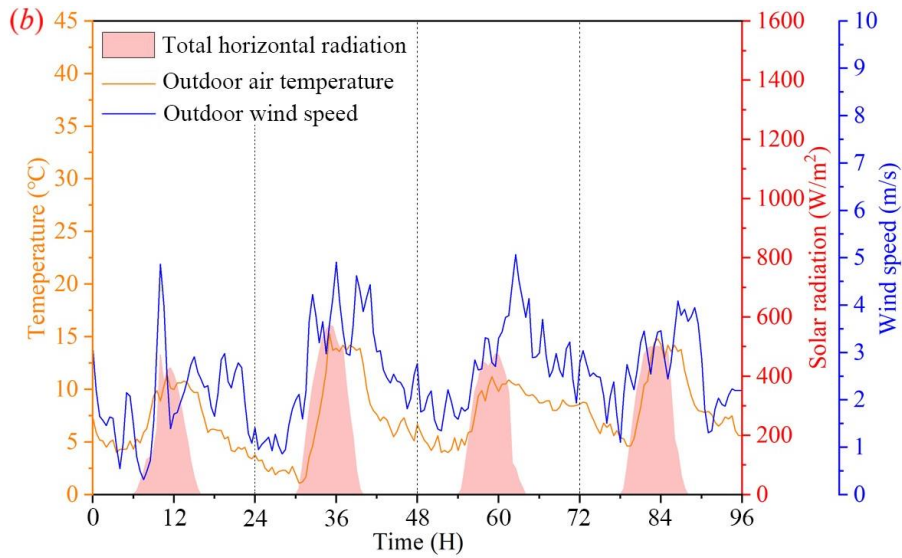
Fig. 7-2. Variation of solar radiation, air temperature and wind speed with time in (a) summer and (b) winter

7.3.1 Comparison of the regional albedo

The amount of absorbed solar radiation would affect building thermal environment, and the demand for building energy [35]. To assess the building's ability to absorb solar radiation, the index of regional albedo was applied, which was the ratio of reflected solar radiation to incident solar radiation. Fig. 7-3 showed the reflected solar radiation of RR-coatings and HR-coatings in summer and winter. It could be seen that RR-coatings had more reflected solar radiation during the experimental periods than HR-coatings. In summer, the maximum values of RR-coatings and HR-coatings were 311.1 W/m^2 and 250.0 W/m^2, respectively, with the difference of 61.1W/m^2. And in winter, the values were 148.1 W/m^2 and 123.8 W/m^2, respectively, with the difference of 24.3 W/m^2. The less difference caused by two coatings in winter could attribute to the less total solar radiation intensity.

Fig. 7-4 showed the albedos of RR-coatings and HR-coatings in summer and winter. It could be seen that the regional albedos of the RR-coatings were higher than HR-coatings in both summer and winter, especially at the noon with highest solar radiation. Table 7-2 showed the maximum and average regional albedos of RR-coating and HR-coating in summer and winter. In summer, the maximum and average regional albedos of RR-coatings and HR-coatings were 40.71% and 35.72%, 29.41% and 24.32%, respectively, with the differences of 4.99% and 5.09%, respectively. And the values were 38.32% and 34.86%, 27.09% and 23.94% in winter, respectively, with the differences of 2.46 % and 3.15%, which indicated that the RR-coatings could obtain the higher albedo in both summer and winter, while the differences were greater in summer than in winter, which would lead to more thermal benefits in summer caused by RR-

coatings than the penalties in winter.
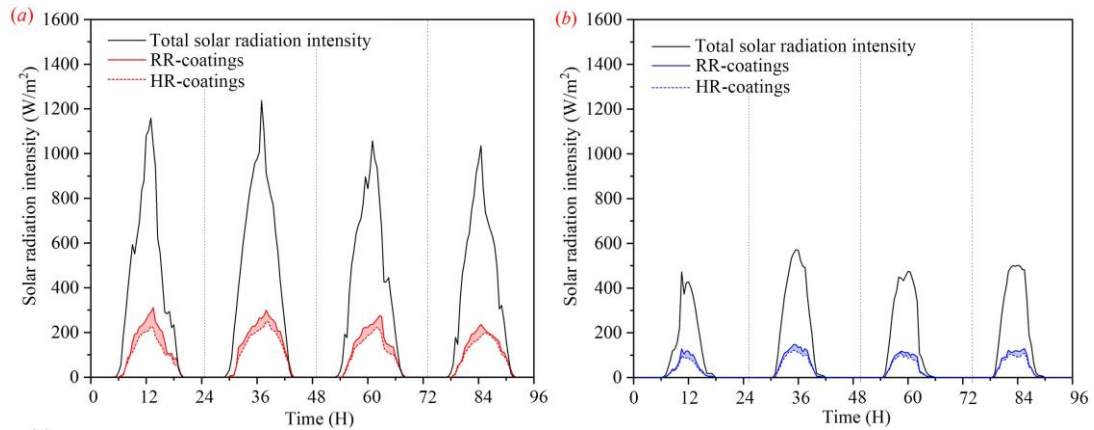
Fig. 7-3. Variation of reflected solar radiation of RR-coatings and HR-coatings in (a) summer and (b) winter
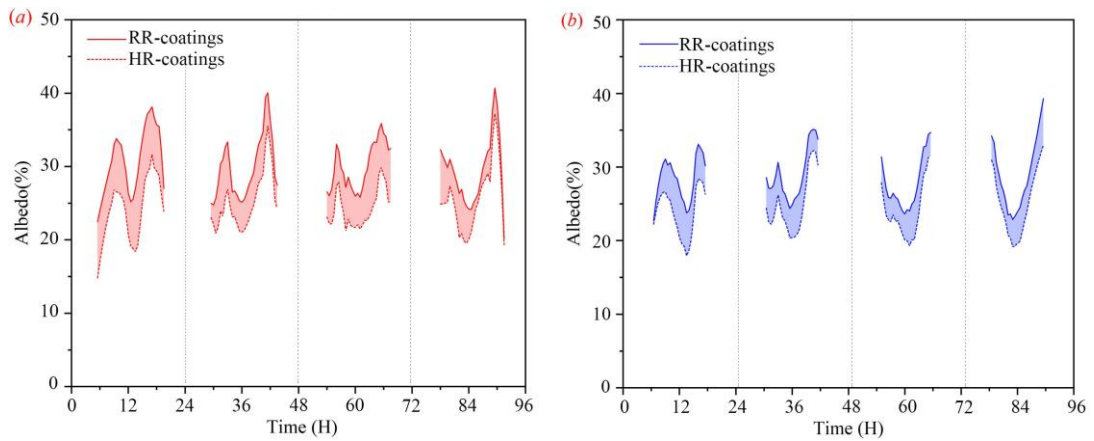
Fig. 7-4. Variation of Albedos of RR-coatings and HR-coatings in (a) summer and (b) winter

Table 7-2 Comparison of maximum and average albedos of RR-coating and HR-coating in summer and winter

Season	Maximum value (%)			Average value (%)		
	RR-coatings	HR-coatings	Difference	RR-coatings	HR-coatings	Difference
Summer	40.71	35.72	4.99	29.41	24.32	5.09
Winter	38.32	34.86	2.46	27.09	23.94	3.15

7.3.2 Comparison of wall temperature

Wall temperature affects the indoor and outdoor thermal environment of buildings, as well as the energy consumption [36-38]. Fig. 7-5. showed the variation of the roof temperatures of two coatings with time in summer and winter. It could be seen that both in summer and winter, the roof temperatures of RR-coatings were always lower than those of HR-coatings. In summer, the maximum and average wall temperature differences were 7.71°C and 3.75°C, respectively. And in winter, the values were 4.50°C and 1.39°C, respectively. Due to the high solar radiation intensity, the maximum wall temperature differences in both summer and winter almost appeared at noon. However, the temperature differences caused by two coatings were larger in summer. This phenomenon was mainly resulted from the optical properties advantage of RR-coatings were amplified resulted by higher solar radiation in summer, moreover, the lower wind speed could also maintain the stability of the formed thermal environment.
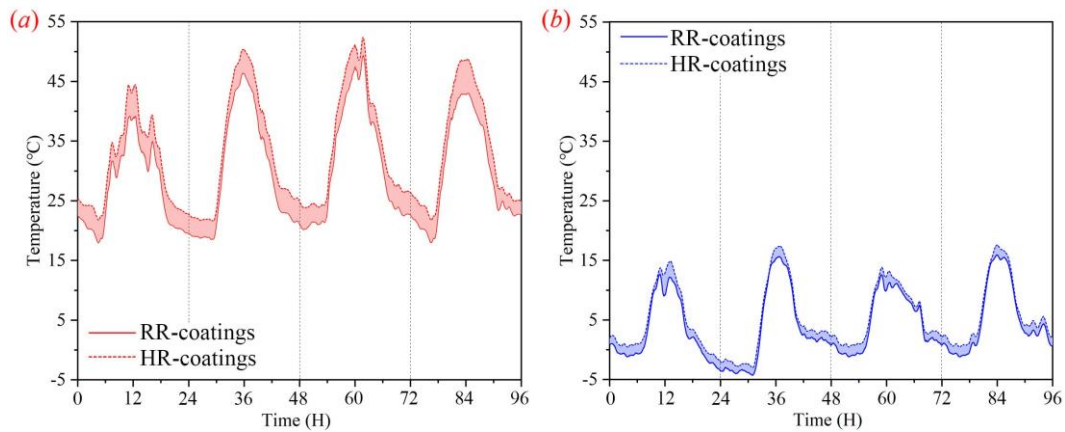
Fig. 7-5. Variation of roof temperatures of RR-coatings and HR-coatings in (a) summer and (b) winter

Fig. 7-6 showed the wall temperatures of RR-coatings and HR-coatings in summer and winter. As shown, in both summer and winter, the wall temperatures of RRC were always lower than those of HR-coatings, although the RR-coatings had a lower solar reflectivity. And for the east wall, the maximum and average wall temperature differences in summer were 11.61°C and 1.71°C, respectively, and the values in winter were 5.61°C and 1.54°C, respectively. For the south wall, the maximum and average wall temperature differences in summer were 7.25°C and 2.90°C, respectively, and the values in winter were 4.32°C and 1.21°C, respectively. For the west wall, the temperature differences were not obvious, and the maximum and average values in summer were 4.63°C and 2.76°C, respectively, and the values in winter were 1.11°C and 0.52°C, respectively. For the north wall, due to the orientation received the least solar radiation, the temperature difference was the smallest, and the maximum and average values in summer

were 2.74℃ and 0.74℃, respectively, and the values in winter were 1.39℃ and 0.39℃, respectively. It was showed that the temperature differences in summer were larger than in winter, no matter what directions of walls. This phenomenon was mainly resulted from the higher solar radiation in summer amplified the optical advantage of RRC, and lower wind speed maintained the formed thermal environment, so the higher thermal benefits were gained in summer caused by RRC than the penalties in winter.

Table 7-3 gave the maximum and average wall temperature differences of RR-coatings and HR-coatings in summer and winter. The maximum and average temperature differences in the roof, east wall and south wall in summer were 7.25℃~11.61℃ & 1.71℃~3.75℃ and 4.32℃~5.61℃ & 1.21℃~1.54℃ in winter. However, these values in west wall and north wall were 2.74℃~4.63℃ & 0.74℃~1.11℃ in summer and 1.39~2.76 & 0.39~0.52℃ in winter. It showed that wall orientations had the same effect between summer and winter on the thermal performance of RR-coatings, and that compared to west wall and north wall, RR-coatings could gain the higher efficiency in the roof, east wall and south wall, which was the same as the conclusion drawn in Qin et al. [34] and Meng et al. [39]. This phenomenon was due to the higher solar radiation in those orientations.
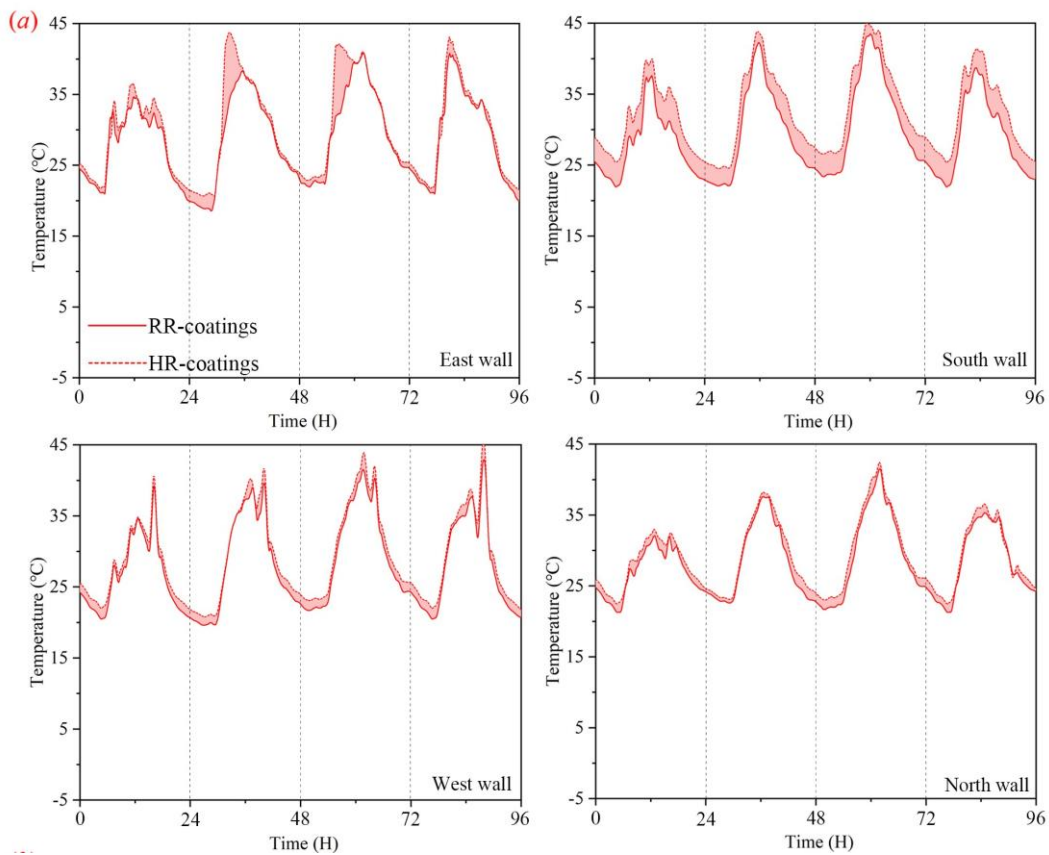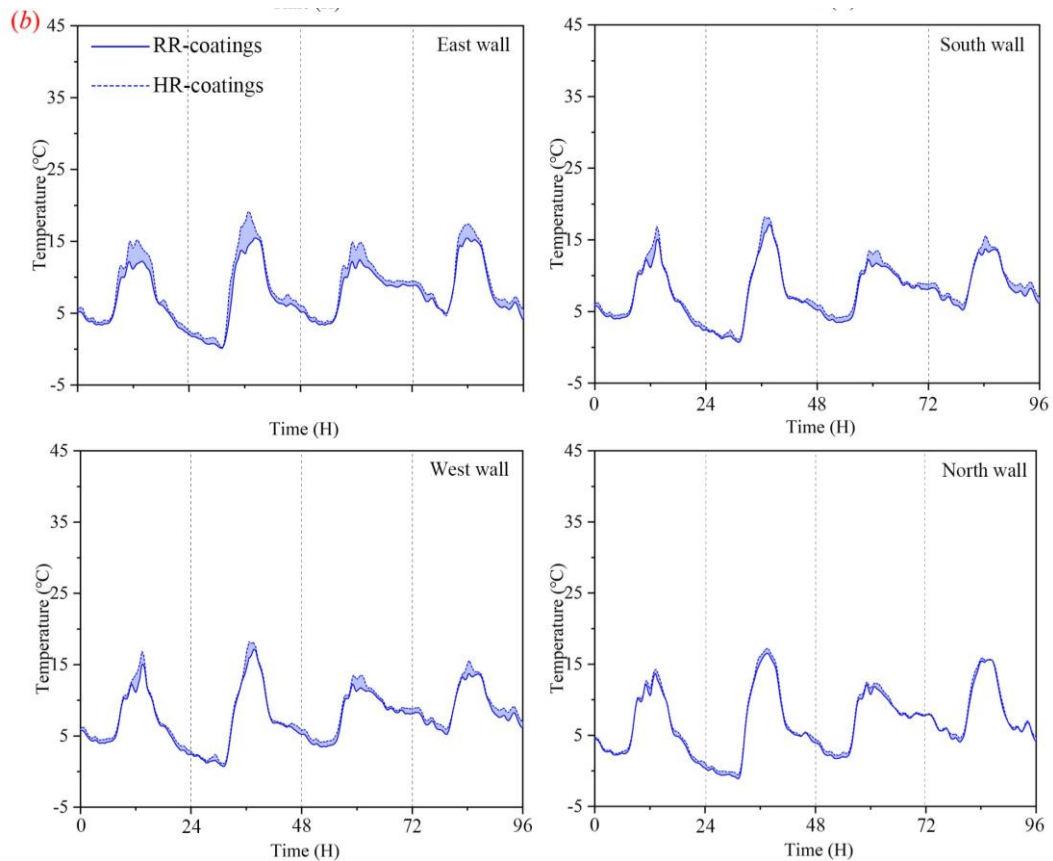
Fig. 7-6. Variation of wall temperature of RR-coatings and HR-coatings in (a) summer and (b) winter

Table 7-3 Comparison of maximum and average wall temperature differences of RR-coatings and HR-coatings models in summer and winter

Wall orientation	Season	Maximum value	Average value
Roof	Summer	7.71	3.75
	Winter	4.50	1.39
East wall	Summer	11.61	1.71
	Winter	5.61	1.54
South wall	Summer	7.25	2.90
	Winter	4.32	1.21
West wall	Summer	4.63	1.11
	Winter	2.76	0.52
North wall	Summer	2.74	0.74
	Winter	1.39	0.39

7.3.3 Comparison of air temperature

Outdoor air temperature directly affects the thermal comfort of human body and indirectly affects the energy consumption of surrounding buildings [40]. Fig. 7-7. showed the variation of air temperature in the enclosed space with time of RR-coatings and HR-coatings in summer and winter. It could be seen that both in summer and winter, the air temperatures in the enclosed space were higher than outdoor air temperature owing to the natural convection between the wall and the air in the enclosed space, and due to the retro-reflection effect, the air temperatures of RR-coatings were lower than those of HR-coatings. However, compared with in summer, the air temperature differences were smaller or even negligible in winter.

Table 7-4 showed the maximum and average air temperature in the enclosed space of RR-coatings and HR-coatings in summer and winter. As shown, in summer, compared to outdoor natural air temperature, the maximum and average air temperature in the enclosed space were increased by 5.70°C and 2.59°C for the RR-coatings, respectively, and the values were 7.80°C and 4.27°C for the HR-coatings, respectively. While in winter, compared to outdoor natural air temperature, the maximum and average air temperature in the enclosed space were increased by 0.91°C and 0.33°C for the RR-coatings, respectively, and the values were 1.30°C and 0.81°C for the HR-coatings, respectively. The above data showed that RR-coatings could reduce air temperatures in the enclosure spaces more than HR-coatings, especially in the summer. The phenomenon could be attributed to the retro-reflection property of RR-coatings, and the higher solar radiation and lower wind speed in summer.
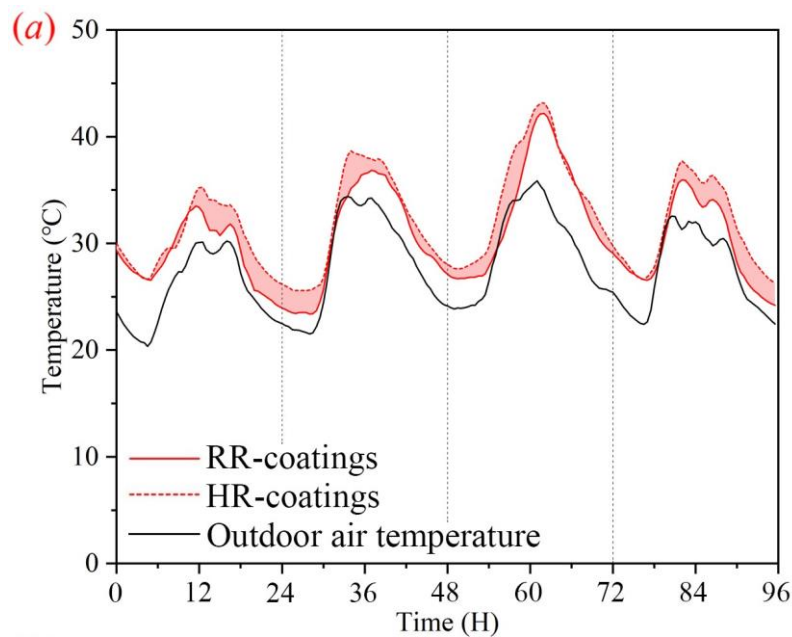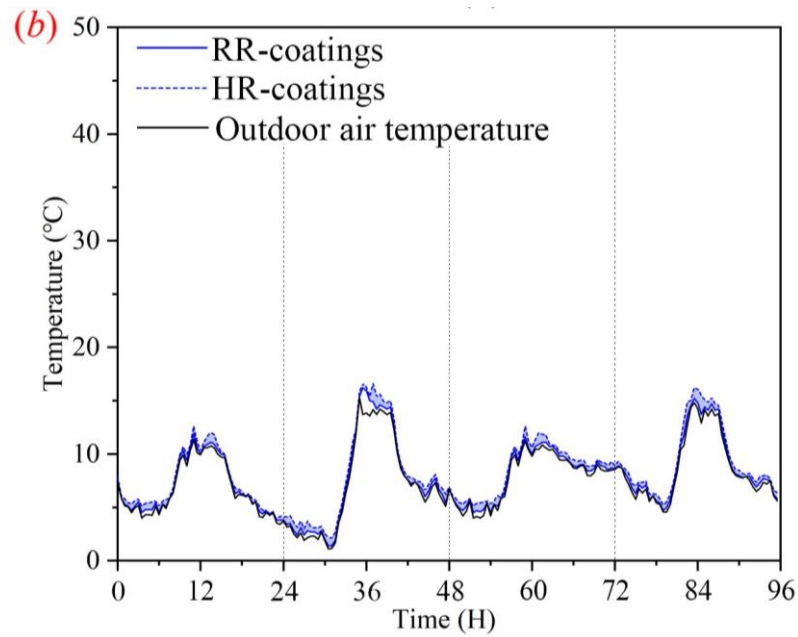
Fig. 7-7. Variation of air temperature of RR-coatings and HR-coatings in (a) summer and (b) winter

Table 7-4 Comparison of maximum and average air temperature of RR-coatings and HR-coatings in summer and winter

Season	Maximum value			Average value		
	Natural air	RR-coatings	HR-coatings	Natural air	RR-coatings	HR-coatings
Summer	38.71	44.41	46.51	27.83	30.42	32.10
Winter	15.32	16.23	16.62	7.56	7.89	8.37

7.4 Conclusion

Given the solar heat gain is one of the important components of urban heat sources, which affects the regional thermal environment directly. Reflective coatings have always been effective way to reduce the effects of solar radiation. However, what cannot be ignored is that in winter, reflective coatings would reduce the solar heat gain, and increase building cooling load. Here RR-coatings and HR-coatings with different optical properties were proposed, thermal performance of two coatings in an enclosed building in both summer and winter were evaluated experimentally. This study mainly focused on the seasonal comparison of the thermal

performance of two coatings in the areas of hot summers and cold winters with great demands for both cooling load and heat load. The regional albedos, wall temperatures and air temperatures in two seasons were monitored. The main results of the above experiments were as follows:

(1) For the regional albedos, the maximum and average values differences of RR-coatings and HR-coatings were 4.99% and 5.09% in summer, 2.46 % and 3.15% in winter, respectively.

(2) For the wall temperatures, the maximum and average values differences of RR-coatings and HR-coatings were 2.74°C~11.61°C and 0.74°C~3.75°C in summer, 1.39°C~5.61°C and 0.39°C~1.54°C in winter.

(3) For the air temperatures in the enclosed space, the maximum and average values differences of RR-coatings and HR-coatings were 2.10°C and 1.68°C in summer, 0.39°C and 0.48°C in winter.

The results showed that RR-coatings had the higher regional albedos, the lower wall temperatures and the lower air temperatures in summer and winter, compared with HR-coatings, but the cooling effect of RR-coatings is weaker in winter than summer. It indicated that RR-coatings could produce non-negligible thermal benefits in summer and relatively small penalties in winter. This work could promote the practical application of coatings in the construction engineering.

References

[1] S.H. Yuan, Z.G. Ren, X.F. Shan, Q.L. Deng, Z. Zhou. Seasonal different effects of land cover on urban heat island in Wuhan's metropolitan area. Urban Climate 49 (2023) 101547.

[2] H. Jie, I. Khan, M. Alharthi, M.W. Zafar, A. Saeed. Sustainable energy policy, socio-economic development, and ecological footprint: The economic significance of natural resources, population growth, and industrial development. Utilities Policy 81 (2023) 101490.

[3] E.S. Darbani, M. Rafieian, D.M. Parapari, J.M. Guldmann. Urban design strategies for summer and winter outdoor thermal comfort in arid regions: The case of historical, contemporary and modern urban areas in Mashhad, Iran. Sustainable Cities and Society 89 (2023) 104339.

[4] X. Wang, H.D. Li, S.H. Sodoudi. The effectiveness of cool and green roofs in mitigating urban heat island and improving human thermal comfort. Building and Environment 217 (2022)

109082.

[5] J.J. Sarralde, D.J. Quinn, D. Wiesmann, K. Steemers. Solar energy and urban morphology: Scenarios for increasing the renewable energy potential of neighborhood in London. Renewable Energy 73 (2015) 10-17.

[6] H. Akbari, D. Kolokotsa. Three decades of urban heat islands and mitigation technologies research. Energy and Buildings 133 (2016) 834-842.

[7] M. Santamouris, A. Synnefa, D. Kolokotsa, V. Dimitriou, K. Apostolakis. Passive cooling of the built environment—use of innovative reflective materials to fight heat islands and decrease cooling needs. International Journal of Low Carbon Technologies 3/2 (2008) 71-82.

[8] A. Synnefa, M. Santamouris, H. Akbari. Estimating the effect of using cool coatings on energy loads and thermal comfort in residential buildings in various climatic conditions. Energy and Buildings 39 (2007) 1167-1174.

[9] M. Alimohammadian, S. Dinarvand, O. Mahian. Innovative strategy of passive sub-ambient radiative cooler through incorporation of a thermal rectifier to double-layer nanoparticlebased coating. Energy 247 (2022) 123411.

[10] S.M. Mousavi, M. Yousefi, M.N. Rostami, H. Tamim, M. Alimohammadian, S. Dinarvand. Zinc oxide–silver/water hybrid nanofluid flow toward an off-centered rotating disk using temperature-dependent experimental-based thermal conductivity. Zinc oxide–silver/water hybrid nanofluid flow toward an off-centered rotating disk using temperature-dependent experimental-based thermal conductivity. Heat Transfer 51 (2022) 1167-1174.

[11] S. Maharjan, K.S. Liao, A.J. Wang, S.A. Curran. Highly effective hydrophobic solar reflective coating for building materials: Increasing total solar reflectance via functionalized anatase immobilization in an organosiloxane matrix. Constr. Build. Mater 243 (2020) 118189.

[12] S. Garshasbi, S.J. Huang, J. Valenta, M. Santamouris. On the combination of quantum dots with near-infrared reflective base coats to maximize their urban overheating mitigation potential. Sol. Energy 211 (2020) 111-116.

[13] P.K. Thejus, K.V. Krishnapriya, K.G. Nishanth. A cost-effective intense blue colour inorganic pigment for multifunctional cool roof and anticorrosive coatings. Sol. Energy Mater. Sol. Cells 219 (2021) 110778.

[14] Y.L. Han, J.E. Taylor, A.L. Pisello. Toward mitigating urban heat island effects: Investigating the thermal-energy impact of bio-inspired retro-reflective building envelopes in

dense urban settings. Energy Build 102 (2015) 380-389.

[15] M. Manni, G. Lobaccaro, F. Goia, A. Nicolini, F. Rossi. Exploiting selective angular properties of retro-reflective coatings to mitigate solar irradiation within the urban canyon. Solar Energy 189 (2019) 74-85.

[16] J.C. Yang, Z.H. Wang, K.E. Kaloush. Environmental impacts of reflective materials: Is high albedo a 'silver bullet' for mitigating urban heat island? Renewable and Sustainable Energy Reviews 47 (2015) 830–843.

[17] I.H. Pérez, Y.O. Gómezb. Thermal evaluation of building roofs with conventional and reflective coatings. Eco-efficient Materials for Reducing Cooling 9 (2021) 247-273.

[18] H. Mohamed, J.D. Chang, M. Alshayed. Effectiveness of High Reflective Roofs in Minimizing Energy Consumption in Residential Buildings in Iraq. Procedia Engineering 118 (2015) 879-885.

[19] M. Baneshi, S. Maruyama. The impacts of applying typical and aesthetically-thermally optimized TiO2 pigmented coatings on cooling and heating load demands of a typical residential building in various climates of Iran. Energy and Buildings 113 (2016) 99-111.

[20] J.H. Yuan, K.Z. Emura, C. Farnham. Potential for application of retroreflective materials instead of highly reflective materials for urban heat island mitigation. Urban Studies Research 2016 (2016) 3626294.

[21] A. Salvati, M. Kolokotroni, A. Kotopouleas, R. Watkins, R. Giriharan, M. Nikolopoulou. Impact of reflective materials on urban canyon albedo, outdoor and indoor microclimates. Building and Environment 207 (2022) 108459.

[22] J. Wang, S.H. Liu, X. Meng, W.J. Gao, J.H. Yuan. Application of retro-reflective materials in urban buildings: A comprehensive review. Energy and Buildings 247 (2021) 111137.

[23] J.E. Hummer, W. Rasdorf, G. Zhang. Linear Mixed-Effects Models for Paint Pavement-Marking Retro reflectivity Data. Journal of Transportation Engineering 137 (2011) 705-716.

[24] R.B. Nilsen, X.J. Lu. Retro reflection Technology. European Symposium on Optics and Photonics for Defence and Security. International Society for Optics and Photonics (2004) 47-60.

[25] H. Sakai, H. Iyota. Development of Two New Types of Retroreflective Materials as Countermeasures to Urban Heat Islands. Int. J. Thermophys. 38 (2017) 31.

[26] J. Yuan, C. Farnham, K. Emura. Development of a retro-reflective material as building coating and evaluation on albedo of urban canyons and building heat loads. Energy and Buildings 103 (2015) 107-117.

[27] S. Yoshida, A. Mochida. Evaluation of effects of windows installed with near-infrared rays retro-reflective film on thermal environment in outdoor spaces using CFD analysis coupled with radiant computation. Build. Simul. 11 (2018) 1053-1066.

[28] T. Inoue, T. Shimo, M. Ichinose, K. Takase, T. Nagahama. Improvement of urban thermal environment by wavelength-selective retro-reflective film. Energy Procedia 122 (2017) 967-972.

[29] L.L. Zhang, X. Meng, F. Liu, L. Xu, E.S. Long. Effect of retro-reflective materials on temperature environment in tents, Case Stud. Therm. Eng. 9 (2017) 122-127.

[30] F. Rossi, E. Morini, B. Castellani, A. Nicolini, E. Bonamente, E. Anderini, F. Cotana. Beneficial effects of retro-reflective materials in urban canyons: results from seasonal monitoring campaign. Journal of Physics: Conference Series 655 (2015) 012012.

[31] J. Wang, S.H. Liu, X. Meng, W.J. Gao. Influence of the building enclosed forms on thermal contribution of retro-reflective and high-reflective coatings. Energy and Buildings 273 (2022) 112400.

[32] S. Yoshida, S. Yumino, T. Uchida, A. Mochida. Effects of windows with heat ray retro-reflective film on outdoor thermal environment and building cooling load. J. Heat Island Institute Int. 2 (2014) 67-72.

[33] Y.F. Gao, R.M. Yao, B.Z. Lia, E. Turkbeylerc, Q. Luo, A. Shortd. Field studies on the effect of built forms on urban wind environments. Renewable Energy 46 (2021) 148-154.

[34] Y.H. Qin, J. Liang, K.G. Tan, F.H. Li. A side by side comparison of the cooling effect of building blocks with retro-reflective and diffuse-reflective walls. Sol.Energy 133 (2016) 172-179.

[35] R. Levinson, H. Akbari1, P. Berdahl. Measuring solar reflectance—Part I: Defining a metric that accurately predicts solar heat gain. Sol. Energy 84 (2010) 1717-1744.

[36] I. Hernández-Pérez, J. Xaman, E.V. Macias-Melo, K.M. Aguilar-Castro, I. Zavala-Guillen, I. Hernandez-Lopez, E. Sima. Experimental thermal evaluation of building roofs with conventional and reflective coatings. Energy Build. 158 (2018) 569-579 .

[37] S. Dinarvand , H. Berrehal, H. Tamim, G. Sowmya, S. Noeiaghdam, M. Abdollahzadeh.

Squeezing flow of aqueous CNTs-Fe3O4 hybrid nanofluid through mass-based approach: Effect of heat source/sink, nanoparticle shape, and an oblique magnetic field. Results in Engineering 17 (2023) 100976.

[38] G. Dharmaiah, S. Dinarvand, J.L. Rama Prasad, S. Noeiaghdam, M. Abdollahzadeh. Non-homogeneous two-component buongiorno model for nanofluid flow towar.d Howarth's wavy cylinder with activation energy. Results in Engineering 17 (2023) 100879.

[39] X. Meng, T. Luo, Z.Y. Wang, W. Zhang, B. Yan, J.L. Ouyang, E.S. Long. Effect of retro-reflective materials on building indoor temperature conditions and heat flow analysis for walls. Energy Build. 127 (2016) 488-498.

[40] A. Aboelata. Reducing outdoor air temperature, improving thermal comfort, and saving buildings' cooling energy demand in arid cities– Cool paving utilization. Sustain. Cities Soc. 68 (2021) 102762.

The effect of building surface retro-reflectivity on energy load and CO_2 emission of an enclosed building

Chapter 8 The effect of building surface retro-reflectivity on energy load and CO_2 emission of an enclosed building

8.1 Introduction

Energy conservation and emission reduction was necessary to ease the energy crisis [1, 2]. In China, the construction industry accounted for 35% of the total electricity consumption [3, 4]. Building cooling and heating energy consumption accounted for more than 65% of the total building energy consumption [5, 6]. The large amount of building energy consumption would deteriorate the regional thermal environment [7, 8] and had a negative impact on human thermal comfort [9, 10]. To reduce it, some green technologies have been proposed, included the increment of green infrastructures [11-13], the employment of spray cooling system [14-16], and so on. However, solar radiation had a great influence on the energy performance of buildings [17, 18], and reflective coatings have attracted much attention due to they could effectively reflect solar radiation, and maintain a low building surface temperature, and reduce the heat transfer of buildings [19-21]. Currently, reflective coatings mainly included high-reflective coatings (HR-coatings) and retro-reflective coatings (RR-coatings).

As for the HR-coatings, Pereza et al. [22] found the high-reflective roof had a daily heat gain 9% smaller than the room with ordinary roof. Guo et al. [23] found the indoor temperature of the room painted the HR-coatings was lower 4.32°C than that of the room without painting the HR-coatings. Mohamed et al. [24] found that compared to typical roof, high-reflective roofs were capable of reducing cooling loads by about 45%. Baneshi et al. [25] found compared to the residential building with typical coatings, the building with optimized coatings which with higher reflectivity could reduced the annual cooling load by 4-31% while increased the annual heating load demand by 1.7-10%. However, the solar radiation reflected by HR-coatings would be intercepted by nearby buildings and roads through the multiple absorption, and thereby, HR-coatings have the low potential of thermal environment improvement, especially for high-density building groups [26].

RR-coatings have attracted more attention of scholars due to the ability of reflecting the solar radiation back along the incident direction [27, 28], which leaded to the reduction of the absorbed solar radiation, and thereby the urban thermal environment and energy consumption in buildings would be affected. Rossi et al. [29] found that when RR-coatings were applied on the vertical surface of the urban canyon, the air temperature decreased by 1% compared with the white diffuse coatings from the result of a summer monitoring campaign. Zhang et al. [30] covered RR-coatings on the tent model and found that the peak temperature of indoor air was lowered by 7.0°C, compared to the ordinary tent. Yoshida et al. [31] adopted the AND model for the calculation of directional reflectivity per unit solid angle for the RR-coatings applied on windows, and it was found the cooling load was reduced by 489 MJ/h, but the heating load was

increased by 534 MJ/h, compared to the window with heat shading film and the Low-E double glass. Yuan et al. [32] simulated the energy consumption of building located in Shanghai, China using a 2-D analytic model and it was found that compared with no RR-coatings, the annual cooling and heating loads were decreased by 157 MJ/m^2 and -71 MJ/m^2, respectively. Andrea et al. [33] simulated a virtual RR-coatings considering its response as almost diffusive but in the same direction of the incident radiation and the energy advantages was investigated by means of a numerical model developed in MATLAB and based on the Gebhart factors theory. Han et al. [34] modeled a bio-inspired retro-reflective building envelope, conducted cross-regional energy simulation of building networks in order to examine its thermal-energy impact, and found the reductions of both total energy consumption and cooling energy consumption could be up to 8.2% and 9.8% in different metropolitan areas. Martin et al. [35] made a 3-D representation of the urban microenvironment, and studied the effect of glass RR-coatings on the thermal environment of street pavements and evaluated the heat transfers through a composite slab. Mauri et al. [36] adopted the methodology of TRNSYS to predict the advantages of the adoption of RR-coatings as envelope cladding in terms of yearly building thermal energy demand.

From the above review, it could be seen that similar to HR-coatings, RR-coatings could reduce the cooling load in summer, however, their negative effect was to increase the heat load in winter. In order to improve the seasonal adaptability and obtain the least annual energy load, it was necessary to select the optimal retro-reflectivity according to the specific climatic characteristics of the regions. However, there was a lack of the research on the optimal retro-reflectivity at present. And due to the retro-reflectance varied with solar altitude angles [32], and most of the building energy simulation techniques only considered construction coatings with a constant and perfectly diffusive solar reflectance, and the adopted models was based on some simplifications which did not permit to fully replicate the entire set of the sun rays' inter-reflections within the building groups. Therefore, it was very hard to simulate RR-coating behavior.

Therefore, based on the results of a previously published paper on the air temperature difference resulted by covering RR-coatings and HR-coatings in the three-sided enclosed building groups [37], the corresponding reduced air temperatures were set varied with building surface reflectivities from 0.1 to 0.9. Based on these values, changes were made to the weather file, and then entered into EnergyPlus to simulate the effect of different retro-reflectivities on the daily, monthly and yearly energy load of an actual three-sided enclosed educational building in Qingdao, China, and CO_2 emissions were also calculated.

8.2 Description of the simulation

8.2.1 Building surface reflectivities

The building surface reflectivity determines the amount of reflected solar radiation, which indirectly affects the cooling and heating load of the buildings [38, 39]. To research the effect of building surface reflectivity on the building energy load, based on the results of a previously published paper on air temperature reduction resulted by covering RR-coatings in the three-sided enclosed building groups [37], which was consistent with the simulation model, that was the prism RR-coatings with a reflectivity of about 50% could reduce the air temperature by about 2∘C, the building surface reflectivities were set to vary from 0 to 1 in the step of 0.1, and the corresponding reduced air temperature displayed a linear variation between 0∘C to 4∘C. However, in view of a perfectly reflecting or absorbing coatings did not exist in reality, the building surface reflectivities of 0 and 1 were deleted. The specific setting of the temperature reduction for different reflectance was shown in Fig. 8-1. And the air temperature value in the weather files were changed accordingly, then taking the values as boundary conditions in EnergyPlus to investigate the effect of building surface reflectivities on energy load of the reference building.
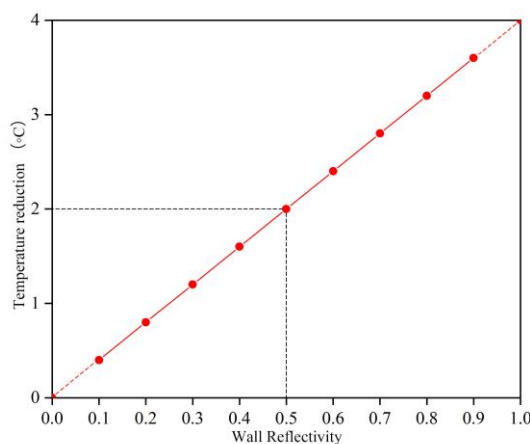
Fig. 8-1. Temperature reduction for different reflectance

8.2.2 Description of the simulation city

Consistent with the experimental site, Qingdao was chosen as the simulation city, as shown in Fig. 8-2. Qingdao was characterized by significant seasonal variation, and had both cooling period and heating period. The heating period was from November to March, and the cooling period was from June to September, and the transition period included April, May, October. Under this condition, both of the air-conditioning and heating energy loads could not be ignored [40].

Fig. 8-3 showed the equipotential diagram of outdoor air and solar radiation all the year in Qingdao city of China. The highest temperature was 29.50°C in summer, the lowest air temperatures were -9.61°C in winter. And the highest solar radiation intensity in summer reached 1.05kW/m^2, and the solar radiation intensity in winter was much lower than that in summer. And from Fig. 8-3, the winter period included November, December, January, February and March with the average air temperatures of about -4.01°C, while the summer period included June, July, August, and September with the average air temperatures of about 27.02°C.
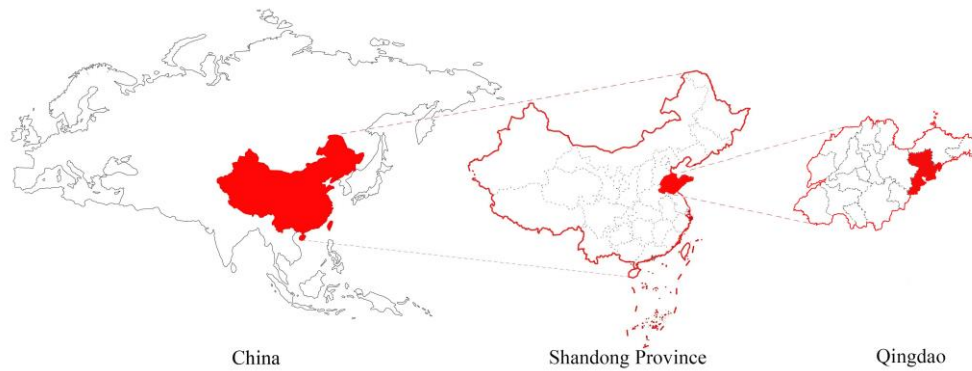
Fig. 8-2. Location of Qingdao in China
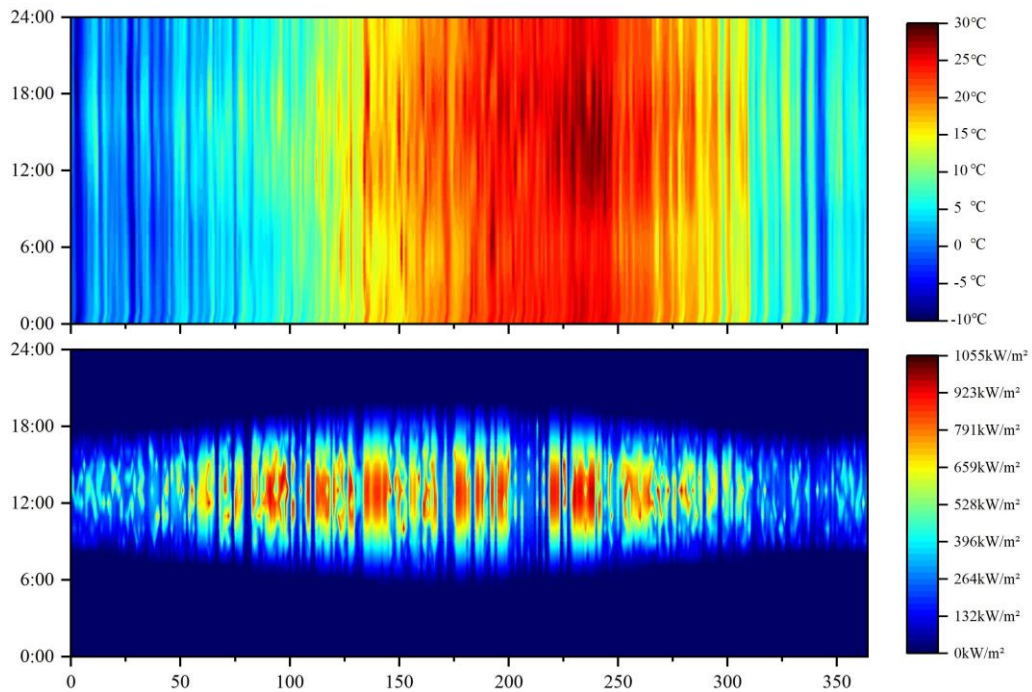
Fig. 8-3. Equipotential diagram of air temperature and solar radiation intensity all the year in Qingdao, China

8.2.3 Description of the simulation model

Consistent with the experimental model, a three-sided enclosed educational building in Qingdao was selected as the simulation object. Educational buildings were the main places for teachers and students to study and work, and it also provided outdoor activity places for teachers and students to adjust their emotions and ensure physical and mental health after learning. Excessive solar radiation heat in atrium would cause a great negative impact on the outdoor thermal environment of enclosed buildings, which would affect the comfort of outdoor activities of teachers and students, reduce their willingness to participate in outdoor activities. In addition, the quality of outdoor thermal environment would also affect the indoor thermal environment of the building, and then affect the air-conditioning energy consumption of educational buildings in summer. Therefore, it was of great significance to improve the outdoor thermal environment of educational buildings by reduced the solar heat gain.

The photo and model of the selected educational building was as shown in Fig. 8-4(*a*) and 8-4(*b*). The building was mainly divided into two functional zones including the classrooms on both sides and offices in the middle, as shown in Fig. 8-4(*c*). Details of the simulation building and conditions of the building load calculation were shown in Table 8-1. The weather data of Qingdao city were from the Energyplus climate file database. The building faced north and south, and total area was $10080.00m^2$ with the classrooms area of $5220.00m^2$, and offices area of $4860.00m^2$. Considering the high personnel density of educational buildings [41, 42], the personnel density was 0.50 person/m^2 and 0.25person/m^2 in classrooms and offices, respectively. The heating powers were 8.00W /m^2 for indoor lighting and 15.00W/m^2 for equipment. The air-conditioning operation time was from 7:00 to 22:00. The indoor design temperature was 25.00°C in cooling period, 20.00°C in heating period and 22.00-25.00°C in middle period. The *K*-value of roof, wall, floor and window were 0.43, 0.49, 0.79 and 2.4 W/m^2·k, respectively, according to the local requirements for the k value. The reflectivity of the roof and walls were changed from 0.1 to 0.9 in the step of 0.1, and that of the floor, window and ground were constant with the value of 0.29, 0.075 and 0.15, respectively.

(*a*)
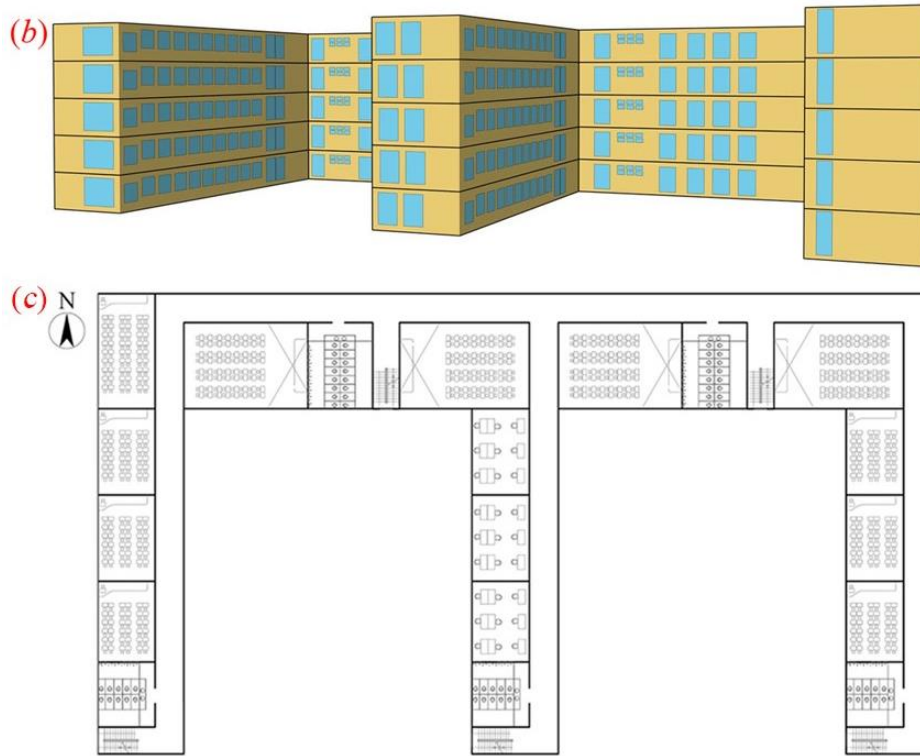
Fig. 8-4(*a*) Building photo, (*b*) model diagram and (*c*) plan function layout diagram

Table 8-1. Details of simulation model and conditions of building load

Location	Qingdao, Shandong, China		
Orientation and area of building	South and North-facing wall		
	Classroom area: 5220.00m^2; Office area:4860.00m^2		
Internal heat generation	Classroom Body: 0.50person/m^2; Office Body: 0.25person/m^2; Light: 8.00W/m^2; Equipment:15.00W/m^2		
Air condition service	7:00-22:00		
Temperature and Humidity settings		Heating season	Cooling season	Middle season
	Temperature (∘C)	20.00	25.00	22.00-25.00
	Humidity (%)	-	60.00	60.00
	K-value (W/m$^{2\cdot}$k)		Reflectivity	

Building exterior wall	Roof	0.43	0.1-0.9 (variable)
	Wall	0.49	0.1-0.9 (variable)
	Floor	0.79	0.29 (constant)
	Window	2.4	0.075 (constant)
Ground		Reflectivity: 0.15 (constant)	

The schedule setting of internal heat generation was shown in Fig. 8-5, including occupant schedule, equipment schedule, lighting schedule and air condition schedule. These were all set to constant value according to the actual situation of the school.
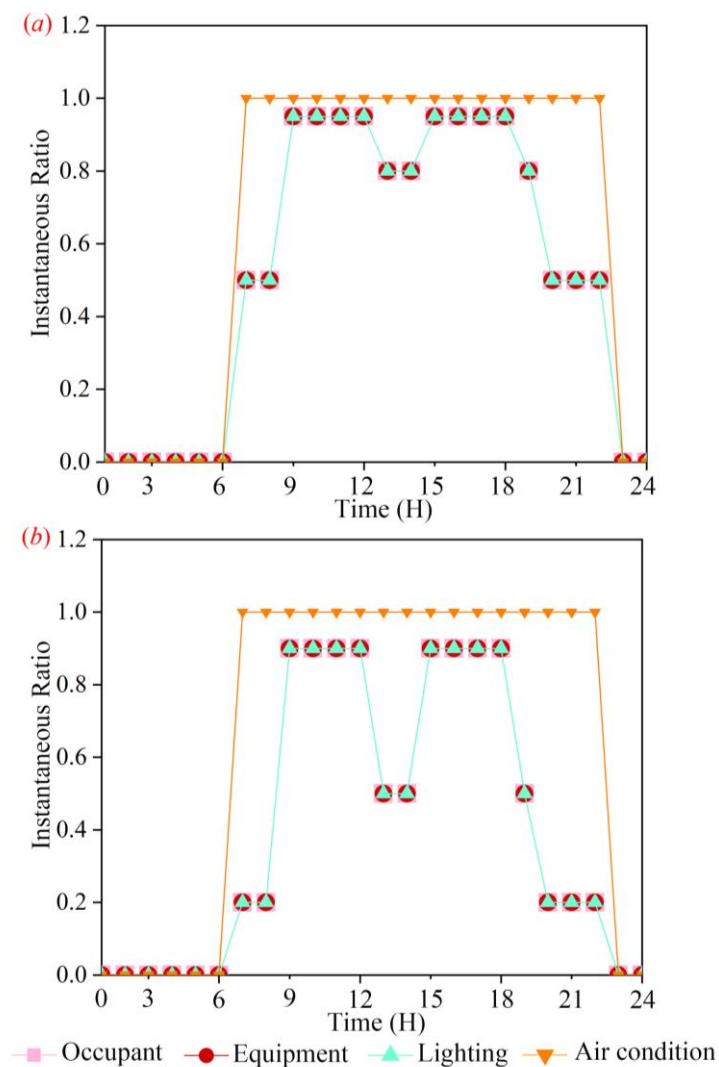
Fig. 8-5. Schedule setting for internal heat generation (a) classroom, (b)office

8.2.4 Energyplus

The research for the effect of building surface reflectivity on energy load was based on the simulation program "Energyplus" which was an energy analysis engine distributed by the U.S. Department of Energy [43]. It was widely used in calculating the indoor temperature, humidity and thermal loads of public buildings, like school buildings [44], office buildings [45], shopping malls [46] and so on. For the purpose of studying the HVAC energy loads of reference building without considering the mechanical efficiency, the Ideal Loads Air System was implemented in this study.

8.2.5 Validation of Numerical method

To guarantee the accuracy of numerical simulation, the published results from Mohamed et al. [47] about the effect of roof solar reflectivity on energy load, and Liu et al. [41] about the effect of exterior wall solar radiation absorption coefficient on total loads in Jinan based on Energyplus were validated. Fig. 8-6 compared the present numerical results with the published values from Liu et al. [41]. As shown, the maximum deviation was just 5.66% between the present numerical results and published values. This indicated the applicability of the simulation software with the research for the effect of building surface reflectivity on the building energy load.
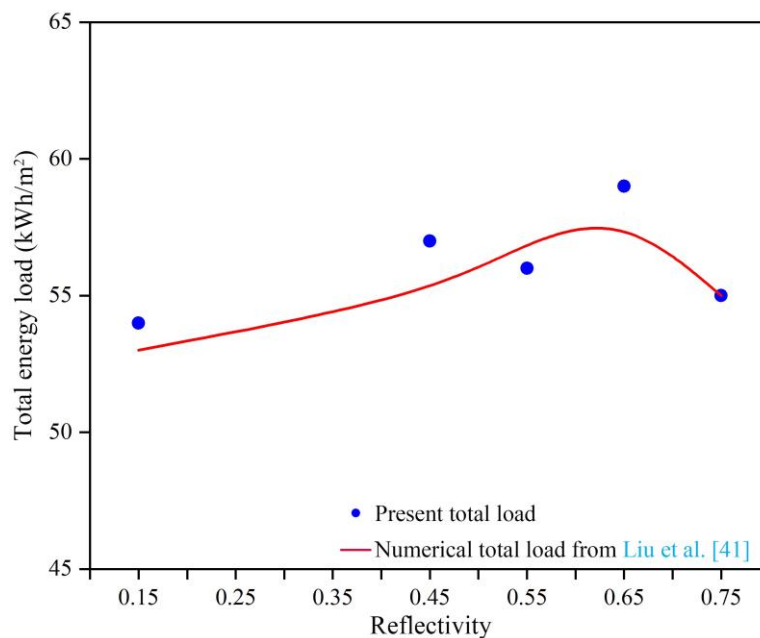
Fig. 8-6. Comparison of the present numerical results with the published values from Liu et al. [41]

8.3 Result and discussion

Building surface reflectivities determined the amount of solar heat gain, and would have a large influence on building surface temperature and the cooling and heating energy load [38]. To research the effect of building surface reflectivity on building energy load, the daily, monthly, and annual heating and cooling energy load were separately simulated, as well as energy associated CO_2 emissions were analyzed.

8.3.1 Daily energy load

Four typical seasonal days in winter, spring, summer and fall were selected to calculate the daily energy load. The day chosen in each season were almost sunny to better clarify the effect of surface reflectivities on building energy load according to the index of Site Total Sky Cover which with a range of 1-10, and the day was the sunny day when the index was less than 3.

Fig. 8-7 showed the variation of daily total and peak energy load with building surface reflectivities in the typical seasons. It could be clearly seen that there was a positive correlation between the daily total and peak energy load and building surface reflectivities in January, April and October, and a negative correlation in July. In January, there was mainly heating load due to Qingdao was in the heating period, when the surface reflectivity was 0.1, the daily total and peak energy load was all the lowest, with the value of 1.33 kWh/m^2 and 0.17kWh/m^2, respectively. And when the surface reflectivity was 0.9, the daily total and peak energy load was all the highest, with the value of 1.57kWh/m^2 and 0.20kWh/m^2, respectively. Compared with the surface reflectivity of 0.1, the daily total and peak energy load saving rate could reach -18.04% and -17.64%, respectively. In July, there was mainly cooling load due to Qingdao was in the cooling period, and the daily total and peak energy load was the highest, with the value of 0.69kWh/m^2 and 0.08kWh/m^2 when the surface reflectivity was 0.1, and the daily total and peak energy load was the lowest when the surface reflectivity was 0.9, with the value of 0.25kWh/m^2 and 0.04kWh/m^2, therefore, the daily total and peak energy load saving rate could reach 63.76% and 50.00%, respectively. Meanwhile, since April and October belonged to the transition seasons in Qingdao, the demand for the daily total and peak energy load was relatively low and mainly heating load, and there was a positive correlation between the daily total and peak energy load and building surface reflectivity. When the surface reflectivity was 0.1, the daily total and peak energy load April and October were the lowest with the values of 0.25kWh/m^2 & 0.05kWh/m^2, and 0.003kWh/m^2 & 0.002kWh/m^2, respectively. And when the surface reflectivity was 0.9, there were the highest values of 0.48kWh/m^2 & 0.08kWh/m^2, and 0.03kWh/m^2 & 0.02kWh/m^2, respectively.
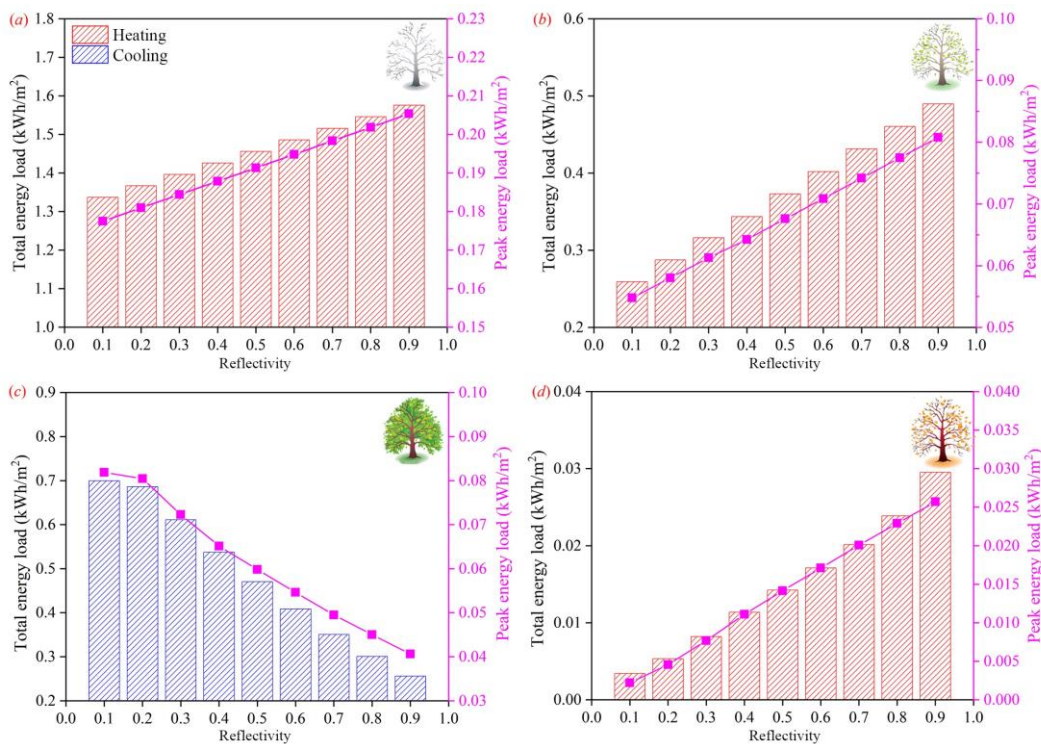
Fig. 8-7. Daily building energy load in the typical seasons (a) Jan., (b) Apr.,(c) Jul., and (d)Oct.

8.3.2 Monthly energy load

Fig. 8-8 showed the variation of monthly energy load with surface reflectivities. According to the weather condition of Qingdao, the heating period was from November to March, and the cooling period was from June to September, and the transition period included April, May, October. As shown, there were mainly heating load in the heating period, and with the increase of surface reflectivities, heating load increased. In January, the heating load was the most, and the value could be up to 29.27 kWh/m^2 when the reflectivity was 0.1, and 36.43 kWh/m^2 when the reflectivity was 0.9, the increase rate was 24.46%. And in November, December, February and March, the heating load was the lowest when the reflectivity was 0.1, with the value of 8.72 kWh/m^2, 19.69 kWh/m^2, 22.26 kWh/m^2 and 16.42 kWh/m^2, respectively. And the heating load was the most when the reflectivity was 0.9, with the value of 14.65 kWh/m^2, 26.84 kWh/m^2, 28.74 kWh/m^2 and 23.58 kWh/m^2, respectively. In the cooling period, there were mainly cooling load, and with the increase of building surface reflectivities, cooling load decreased. In August, the cooling load was most, the value could be up to 27.14 kWh/m^2 when the reflectivity was 0.1, and 8.93 kWh/m^2 when the reflectivity was 0.9, the decrease rate was 67.09%. And in June, July and September, the cooling load was the most when the reflectivity was 0.1, with the value of 2.18 kWh/m^2, 17.12 kWh/m^2 and 9.28 kWh/m^2, respectively. And the cooling load was the lowest when the reflectivity was 0.9, with the value of 0.23 kWh/m^2, 3.06 kWh/m^2 and 2.48

kWh/m^2, respectively. Compared with cooling period and heating period, the energy load in transition seasons were relatively lower. However, it could be seen that there were mainly heating load, and which were the most when the reflectivity was 0.9, with the value of 13.63 kWh/m^2, 3.12 kWh/m^2 and 2.17 kWh/m^2, respectively.

Table 8-2 compared the annual heating and cooling load resulted by walls with different reflectivities. As shown, the higher the surface reflectivity, the less the cooling load and the more heating load. For the cooling load, when the building surface reflectivity was 0.1, the value was 57.13 kWh/m^2, when the surface reflectivity was 0.9, the value was 10.83 kWh/m^2, the cooling load decreased by an amount of 46.30 kWh/m^2, making a percentage decrease of 81.04%. For the heating load, hen the building surface reflectivity was 0.1, the value was 115.98 kWh/m^2, when the surface reflectivity was 0.9, the value was 139.41 kWh/m^2, whereas the heating load increased by an amount of 23.43 kWh/m^2, representing 20.19% increase. It was worth noting that there was the least total energy load when the building surface reflectivity was 0.7, with the value of 148.23kWh/m^2, and the total energy load was the most when the building surface reflectivity was 0.1, with the value of 173.11kWh/m^2, with the difference of 24.88 kWh/m^2, representing 16.78% increase. Therefore, when the building surface reflectivity of the enclosed educational building was 0.7, the energy-saving effect was the best.
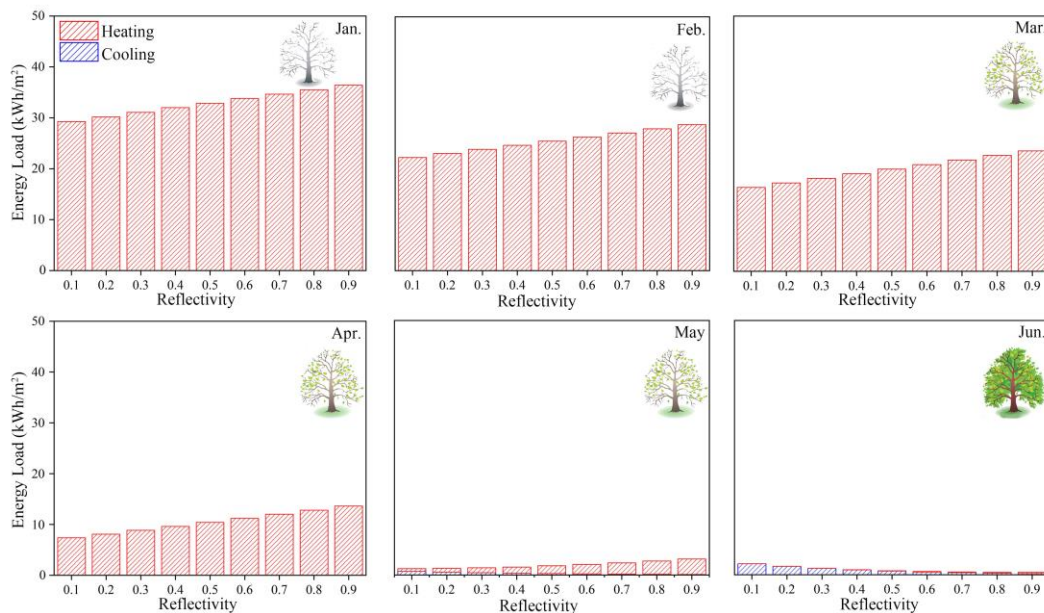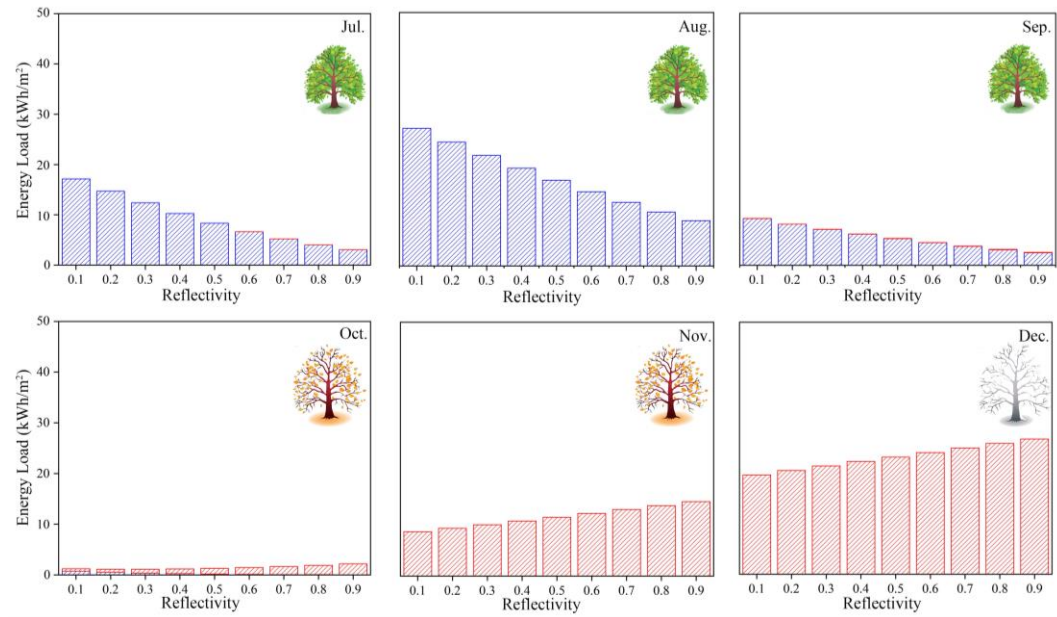
Fig. 8-8. Monthly building energy load in a year

Table 8-2. Comparison of annual heating and cooling load resulted by building surface with different reflectivities

Building surface reflectivity	Cooling (kWh/m^2)	Heating (kWh/m^2)	Cooling& heating (kWh/m^2)
0.1	57.13	115.98	173.11
0.2	50.00	118.04	168.04
0.3	43.37	121.4	164.77
0.4	37.27	124.85	162.12
0.5	30.67	127.35	158.02
0.6	23.62	130.98	154.6
0.7	15.14	133.09	148.23
0.8	13.21	136.51	149.71
0.9	10.83	139.41	150.23

8.3.3 CO_2 emissions

Both heating and cooling energy loads contributed to CO_2 emission [48]. Since the ideal loads air system was implemented in this study, which was equivalent to the room hang-up air conditioner, associated electricity load was calculated by dividing the heating and cooling energy efficiency ratios of 3.50 and 3.25, respectively [49], then according to the Guidance on Accounting Methods and Reporting of Greenhouse Gas Emissions for Enterprises Power Generation Facilities (Revised 2022) [50], the energy associated carbon emission was calculated by multiplying grid carbon emission factor of 0.581kg CO_2/kWh. Therefore, the results of CO_2 emissions were outline in Fig. 8-9. As shown, with the increase of surface

reflectivities, CO_2 emissions resulted by heating load increased and which resulted by cooling load decreased. And from Table 8-3, as for the CO_2 emissions resulted by cooling load, the values were $10.21kg/m^2$ and $1.93kg/m^2$ when the surface reflectivity was 0.1 and 0.9, respectively, the decrease rate was 81.09%. As for the CO_2 emissions resulted by heating load, the value was $19.25kg/m^2$ when the surface reflectivity was 0.1, and $23.14kg/m^2$ when the surface reflectivity was 0.9, the increase rate was 20.20%. It was worth noting that there was the least total CO_2 emissions when the surface reflectivity was 0.7, with the value of $24.79kg/m^2$. Therefore, the surface reflectivity of 0.7 was the best for saving energy and alleviating global warming.
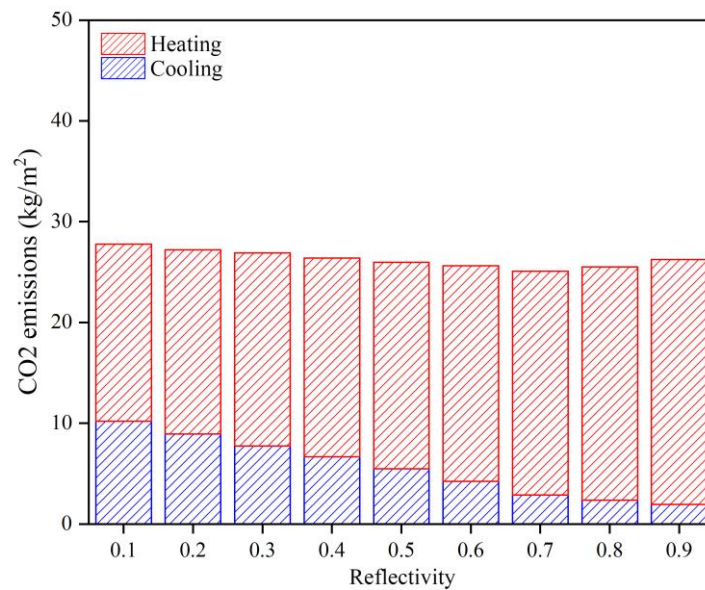
Fig. 8-9. CO_2 emissions resulted by building surface with different reflectivities

Table 8-3. Comparison of CO_2 emissions resulted by energy load of building with different reflectivities

Building surface reflectivity	CO_2 resulted by cooling (kg/m^2)	CO_2 resulted by heating (kg/m^2)	Total CO_2 (kg/m^2)
0.1	10.21	19.25	29.46
0.2	8.94	19.59	28.53
0.3	7.75	20.15	27.90
0.4	6.66	20.73	27.39
0.5	5.48	21.14	26.62
0.6	4.22	21.74	25.96
0.7	2.71	22.09	24.80
0.8	2.36	22.66	25.02
0.9	1.94	23.14	25.08

From the above analysis, it could be seen that when the surface reflectivity was 0.7, the annual energy load and CO_2 emissions were all the least. According to the relation between solar reflectivities and retro-reflectivities of prism RR-coatings mentioned in only two published articles [51, 52], that the retro-reflectivity could be at most 67.06% of the total solar reflectivity, which meant that building surface with the retro-reflectivity of 0.47 could obtain the best energy saving and emission reduction for the enclosed educational building in Qingdao, China.

8.4 Conclusion

This study explored the effect of building surface retro-reflectivities on the energy load and CO_2 emissions of a educational building in Qingdao city using the simulation program "Energyplus". The input variables for the building were the building surface reflectivities varying from 0.1 to 0.9 in steps of 0.1. The output data were daily, monthly and yearly energy load, and energy associated CO_2 emissions of building. The main conclusions could be gained as followings:

(1) For daily energy load in four typical seasons, there was a positive correlation between the daily total and peak energy load and building surface reflectivities in January, April and October, and a negative correlation in July. In January, compared with the building surface reflectivity of 0.1, the daily total and peak energy load saving rate could reach -18.04% and -17.64% when the building surface reflectivity was 0.9. In July, the energy load saving rate could reach 63.76% and 50.00%. And in April and October, when the building surface reflectivity was 0.9, there were the highest values of $0.48 kWh/m^2$ & $0.08 kWh/m^2$, and $0.03 kWh/m^2$ & $0.02 kWh/m^2$, respectively.

(2) For monthly energy load, the building heating energy load was the most in January, the value could be up to $29.27 \ kWh/m^2$ when the reflectivity was 0.1, and $36.43 \ kWh/m^2$ when the reflectivity was 0.9, the increase rate was 24.46%. The building cooling energy load was the most in August, the value could be up to $27.14 \ kWh/m^2$ when the reflectivity was 0.1, and $8.93 \ kWh/m^2$ when the reflectivity was 0.9, the decrease rate was 67.09%.

(3) For annual energy load, the higher the building surface reflectivity, the less the cooling load and the more heating load. But in general, there was the least total energy load when the building surface reflectivity was 0.7, with the value of $148.23 \ kWh/m^2$.

(4) For CO_2 emissions, with the increase of building surface reflectivities, CO_2 emissions resulted by heating load increased and which resulted by cooling load decreased. There was the least total CO_2 emissions when the building surface reflectivity was 0.7, with the value of

24.79kg/m^2.

(5) According to the relation between solar reflectivities and retro-reflectivities of prism RR-coatings mentioned in the published articles, When the building surface retro-reflectivity was 0.47, the total annual energy load and CO$_2$ emissions were the least.

Reference

[1] F. He, R.F. Bo, C.X. Hu, X. Meng, W.J. Gao. Employing spiral fins to improve the thermal performance of phase-change materials in shell-tube latent heat storage units. Renewable Energy 203 (2023) 518-528.

[2] J.L. Zou , X. Meng. Investigating the effect of distribution form of copper foam fins on the thermal performance improvement of latent thermal energy storage units. International Communications in Heat and Mass Transfer 141 (2023) 106571.

[3] Z. Wu, Q.S. Jia , X. Guan. Optimal control of multiroom HVAC system: An event-based approach. IEEE Transactions on Control Systems Technology 24 (2015) 662-669.

[4] J.L. Zou, F. He, Y.Y. Qi, X. Meng, W.K. Ma. Thermal performance improvement of thermal energy storage systems by employing a contrastive experiment. Case Studies in Thermal Engineering 41 (2023) 102647.

[5] D.D. Kim, H.S. Suh. Heating and cooling energy consumption prediction model for high-rise apartment buildings considering design parameters. Energy for Sustainable Development 61 (2021) 1-14.

[6] Y. Gao, X. Meng. A comprehensive review of integrating phase change materials in building bricks: Methods, performance and applications. Journal of Energy Storage 62 (2023) 106913.

[7] L. Gustavsson, T. Nguyen, R. Sathre, U.Y.A. Tettey. Climate effects of forestry and substitution of concrete buildings and fossil energy. Renewable and Sustainable Energy Reviews 136 (2021) 110435.

[8] F. Rosso, A.L. Pisello, V.L. Castaldo, C. Fabiani, F. Cotana, M. Ferrero, W. Jin. New cool concrete for building envelopes and urban paving: Optics-energy and thermal assessment in dynamic conditions, Energy and Buildings. 151 (2017) 381-392.

[9] C.X. Hu, Z.H. Wang, R.F. Bo, C.Y. Li, X. Meng. Effect of the cooling clothing integrating with phase change material on the thermal comfort of healthcare workers with personal

protective equipment during the COVID-19. Case Studies in Thermal Engineering 42 (2023) 102725.

[10] L.A.C. Jiron, K. Graw, M. Gangwisch, A. Matzarakis. Influence of street configuration on human thermal comfort and benefits for climate-sensitive urban planning in Santiago de Chile. Urban Climate 47 (2023) 101361.

[11] X. Wang, H.D. Li, S.H. Sodoudi. The effectiveness of cool and green roofs in mitigating urban heat island and improving human thermal comfort. Building and Environment 217 (2022) 109082.

[12] X. Meng, L.Y. Yan , F.D. Liu. A new method to improve indoor environment: Combining the living wall with air-conditioning. Building and Environment 216 (2022) 108981.

[13] F.D. Liu, L.Y. Yan, X. Meng, C. Zhang. A review on indoor green plants employed to improve indoor environment. Journal of Building Engineering 53 (2022) 104542.

[14] X. Meng, L. Meng, Y. Gao, H.R. Li. A comprehensive review on the spray cooling system employed to improve the summer thermal environment: Application efficiency, impact factors, and performance improvement. Building and Environment 217 (2022) 109065.

[15] Y.J. Wang, F.Y. He, Z.H. Lv, W.B. Yang, Q. Wang. Experimental investigations on thermal performance of spray cooling double skin façade in hot humid climate region. Energy and Buildings 277 (2022) 112605.

[16] J.S. Wang, Q.L. Meng, C. Yang, P. Ren, M. Santamouris. Spray optimization to enhance the cooling performance of transparent roofs in hot-humid areas. Energy and Buildings 286 (2023) 112929.

[17] F. He, B.W. Yan, J.L. Zou, C.X. Hu, X. Meng, W.J. Gao. Experimental evaluation of the effect of perforated spiral fins on the thermal performance of latent heat storage units. Journal of Energy Storage 58 (2023) 106359.

[18] Y. Azegami, M. Imanishi, K. Fujiwara, H. Kusaka. Effects of solar radiation in the streets on pedestrian route choice in a city during the summer season. Building and Environment 235 (2023) 110250.

[19] H. Akbari, D. Kolokotsa. Three decades of urban heat islands and mitigation technologies research. Energy and Buildings 133 (2016) 834-842.

[20] M. Santamouris, A. Synnefa, D. Kolokotsa, V. Dimitriou, K. Apostolakis. Passive cooling of the built environment—use of innovative reflective materials to fight heat islands

and decrease cooling needs. International Journal of Low Carbon Technologies 3/2 (2008) 71-82.

[21] A. Synnefa, M. Santamouris, H. Akbari. Estimating the effect of using cool coatings on energy loads and thermal comfort in residential buildings in various climatic conditions. Energy and Buildings 39 (2007) 1167-1174.

[22] I.H. Pereza Y.O. Gomezb. Thermal evaluation of building roofs with conventional and reflective coatings. Eco-efficient Materials for Reducing Cooling Needs in Buildings and Construction 9 (2021) 247-273.

[23] X.G. Guo, J. Wang, Y. Wu, Y.Q. Ao, X.W. Liu. Experimental Study of the Thermal Performance of a New Type of Building Reflective Coating in Hot Summer and Cold Winter Zone of China. Procedia Engineering 205 (2017) 603-608.

[24] H. Mohamed, J.D. Chang, M. Alshayed. Effectiveness of High Reflective Roofs in Minimizing Energy Consumption in Residential Buildings in Iraq. Procedia Engineering 118 (2015) 879-885.

[25] M. Baneshi, S. Maruyama. The impacts of applying typical and aesthetically-thermally optimized TiO_2 pigmented coatings on cooling and heating load demands of a typical residential building in various climates of Iran. Energy and Buildings 113 (2016) 99-111.

[26] J. Yang, Z. H. Wang, K.E. Kaloush, Environmental impacts of reflective materials: Is high albedo a 'silver bullet' for mitigating urban heat island? Renewable and Sustainable Energy Reviews 47 (2015) 830–843.

[27] J. Wang, S.H. Liu, X. Meng, W.J. Gao, J.H. Yuan. Application of retro-reflective materials in urban buildings: A comprehensive review. Energy and Buildings 247 (2021) 111137.

[28] J. Wang, S.H. Liu, Z.F. Liu, X. Meng, C.B. Xu, W.J. Gao. An experimental comparison on regional thermal environment of the high-density enclosed building groups with retro-reflective and high-reflective coatings. Energy and Buildings 259 (2022) 111864.

[29] F. Rossi, E. Morini, B. Castellani, A. Nicolini, E. Bonamente, E. Anderini, F. Cotana. Beneficial effects of retro-reflective materials in urban canyons: results from seasonal monitoring campaign. Journal of Physics: Conference Series 655 (2015) 012012.

[30] L.L. Zhang, X. Meng, F. Liu, L. Xu, E.S. Long. Effect of retro-reflective materials on temperature environment in tents. Case Studies in Thermal Engineering 9 (2017) 122-127.

[31] S. Yoshida, S. Yumino, T. Uchida, A. Mochida. Effects of windows with heat ray retro-reflective film on outdoor thermal environment and building cooling load. Journal of Heat Island Institute International 2 (2014) 67-72.

[32] J. Yuan, C. Farnham, K. Emura. Development of a retro-reflective material as building coating and evaluation on albedo of urban canyons and building heat loads. Energy and Buildings 103 (2015) 107-117.

[33] V. Andrea, M. Luca, C. Chiara, D.L.V. Roberto. Numerical Model for the Characterization of Retro-reflective Materials Behavior in an Urban Street Canyon. Journal of Thermal Science 27 (2018) 456-462.

[34] Y.L. Han, J.E. Taylor, A.L. Pisello. Toward mitigating urban heat island effects: Investigating the thermal-energy impact of bio-inspired retro-reflective building envelopes in dense urban settings. Energy and Buildings 102 (2015) 380–389.

[35] M. Martin, N.H. Wong, M. Ichinose. Impact of retro-reflective glass façades on the surface temperature of street pavements in business areas of Singapore and Tokyo. IOP Conf. Series: Earth and Environmental Science 294 (2019) 012020.

[36] L. Mauri, G. Battista, E.D.L. Vollaro, R.D.L. Vollaro. Retroreflective materials for building's façades: Experimental characterization and numerical simulations. Solar Energy 171(2018) 150-156.

[37] J. Wang, S.H. Liu, X. Meng, W.J. Gao. Influence of the building enclosed forms on thermal contribution of retro-reflective and high-reflective coatings. Energy and Buildings 273 (2022) 112400.

[38] H. Shen, H.W. Tan, A. Tzempelikos. The effect of reflective coatings on building surface temperatures, indoor environment and energy consumption-An experimental study. Energy and Buildings 43 (2011) 573-580.

[39] M. Xu. Impacts of Building Geometries and Radiation Properties on Urban Thermal Environment. Procedia Computer Science 108C (2017) 2517-252.

[40] W.G. Hao, Y.F. Lu, Y.H. Lai, M.X. Lyu. Application of earth-air heat exchanger cooling technology in an office building in Jinan city. Energy Procedia 158 (2019) 6105-6111.

[41] Z.A. Liu, J.W. Hou, L.L. Zhang, B.J. Dewancker, X. Meng, C.P. Hou. Research on energy-saving factors adaptability of exterior envelopes of university teaching-office buildings under different climates (China) based on orthogonal design and EnergyPlus. Heliyon 8 (2022)

10056.

[42] M.D. Orazio, E.D. Giuseppe, G. Bernardini. All rights reserved.Occupant density impact on building maintenance: Data-driven approach for university buildings. Automation in Construction 141 (2022) 104451.

[43] T.E. Jiru. Combining HVAC energy conservation measures to achieve energy savings over standard requirements. Energy and Buildings 73(2014) 171-175.

[44] G. Rospi, N. Cardinale, F. Intini. Analysis of energy consumption of different typologies of school buildings in the city of matera (southern Italy). Energy Procedia 82(2015) 512-518.

[45] A. Boyano, P. Hernandez, O. Wolf. Energy demands and potential savings in European office Buildings: Case studies based on EnergyPlus simulations. Energy and Buildings 65(2013) 19-28.

[46] S. Zheng, H. Liang. Simulation and study on energy-saving of air-conditioning system energy consumption of a shopping plaza in Xi'an. Building Energy and Environment 33(2014) 38-41.

[47] H. Mohamed, J.D. Chang, M. Alshayeb. Effectiveness of High Reflective Roofs in Minimizing Energy Consumption in Residential Buildings in Iraq. Procedia Engineering 118 (2015) 879-885.

[48] J.Y. Hu, X. Yu. Thermo and light-responsive building envelope: Energy analysis under different climate conditions. Solar Energy 193(2019)866-877.

[49] GB 12021.3-2010: The minimum allowable value of the energy efficiency and energy efficiency grades for room air conditioners. National Standardization Administration Committee.

[50] Guidance on Accounting Methods and Reporting of Greenhouse Gas Emissions for Enterprises Power Generation Facilities (Revised 2022). Ministry of Ecology and Environment.

[51] S.H. Liu, J.Wang, X.Meng. Spectral properties of retro-reflective materials from experimental measurements. Case Studies in Thermal Engineering 39 (2022) 102434.

[52] J.H. Yuan, K.Emura, C. Farnham. A method to measure retro-reflectance and durability of retro-reflective materials for building outer walls. Journal of Building Physics 38 (2015) 500-516.

Chapter 9

Conclusion and prospect

Chapter 9 Conclusion and prospect

9.1 Conclusion

Retro-reflective coatings (RR-coatings) was a kind of special coatings which could reflect incident light back along the incident direction. Theoretically, when the coatings were applied on the exterior surface of buildings, it could not only reduce the temperature of the exterior surface of buildings, save energy, but also alleviate the urban heat island effect and improve the urban thermal environment. At present, the application research of this coatings in the field of building energy conservation was a brand-new topic.

Based on the deep understanding of the thermal environment formation mechanism of high-rise and high-density buildings, the influence of RR-coatings on regional thermal environment was put forward to alleviate the deterioration of outdoor thermal environment. On the one hand, the optical properties of RR-coatings, including solar reflectance and retro-reflectance, were studied. On the other hand, the RR-coatings and HR-coatings were applied on the outer surface of the scaled model. Under the same outdoor climate conditions, the influence of the RR-coatings and HR-coatings on the thermal environment of the building was studied by monitoring the changes of the regional albedo, wall temperature and air temperature through comparative experiments. In addition, the influence of the architectural form on the thermal contribution of coatings was also paid attention to. And for a more comprehensive assessment of thermal contribution of HR-coatings and RR-coatings, the summer benefit and winter loss of the RR-coatings was studied through experiment. Finally, the effect of building surface retro-reflectivities on energy load of an actual three-sided enclosed educational building in Qingdao was simulated based on the software of Energyplus, and CO_2 emissions were also calculated.

The main works and results could be summarized as follows:

In Chapter 1, Background and Purpose of the Study:

The research backgrounds were introduced, including due to the increase of population and high-rise and high density buildings caused by urbanization, the thermal environment of regional buildings deteriorated and energy consumption increased. After demonstrating the limitation of other green technologies, based on the fact that solar radiation was the main source of building thermal gain, RR-coatings and HR-coatings were proposed. The research status of these coatings was introduced in detail. It was pointed out that due to their special optical properties, the application potential of RR-coatings in architecture was great. The purpose and significance of this paper were introduced. Finally, the chapter structure of the study was explained.

In Chapter 2, Literature review of the application of RR-coatings in buildings:

The relevant research of this paper was reviewed, and the focuses were the development, performance measurement and significant outcomes of RR-coatings, while the application efficiency of RR-coatings was described, mainly included the urban thermal environment and building energy consumption. Finally, future directions were proposed on possible studies and applications.

In Chapter 3, Methodology and performance evaluation index:

This chapter introduced the basic experimental system, simulation system and evaluation index of the impact of RR-coatings on the thermal environment and energy load of regional buildings, which laid the foundation for the analysis of related research in the following chapters. Firstly, the optical performance experiment was introduced. The solar reflectance and angle distribution of glass bead RR-coatings and prism RR-coatings were measured using the optical property measuring instruments. Secondly, the thermal performance experiment was introduced, including the experimental plans and the basic experimental models, and the performance evaluation index, which mainly included the regional albedo, wall temperature and air temperature. Thirdly, based on the software of Energyplus, the impact of RR-coating on the thermal environment of buildings was preliminarily determined and the effect of wall reflectivities on energy load of an enclosed educational building in Qingdao was simulated, and the evaluation index included daily, monthly and yearly energy load.

In Chapter 4, Experimental study on spectral properties of retro-reflective coatings:

The spectral characteristics of glass bead RR-coatings and prism RR-coatings were measured. The integrating sphere was used to measure the global reflectivity, and a self-developed instrument was used to measure the angular distribution at different incident angles. The result showed that the global reflectivity of glass bead RR-coatings and prism RR-coatings were 64.74% and 51.44%, respectively. However, the retro-reflectivity of prism RR-coatings was higher than glass bead RR-coatings at the smaller incident angles with the values of 25.22% and 21.67%, respectively (at 10◦ and 30◦ of incidence). For larger incidence angles including 50◦ and 70◦, two RR-coatings mainly showed specular-reflection property. RR-pattern facades could reduce the wall surface temperature, compared to general facades.

In Chapter 5, An experimental comparison on regional thermal environment of the high-density enclosed building groups with retro-reflective and high-reflective coatings:

This chapter built two small-scale high-density enclosed building group models and covered by RR-coatings and HR-coatings, respectively. The urban albedo, wall surface temperature and air temperature were contrastively analyzed in two models. Experimental results showed

compared with HR-coating model, RR-coating model had better cooling potential, and its regional albedo was increased by 5.53%. And air temperature in enclosed space of RR-coating model was 2.24°C lower than that of HR-coating model, but they were higher than outdoor natural air temperature. Moreover, compared to HR-coatings, covering RR-coatings could reduce the peak and average wall temperature by 2.47°C~15.25°C & 0.30°C~3.82°C in the daytime and 1.35°C~7.91°C% & 0.25°C~4.38°C in the nighttime, and its application in the roof and east wall had the high efficiency.

In Chapter 6, Influence of the building enclosed forms on thermal contribution of retro-reflective and high-reflective coatings:

The contribution efficiency of reflective coatings was reevaluated to improve the regional thermal environment. Three typical forms of high-density buildings, namely the Determinant Form (D-Form), Three-Sided Enclosed Form (TSE-Form) and Four-Sided Enclosed Form (FSE-Form), were proposed. High-reflective coatings (HR-coatings) and retro-reflective coatings (RR-coatings) were employed with the different reflective mechanisms, while the albedo, wall temperature, and air temperature were monitored. Experimental results showed that the higher the enclosed degree of buildings covered by HR-coatings, the poorer the regional thermal environment and the higher the heat island efficiency. However, the opposite was true for enclosed buildings with RR-coatings. RR-coatings had a better thermal contribution than HR-coatings, and the higher the enclosure degree of buildings, the higher the improvement efficiency of RR-coatings. Compared with HR-coatings, RR-coatings increased the maximum and average regional albedos by 0.67%~3.42% and 1.36%~5.59%, respectively, and lowered the maximum and average temperatures by 0.26°C~7.05°C and 0.02°C~4.83°C for model walls and 0.59°C~4.41°C and 1.80°C~3.06°C for outdoor air, respectively.

In Chapter 7, An experimental evaluation on thermal contribution of retro-reflective and high-reflective coatings in an enclosed building in summer and winter:

This chapter evaluated the thermal contribution of retro-reflective coatings (RR-coatings) and high-reflective coatings (HR-coatings) with the different reflective mechanisms in an enclosed building in both summer and winter. And the regional albedos, wall temperatures, and air temperatures were measured. Experimental results showed that both in summer and winter, compared with HR-coatings, RR-coatings had higher regional albedos, lower wall temperatures and air temperatures, however, the differences were smaller in winter, which would lead to more thermal benefits in summer caused by RR-coatings than thermal penalties in winter. For the regional albedos, the maximum differences in summer and winter were 4.99% and 2.46%, and the values were 2.74°C~11.61°C and 1.39°C~5.61°C for the wall temperatures, 2.10°C and

0.39°C for the air temperatures.

In Chapter 8, The effect of building surface retro-reflectivity on energy load and CO_2 emission of an enclosed building.

This chapter analyzed the effect of building surface reflectivity on daily, monthly and yearly energy load of an educational building based on the Energyplus software, and CO_2 emissions were also calculated. The numerical results showed for daily energy load in four typical seasons, there was a positive correlation between the daily energy load and building surface reflectivities in January, April and October, and a negative correlation in July. For monthly energy load, the building cooling and heating load were the most in January and August, respectively. For annual energy load, the higher the reflectivity, the lower the cooling load and the higher the heating load. When the building surface reflectivity was 0.7, the annual energy load were the least, with the value of 148.23 kWh/m^2. In addition, the CO_2 emissions was also the lowest, with the value of 24.79 kg/m^2. According to the relation between solar reflectivities and retro-reflectivities of prism RR-coatings mentioned in the published articles, When the building surface retro-reflectivity was 0.47, the total annual energy load and CO_2 emissions were the least.

In Chapter 9, Conclusion and prospect：

The main research conclusions of each chapter were summarized, and the contents of the future research was expounded.

9.2 Prospect

In this paper, a certain amount of research and exploration has been carried out in determining the spectral properties of RR-coatings and the effect on thermal environment , but there are still a lot of work worth further in-depth, which mainly include:

(1) If the experimental conditions permit, the RR-coatings can be pasted on the actual building to further test the cooling data of the building under real conditions.

(2) RR-coatings have been proved to reduce cooling energy consumption, but increase heating energy consumption to a certain extent. Therefore, the contribution of RR-coatings to energy consumption is closely and directly related to the local climate conditions, so it is necessary to study the adaptability of RR-coatings in five different climate zones under the premise of experimental conditions.

(3) Building coatings will produce fading, peeling, cracking, embrittlement, delamination and loss of tensile strength and thermal properties over time. In order to evaluate the best service

life and predict the long-term performance of the sample, it is necessary to test the weather resistance of the RR-coatings through long-term experimental observation.

(4) The retro-reflectance of existing RR-coatings will attenuate sharply at relatively large incidence angles of solar radiation, so the RR-coatings should be developed and further optimized.